

Complementary quadruple hydrogen bonding

Citation for published version (APA):

Ligthart, G. B. W. L. (2006). *Complementary quadruple hydrogen bonding*. [Phd Thesis 1 (Research TU/e / Graduation TU/e), Chemical Engineering and Chemistry]. Technische Universiteit Eindhoven.
<https://doi.org/10.6100/IR608314>

DOI:

[10.6100/IR608314](https://doi.org/10.6100/IR608314)

Document status and date:

Published: 01/01/2006

Document Version:

Publisher's PDF, also known as Version of Record (includes final page, issue and volume numbers)

Please check the document version of this publication:

- A submitted manuscript is the version of the article upon submission and before peer-review. There can be important differences between the submitted version and the official published version of record. People interested in the research are advised to contact the author for the final version of the publication, or visit the DOI to the publisher's website.
- The final author version and the galley proof are versions of the publication after peer review.
- The final published version features the final layout of the paper including the volume, issue and page numbers.

[Link to publication](#)

General rights

Copyright and moral rights for the publications made accessible in the public portal are retained by the authors and/or other copyright owners and it is a condition of accessing publications that users recognise and abide by the legal requirements associated with these rights.

- Users may download and print one copy of any publication from the public portal for the purpose of private study or research.
- You may not further distribute the material or use it for any profit-making activity or commercial gain
- You may freely distribute the URL identifying the publication in the public portal.

If the publication is distributed under the terms of Article 25fa of the Dutch Copyright Act, indicated by the "Taverne" license above, please follow below link for the End User Agreement:

www.tue.nl/taverne

Take down policy

If you believe that this document breaches copyright please contact us at:

openaccess@tue.nl

providing details and we will investigate your claim.

Complementary Quadruple Hydrogen Bonding

Proefschrift

ter verkrijging van de graad van doctor aan de Technische Universiteit Eindhoven,
op gezag van de Rector Magnificus, prof.dr.ir. C.J. van Duijn, voor een commissie
aangewezen door het College voor Promoties in het openbaar te verdedigen op
dinsdag 30 mei 2006 om 16.00 uur

door

Godefridus Bernardus Wilhelmus Leonardus Ligthart

geboren te Breda

Dit proefschrift is goedgekeurd door de promotor:

prof.dr. E.W. Meijer

Copromotor:

dr. R.P. Sijbesma

This research has been financially supported by the Netherlands Organization for Scientific Research, Chemical Sciences (NWO-CW).

Omslagontwerp: JWL Producties te Eindhoven

Druk: PrintPartners Ipskamp te Enschede

A catalogue is available from the Library Eindhoven University of Technology

ISBN-10: 90-386-2628-2

ISBN-13: 978-90-386-2628-4

Contents

1 Multiple hydrogen bonding in supramolecular polymers	1
1.1 The molecular world	2
1.2 Supramolecular chemistry and supramolecular polymers	2
1.3 Hydrogen bonding	5
1.4 Supramolecular polymers	8
1.4.1 Small building blocks	8
1.4.1.1 Supramolecular polymers based on liquid-crystalline monomers	9
1.4.1.2 Supramolecular polymers in isotropic solution	10
1.4.2 Large building blocks	15
1.4.2.1 Main-chain supramolecular polymers	16
1.4.2.2 Supramolecular block copolymers	20
1.4.2.3 Side-chain supramolecular polymers	22
1.5 Aim of the thesis	27
1.6 Outline of the thesis	27
1.7 References	28
2 Complementary hydrogen bonding based on benzotriazine-N-oxide and imide motifs	33
2.1 Introduction	34
2.2 Quadruple hydrogen bonding based on a benzo-1,2,4-triazine-N-oxide motif	36
2.2.1 Synthesis and characterization	36
2.2.2 Binding studies	38
2.2.3 Quantum mechanical calculations	39
2.2.3.1 Geometry optimization	40
2.2.3.2 Hydrogen bonding abilities with complementary motifs	41
2.3 Hydrogen bonding based on an imide motif	43
2.3.1 Synthesis and characterization	45
2.3.2 Binding studies	46
2.4 Conclusions	48
2.5 Experimental procedures	49
2.6 References	53
3 Pd-catalyzed amidation of 2-chloro- and 2,7-dichloro-1,8-naphthyridines	57
3.1 Introduction	58
3.2 Pd-catalyzed amidation of arylhalides	60
3.2.1 Optimization of Pd-catalyzed amidation of 2,7-dichloro-1,8-naphthyridine	60
3.2.2 Symmetric bisamidation of 2,7-dichloro-1,8-naphthyridine	61
3.2.3 Mono-amidation of 2,7-dichloro-1,8-naphthyridine	62
3.2.4 Amidation of 7-amido-2-chloro-1,8-naphthyridine	65
3.3 Hydrolysis of 2,7-diamido-1,8-naphthyridines	67
3.4 Conclusions	71
3.5 Experimental procedures	72

3.6 References	79
4 Pd-catalyzed amination to 2-amino- and 2,7-diamino-1,8-naphthyridines	81
4.1 Introduction	82
4.2 Pd-catalyzed amination to 2-amino- and 2,7-diamino-1,8-naphthyridine	84
4.2.1 Pd-catalyzed amination of 2,7-dichloro-1,8-naphthyridine	84
4.2.2 Pd-catalyzed mono-amination of 2-chloro-1,8-naphthyridine	86
4.2.3 Synthetic strategy to 2,7-diamino-1,8-naphthyridines	88
4.3 Degradation of 2-amido-7-arylamino- and 2,7-di(arylamino)-1,8-naphthyridines	92
4.4 Reactivity of naphthyridine substrates in Pd-catalyzed aminations and arylations	94
4.5 Conclusions	96
4.6 Experimental procedures	96
4.7 References	105
5 Complementary quadruple hydrogen bonding based on the UPy – Napy binding motif	107
5.1 Introduction	108
5.2 The association constant of the 2-ureido-6-[1H]-pyrimidinone – 2,7-diamido-1,8-naphthyridine dimer	110
5.2.1 Introduction	110
5.2.2 NMR measurements	111
5.2.3 Fluorescence measurements	116
5.2.4 Theoretical model of concentration dependent UPy – Napy association	117
5.2.5 UV/Vis measurements	119
5.3 Evaluation of substituent effects on binding strengths	121
5.3.1 Association of substituted 2,7-amino-1,8-naphthyridines	121
5.3.2 Influence of bulky substituents	122
5.3.3 Electronic effects on binding strength	124
5.4 The lifetime of the 2-ureido-6-[1H]-pyrimidinone – 2,7-diamido-1,8-naphthyridine dimer	127
5.4.1 Introduction	127
5.4.2 2D-EXSY measurements	128
5.4.3 Kinetic equilibration measurements	131
5.5 Discussion	132
5.6 Conclusions	135
5.7 Experimental procedures	135
5.8 References	138
6 Supramolecular block copolymers based on the UPy – Napy binding motif	141
6.1 Introduction	142
6.2 Supramolecular systems based on small bifunctional Napy molecules	145
6.2.1 Synthesis and characterization	145
6.2.2 Towards UPy – Napy based supramolecular alternating copolymers	146

6.2.3 Diffusion-ordered 2D NMR (DOSY) experiments	148
6.2.4 Increasing spacer length to induce alternating copolymer formation	149
6.3 Supramolecular systems based on polymeric bifunctional Napy molecules	151
6.3.1 Introduction	151
6.3.2 Synthesis and characterization	154
6.3.2.1 UPy protecting groups	154
6.3.2.2 Bifunctional UPy and Napy CTAs	155
6.3.2.3 UPy and Napy telechelic polymers	157
6.3.3 Supramolecular block copolymer formation in solution	161
6.3.4 Supramolecular block copolymer formation in the bulk	162
6.4 Discussion and conclusions	165
6.5 Experimental procedures	167
6.6 References	176
7 Supramolecular graft-copolymers based on 2,7-diamido-1,8-naphthyridines	179
7.1 Introduction	180
7.2 Oligo-2,7-bis(9-decenoylamino)-1,8-naphthyridines via Acyclic Diene Metathesis polymerization	181
7.2.1 Synthesis of oligo-2,7-bis(9-decenoylamino)-1,8-naphthyridines	182
7.2.2 Characterization of ADMET-polymer 2	184
7.2.2.1 NMR spectroscopy	184
7.2.2.2 Size exclusion chromatography	186
7.3 Oligo-2,7-diamido-1,8-naphthyridines via polycondensation	186
7.3.1 Synthesis and characterization of oligo-2,7-diamido-1,8-naphthyridines	188
7.3.2 Recognition properties of oligo-2,7-diamido-1,8-naphthyridines	190
7.4 Supramolecular grafting	191
7.5 Discussion and conclusions	193
7.6 Experimental procedures	194
7.7 References	196
Summary	199
Samenvatting	201
Curriculum Vitae	203
Publications	204
Dankwoord	205

1

Multiple hydrogen bonding in supramolecular polymers

Abstract

The assembly of small and large molecules into larger structures plays an important role in life. The non-covalent interactions that determine the properties of these assemblies can be used to design new supramolecular structures with unique material properties. This chapter serves as an overview on supramolecular polymers based on multiple hydrogen bonding with a focus on the resulting material properties. With the area of supramolecular architectures as a target, the aim and scope of the thesis are subsequently formulated.

1.1 The molecular world

Molecules are assemblies of atoms that are connected by chemical bonds. They can be synthesized from smaller molecules by the selective formation of kinetically stable covalent bonds (typical bond enthalpies 100-400 kJ/mol). Molecules can also interact without forming such strong bonds through weaker and kinetically labile non-covalent interactions. In biology such interactions are responsible for the transduction of signals, the selective transport of ions or small molecules such as drugs across cell membranes or for the folding of large proteins into a 3D-structure. In Nature as well as in the abiotic world, such non-covalent interactions determine the physical properties of common materials such as wood and plastic. A variety of non-covalent interactions exist: metal-ligand (50-200 kJ/mol), hydrogen bonds (4-120 kJ/mol), dipole-dipole (4-40 kJ/mol), π - π stacking (1-20 kJ/mol) and van der Waals (dispersion) attractions (1-10 kJ/mol). Although single non-covalent interactions are often too weak to survive the thermal motions that keep molecules apart, strong binding is obtained when several of these interactions are combined or multiple non-covalent bonds interact cooperatively. In order to get a better understanding of natural processes and the influence of these non-covalent interactions in both natural and synthetic materials, it is important to study the characteristics of such interactions.

This thesis will deal with the investigation of small and large molecules that were designed to display strong and specific interactions.

1.2 Supramolecular chemistry and supramolecular polymers

The directed association of synthetic molecules into defined architectures is the area of supramolecular chemistry, which is also known as chemistry beyond the molecule.¹ Much of the field of supramolecular chemistry finds its origin in the remarkable observations and findings of Pedersen,² Cram³ and Lehn⁴ in their research on crown ethers, spherands, carcerands and, in general, pre-organization. Their studies allowed for the development of many synthetic binding motifs for a guest molecule in a specific orientation into a host molecule. These host-guest complexes display size and shape selectivity and include compounds such as crown ethers,⁵ cyclodextrins⁶ or cucurbit[n]urils⁷ as hosts and ammonium salts or small organics as guests. Over the last four decades, synthetic host-guest systems have led to a large number of reports on the construction of discrete architectures and turned from

scientific curiosity into applications such as sensors. The non-covalent interactions resulting in these complexes are usually combinations of solvophobic effects and ion-dipole interactions.

A particularly interesting concept in supramolecular chemistry is the supramolecular polymer which is a macromolecular architecture that is formed by the self-assembly of monomers bearing two or more binding sites. Polymers based on this concept hold promise as a unique class of polymeric materials, because they potentially combine many of the attractive features of conventional polymers with properties that result from the dynamic nature of non-covalent interactions between monomeric units. Structural parameters that determine covalent polymer properties, such as degree of polymerization (DP) and its conformation are also valid for supramolecular polymers. In addition, dynamic parameters such as lifetime of the chain which is unique to supramolecular polymers are a function of the strength and dissociation rate of the non-covalent interaction, which can be adjusted by external parameters. This dynamic nature results in materials that are able to respond to external stimuli in a way that is not possible for traditional polymers.

In general, supramolecular polymers can be classified into two classes: a) main-chain and b) side-chain (Figure 1.1a & b). Main-chain polymers are usually divided in i) linear main-chain polymers, ii) networks and iii) linear main-chain based on bidirectional units. On the other hand, there are two types of side-chain polymers: i) polymers bearing binding motifs in the side-chain and ii) polymers bearing binding motifs in the main-chain.

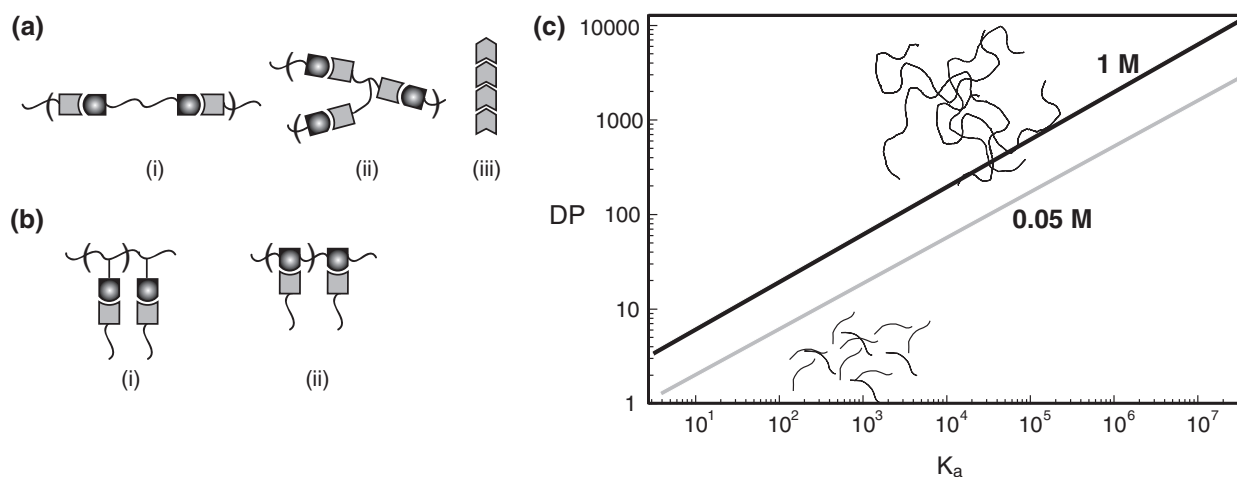


Figure 1.1 Schematic representation of two classes of supramolecular polymers: (a) main-chain supramolecular polymers and (b) side-chain supramolecular polymers; (c) theoretical relationship between the association constant K_a and DP, using a simple isodesmic association function or “multistage open association” model.

In a linear main-chain type, supramolecular polymers can either be formed by assembling bi- or multifunctional molecules (i and ii) or planar structures that have the

possibility to assemble on both sides of the plane (iii). In the latter, one structural element is responsible for the formation of the polymer and chain stoppers are more difficult to design than stoppers for subclasses i and ii. When this is the case, the DP is completely governed by the association constant and the concentration. Supramolecular polymers formed from bidirectional units are rather stiff and resemble rod-like polymers with interesting architectural properties yet they exhibit poor mechanical properties in the bulk due to a limited variation in molecular structure. Using a directional complementary couple (A-B) or a self-complementary binding motif (A-A), it is possible to form all known structures of polymers, including linear homo- and copolymers, cross-linked networks and branched structures.⁸ In contrast to when self-complementary motifs are employed, the use of complementary motifs allows for controlled introduction of different structural elements into a supramolecular architecture. Generally, the assembly of bi- or multifunctional monomers can be considered as a step-growth process, with the DP of bifunctional monomers defined by Carothers' equation.⁹ If the stepwise polymerization of bifunctional monomers is considered non-cooperative (i.e. equal association constants for each step) and the association constant for the non-covalent interaction is known, the DP can be calculated. The degree of polymerization is dependent on the concentration of the solution and the association constant and the theoretical relationship is given in Figure 1.1c.¹⁰ As can be seen, a high association constant between the repeating units is of great importance to obtain polymers with high molecular weights. In analogy with covalent condensation polymers, the chain length of supramolecular polymers can be tuned by the addition of monofunctional "chain stoppers". This also implies that a high purity of bifunctional monomers is essential, since a small fraction of monofunctional impurity will dramatically decrease DP. Therefore, as in condensation polymerization, monomer purification is extremely important to obtain high molecular weight (MW) materials.

When designing supramolecular polymers, the use of each non-covalent interaction has its own advantages as well as limitations, and the choice of which interaction to use, should be considered carefully for each application. For example, while metal-coordination is directional, the strength of the interaction often restricts its dynamic nature and consequently its reversibility. Coulombic interactions between ionic groups on the other hand suffer from the fact that these interactions are non-directional in many cases, giving rise to ill-defined aggregation. Solvophobic interactions have the same limitations and are generally weak in solvents other than water. Although (multiple) hydrogen bonds are not the strongest non-covalent interactions, they hold a prominent place in supramolecular chemistry due to their synthetic accessibility, their directionality and because they allow for the tuning of binding constants between $10\text{-}10^9\text{ M}^{-1}$ in organic solvents.¹¹

This introductory chapter will discuss the scope and limitations of multiple hydrogen bonding in polymeric materials, with an emphasis on resulting materials properties. For information on well-defined synthetic macromolecular systems the reader is referred to some recent reviews on the use of hydrogen bonds in discrete self-assembly.¹¹⁻¹⁶

1.3 Hydrogen bonding

Hydrogen bonds between neutral organic molecules play an important role in determining the three-dimensional structure of chemical and biological systems as a consequence of their specificity and directionality. The most familiar hydrogen bond motifs are the nucleobases found in DNA and RNA. Hydrogen bonding arises from a combination of electrostatic, induction, charge-transfer and dispersion forces.¹⁷ Of these effects, electrostatic interactions are generally believed to play the largest role. Hydrogen bonds connect atoms X and Y such as oxygen and nitrogen that have electronegativities larger than that of hydrogen. Generally, the XH group is called the hydrogen bond donor (D) while the Y atom is referred to as the hydrogen bond acceptor (A). Typically, the energy of a hydrogen bond in the gas phase is 10-80 kJ/mol. Although this is significantly lower than covalent bonds, it is stronger than dipolar or London dispersion force energies (< 10 kJ/mol). The thermodynamic stabilities of hydrogen bonded complexes in solution are strongly solvent dependent. Stabilities are generally high in apolar solvents without hydrogen bonding properties such as alkanes. In contrast, lower stabilities are displayed in solvents that can act as hydrogen bond acceptor or donor themselves such as dimethylsulfoxide or methanol.

The strong dependence of hydrogen bond strength on electron distribution provides an easy means of influencing the strength. A straightforward way to do so is through electron-donating and withdrawing substituents. A second approach is the combination of multiple donor and acceptor sites in one molecule. While there are two arrays possible for double hydrogen bond arrays (AA-DD and DA-AD), there are three types of triple hydrogen bonded dimers and six different quadruple hydrogen bonded motifs. Although most motifs consist of complementary molecules, there are also three self-complementary arrays (DA, AADD and ADAD). The association for these molecules is normally expressed in a dimerization constant (K_{dim}), while binding strength of complementary or heterodimeric complexes is expressed in association constants (K_a). Although the number of primary hydrogen bonds is equal for each double, triple or quadruple hydrogen bonded unit, these complexes have been found to have very different binding strengths. This observation led Jorgenson and Pranata to propose that

secondary electrostatic interactions are important determinants of complex stability.^{18,19} Early experimental studies on a series of triply hydrogen bonded complexes by Zimmerman and co-workers provided empirical support of this hypothesis.^{20,21} These effects have been quantified by Schneider and Sartorius for the prediction of multiple hydrogen bonded complexes in chloroform.²² Analysis of free energies of complexation for a large number of complexes showed a contribution of ~8 kJ/mol for each primary interaction, while each secondary interaction indicated either an increase or decrease of 2.9 kJ/mol depending on the interaction being attractive or repulsive. Although good agreement is obtained for small complexes, the validity of this hypothesis has been questioned for complexes with more than three hydrogen bonds in a linear array.^{23,24}

In the last two decades, several reports have described the synthesis of building blocks capable of forming very robust complexes and their association constants have been determined. An illustrative set of complexes is shown in (Figure 1.2). Similar to Nature, the majority of molecules capable of forming multiple hydrogen bonding, including those in Figure 1.2, are heterocycles. In search of a suitable receptor for barbiturate **1**, Hamilton and co-workers developed one of the first strongly associating complexes based on multiple hydrogen bonding.²⁵ Host **2** shows an inwardly facing cleft capable of making a two triple hydrogen bond arrays with a complementary barbiturate and an association constant of $2.1 \times 10^4 \text{ M}^{-1}$ in chloroform. Almost one decade later, in studies aimed at extending hydrogen bonding arrays from three to four linear sites, our group developed the ureido-*s*-triazine (UTr) dimer **3 – 3** which has a dimerization constant (K_{dim}) of $2.0 \times 10^4 \text{ M}^{-1}$ in chloroform.²⁶ As can be seen in the structure, an intramolecular hydrogen bond stabilizes the urea group in the desired conformation. The importance of this interaction becomes clear when the urea is replaced by an amide resulting in a decrease of K_{dim} of nearly two orders of magnitude to 530 M^{-1} in chloroform. Two structurally similar self-complementary molecules **4** and **5** were developed by our group²⁷⁻²⁹ and Zimmerman and co-workers,^{30,31} respectively. The ureido-pyrimidinone (UPy) **4** was synthesized very easily in one step from commercially available isocytosines. Crystal structure determination verified the design, as it shows dimers of **4**, which are held together by quadruply hydrogen bonding *via* a DDAA array.²⁸ Accurate measurements using a fluorescently-tagged UPy derivative determined K_{dim} values of $6 \times 10^7 \text{ M}^{-1}$ and $6 \times 10^8 \text{ M}^{-1}$ in chloroform and toluene, respectively.²⁹ Corbin *et al.* had pointed out previously that prototropy (i.e. tautomerism involving proton shifts) can be detrimental to hydrogen-bonded complex formation.³⁰ Therefore, **5** was designed to display self-complementary quadruple hydrogen bonding arrays irrespective of its tautomeric form. Fluorescence studies analogous to those

reported by Söntjens *et al.* indicated a lower limit of $K_{\text{dim}} = 5 \times 10^8 \text{ M}^{-1}$ in chloroform.³¹ Although the previous three dimers form self-complementary arrays, the possibility of complementary quadruple hydrogen bond arrays remained largely unexplored until 5 years ago. An early example was reported by Corbin and Zimmerman, who reported the strong selectivity of 2,7-diamido-1,8-naphthyridines **6** for **5**.³⁰ Using DMSO as a competing cosolvent they determined a K_a value of 3300 M^{-1} for dimer **5** – **6** in 5% DMSO- d_6 /CDCl₃. The importance of the intramolecular hydrogen bond present in **5** is evident when **5** is replaced by N,N'-di-2-pyridylurea **7**. These derivatives are known to form inter- and intramolecular hydrogen bonds in solution,³² therefore increasing the energy barrier for formation of heterocomplexes **6** – **7** resulting in K_a values of $2 \times 10^3 \text{ M}^{-1}$ in chloroform.^{33,34} Non-heterocyclic compounds **8** and **9** were reported by Gong and co-workers to associate via amide-donor-acceptor interactions which are reminiscent of those responsible, in part, for the ordered secondary structures of oligopeptides and proteins.^{35,36} Isothermal microcalorimetry was applied to determine an extre-

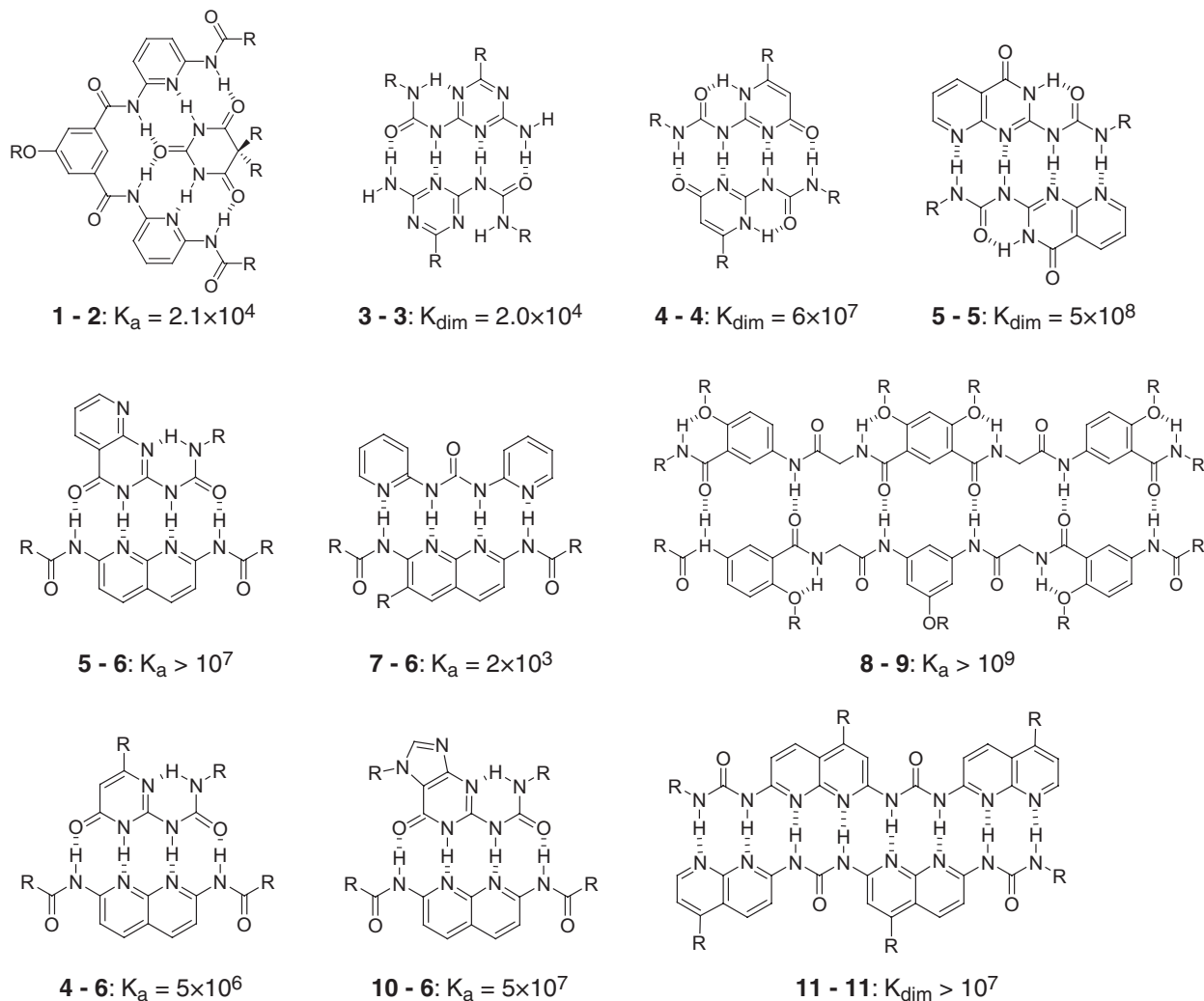


Figure 1.2 Selected multiple hydrogen bonded complexes with high association constants. Association and dimerization constants for chloroform solutions are given in M^{-1} .

mely high association constant of 10^9 M^{-1} in chloroform. This strategy of using multiple amide groups not only eliminates repulsive secondary interactions but its modular approach enables the synthesis of a variety of complementary as well as self-complementary multiple hydrogen bonding units.³⁷ More recently, the groups of Li, Zimmerman and our group have studied the association behavior of naphthyridine derivatives **6** with complementary tautomeric forms of compounds **4** and **10**.³⁸⁻⁴¹ Heterodimer **4** – **6** was shown to exhibit concentration dependent selectivity with an association constant of $5 \times 10^6 \text{ M}^{-1}$ in chloroform.³⁹ A stronger dimerization of $5 \times 10^7 \text{ M}^{-1}$ in chloroform was determined for ureido-guanosine **10** with **6** by fluorescence resonance energy transfer experiments.⁴¹ An example of a modular approach in extending linear multiple hydrogen bonding arrays to 8 hydrogen bonds in dimer **11** – **11** was shown recently by Zimmerman and co-workers.⁴² NMR dilution experiments in 10% DMSO-*d*₆/CDCl₃ were performed to assess the stability of the dimer indicating a K_a value larger than $5 \times 10^5 \text{ M}^{-1}$.

It is important to note that the hydrogen bonding modules described above are illustrative examples of the types of building blocks that have the potential to be useful in the construction of supramolecular materials. Although there is ample opportunity for developing new multiple hydrogen bonding units, the most important feature for application in supramolecular (co)polymers is the ease of synthesis since molecules **1** – **11**, with the single exception of **4**, require multi-step syntheses.

1.4 Supramolecular polymers

1.4.1 Small building blocks

Application of units as associating end-groups in bifunctional or multifunctional molecules results in the formation of supramolecular polymers with varying degrees of polymerization. The early examples of hydrogen bonded supramolecular polymers rely on units, which associate using single, double or triple hydrogen bonds that all have association constants below 10^3 M^{-1} in chloroform. In isotropic solution, the DP of these polymers is expected to be low (see Figure 1.1c). However, in the liquid crystalline state stabilization occurs by excluded volume interactions, and the resulting DP is much higher. In the first part of this section, examples of linear supramolecular polymers based on weak hydrogen bonding interactions assisted by liquid crystallinity or phase separation is discussed, followed by a more thorough discussion of supramolecular polymers based on strong hydrogen bonding and other non-covalent interactions that persist in the isotropic state (melt or solution) in the second part.

1.4.1.1 Supramolecular polymers based on liquid-crystalline monomers

The use of directional hydrogen bonds to construct low-molecular weight complexes was initially investigated to explain the mesomorphic behavior of carboxylic acids. The first examples of assembly of mesogens based on benzoic acids and pyridines were reported by Kato and Fréchet and Lehn and co-workers.^{43,44} Although the separate components of these assemblies display a narrow liquid crystalline (LC) regime or no liquid crystallinity at all, the complexes exhibit thermally stable nematic and smectic (layered) liquid crystalline phases. Shortly thereafter, multisite (≥ 2) mesogens were studied that are considered to be the precursors to main-chain supramolecular polymers.⁴⁵⁻⁴⁷ The group of Lehn is recognized to be the first to develop a supramolecular main-chain polymer based on a ditopic molecule equipped with multiple hydrogen bonding units. These supramolecular polymers are held together by triple hydrogen bonding between diamidopyridines and uracil derivatives (Figure 1.3a), with an association constant in the order of 10^3 M^{-1} .^{48,49} A 1:1 mixture of the ditopic molecules resulted in aggregates (**12**) that exhibit liquid crystallinity over a broad temperature window, whereas the pure compounds are solids melting in an isotropic liquid without displaying a liquid crystalline phase. Due to the chirality of the tartaric acid spacer used, the fibers observed by electron microscopy showed biased helicity.⁵⁰ The scope of supramolecular polymers was soon expanded by the development of rigid rod polymers (**13**) based on the same triple hydrogen bonding motif.⁵¹ In these polymers, a rigid 9,10-dialkoxanthracene core connects the hydrogen bonded groups via a phthalimide group. Due to the increased molecular rigidity, the system is not thermotropic liquid crystalline, but displays a lyotropic liquid crystalline phase that is birefringent. In addition, solutions of these polymers in apolar solvents are highly viscous. Also, by using multifunctional low molecular weight building blocks, Griffin was able to obtain materials that exhibit polymer-like properties.⁵² Hydrogen bonding between pyridine units in a tetrafunctional compound and benzoic acid units in bifunctional compounds (Figure 1.3b) resulted in the formation of thermoreversible networks (**14**). These materials exhibit properties typical of low MW compounds at high T and of polymers at low T. DSC studies on these networks revealed a memory effect, resulting in a consistent decrease of crystallinity as the time the material experiences in the isotropic state increases.⁵³

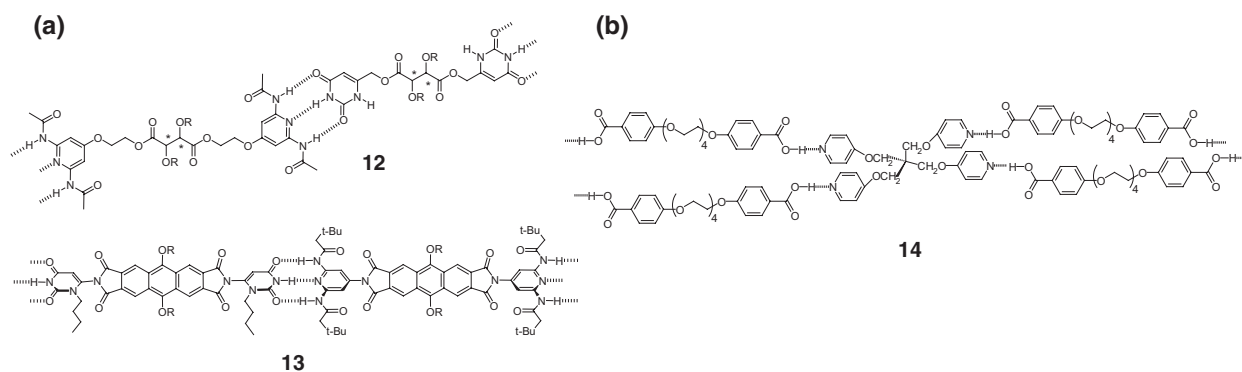


Figure 1.3 Liquid crystalline supramolecular polymers; (a) based on triple hydrogen bonding from ditopic chiral monomers (**12**) and from rigid monomers (**13**); (b) based on single hydrogen bonding between multivalent molecules (**14**).

1.4.1.2 Supramolecular polymers in isotropic solution

Although chain extension based on single hydrogen bonding can be observed, supramolecular polymers based on non-covalent interactions with $K_a < 10^3 \text{ M}^{-1}$ are not sufficiently stable to display high DPs in solution and in most aspects these aggregates resemble small molecules more than polymer chains in solution. Only the triple hydrogen bonded supramolecular polymers based on bifunctional molecules reported by Lehn and multifunctional molecules, such as those reported by Griffin,⁵² displayed some typical polymer properties, like the ability to draw fibers from the melt.

Up to a decade ago, the number of supramolecular polymers based on very strong non-covalent interactions was relatively small. This was mainly due to the synthetic inaccessibility of most of the monomers. Intriguing architectures such as nanotubes⁵⁴ and nanorods^{55,56} are obtained when bifunctional compounds with multiple arrays of hydrogen bonding sites are used. Ghadiri has studied nanotubes which self-assemble from bidirectional cyclic peptides, composed of an even number of alternating D- and L-amino acids.⁵⁷ These nanotubes were found to be very robust and turned out to be stable to a wide range of pH and solvents as well as to physical stress.⁵⁸ Independently, the groups of Reinhoudt⁵⁵ and of Whitesides⁵⁶ have reported the formation of supramolecular “nanorods” based on assembly of multiple cyanuric acid – melamine motifs. The nature of these and similar aggregates has been investigated by NMR spectroscopy, gel permeation chromatography (GPC) and transmission electron microscopy (TEM). Furthermore, similar aggregates display remarkably high thermodynamic as well as kinetic stabilities.^{59,60} Other examples of this subclass of supramolecular main-chain polymers which are based on bidirectional monomers include the polymers based on bisurea

motifs developed by Bouteiller and co-workers. These compounds form rigid linear chains in various apolar organic solvents by the cooperative formation of four hydrogen bonds per monomer as was found by IR spectroscopy, small angle neutron scattering (SANS), static light scattering and viscometry.⁶¹⁻⁶⁴ More recently, Lehn and co-workers reported the assembly of a bow-shaped molecule into highly ordered sheet-type aggregates via quadruple hydrogen bonds.⁶⁵ Although this subclass of supramolecular polymers exhibits many interesting features, they will not be treated further in this chapter.

An important development in the preparation of supramolecular polymers in isotropic solution has been the development of the ureidopyrimidinone (UPy) functionality (**4**), a synthetically accessible quadruple hydrogen bonding unit with a very high association constant.^{27,29} The UPy unit can be made in a one-step procedure from commercially available isocytosines and isocyanates²⁸ or amines.⁶⁶ Bifunctional monomers (**15**) form long polymer chains in solution as well as in the bulk (Figure 1.4a).²⁷ The viscosities of chloroform solutions of **15** are high and exhibit a concentration dependence that can be attributed to changes in DP. The average DP for highly purified **15** at 40 mM was estimated to be 700 which is consistent with the very high dimerization constant and indicates that no uncontrolled multidirectional gelation occurs. The presence of monofunctional impurities was shown to lead to a dramatic decrease in DP since they act as chain stoppers and hence limit growth. This was shown by the deliberate addition of monofunctional UPy to a solution of bifunctional UPy monomers (Figure 1.4b) and by photogeneration of a monofunctional UPy in a solution of **15**.⁶⁷

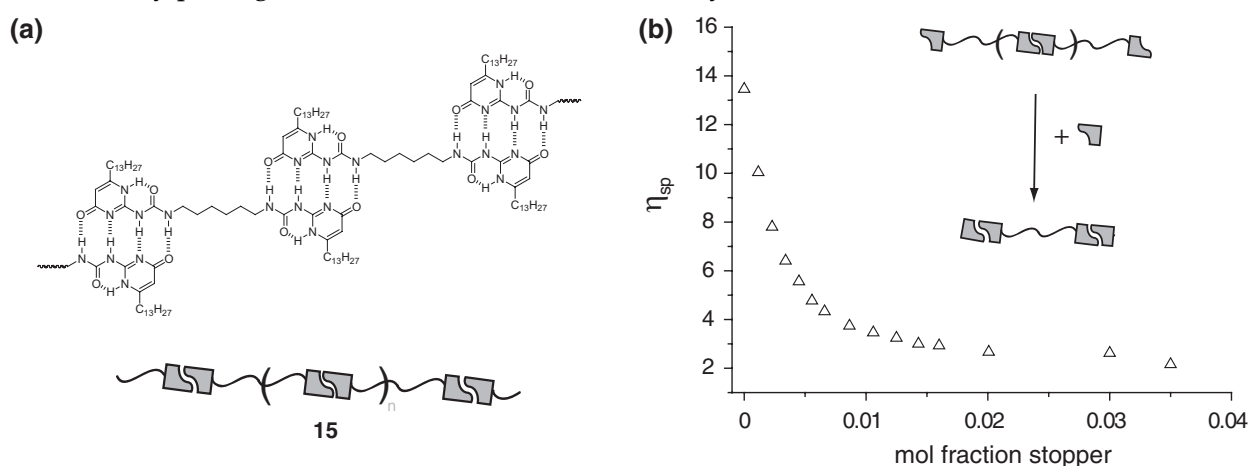


Figure 1.4 (a) Supramolecular polymer of bifunctional UPy monomer **15**; (b) the effect of a UPy chain stopper on a supramolecular main-chain polymer based on bifunctional UPy monomers.

Although supramolecular polymers based on small bifunctional UPy monomers in many ways behave like conventional polymers, the strong temperature dependence of their

mechanical properties really sets them apart from traditional polymers. At room temperature, the supramolecular polymers show polymer-like viscoelastic behavior in bulk and solution, whereas at elevated temperatures liquid-like properties are observed. Noncrystallizing UPy derivative **16** was studied using dynamic mechanical thermal analysis (DMTA), rheology and dielectric relaxation spectroscopy in order to obtain information about the bulk viscoelastic properties.⁶⁸ One of the salient features of this material, with high relevance for applications, is the extremely high activation energy for viscous flow of 105 kJ·mol⁻¹ (Figure 1.5), determined with the Andrade-Eyring equation. This results in a strongly temperature dependent melt viscosity, which increases processability of these materials at temperatures just above the melting point or T_g . The high activation energy can be attributed to the contribution of three mechanisms to stress relaxation in sheared melts of supramolecular polymers: i) one is a mechanism that is shared with covalent polymers, i.e. escape from entanglements by reptation;⁶⁹ ii) supramolecular polymers have enhanced relaxation at higher temperatures because the chains become shorter and iii) the supramolecular polymers can lose strain by breaking, followed by recombination of free chain ends without strain.⁷⁰ Breaking rates increase with temperature and therefore contribute to the temperature dependent behavior of supramolecular polymers.

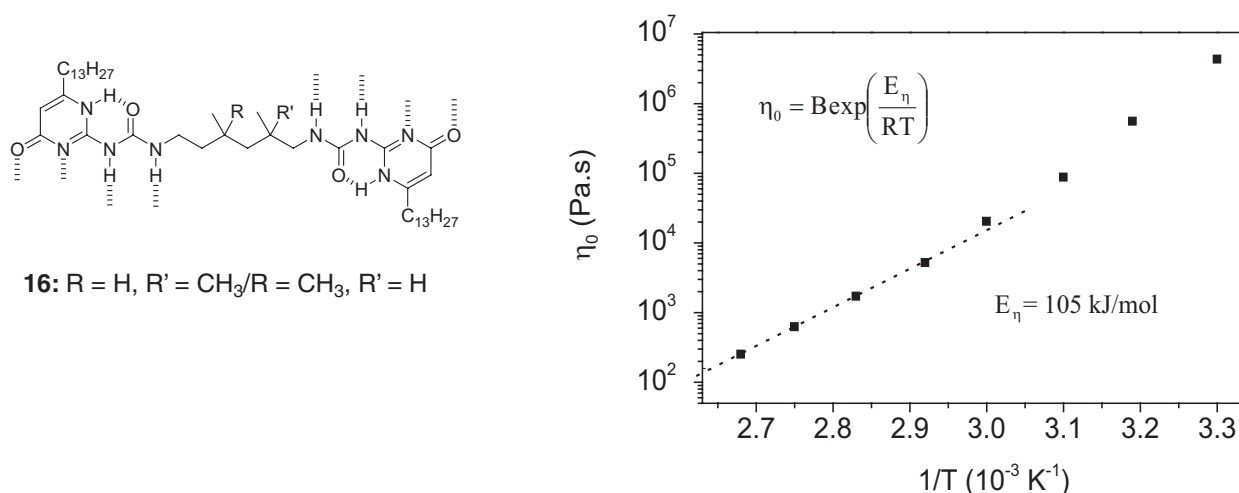


Figure 1.5 Zero shear viscosity of **16** vs. reciprocal temperature; the apparent activation energy is determined according to the Andrade-Eyring equation (dotted line).

In addition to the work on UPy derivatives, our group also reported studies of bifunctional ureido-s-triazine²⁶ (UTr) derivatives (**17** – **20**) (Figure 1.6a).^{71,72} Polymeric aggregates of these derivatives provided with either achiral (**17**) or chiral (**18**) alkyl side chains are able to self-assemble into columnar structures in dodecane via dimerization and solvophobic stacking of the disc-like dimer as evidenced by small-angle neutron scattering (SANS).⁷¹ Solutions of **17** in dodecane are highly viscous and show pronounced shear thinning.

Furthermore, lateral interactions between the columns cause lyotropic mesophases to form at high concentrations. The combined non-covalent interactions are sufficiently strong to induce formation of columns in water by derivatives **19** and **20** equipped with achiral and chiral penta(ethyleneoxide) side chains, respectively.⁷² Figure 1.6b shows a schematic representation of the assembly processes. The monomers dimerize into polymeric aggregates in chloroform and are able to organize into columnar disks in dodecane or water. Circular dichroism studies revealed a helical bias in columns formed from monomers **18** and **20**. Moreover, it was shown that introduction of a chiral monofunctional UTr derivative leads to the formation of smaller helices with biased helicity through cooperative interactions.

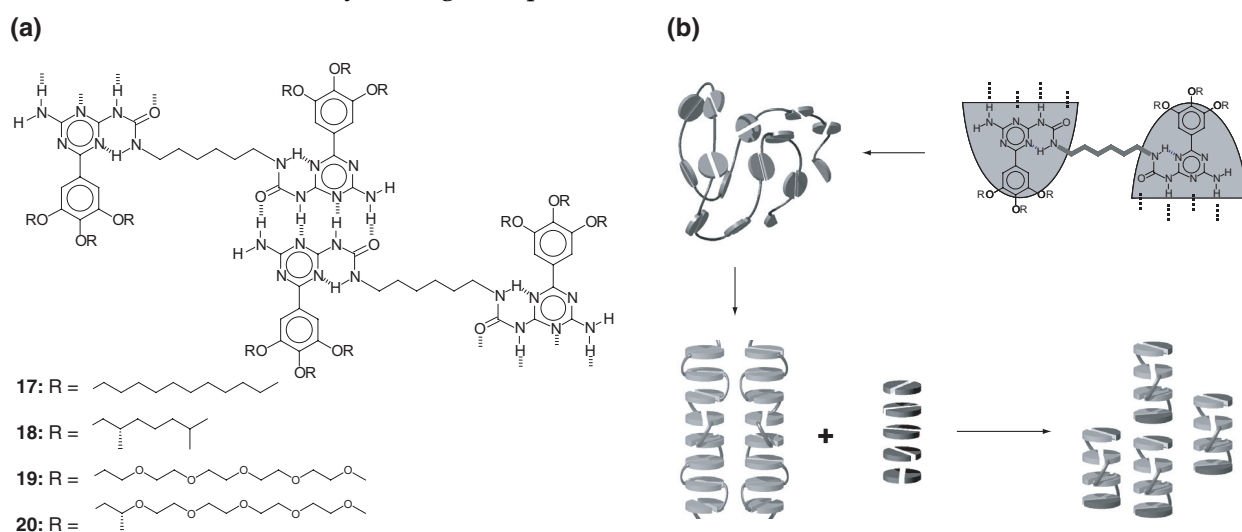


Figure 1.6 (a) Supramolecular polymer of bifunctional UTr derivatives **17** – **20**; (b) schematic representation of the formation of columnar aggregates.

Another example which used strong self-complementary binding units was reported by Rebek Jr. and co-workers. They described the assembly of ditopic calixarene units functionalized with urea groups on the upper rim (**21**) into polymeric capsules (also termed “polycaps”) by hydrogen bonding in cooperation with complexation of a solvent molecule or a small guest (**G**) (Figure 1.7).⁷³ Solutions of these molecules in *o*-dichlorobenzene exhibit a strongly concentration-dependent viscosity.⁷⁴ The physical integrity of the polycaps under shear was demonstrated by the observation of strong normal forces in rheometry experiments. Additionally, the polycaps can be drawn into fibers with high tensile strengths (10^8 Pa). Networks from tetrafunctional molecules in solution display a stronger elastic component in their rheological behavior, and have complicated time-dependent properties, such as shear thickening. Furthermore, it was shown that concentrated polycap solutions in chloroform display liquid crystallinity and shear can be used to orient the liquid crystal formulations.⁷⁵

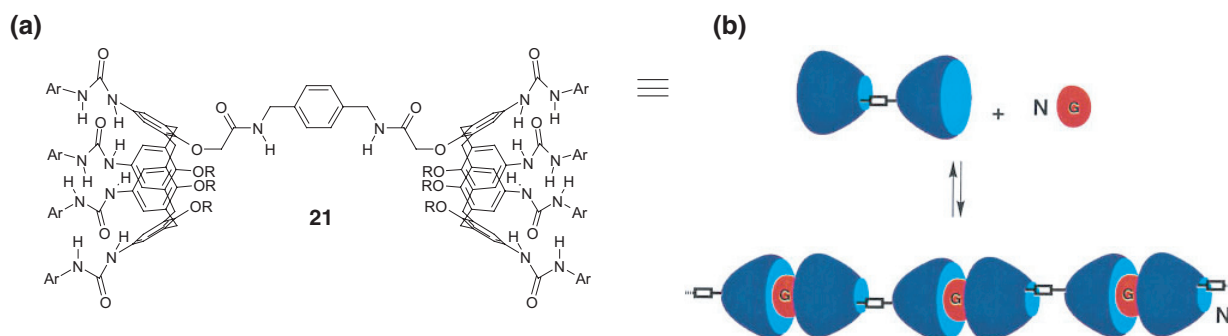


Figure 1.7 (a) Ditopic calixarene (**21**) and (b) a schematic representation of polycap formation of **21** with guest molecules (**G**).

Although the aforementioned polymers were prepared by assembly of monomers equipped with self-complementary hydrogen bonding motifs, supramolecular polymers have also been prepared in isotropic solution with complementary motifs A and B. In this way, directionality can be introduced into the supramolecular polymer chain. One of the first examples employing strong complementary hydrogen bonding was reported by Rebek and co-workers who studied the assembly of bi- and trifunctional polycaps based on the heterodimerization of calixarenes equipped with arylurea and sulfonylurea.⁷⁶ The resulting structures were analyzed by ¹H NMR and GPC techniques. Inspired by work on multiple hydrogen bond motifs by Hamilton, the group of Lehn reported supramolecular polymers based on the six-fold hydrogen bonding between a 2,6-bis(diamidopyridine)-phenol (**2**) and a double-faced cyanuric acid type wedge (**22**) in apolar and chlorinated solvents (Figure 1.8a). ¹H NMR spectroscopy, viscometry and electron microscopy (EM) revealed the formation of polymeric aggregates in tetrachloroethane (TCE) and fibers were observed in micrographs of samples of various mixtures. Moreover, a marked influence of stoichiometry, as well as end-capping and cross-linking upon fiber formation is revealed in solution and by EM. While stoi-

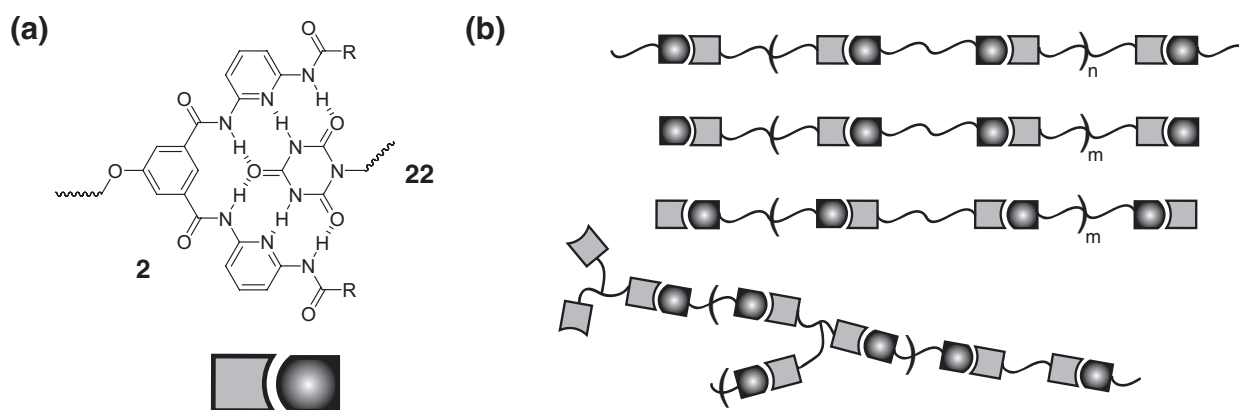


Figure 1.8. Supramolecular polymerization of heterocomplementary binding units; (a) heterocomplex **2** – **22**; (b) schematic representation of prepared structures with mono-, bi- and trifunctional building blocks ($m < n$).

chiometric imbalance and the addition of monofunctional molecules lead to a decrease in DP, the introduction of trifunctional molecules lead to a cross-linked network (Figure 1.8b).

A last example based on the assembly of bifunctional low MW monomers equipped with complementary hydrogen bonding motifs are the polymers of Craig and co-workers, which assemble by complementary base pairing within oligonucleotides (Figure 1.9).^{77,78} Among several studies of the assembly of various oligonucleotides, polymerization of A-B type monomer **23** (X = no spacer) was substantiated with UV/Vis melting studies. Static and dynamic light scattering (SLS and DLS) and size exclusion chromatography (SEC) were used to probe the size, structure and dynamics of the system and demonstrated that polymers based on **23** resemble rodlike double-stranded DNA. Specifically, viscometry measurements on **23** are in very good agreement with theoretical predictions by Cates since a slope of 3.7 is found for the semidilute regime in a double logarithmic plot of specific viscosity vs. concentration. Remarkably, incorporation of short spacers for X within the monomer results in an increased probability for cyclization and increased time scales of equilibration. This is in contrast to other systems where an increase in spacer length ($X = -(\text{CH}_2)_3-$ or $-((\text{CH}_2)_2\text{O})_6-$) results in a decreased tendency to form cyclic aggregates.

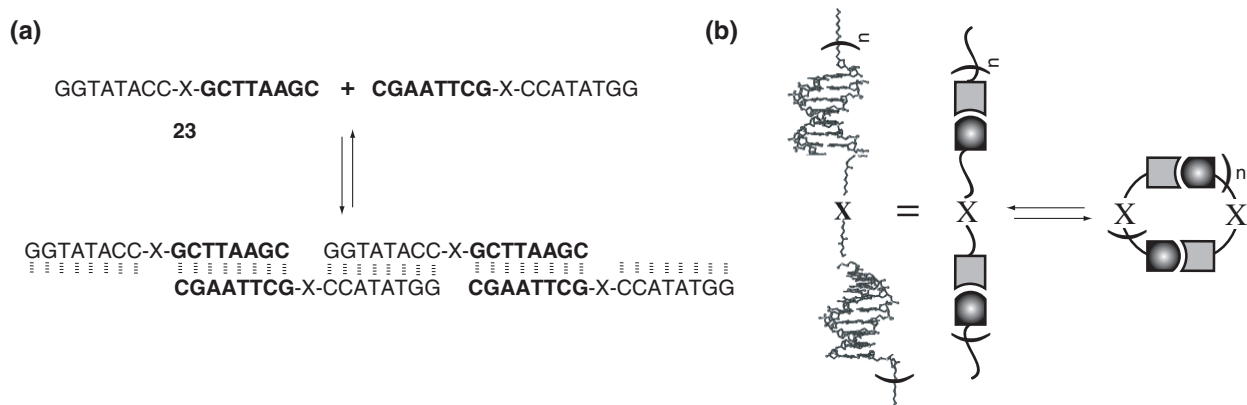


Figure 1.9 Supramolecular polymerization of complementary oligonucleotides; (a) self-assembly of oligonucleotide **23** (X = no spacer); (b) schematic representation of the dynamic equilibrium in nucleotide based polymers.

1.4.2 Large building blocks

Although the supramolecular polymers based on small building blocks possess intriguing new properties, the need for large amounts of material for e.g. melt-rheological experiments and tensile testing in combination with synthetic barriers do not allow extensive study of the mechanical properties of these materials. Furthermore, low MW monomers have an increased tendency to form small discrete assemblies through cyclization.^{11,79} Therefore, in

order to obtain supramolecular polymers with tunable and macroscopic material properties, the supramolecular functionalities need to be separated by polymeric spacers (or appended to polymer chains). In this way, macromonomers can be elongated or functionalized by reversible interactions. This section will focus on supramolecular polymers based on polymeric monomers that are equipped with multiple hydrogen bonding motifs and their materials properties in solution as well as in the bulk.

1.4.2.1 Main-chain supramolecular polymers

The physical properties of linear polymers and organic molecules are expected to be strongly modified when they are provided with associating end groups due to the reversible nature of non-covalent interactions. One of the first to acknowledge this were Lenz and co-workers who proposed that the liquid-crystalline behavior and the ability to form elastomeric films of polymeric glycols terminated with diacids could be explained by dimerization of the carboxylic end-groups.⁸⁰ Lillya et al. also have demonstrated that dimerization of the carboxylic acid moieties in benzoic acid telechelic polytetrahydrofuran (poly-THF) results in a significant improvement in material properties due to the formation of large crystalline domains of the hydrogen bonded units.⁸¹ A smaller improvement in material properties was observed when polydimethylsiloxanes (PDMS) were provided with benzoic acid groups.⁸² Based on detailed FT-IR and NMR spectroscopy and viscometry studies, a quantitative model for the chain length and weight distribution of the functionalized PDMS in solution was described by Bouteiller and co-workers.⁸³⁻⁸⁵

Utilizing a post-polymerization modification route, the groups of Rowan and Long applied nucleobases as recognition motifs to functionalize low MW poly-THF ($M_n = 1.4$ kg/mol) and polystyrene (PS) ($M_n = 2.6$ kg/mol).⁸⁶⁻⁸⁸ ^1H NMR-analysis confirmed the formation of assemblies in a 1:1 mixture of adenine-PS and thymine-PS and thermoreversibility was substantiated in toluene-*d*₈. In addition, attachment of a nucleobase derivative at the chain ends of bisamino telechelic poly-THF (Figure 1.10a) results in a profound change in the properties of the material with an increase of over 100 °C in the T_m . While amine-terminated poly-THF is a soft waxy solid, both adenine- and cytosine-derived telechelic polymers **24** and **25** self-assemble in the bulk to yield materials with enough mechanical stability to be melt processed (Figure 1.10b & c). Both materials show extreme temperature sensitivity, resulting in the formation of very low viscosity melts. A combination of FT-IR, wide-angle x-ray scattering (WAXS) and rheological experiments demonstrated that the combination of phase segregation

between the hard nucleobase components and the soft poly-THF core combined with aromatic amide hydrogen bonding is responsible for the highly thermosensitivity of the materials. Interestingly, thymine functionalized material **26** did not exhibit such properties which was attributed to its high crystallization temperature.

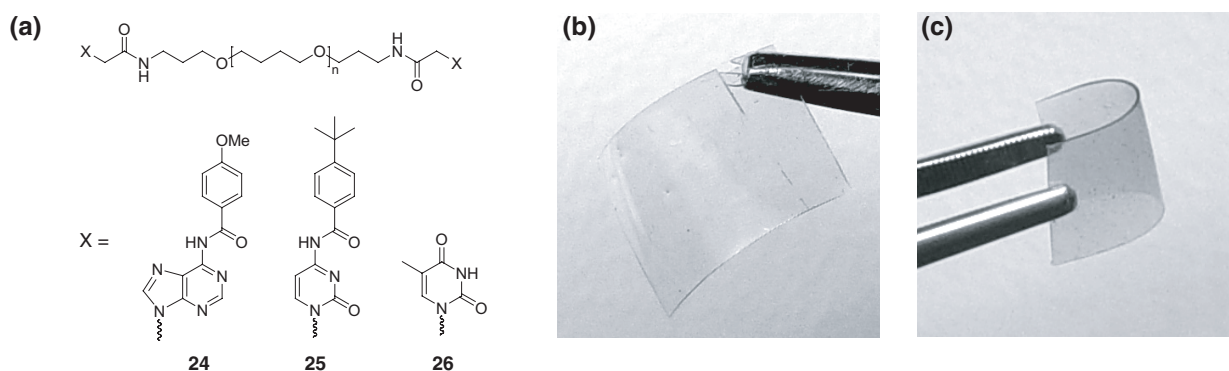


Figure 1.10. (a) bifunctional macromonomers with nucleobase derivatives and pictures of films formed from (b) **24** and (c) **25**.

Although the strength of association between units with such weak non-covalent interactions is low, it was demonstrated that chain extension is a versatile tool to gain a significant improvement in material properties. A modest degree of polymerization in combination with physical inter-chain interactions by means of domain formation results in high MW assemblies with improved material properties. Without domain formation, however, it is generally believed that high association constants are required in order to obtain high MW polymers.

The quadruple hydrogen bond unit developed by our group has been further employed in the chain extension of telechelic PDMS,⁸⁹ poly(ethylene/butylenes) (PEB),^{90,91} polyethers,^{90,92,93} polycarbonates⁹⁰ and polyesters^{90,94,95} (Figure 1.11a). Solution viscosity studies and bulk rheological measurements with UPy-telechelic oligo-dimethylsilane **27a** indicated the formation of high MW PDMS. Likewise, UPy-telechelic PDMS **27b** exhibited viscoelastic bulk properties that differed from a non-hydrogen bonding PDMS of similar MW. As was demonstrated previously, the purity of the supramolecular materials is extremely important. Therefore, UPy-synthon **28** containing a highly reactive isocyanate functionality was designed which is synthetically accessible on large scale by reaction of commercially available isocytosines in neat diisocyanates. Reaction of synthon **28** with amino or hydroxy-telechelic polymers subsequently allows for an easy work-up procedure to obtain UPy-telechelics **29a - e** (Figure 1.11b). For example, reaction of hydroxyl-telechelic PEB ($M_n = 3.5$ kg/mol, degree of functionalization: $F_n = 1.93$) with synthon **28a** on large scale led to supramolecular polymer **29a** with < 0.2 % residual OH groups.⁹¹ The mechanical properties of the polymer are dramatically

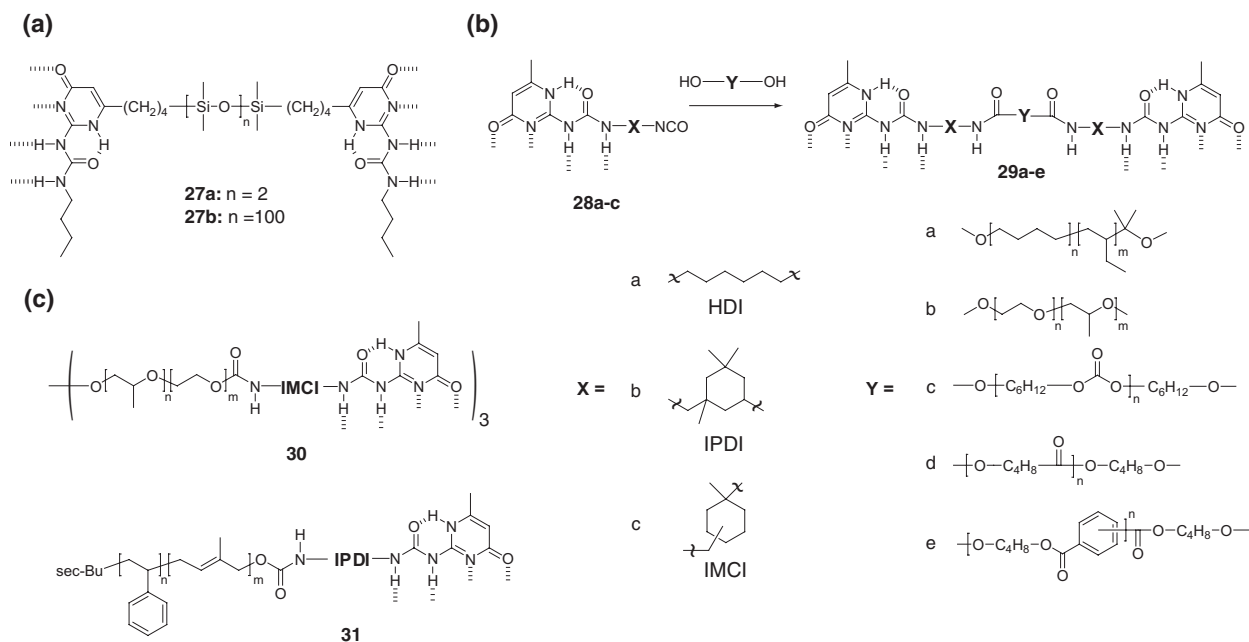


Figure 1.11. Examples of UPy-telechelic polymers (a) UPy-telechelic PDMS **27**; (b) synthesis of various UPy-telechelic supramolecular polymers **29a - e** with UPy-synthons **28a - c** and amine or hydroxy-telechelic polymers; (c) trifunctionalized star copolymer of poly(ethyleneoxide/propyleneoxide) **30** and monofunctional UPy poly(isoprene)-block-polystyrene **31**. Note: HDI, IPDI and IMCI are abbreviations of the commercially available starting diisocyanates.

different from those of the starting material. Whereas the starting material is a viscous liquid, **29a** is a rubber-like material with a Young's modulus of 5 MPa (Figure 1.12a and b). Similarly, functionalization of more polar hydroxyl-telechelic polymers with synthon **28a** resulted in improved materials properties. Functionalized polyether **29b** displays a rubber plateau in DMTA measurements and a storage modulus of 10 MPa, while the starting material is a viscous liquid. The properties of functionalized polycarbonate **29c** and polyester **29d** and **29e** are those of semicrystalline polymers, whereas the starting materials are brittle solids (Figure 1.12c and d). Especially interesting was polyester material **29d** since it could easily be processed by different techniques into several scaffolds varying from films and fibres to meshes and grids.⁹⁴ An additional noticeable feature in these polymers is the high activation energy for viscous flow as compared to their unfunctionalized counterparts (e.g. 105 kJ/mol for **29a**). From trifunctional UPy poly(ethyleneoxide/propyleneoxide) copolymer **30** supramolecular networks have also been assembled. Solution viscometry measurements, including chain stopper studies, indicated formation of a reversible network. In addition, due to the formation of reversible cross-links, a higher plateau modulus was observed in dynamic mechanical analysis. Monofunctional UPy-telechelics **31** were synthesized via living anionic polymerization and end-group modification of PS-*block*-PI of variable length with UPy synthon **28b**.

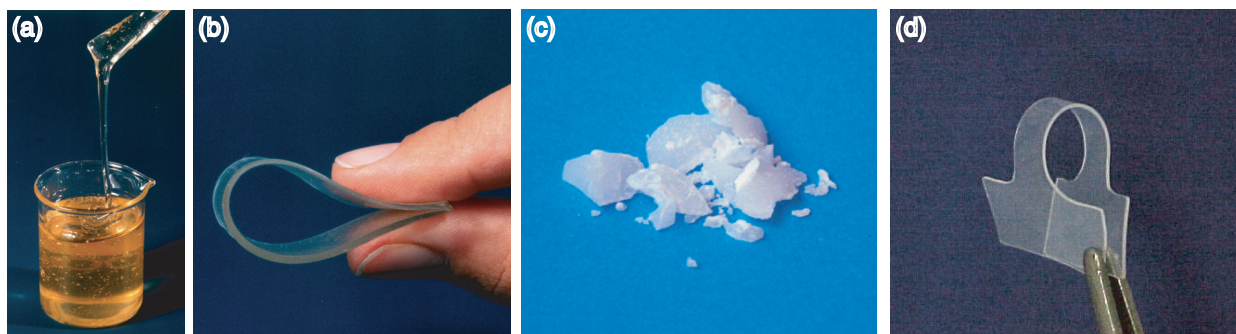


Figure 1.12. (a) Hydroxy-telechelic PEB ($M_n = 3.5$ kg/mol); (b) UPy-telechelic PEB; (c) hydroxy-telechelic PCL ($M_n = 2.0$ kg/mol); (d) UPy-telechelic PCL.

In summary, the material properties of UPy-telechelic polymers were shown to improve dramatically upon functionalization and materials were obtained that combine many of the mechanical properties of conventional macromolecules with the low melt viscosity of oligomeric compounds. An important aspect which sets these materials apart from the previously mentioned low MW supramolecular polymers is that the viscoelastic properties of UPy-telechelic polymers can be attributed to the entanglement of high MW hydrogen bonded polymer chains as opposed to physical cross-links by aggregation of the recognition groups into microcrystalline domains.

A very elegant supramolecular polymer based on UPy dimerization was recently reported by Guan and co-workers.⁹⁶ Inspired by titin, a giant protein of muscle sarcomere that has $> 10^2$ repeating modules and displays high strength, toughness and elasticity, they synthesized a poly-THF containing UPy functionalities in the main-chain (Figure 1.13a). Analo-

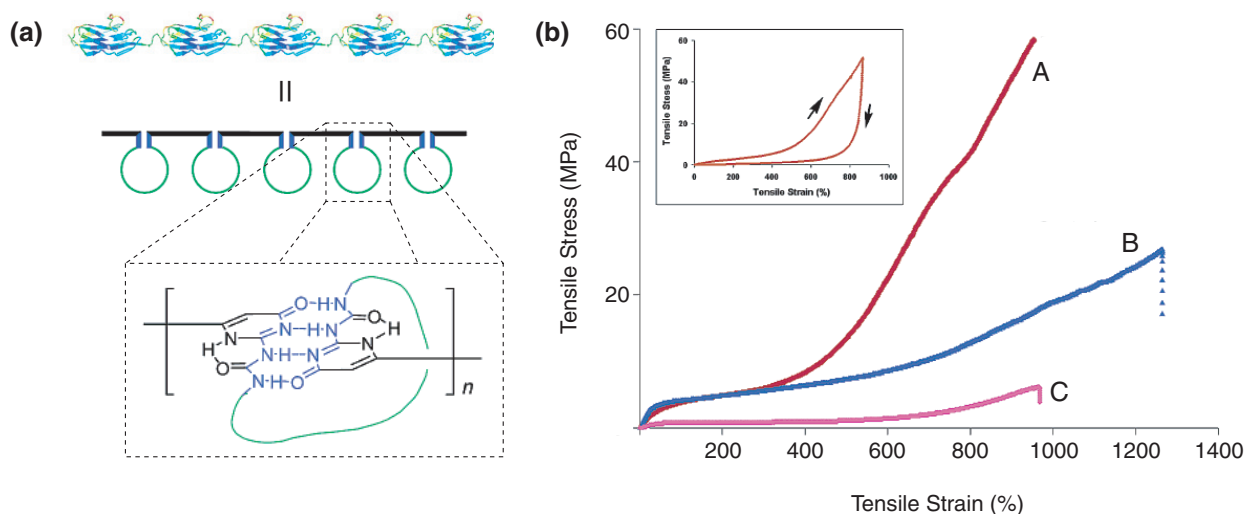


Figure 1.13 Biomimetic UPy polymer inspired by titin protein; (a) concept of design; (b) stress-strain curves for the UPy-based polymer (A), control polymer (B) and a high MW polyurethane (C, $M_n = 10^3$ kg/mol); a stretching – retraction cycle for A is shown in the inset.

gous to biopolymers, single-molecule nanomechanical properties were studied with atomic force microscopy (AFM) and demonstrated the sequential breaking of UPy dimers. Stress-strain profiles obtained from mechanical analysis of solution-cast films of the UPy-based polymer, revealed that the polymer was very elastic, as evidenced by the high strain up to 900% and complete recovery to its original length (Figure 1.13b). Moreover, the observed hysteresis (see inset) demonstrates the great energy dissipation capability of the system which is an important feature for high toughness.

1.4.2.2 Supramolecular block copolymers

As a rule, most polymer blends are immiscible, which results in macrophase separation. The formation of such a macrophase morphology generally results in poor mechanical properties. In block copolymers, however, two or more polymer blocks are linked by means of a strong chemical interaction. The competition between the strong chemical connection and repulsion between different polymer blocks leads to a wealth of interesting microphase structures (typical length scale is about 5 - 50 nm, depending on the individual length of the blocks).⁹⁷ Although non-covalent interactions like hydrogen bonding play a very important role in the phase-segregation in many block-copolymer systems such as polyamides, only copolymers based on multiple hydrogen bonding arrays between two end-functionalized blocks will be discussed in this section.

Recent developments in the field of supramolecular chemistry have shown that complementary as well as self-complementary building blocks can lead to large, well-defined structures through self-assembly. Advantages of assembling multi-block copolymers through strong reversible non-covalent interactions include a modular approach in synthesis, ease of processing, self-healing properties, facile and selective removal of sacrificial blocks, and an extra level of hierarchical control in self-organization of functional materials.⁹⁸⁻¹⁰¹ It has been known that multiple weak hydrogen bonds between two chemically different polymer blocks can result in a homogeneous polymer blend while when these interactions are absent the polymers would be immiscible (see examples in the next section on side-chain supramolecular polymers). However, examples using strong non-covalent interactions are scarce. It is generally believed that strong recognition motifs affixed to the polymers will be essential in overcoming the phase separation force and induce the formation of small regular domains. When the non-covalent interaction between two monomers is self-complementary, the block-size is not fixed, and depending on the conditions the structure may vary from a random copolymer through a microstructure to a macrophase separated blend. Using strong, self-complementary ureido-s-

triazine units (**3**) in a supramolecular main-chain rod-coil block-copolymer, Hirschberg *et al.* demonstrated that the presence of kinetically stable microphases in the bulk that double in size upon annealing.¹⁰² Therefore, the use of complementary binding motifs is a prerequisite for thermodynamically stable microphase-separated structures. Mixtures of poly(etherketones) (PEK) and poly(isobutylenes) (PIB) functionalized on the termini with multiple hydrogen bonding arrays were systematically investigated by Binder and co-workers (Figure 1.14a).¹⁰³⁻¹⁰⁵ They reported that high strength of the hydrogen bonding motifs is essential in preventing macrophase separation in the solid state. High association constants ($K_a = 10^3 - 10^5 \text{ M}^{-1}$, Figure 1.14b) lead to the formation of regular arrays of alternating polymers, whereas low K_a values lead to immiscibility of the individual polymers in the bulk.¹⁰⁶ Both small angle x-ray scattering (SAXS) and transmission electron microscopy (TEM) demonstrated the presence of 14 nm sized PIB and PEK microphases in 1:1 mixtures of **32** and **33**. As expected from the molecular design, sheetlike structures consisting of alternating layers of PEK and PIB were observed (Figure 1.14c & d). Moreover, clear films of these materials can be obtained indicating that macrophase separation is prevented. Furthermore, the reversibility of the binding process induced by temperature mediated breaking of the bonds was revealed by temperature dependent SAXS measurements. While weak binding motifs such as in **32a** – **33a** can be broken at temperatures below the glass transition temperature, the regular structure is retained with strong binding motifs **32b** – **33b**.

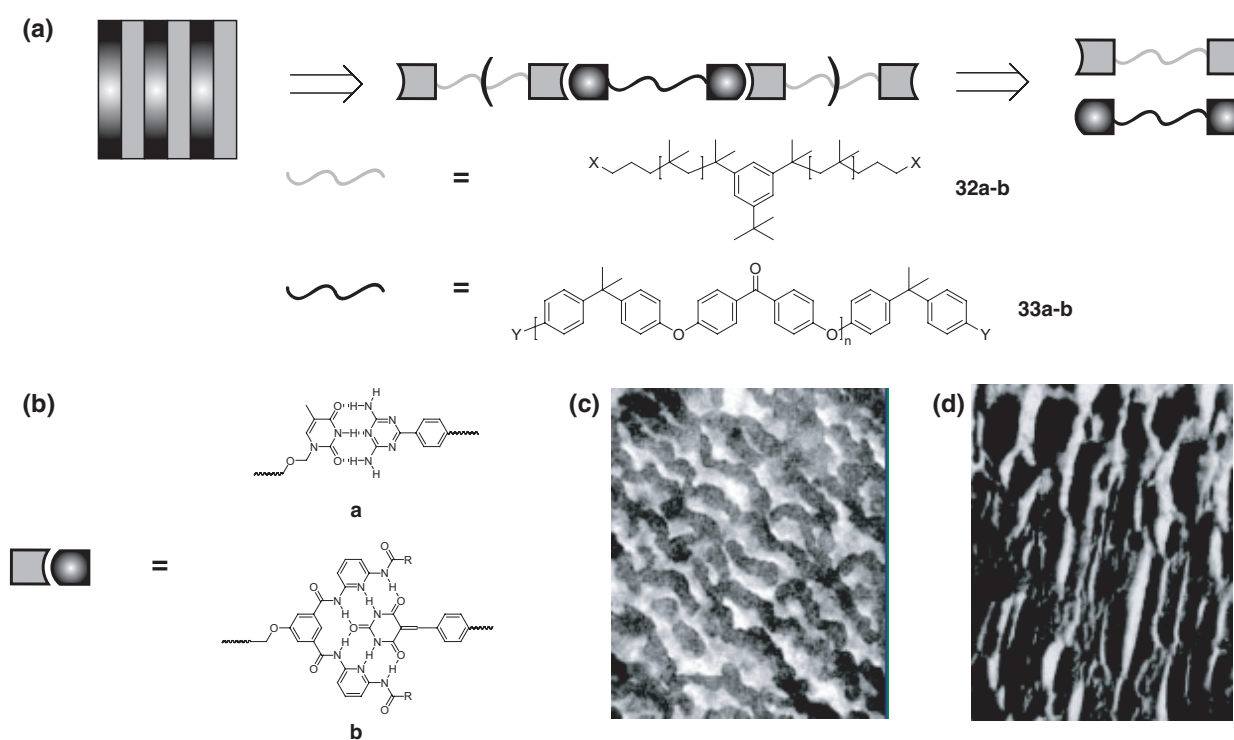


Figure 1.14 (a) Self-assembly of telechelic polymers (PIB, **32** and PEK, **33**) into pseudo block copolymers; (b) binding motifs **a** and **b**; (c) TEM image of **32a** – **33a**; (d) TEM image of **32b** – **33b**.

Gong and co-workers reported the microphase separation of supramolecular AB diblock copolymers based on PS and poly(ethylene glycol) (PEG) polymers which were functionalized with a linear complementary six-fold hydrogen bond motif based on oligoamide complex **8** – **9** ($K_a > 10^9 \text{ M}^{-1}$, Figure 1.15a).^{107,108} NMR and GPC studies clearly indicated that PS and PEG strand are linked through strong hydrogen bonding. In addition, DSC and AFM measurements suggested the formation of microphase-separated PEG domains when polymers **34a** and **35a** were used (Figure 1.15b). In contrast, the AFM image of low MW polymers **34b** and **35b** was completely different (Figure 1.15c). This was explained by regarding the recognition motif as a third block with comparable MW to the polymers resulting in a coil-rod-coil triblock type copolymer.

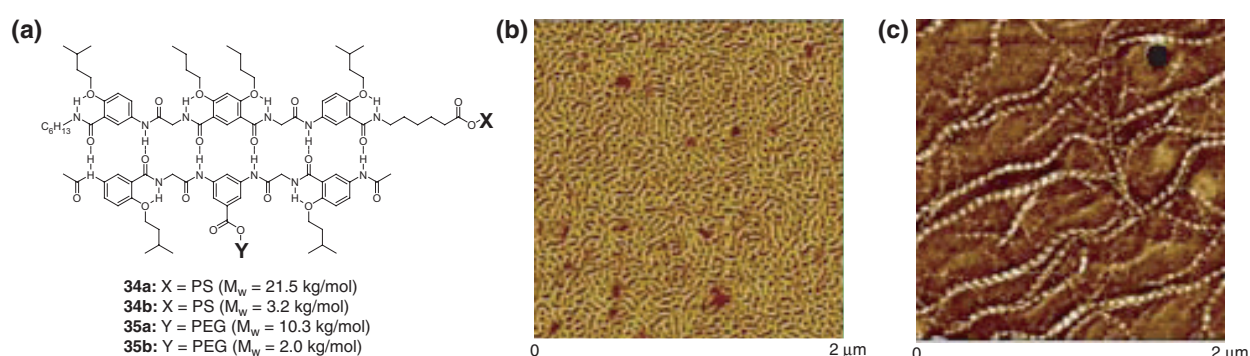


Figure 1.15 (a) Supramolecular PS/PEG diblock copolymer functionalized with complementary oligoamide strands; AFM images (height) of (b) **34a** – **35a** and (c) **34b** – **35b**.

1.4.2.3 Side-chain supramolecular polymers

The second generic class of supramolecular polymers is formed by side-chain polymers. The general design for this class entails either incorporation of recognition units into a covalent polymer main-chain or as pendant groups onto a covalent polymer. Several reviews have appeared recently on this topic^{109,110} so this section is limited to the most illustrative examples of the last two decades. Non-covalent side-chain functionalization strategies were first reported for the synthesis of LC materials (Figure 1.16a).^{111,112} Specifically, the benzoic acid/pyridine mesogenic complexes **36** that were first described by Kato and Fréchet have been the most studied side-chain supramolecular polymers.¹¹³ They exhibit thermally stable smectic or nematic phases over broad temperature ranges. Additionally, when bifunctional pyridines are used, LC networks **37** are formed.¹¹⁴ Likewise, mesomorphic molecular assemblies that are based on two components, neither of which is liquid crystalline can also be obtained through double hydrogen bonding.^{115,116} For example, complex **38** displays a columnar LC-phase¹¹⁶ and supramolecular liquid crystalline polyamide **39** exhibits stable and enantiotropic

mesophases.¹¹⁷ An illustrative example of the effect of multiple weak interactions between two immiscible polymer chains was reported by Meftahi and Fréchet. In these studies, blends were prepared from poly(4-vinylpyridine) (P4VP) **40** and poly(4-hydroxystyrene) **41** (Figure 1.16b). Contrary to mixtures of **40** and PS which showed two separate glass-transition temperatures, a single T_g was observed for a 1:1 mixture of **40** and **41** and both polymers were miscible over the whole composition range.¹¹⁸

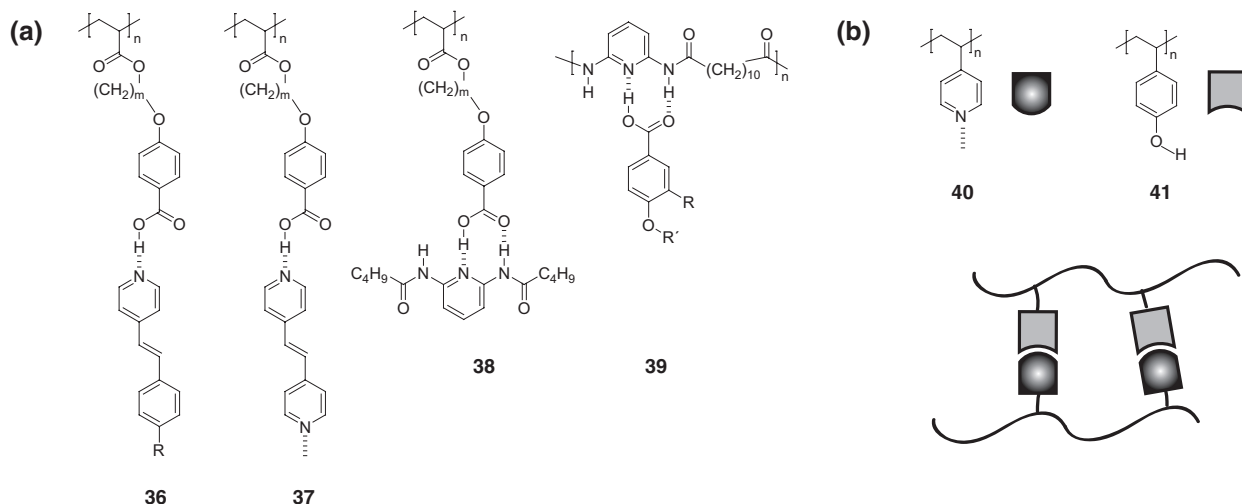


Figure 1.16 (a) Representative examples of side-chain LC polymers **36** - **39**; (b) schematic representation of a blend of poly(4-vinylpyridine) (P4VP) **40** and poly(4-hydroxystyrene) **41**.

Excellent accounts of applying side-chain self-assembly for the design of new polymeric materials have been reported by Ikkala and ten Brinke.^{101,119,120} An illustrative example is the hierarchical assembly of a comb-coil supramolecular diblock copolymer which is a hydrogen

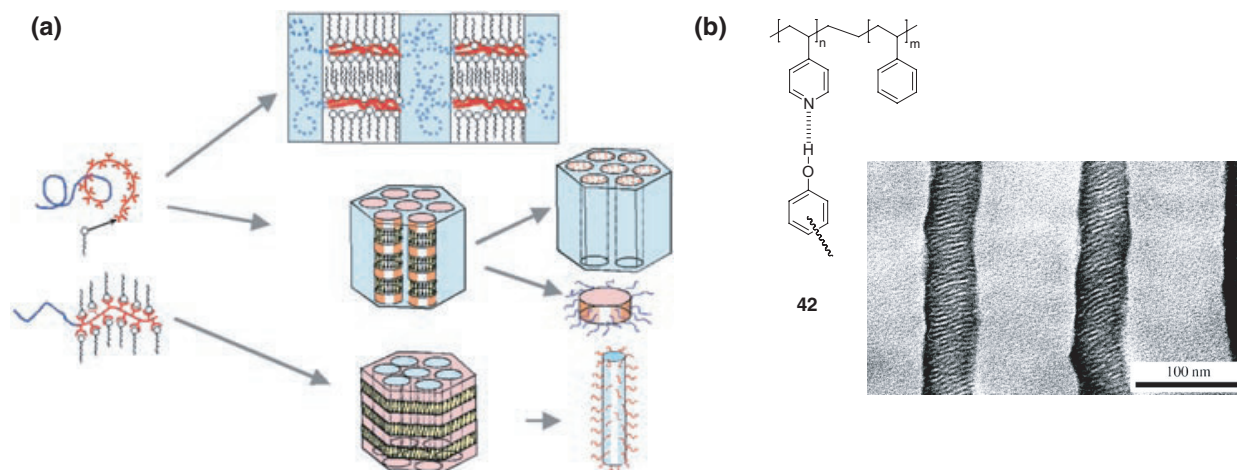


Figure 1.17 (a) Illustration of hierarchical structure formation by self-assembly of block copolymer-based supramolecular side-chain polymers and subsequent preparation of nano-sized architectures by selective removal of a sacrificial block; (b) transmission electron micrograph showing hierarchical self-assembly of PS-block-P4VP(PDP)_{1.0} **42** where nominally one pentadecylphenol (PDP) is hydrogen bonded to a pyridine moiety.

bonded complex of a PS-*block*-P4VP with a non-mesogenic alkylphenol **42** (Figure 1.17).¹²¹ In this manner, a lamellar substructure within a cylindrical mesomorphic architecture is formed (Figure 1.17b).¹²² In addition, the dimensions and properties of the periods can easily be tailored by modifications of the surfactant. Nano-sized objects can be obtained by subsequent selective removal of one of the blocks. A number of materials prepared via this hierarchical self-assembly approach have already been applied for the preparation of photofunctional,^{123,124} optical,¹²⁵ and conductive materials.^{101,126,127}

Stadler and co-workers made an impressive contribution to the field of supramolecular side-chain homopolymers by studying the properties of polybutadienes functionalized with hydrogen bonded phenylurazole derivatives.¹²⁸⁻¹³⁶ Due to reversible chain extension and the subsequent formation of small crystalline domains, the functionalized polymers exhibit properties typical for thermoplastic elastomers. At low temperatures the hydrogen bond interaction contributes to the properties in a manner comparable to covalent interactions, while at high temperature these interactions disappear and the materials exhibit flow behavior typical for a low molecular weight polymer. The properties of these materials were analyzed by DSC,¹²⁹ light and x-ray scattering,¹³⁰ dynamical mechanical analyses,¹³¹⁻¹³³ dielectric spectroscopy¹³⁴ and IR spectroscopy.¹³⁵ A similar strategy was used by Lange *et al.* who described the use of triple hydrogen bonding interactions between the alternating copolymer of styrene and maleimide with melamine and 2,4-diamino-6-vinyl-*s*-triazine.¹³⁷ They demonstrated the formation of a polymer network and showed that the presence of the triple hydrogen bonding motif was essential to guarantee complete miscibility of the polymer blend.

Similarly, triple hydrogen bonding moieties have been incorporated into the side-chain of polymers for versatile approaches to polymer functionalization. Especially, Rotello and co-workers have developed “plug and play” polymers¹³⁸ based on a post-functionalization strategy of random PS copolymers with either diaminotriazine (**43**), diamidopyridine (**44**) or thymine (**45**) hydrogen bonding groups (Figure 1.18a). Initial reports were on the self-assembly of flavin (**46**) onto polymeric scaffolds. Because of an increased intramolecular association of triazines, **44** was more effective in binding **46**.¹³⁸ In addition, polymer **43** and thymine functionalized gold colloids were reported to self-assemble into discrete microspheres that are highly ordered on the molecular as well as the micrometer scale.¹³⁹⁻¹⁴¹ Other reports describe the formation of recognition-induced polymersomes (RIPs) from **44** and **45** or other bifunctional thymine derivatives (Figure 1.18b).¹⁴²⁻¹⁴⁶ These vesicular aggregates were studied with differential interference contrast (DIC), laser confocal scanning microscopy (LCSM) (Figure 1.18c), TEM and AFM. Microsphere formation (2-10 μm) was thermally reversible at 50 °C and subsequent reconstruction of the structures was observed upon cooling demonstrating the

ability to self-optimize.^{144,145} The strength of this recognition methodology was recently illustrated by an elegant study of the incorporation of thymine functionalized dendrimer wedges into block copolymer films of analogues of **44**. Using dynamic secondary ion mass spectrometry (SIMS), DSC, TEM and x-ray diffraction, the extent of guest induced phase segregation was analyzed.

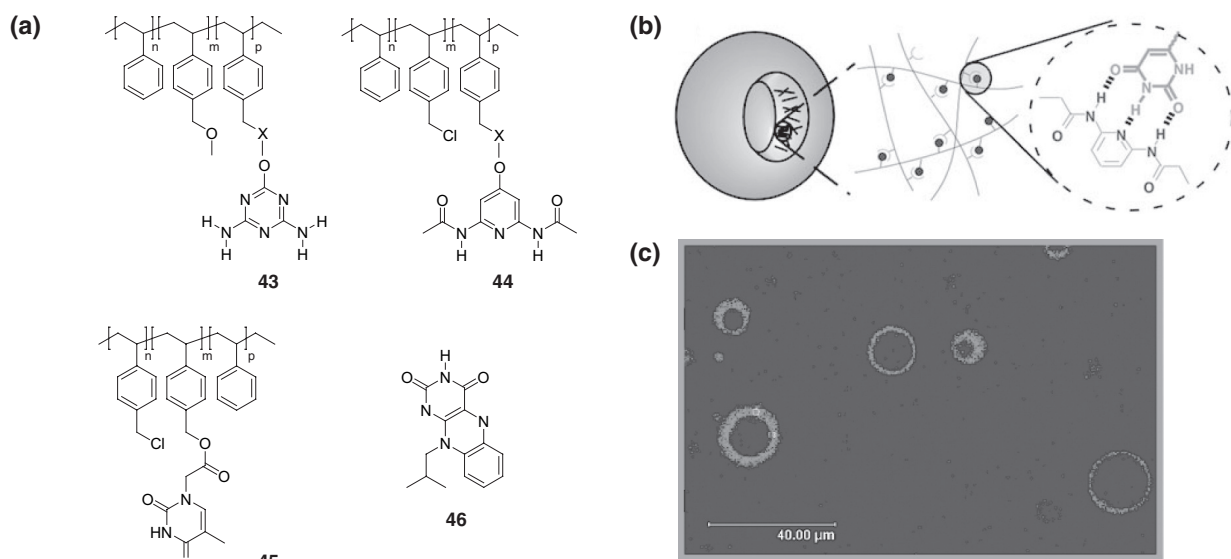


Figure 1.18 (a) PS copolymers functionalized with triple hydrogen bonding units **43** – **45** and flavin **46**; (b) schematic representation of Recognition Induced Polymersomes (RIP) and the recognition unit; (c) laser confocal scanning micrograph of vesicular morphology of RIPs from **44** – **45** in which **45** was functionalized with Rhodamine B.

Currently, a number of groups study the possibility of incorporating multiple recognition groups in order to introduce dynamic multifunctionality into a polymeric material.^{147,148} A system that was reported by Weck and co-workers is the “universal polymer backbone” which is based on a polymeric scaffold that contains metal-ligand and triple hydrogen bonding complexes.¹⁴⁹ This design was conceptually illustrated by Lehn in 2002.¹⁵⁰

A different approach applying self-complementary hydrogen bonding units was taken by the groups of Coates and Long. Coates and coworkers incorporated vinyl-substituted UPy monomer **47** in poly(1-hexene), using a nickel-based polymerization catalyst which is tolerant to Lewis basic groups (Figure 1.19a).¹⁵¹ With small amounts (< 2%) of UPy monomer **47** in the polymer chain, the polyolefins show thermoplastic elastomeric behavior. Long and coworkers described the synthesis and characterization of poly(alkyl methacrylates) containing pendant UPy functionalities (Figure 1.19b).¹⁵²⁻¹⁵⁵ Interestingly, copolymer **48** exhibited significantly better adhesive properties to glass than a similar unadorned polymer.¹⁵² In addition, these

copolymers could easily be spun into fibers (0.1-50 μm) by electrospinning.¹⁵³ Tensile experiments on **49** revealed that at low levels of UPy incorporation, copolymers display a high elongation and low tensile strength.¹⁵⁵ However, with increasing UPy content, the percentage elongation decreased and tensile strength increased. Melt rheological analysis demonstrated that the extent of non-covalent inter-chain interactions largely dictates the physical properties of the polymers. In contrast to supramolecular main-chain polymers, these materials displayed increased creep resistance which enhances performance properties.

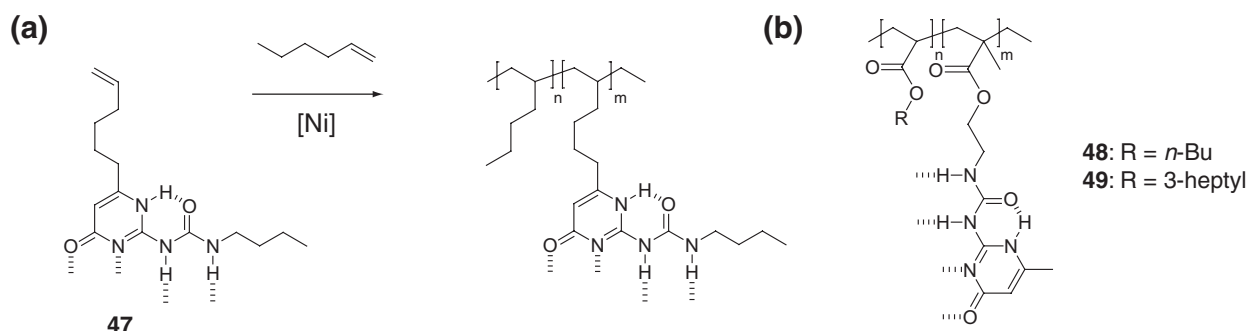


Figure 1.19 (a) Synthesis of UPy-functionalized poly(1-hexene) copolymer; (b) poly(alkyl methacrylates) copolymer containing pendant UPy-units.

More recently, Zimmerman and co-workers reported the utility of a complementary quadruple hydrogen bonding complex by the formation of polymer blends of poly(butyl methacrylate) (PBMA) and PS containing a controlled number of units **6** and **10** (Figure 1.20).⁴⁰ The polymer blends were characterized by DSC, SEC and viscometry which confirmed the formation of reversible networks. Moreover, transparent films could be obtained.

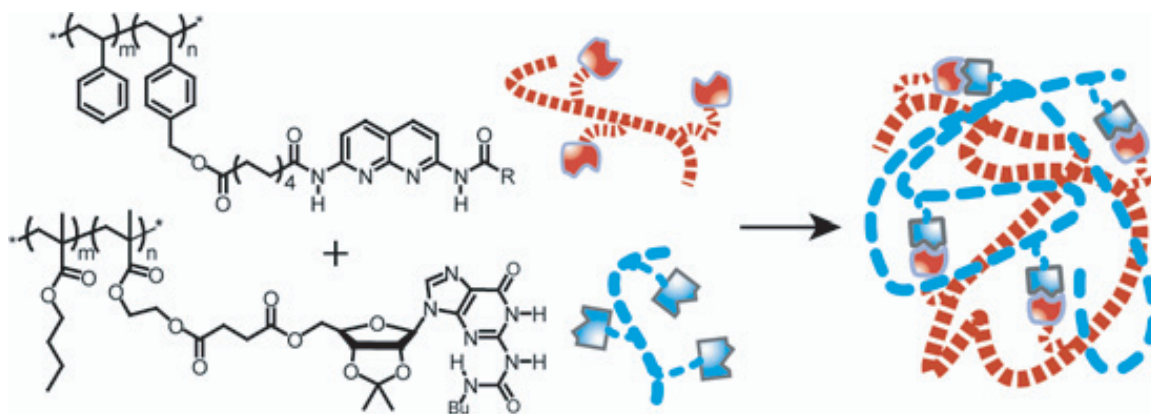


Figure 1.20 Supramolecular side-chain polymers equipped with complementary quadruple hydrogen bonding motifs (**6** and **10**) and schematic representation of copolymer network formation.

1.5 Aim of the thesis

Whereas supramolecular chemistry has focused on the development of well-defined, discrete aggregates using either complementary or self-complementary non-covalent interactions between individual building blocks, supramolecular polymer chemistry has applied these reversible interactions for the development of polymeric aggregates. This class of materials has the potential for possessing unprecedented properties not found in traditional polymers as a result of the reversibility of the non-covalent interactions employed. However, while a large number of recognition units have been developed with a broad range of association constants, only strong self-complementary and weak complementary binding motifs based on multiple hydrogen bonding have been used in supramolecular polymeric materials. Although a modest degree of polymerization by means of weak recognition units in combination with physical inter-chain interactions through domain formation can result in high MW assemblies with improved material properties, it is generally believed that recognition units with high K_a values ($> 10^4 \text{ M}^{-1}$) are necessary to provide polymeric properties in the bulk as well as in solution. Hence, there is a clear need for strong complementary binding motifs. Even though several exciting examples of such recognition units have been reported in literature, their multi-step syntheses hamper their use in materials science.

The aim of this thesis is to design and synthesize new complementary binding motifs based on multiple hydrogen bond interactions and to explore their application in supramolecular polymeric architectures such as those described in the previous sections. Since substantial quantities of material are often needed in material science, ease of synthesis is a prerequisite for these binding motifs. Therefore, the use of highly active catalysts will be explored.

1.6 Outline of the thesis

A general overview of the field of supramolecular polymers is given in *Chapter 1* and focuses on the use of hydrogen bonding units to obtain polymeric properties in solution or in the bulk. The synthesis and characterization of two new hydrogen bonded complexes based on a benzotriazine-N-oxide or imide motif are described in *Chapter 2*. Ab initio quantum mechanical calculations were performed in order to evaluate and confirm the experimentally found binding properties of the benzotriazine-N-oxide complex. A generally applicable palladium-catalyzed amidation procedure of 2-chloro- and 2,7-dichloro-1,8-naphthyridines

towards 2,7-diamido-1,8-naphthyridines (Napy) which display DAAD hydrogen bonding motifs is described in **Chapter 3**. Since these 2,7-diamido-1,8-naphthyridines are prone to acidic and alkaline hydrolysis, a palladium-catalyzed amination and arylation route was explored and optimized for the synthesis of 2-arylamino- and 2,7-di(arylamino)-1,8-naphthyridines in **Chapter 4**. These derivatives are not susceptible to alkaline degradation. In **Chapter 5** the heterodimer based on the association of 2-ureido-6[1H]-pyrimidinones (UPy) and 2,7-diamino-1,8-naphthyridines was studied in solution by a variety of spectroscopic techniques, which revealed insights into the steric and electronic effects of the amino-substituents of the 1,8-naphthyridine on the binding event. With an interesting complementary quadruple hydrogen bonding array available, the results described in **Chapter 6** focus on an application of this array in supramolecular block copolymers. In order to synthesize large bifunctional UPy and Napy telechelics via ring-opening metathesis polymerization, a protecting group strategy based on quadruple hydrogen bonding with a UPy protecting group is introduced. Supramolecular block copolymer formation was substantiated in solution as well as in the bulk using a variety of techniques. Finally, acyclic diene metathesis polymerization employing the UPy-protection strategy and a polycondensation procedure using bifunctional Napy units are described in **Chapter 7** to obtain strictly linear polymers with a high degree of DAAD quadruple hydrogen bond motifs in the main chain. These polymers were characterized as grafted and ungrafted copolymers in solution.

1.6 References

- (1) Lehn, J.-M. *Supramolecular Chemistry*; Wiley-VCH, 1995.
- (2) Pedersen, C. J. *J. Am. Chem. Soc.* **1967**, *89*, 7017-36.
- (3) Cram, D. J.; Cram, J. M. *Science* **1974**, *183*, 803-9.
- (4) Dietrich, B.; Lehn, J. M.; Sauvage, J. P. *Tetrahedron Lett.* **1969**, 2889-92.
- (5) Loeb, S. J.; Tiburcio, J.; Vella, S. J. *Org. Lett.* **2005**, *7*, 4923-4926.
- (6) Connors, K. A. *Chem. Rev.* **1997**, *97*, 1325-1357.
- (7) Lagona, J.; Mukhopadhyay, P.; Chakrabarti, S.; Isaacs, L. *Angew. Chem. Int. Ed.* **2005**, *44*, 4844-4870.
- (8) Ciferri, A. *Supramolecular Polymers*; 2 ed.; CRC Press: Boca Raton, 2005.
- (9) Flory, P. J. *Principles of Polymer Chemistry*; Cornell University Press: Ithaca, 1953.
- (10) Ciferri, A. *Macromol. Rapid Commun.* **2002**, *23*, 511-529.
- (11) Prins, L. J.; Reinhoudt, D. N.; Timmerman, P. *Angew. Chem. Int. Ed.* **2001**, *40*, 2382-2426.
- (12) Lawrence, D. S.; Jiang, T.; Levett, M. *Chem. Rev.* **1995**, *95*, 2229-60.
- (13) Sherrington, D. C.; Taskinen, K. A. *Chem. Soc. Rev.* **2001**, *30*, 83-93.
- (14) Cooke, G.; Rotello, V. M. *Chem. Soc. Rev.* **2002**, *31*, 275-286.
- (15) Sijbesma, R. P.; Meijer, E. W. *Chem. Commun.* **2003**, 5-16.
- (16) Zimmerman, S. C.; Corbin, P. S. *Structure and Bonding (Berlin)* **2000**, *96*, 63-94.
- (17) Stone, A. J. *The Theory of Intermolecular Forces*; Clarendon: Oxford, 1996.
- (18) Jorgensen, W. L.; Pranata, J. *J. Am. Chem. Soc.* **1990**, *112*, 2008-10.

- (19) Pranata, J.; Wierschke, S. G.; Jorgensen, W. L. *J. Am. Chem. Soc.* **1991**, *113*, 2810-19.
- (20) Murray, T. J.; Zimmerman, S. C. *J. Am. Chem. Soc.* **1992**, *114*, 4010-11.
- (21) Zimmerman, S. C.; Murray, T. J. *Philosophical Transactions of the Royal Society of London, Series A: Mathematical, Physical and Engineering Sciences* **1993**, *345*, 49-56.
- (22) Sartorius, J.; Schneider, H.-J. *Chem. Eur. J.* **1996**, *2*, 1446-1452.
- (23) Lukin, O.; Leszczynski, J. *J. Phys. Chem. A* **2002**, *106*, 6775-6782.
- (24) Schneider, H.-J. *J. Phys. Chem. A* **2003**, *107*, 9250.
- (25) Chang, S. K.; Hamilton, A. D. *J. Am. Chem. Soc.* **1988**, *110*, 1318-19.
- (26) Beijer, F. H.; Kooijman, H.; Spek, A. L.; Sijbesma, R. P.; Meijer, E. W. *Angew. Chem. Int. Ed.* **1998**, *37*, 75-78.
- (27) Sijbesma, R. P.; Beijer, F. H.; Brunsveld, L.; Folmer, B. J. B.; Hirschberg, J. H. K. K.; Lange, R. F. M.; Lowe, J. K. L.; Meijer, E. W. *Science* **1997**, *278*, 1601-1604.
- (28) Beijer, F. H.; Sijbesma, R. P.; Kooijman, H.; Spek, A. L.; Meijer, E. W. *J. Am. Chem. Soc.* **1998**, *120*, 6761-6769.
- (29) Söntjens, S. H. M.; Sijbesma, R. P.; van Genderen, M. H. P.; Meijer, E. W. *J. Am. Chem. Soc.* **2000**, *122*, 7487-7493.
- (30) Corbin, P. S.; Zimmerman, S. C. *J. Am. Chem. Soc.* **1998**, *120*, 9710-9711.
- (31) Corbin, P. S.; Lawless, L. J.; Li, Z. T.; Ma, Y. G.; Witmer, M. J.; Zimmerman, S. C. *Proc. Natl. Acad. Sci. USA* **2002**, *99*, 5099-5104.
- (32) Corbin, P. S.; Zimmerman, S. C. *J. Am. Chem. Soc.* **2000**, *122*, 3779-3780.
- (33) Luning, U.; Kuhl, C. *Tetrahedron Lett.* **1998**, *39*, 5735-5738.
- (34) Corbin, P. S.; Zimmerman, S. C.; Thiessen, P. A.; Hawryluk, N. A.; Murray, T. J. *J. Am. Chem. Soc.* **2001**, *123*, 10475-10488.
- (35) Zeng, H.; Miller, R. S.; Flowers, R. A., II; Gong, B. *J. Am. Chem. Soc.* **2000**, *122*, 2635-2644.
- (36) Gong, B. *Synlett.* **2001**, 582-589.
- (37) Gong, B.; Yan, Y.; Zeng, H.; Skrzypczak-Jankunn, E.; Kim, Y. W.; Zhu, J.; Ickes, H. J. *Am. Chem. Soc.* **1999**, *121*, 5607-5608.
- (38) Wang, X.-Z.; Li, X.-Q.; Shao, X.-B.; Zhao, X.; Deng, P.; Jiang, X.-K.; Li, Z.-T.; Chen, Y.-Q. *Chem. Eur. J.* **2003**, *9*, 2904-2913.
- (39) Ligthart, G. B. W. L.; Ohkawa, H.; Sijbesma, R. P.; Meijer, E. W. *J. Am. Chem. Soc.* **2005**, *127*, 810-811.
- (40) Park, T.; Zimmerman, S. C.; Nakashima, S. *J. Am. Chem. Soc.* **2005**, *127*, 6520-6521.
- (41) Park, T.; Todd, E. M.; Nakashima, S.; Zimmerman, S. C. *J. Am. Chem. Soc.* **2005**, *127*, 18133-18142.
- (42) Mayer, M. F.; Nakashima, S.; Zimmerman, S. C. *Org. Lett.* **2005**, *7*, 3005-3008.
- (43) Brienne, M. J.; Gabard, J.; Lehn, J. M.; Stibor, I. *J. Chem. Soc., Chem. Commun.* **1989**, 1868-70.
- (44) Kato, T.; Frechet, J. M. J. *J. Am. Chem. Soc.* **1989**, *111*, 8533-4.
- (45) Kato, T.; Wilson, P. G.; Fujishima, A.; Frechet, J. M. J. *Chem. Lett.* **1990**, 2003-6.
- (46) Alexander, C.; Jariwala, C. P.; Lee, C. M.; Griffin, A. C. *Macromol. Symp.* **1994**, *77*, 283-94.
- (47) Kihara, H.; Kato, T.; Uryu, T.; Frechet, J. M. J. *Chem. Mater.* **1996**, *8*, 961-8.
- (48) Fouquey, C.; Lehn, J. M.; Levelut, A. M. *Adv. Mater.* **1990**, *2*, 254-7.
- (49) Lehn, J. M. *Macromol. Chem., Macromol. Symp.* **1993**, *69*, 1-17.
- (50) Gulik-Krzywicki, T.; Fouquey, C.; Lehn, J. M. *Proc. Natl. Acad. Sci. USA* **1993**, *90*, 163-7.
- (51) Kotera, M.; Lehn, J. M.; Vigneron, J. P. *J. Chem. Soc., Chem. Commun.* **1994**, 197-9.
- (52) St.Pourcain, C. B.; Griffin, A. C. *Macromolecules* **1995**, *28*, 4116-21.
- (53) Wiegel, K. N.; Griffin, A. C.; Black, M. S.; Schiraldi, D. A. *J. Appl. Polym. Sci.* **2004**, *92*, 3097-3106.
- (54) Bong, D. T.; Clark, T. D.; Granja, J. R.; Ghadiri, M. R. *Angew. Chem. Int. Ed.* **2001**, *40*, 988-1011.
- (55) Klok, H. A.; Jolliffe, K. A.; Schauer, C. L.; Prins, L. J.; Spatz, J. P.; Moller, M.; Timmerman, P.; Reinhoudt, D. N. *J. Am. Chem. Soc.* **1999**, *121*, 7154-7155.
- (56) Choi, I. S.; Li, X. H.; Simanek, E. E.; Akaba, R.; Whitesides, G. M. *Chem. Mater.* **1999**, *11*, 684-690.

- (57) Ghadiri, M. R.; Granja, J. R.; Milligan, R. A.; McRee, D. E.; Khazanovich, N. *Nature* **1993**, 366, 324-7.
- (58) Hartgerink, J. D.; Ghadiri, M. R. *New Macromolecular Architecture and Functions*; Springer-Verlag: Berlin, 1996.
- (59) Seto, C. T.; Whitesides, G. M. *J. Am. Chem. Soc.* **1993**, 115, 1330-40.
- (60) Mammen, M.; Simanek, E. E.; Whitesides, G. M. *J. Am. Chem. Soc.* **1996**, 118, 12614-12623.
- (61) Boileau, S.; Bouteiller, L.; Laupretre, F.; Lortie, F. *New J. Chem.* **2000**, 24, 845-848.
- (62) Lortie, F.; Boileau, S.; Bouteiller, L.; Chassenieux, C.; Deme, B.; Ducouret, G.; Jalabert, M.; Laupretre, F.; Terech, P. *Langmuir* **2002**, 18, 7218-7222.
- (63) Simic, V.; Bouteiller, L.; Jalabert, M. *J. Am. Chem. Soc.* **2003**, 125, 13148-13154.
- (64) van der Gucht, J.; Besseling, N. A. M.; Knoben, W.; Bouteiller, L.; Cohen Stuart, M. A. *Phys. Rev. E* **2003**, 67.
- (65) Ikeda, M.; Nobori, T.; Schmutz, M.; Lehn, J. M. *Chem. Eur. J.* **2005**, 11, 662-668.
- (66) Keizer, H. M.; Sijbesma, R. P.; Meijer, E. W. *Eur. J. Org. Chem.* **2004**, 2553-2555.
- (67) Folmer, B. J. B.; Cavini, E.; Sijbesma, R. P.; Meijer, E. W. *Chem. Commun.* **1998**, 1847-1848.
- (68) Wubbenhorst, M.; van Turnhout, J.; Folmer, B. J. B.; Sijbesma, R. P.; Meijer, E. W. *IEEE Trans. Dielectr. Electr. Insul.* **2001**, 8, 365-372.
- (69) Doi, M.; Edwards, S. F. *The Theory of Polymer Dynamics*; Clarendon: Oxford, 1986.
- (70) Cates, M. E. *Macromolecules* **1987**, 20, 2289-96.
- (71) Hirschberg, J. H. K. K.; Brunsveld, L.; Ramzi, A.; Vekemans, J. A. J. M.; Sijbesma, R. P.; Meijer, E. W. *Nature* **2000**, 407, 167-170.
- (72) Brunsveld, L.; Vekemans, J.; Hirschberg, J.; Sijbesma, R. P.; Meijer, E. W. *Proc. Natl. Acad. Sci. USA* **2002**, 99, 4977-4982.
- (73) Castellano, R. K.; Rudkevich, D. M.; Rebek, J., Jr. *Proc. Natl. Acad. Sci. USA* **1997**, 94, 7132-7137.
- (74) Castellano, R. K.; Clark, R.; Craig, S. L.; Nuckolls, C.; Rebek, J., Jr. *Proc. Natl. Acad. Sci. USA* **2000**, 97, 12418-12421.
- (75) Castellano, R. K.; Nuckolls, C.; Eichhorn, S. H.; Wood, M. R.; Lovinger, A. J.; Rebek, J. *Angew. Chem. Int. Ed.* **1999**, 38, 2603-2606.
- (76) Castellano, R. K.; Rebek, J., Jr. *J. Am. Chem. Soc.* **1998**, 120, 3657-3663.
- (77) Fogleman, E. A.; Yount, W. C.; Xu, J.; Craig, S. L. *Angew. Chem. Int. Ed.* **2002**, 41, 4026-4028.
- (78) Xu, J.; Fogleman, E. A.; Craig, S. L. *Macromolecules* **2004**, 37, 1863-1870.
- (79) ten Cate, A. T.; Sijbesma, R. P. *Macromol. Rapid Commun.* **2002**, 23, 1094-1112.
- (80) Hoshino, H.; Jin, J. I.; Lenz, R. W. *J. Appl. Polym. Sci.* **1984**, 29, 547-54.
- (81) Lillya, C. P.; Baker, R. J.; Hutte, S.; Winter, H. H.; Lin, Y. G.; Shi, J.; Dickinson, L. C.; Chien, J. C. W. *Macromolecules* **1992**, 25, 2076-80.
- (82) Abed, S.; Boileau, S.; Bouteiller, L.; Lacoudre, N. *Polym. Bull.* **1997**, 39, 317-324.
- (83) Abed, S.; Boileau, S.; Bouteiller, L. *Macromolecules* **2000**, 33, 8479-8487.
- (84) Abed, S.; Boileau, S.; Bouteiller, L. *Polymer* **2001**, 42, 8613-8619.
- (85) Duweltz, D.; Laupretre, F.; Abed, S.; Bouteiller, L.; Boileau, S. *Polymer* **2003**, 44, 2295-2302.
- (86) Yamauchi, K.; Lizotte, J. R.; Long, T. E. *Macromolecules* **2002**, 35, 8745-8750.
- (87) Rowan, S. J.; Suwanmala, P.; Sivakova, S. *J. Polym. Sci., Part A : Polym. Chem.* **2003**, 41, 3589-3596.
- (88) Sivakova, S.; Bohnsack, D. A.; Mackay, M. E.; Suwanmala, P.; Rowan, S. J. *J. Am. Chem. Soc.* **2005**, 127, 18202-18211.
- (89) Ky Hirschberg, J. H. K.; Beijer, F. H.; van Aert, H. A.; Magusin, P. C. M. M.; Sijbesma, R. P.; Meijer, E. W. *Macromolecules* **1999**, 32, 2696-2705.
- (90) Folmer, B. J. B.; Sijbesma, R. P.; Versteegen, R. M.; van der Rijt, J. A. J.; Meijer, E. W. *Adv. Mater.* **2000**, 12, 874-878.
- (91) Keizer, H. M.; van Kessel, R.; Sijbesma, R. P.; Meijer, E. W. *Polymer* **2003**, 44, 5505-5511.
- (92) Lange, R. F. M.; Van Gurp, M.; Meijer, E. W. *J. Polym. Sci., Part A : Polym. Chem.* **1999**, 37, 3657-3670.

- (93) Keizer, H. M.; Sijbesma, R. P.; Jansen, J. F. G. A.; Pasternack, G.; Meijer, E. W. *Macromolecules* **2003**, *36*, 5602-5606.
- (94) Dankers, P. Y. W.; Harmsen, M. C.; Brouwer, L. A.; Van Luyn, M. J. A.; Meijer, E. W. *Nature materials* **2005**, *4*, 568-574.
- (95) Yamauchi, K.; Kanomata, A.; Inoue, T.; Long, T. E. *Macromolecules* **2004**, *37*, 3519-3522.
- (96) Guan, Z. B.; Roland, J. T.; Bai, J. Z.; Ma, S. X.; McIntire, T. M.; Nguyen, M. J. *Am. Chem. Soc.* **2004**, *126*, 2058-2065.
- (97) Hamley, I. W. *The Physics of Block Copolymers*; Oxford Science Publications: Oxford, 1998.
- (98) Whitesides, G. M.; Grzybowski, B. *Science* **2002**, *295*, 2418-2421.
- (99) Muthukumar, M.; Ober, C. K.; Thomas, E. L. *Science* **1997**, *277*, 1225-1232.
- (100) Stupp, S. I.; LeBonheur, V.; Walker, K.; Li, L. S.; Huggins, K. E.; Keser, M.; Amstutz, A. *Science* **1997**, *276*, 384-389.
- (101) Ikkala, O.; ten Brinke, G. *Chem. Commun.* **2004**, 2131-7.
- (102) Hirschberg, J. H. K. K.; Ramzi, A.; Sijbesma, R. P.; Meijer, E. W. *Macromolecules* **2003**, *36*, 1429-1432.
- (103) Binder, W. H.; Kunz, M. J.; Ingolic, E. J. *Polym. Sci., Part A : Polym. Chem.* **2003**, *42*, 162-172.
- (104) Kunz, M. J.; Hayn, G.; Saf, R.; Binder, W. H. *J. Polym. Sci., Part A : Polym. Chem.* **2004**, *42*, 661-674.
- (105) Binder, W. H.; Kunz, M. J.; Kluger, C.; Hayn, G.; Saf, R. *Macromolecules* **2004**, *37*, 1749-1759.
- (106) Binder, W. H.; Bernstorff, S.; Kluger, C.; Petraru, L.; Kunz, M. J. *Adv. Mater.* **2005**, *17*, 2824-2828.
- (107) Yang, X.; Hua, F.; Yamato, K.; Ruckenstein, E.; Gong, B.; Kim, W.; Ryu, C. Y. *Angew. Chem. Int. Ed.* **2004**, *43*, 6471-6474.
- (108) Gong, B.; Yang, X.; Kim, W.; Ryu, C. Y. *Polym. Prepr.* **2005**, *46*, 1128-1129.
- (109) Pollino, J. M.; Weck, M. *Chem. Soc. Rev.* **2005**, *34*, 193-207.
- (110) Kato, T.; Mizoshita, N.; Kishimoto, K. *Angew. Chem. Int. Ed.* **2006**, *45*, 38-68.
- (111) Kato, T.; Frechet, J. M. J. *Macromolecules* **1989**, *22*, 3818-19.
- (112) Ujiie, S.; Iimura, K. *Macromolecules* **1992**, *25*, 3174-8.
- (113) Kato, T.; Frechet, J. M. J. *Macromol. Symp.* **1995**, *98*, 311-26.
- (114) Kato, T.; Kihara, H.; Kumar, U.; Uryu, T.; Frechet, J. M. J. *Angew. Chem.* **1994**, *106*, 1728-30.
- (115) Malik, S.; Dhal, P. K.; Mashelkar, R. A. *Macromolecules* **1995**, *28*, 2159-64.
- (116) Kato, T.; Nakano, M.; Moteki, T.; Uryu, T.; Ujiie, S. *Macromolecules* **1995**, *28*, 8875-6.
- (117) Kato, T.; Ihata, O.; Ujiie, S.; Tokita, M.; Watanabe, J. *Macromolecules* **1998**, *31*, 3551-3555.
- (118) Vivas de Meftahi, M.; Frechet, J. M. J. *Polymer* **1988**, *29*, 477-82.
- (119) Ikkala, O.; ten Brinke, G. *Science* **2002**, *295*, 2407-9.
- (120) Ten Brinke, G.; Ikkala, O. *Chemical Record* **2004**, *4*, 219-230.
- (121) Ruokolainen, J.; ten Brinke, G.; Ikkala, O.; Torkkeli, M.; Serimaa, R. *Macromolecules* **1996**, *29*, 3409-15.
- (122) Ruokolainen, J.; Saariaho, M.; Ikkala, O.; Ten Brinke, G.; Thomas, E. L.; Torkkeli, M.; Serimaa, R. *Macromolecules* **1999**, *32*, 1152-1158.
- (123) Osuji, C.; Chao, C.-Y.; Bitá, I.; Ober, C. K.; Thomas, E. L. *Adv. Funct. Mater.* **2002**, *12*, 753-758.
- (124) Valkama, S.; Kosonen, H.; Ruokolainen, J.; Haatainen, T.; Torkkeli, M.; Serimaa, R.; ten Brinke, G.; Ikkala, O. *Nature materials* **2004**, *3*, 872-876.
- (125) Chao, C.-Y.; Li, X.; Ober, C. K.; Osuji, C.; Thomas, E. L. *Adv. Funct. Mater.* **2004**, *14*, 364-370.
- (126) Maki-Ontto, R.; de Moel, K.; Polushkin, E.; van Ekenstein, G. A.; ten Brinke, G.; Ikkala, O. *Adv. Mater.* **2002**, *14*, 357-361.
- (127) Ruokolainen, J.; Makinen, R.; Torkkeli, M.; Makela, T.; Serimaa, R.; Ten Brinke, G.; Ikkala, O. *Science* **1998**, *280*, 557-560.
- (128) Mueller, M.; Dardin, A.; Seidel, U.; Balsamo, V.; Ivan, B.; Spiess, H. W.; Stadler, R. *Macromolecules* **1996**, *29*, 2577-83.
- (129) Hilger, C.; Stadler, R.; De Lucca Freitas, L. L. *Polymer* **1990**, *31*, 818-23.
- (130) Bica, C. I. D.; Burchard, W.; Stadler, R. *Macromol. Chem. Phys.* **1996**, *197*, 3407-3426.

- (131) De Lucca Freitas, L. L.; Stadler, R. *Macromolecules* **1987**, *20*, 2478-85.
- (132) De Lucca Freitas, L.; Stadler, R. *Colloid Polym. Sci.* **1988**, *266*, 1095-101.
- (133) Müller, M.; Seidel, U.; Stadler, R. *Polymer* **1995**, *36*, 3143-50.
- (134) Müller, M.; Stadler, R.; Kremer, F.; Williams, G. *Macromolecules* **1995**, *28*, 6942-9.
- (135) Seidel, U.; Stadler, R.; Fuller, G. G. *Macromolecules* **1994**, *27*, 2066-72.
- (136) Hilger, C.; Stadler, R. *Macromolecules* **1992**, *25*, 6670-80.
- (137) Lange, R. F. M.; Meijer, E. W. *Macromolecules* **1995**, *28*, 782-3.
- (138) Ilhan, F.; Gray, M.; Rotello, V. M. *Macromolecules* **2001**, *34*, 2597-2601.
- (139) Boal, A. K.; Ilhan, F.; DeRouchey, J. E.; Thurn-Albrecht, T.; Russell, T. P.; Rotello, V. M. *Nature* **2000**, *404*, 746-748.
- (140) Frankamp, B. L.; Uzun, O.; Ilhan, F.; Boal, A. K.; Rotello, V. M. *J. Am. Chem. Soc.* **2002**, *124*, 892-893.
- (141) Boal, A. K.; Frankamp, B. L.; Uzun, O.; Tuominen, M. T.; Rotello, V. M. *Chem. Mater.* **2004**, *16*, 3252-3256.
- (142) Ilhan, F.; Galow, T. H.; Gray, M.; Clavier, G.; Rotello, V. M. *J. Am. Chem. Soc.* **2000**, *122*, 5895-5896.
- (143) Thibault, R. J., Jr.; Galow, T. H.; Turnberg, E. J.; Gray, M.; Hotchkiss, P. J.; Rotello, V. M. *J. Am. Chem. Soc.* **2002**, *124*, 15249-15254.
- (144) Thibault, R. J.; Hotchkiss, P. J.; Gray, M.; Rotello, V. M. *J. Am. Chem. Soc.* **2003**, *125*, 11249-11252.
- (145) Uzun, O.; Sanyal, A.; Nakade, H.; Thibault, R. J.; Rotello, V. M. *J. Am. Chem. Soc.* **2004**, *126*, 14773-14777.
- (146) Uzun, O.; Xu, H.; Jeoung, E.; Thibault, R. J.; Rotello, V. M. *Chem. Eur. J.* **2005**, *11*, 6916-6920.
- (147) Gerhardt, W.; Crne, M.; Weck, M. *Chem. Eur. J.* **2004**, *10*, 6212-6221.
- (148) Hofmeier, H.; Schubert Ulrich, S. *Chem. Commun.* **2005**, 2423-32.
- (149) Pollino, J. M.; Stubbs, L. P.; Weck, M. *J. Am. Chem. Soc.* **2004**, *126*, 563-567.
- (150) Lehn, J. M. *Polym. Int.* **2002**, *51*, 825-839.
- (151) Rieth, L. R.; Eaton, R. F.; Coates, G. W. *Angew. Chem. Int. Ed.* **2001**, *40*, 2153-2156.
- (152) Yamauchi, K.; Lizotte, J. R.; Long, T. E. *Macromolecules* **2003**, *36*, 1083-1088.
- (153) McKee, M. G.; Elkins, C. L.; Long, T. E. *Polymer* **2004**, *45*, 8705-8715.
- (154) McKee, M. G.; Elkins, C. L.; Park, T.; Long, T. E. *Macromolecules* **2005**, *38*, 6015-6023.
- (155) Elkins, C. L.; Park, T.; McKee, M. G.; Long, T. E. *J. Polym. Sci., Part A : Polym. Chem.* **2005**, *43*, 4618-4631.

2

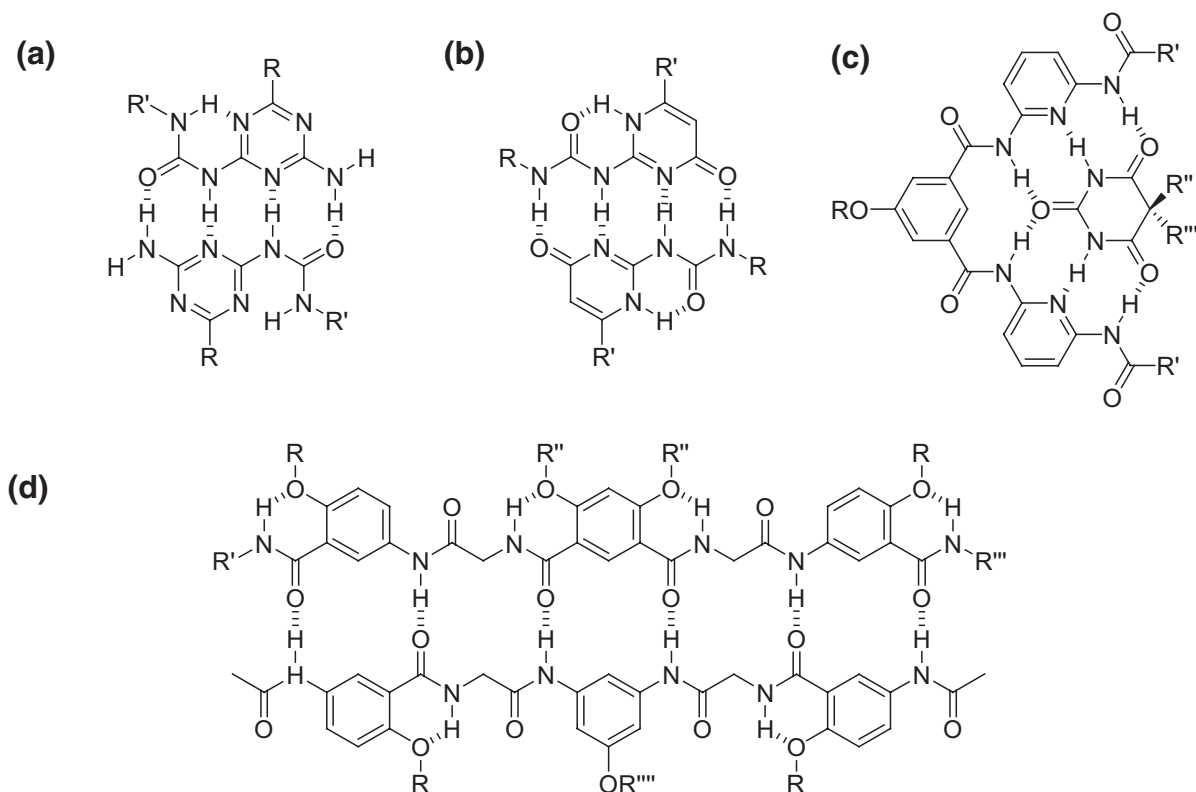
Complementary hydrogen bonding based on benzotriazine-N-oxide and imide motifs

Abstract

*A 3-ureido-benzo-1,2,4-triazine-1-N-oxide **1** was synthesized successfully. The derivative displays an Acceptor-Donor-Acceptor-Acceptor (ADAA) hydrogen bonding motif in CDCl₃ and DMSO-d₆ solution as well as in the solid state. Although moderately strong association of **1** with DAD motifs was observed, non-specific binding is seen with ureidopyridines featuring a complementary DADD array. Quantum mechanical calculations of conformations **1a** and **1b** together with two complexes at DFT levels of theory were performed, which result in positive free energies of association predicting the absence of specific assembly of the components. A rational design using intramolecular hydrogen bonding of pre-organized acyclic imides into the Z,Z conformation to display an AA hydrogen bonding array is presented. Pre-organization of the imide by an intramolecular hydrogen bond is observed in the solid state and in CDCl₃ solution. A significant increase in binding to complementary ureas is observed for the pre-organized imides.*

2.1 Introduction

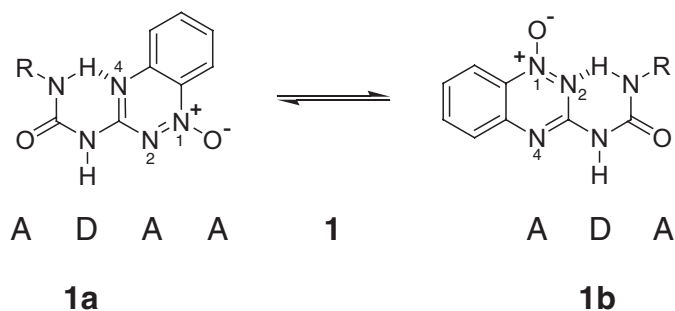
Inspired by the generic storage mechanism of DNA, arrays of multiple parallel or near-parallel hydrogen bonds have been commonly used in motifs for molecular recognition for the last 20 years,¹⁻³ since strength, specificity and directionality are increased compared to single hydrogen bonds. The strength of multiple hydrogen bonded complexes has been found to depend not only on the number of hydrogen bonds – and the donor acidity and acceptor basicity of the individual hydrogen bonds⁴⁻⁷ – but also strongly on the particular arrangement of the donor and acceptor functional groups.^{8,9} Linear arrays of two and three hydrogen bonds have been studied in detail, and the strength of triple hydrogen bonds was found to vary from moderate ($K_a = 10^2$ – 10^3 M⁻¹ for the DAD-ADA couple in chloroform), to strong ($K_a > 10^5$ M⁻¹ for the DDD-AAA couple in chloroform).¹⁰ Despite its moderate strength, the DAD-ADA couple is by far the most frequently encountered array in supramolecular engineering due to its ease of synthesis and chemical stability. The synthesis of the components of much stronger binding motifs generally requires much more effort. A large number of strongly bonded complexes held together by more than three hydrogen bonds have been described in the last decade, of which a few illustrative examples are given in Scheme 2.1.¹¹⁻¹⁵



Scheme 2.1 Molecular recognition based on multiple hydrogen bonding motifs. (a) Ureido-s-triazine dimer, $K_{dim} = 2 \cdot 10^4$ M⁻¹ in CDCl₃;¹¹ (b) Ureido-pyrimidinone, $K_{dim} = 6 \cdot 10^6$ M⁻¹ in CDCl₃;^{12,13} (c) Barbiturate – bis(diamidopyridine) complex, $K_a = 2 \cdot 10^4$ M⁻¹ in CDCl₃;¹⁴ (d) Oligoamide complex, $K_a > 10^9$ M⁻¹ in CDCl₃.¹⁵

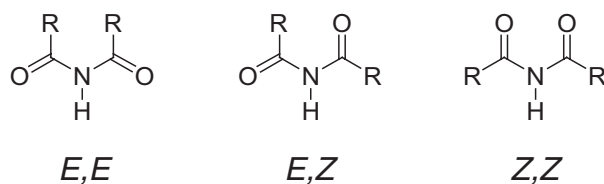
For a number of applications, such as self-assembling container molecules¹⁶ and supramolecular tubes,¹⁷ self-complementarity is used. Especially, strongly associating self-complementary molecules are advantageous for the assembly of linear hydrogen-bonded polymers. The development of the ureido-s-triazine (Scheme 2.1a) and ureido-pyrimidinone (Scheme 2.1b) groups which are easy to prepare and have high dimerization constants has been a breakthrough towards supramolecular polymers.¹⁸⁻²² However, the self-complementarity of these units imposes restrictions to the self-assembly of copolymers and the construction of supramolecular architectures consisting of more than one compound. Even though a number of complementary multiple hydrogen bonding arrays have been developed recently (see also Scheme 2.1c & d), the individual components either lack synthetic accessibility or selective association to the heterocomplexes.²³⁻²⁸

In this chapter a study into new complementary hydrogen bonding modules is explored. In the first part of the chapter, the synthetic accessibility of 3-ureido-1,2,4-triazine-1-N-oxide **1** and suitability as an ADAA hydrogen bonding scaffold is reported. Since N-oxides of nitrogen heterocycles have been reported to be stronger hydrogen bond acceptors than the corresponding pyridine, strong binding would be expected.^{4,29-33} Although **1** can be present in two possible conformations **1a** and **1b**, as displayed in Scheme 2.2, the equilibrium might be shifted towards the ADAA form upon presenting a complementary DADD partner. These experimental studies are complemented by density functional quantum mechanical calculations to evaluate the experimentally found binding properties of the compound, and both experimental and theoretical data will be discussed in detail.



Scheme 2.2 3-Ureido-1,2,4-triazine-1-N-oxide **1** in two possible conformations.

In the second half of the chapter, an approach is presented towards the use of imide-urea motifs as complementary AA-DD arrays. Because of rotation about the C-N bond, acyclic imides exhibit *E-Z* isomerism.³⁴ Three conformations are possible for acyclic, symmetrical imides (Scheme 2.3). The possibility of fixing the imide in the *Z,Z* conformation by intramolecular hydrogen bonding was examined next to the influence of binding to urea molecules.



Scheme 2.3 Three conformations in acyclic imides.

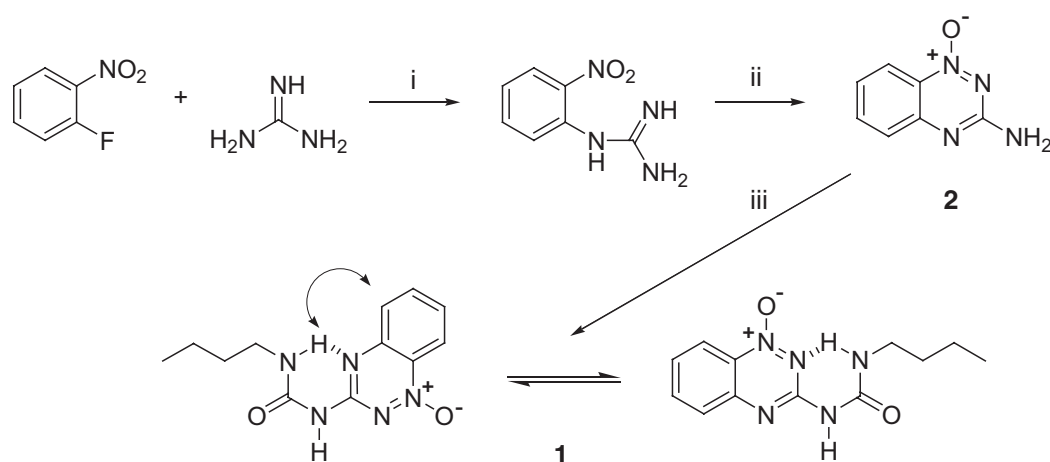
2.2 Quadruple Hydrogen Bonding based on a Benzo-1,2,4-triazine-N-oxide motif

2.2.1 Synthesis and characterization

In general, 1,2,4-triazine-N-oxides can be obtained by two methods: by direct oxidation of the parent triazine with organic peroxides or by the formation of the triazine-N-oxide ring by cyclization.³⁵ 3-Amino-benzo-1,2,4-triazine-1-N-oxide **2**, is a precursor to Tirapazamine (3-amino-benzo-1,2,4-triazine-1,4-dioxide), which is a bioelectronically activated DNA-damaging agent that selectively kills the hypoxic cells found in solid tumors.^{36,37} A common method to obtain **2** involves a (violent exothermic) reaction of 2-nitroaniline with cyanamide.³⁸⁻⁴⁰ However, a more elegant approach was introduced by Suzuki *et al.* who reported the nucleophilic aromatic substitution between nitroarenes and free guanidine base followed by base-induced cyclization.^{41,42} Because of the notorious difficulty in handling free guanidine, which is such a strong base that it rapidly absorbs carbon dioxide and moisture from the air to form the stable guanidinium carbonate, the free base was prepared by passing an aqueous solution of guanidine hydrochloride through an ion exchange column (DOWEX 550A OH) and evaporation of the eluate in vacuo. 3-Amino-benzo-1,2,4-triazine-1-oxide **2** was subsequently obtained in 96% yield through reaction of *o*-fluoronitrobenzene with free guanidine followed by in situ cyclization with KO-*t*-Bu. Condensation of **2** with butylisocyanate gave the desired product **1** as bright yellow crystals in 31% yield.

Compound **1** can potentially exist in two conformers, each of them characterized by a different intramolecular hydrogen bond (Scheme 2.2, structures **1a** and **1b**). It was anticipated that compound **1** would feature an ADAA array of hydrogen bonding sites (conformation **1a**), presumably because N4 bears a larger electron density than N2 (NPA charges roughly (-0.6 and -0.4, respectively)). To elucidate the conformation in solution, Nuclear Overhauser Effect (NOE) experiments using selective excitation were performed.⁴³ The presence of conformation **1a** in CDCl₃ and in DMSO-*d*₆ was indeed confirmed by observation of the intramolecular NOE contact indicated in Scheme 2.4. X-ray analysis of the product showed that the molecule features an intramolecular hydrogen bond from the urea NH to N4 in the triazine ring to

display an ADAA array of hydrogen bonding sites in the solid state. The unit cell contains two independent molecules, one of which exhibits disorder in the butylureido group. The N-N distance between the nitrogen atoms involved in the intramolecular hydrogen bond (average distance 2.68 Å) is larger than the C-C distance between the atoms connected to the central N-H (average distance 2.58 Å). In addition, the corresponding C-N-C angles for the two independent molecules are 129.38° and 129.18°. The molecule is also not fully planar since the triazine ring is at an angle of 8.0° and 2.0° with the ureido group for the non-equivalent molecules in the unit cell. Specifically, the observed deviations from linearity in the hydrogen bond array could have an effect on the capability of **1** to form multiple hydrogen bonded arrays with complementary molecules.



Scheme 2.4 Synthesis of 3-butylureido-benzo-1,2,4-triazine-1-N-oxide **1**; i: 4 h, THF, 70 °C; ii: KO-*t*-Bu, 2 h, THF, 70 °C, 96%; iii: *n*-butylisocyanate, 20 h, pyridine, 110 °C, 31%. The observed NOE effect is indicated with a double headed arrow.

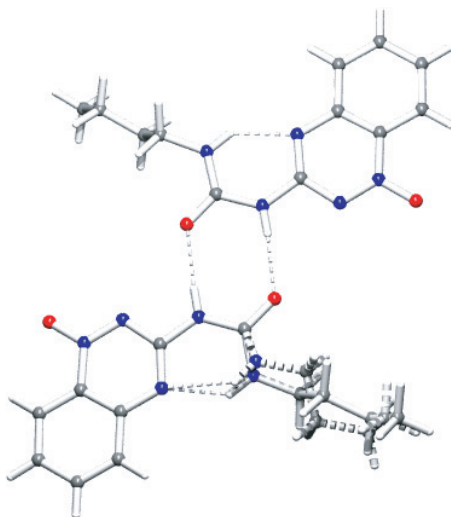
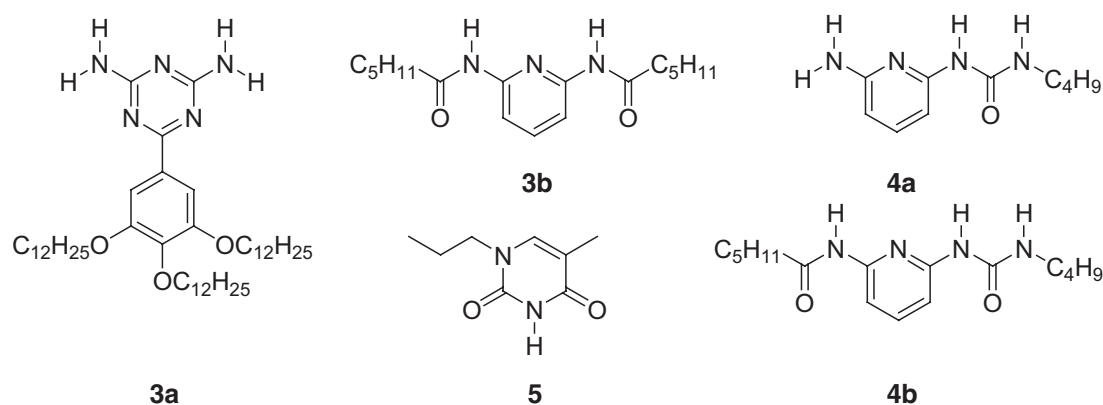


Figure 2.1 Pluton representation of the single-crystal X-ray structure of compound **1**.

2.2.2 Binding studies

Since dimerization of **1** by double hydrogen bonds was observed in the solid state, dimerization in CDCl₃ solution was determined by ¹H NMR dilution experiments. To a minor extent **1** was found to self associate ($K_{\text{dim}} < 5 \text{ M}^{-1}$ in CDCl₃ at 25 °C). Association of **1** with compounds **3** and **4**, featuring DAD and DADD arrays respectively, was investigated by ¹H NMR titration experiments (Scheme 2.5). For comparison, association constants of compounds **3** and **4** with 1-N-propylthymine **5** are included in Table 2.1.



Scheme 2.5 Compounds used in the association with **1**.

Table 2.1 Association constants in M^{-1} of **1** and **5** with **3** and **4** determined in CDCl₃ at 25 °C.

compound	1	probe (signal)	5
3a	106 ± 13 (1.7) ^a	3a (NH ₂)	845 ^d
3b	83 ± 17 (1.8) ^a	3b (NH-amide)	460 ^e
4a	< 10 ^b	4a (NH ₂)	57 ^d
4b	< 10 ^c	4b (NH-amide)	110 ^d

^a CIS values (ppm) given in parentheses. ^b The fit was obtained for 5 data points due to broadening of the NH₂ hydrogen signals. ^c The fit was obtained for 5 data points due to overlap in signals. ^d literature data from Söntjens *et al.*²³ ^e literature data from Beijer *et al.*⁴⁴

Although 1-N-propylthymine binds moderately to DAD molecules **3a** and **3b** (845 and 460 M^{-1} respectively), compound **1** displays a lower binding constant (106 and 83 M^{-1} , respectively). In this case, the complementary ADA binding motif of **1** can be both conformation **1a** which is observed in solution and solid state as described in the previous paragraph, as well as conformation **1b** with the intramolecular hydrogen bond towards N2 in the triazine ring (see Scheme 2.2). However, association of **1** with **3a** and **3b** is not accompanied with a significant shift of the intramolecular hydrogen bond indicating that no structural

adjustment occurs upon binding, and the intramolecular hydrogen bond to N4 in the triazine ring is maintained. Moreover, no NOE contacts as indicated in Scheme 2.4 could be observed. Binding of pyridylureas **4** to **1** forming DADD-ADAA arrays was investigated to determine the existence of an energy gain due to favorable hydrogen bonding with the N-oxide. In solution as well as in the solid state, pyridylureas are known to display an intramolecular hydrogen bond from the urea NH to the nitrogen in the pyridine ring and double hydrogen bonds between two individual molecules.^{45,46} Upon complexation with a complementary binding motif, these bonds can be broken.⁴⁶⁻⁴⁸ The ability of **5** to bind to **4** confirms the low energetic penalty in the disruption of this process. However, ¹H NMR titrations of **1** with **4** show very low association constants ($< 10 \text{ M}^{-1}$). These at first glance surprising results suggest a weak to no ability of the N-oxide to form a hydrogen bond.

2.2.3 Quantum mechanical calculations

Even though the presence of an AADA array is indicated in solution and in the crystal structure of **1**, formation of quadruple hydrogen bonded complexes in solution was not found with seemingly complementary agents. Two questions might be answered with computational calculations: i) is there a large difference in energy between conformations **1a** and **1b**, and ii) what are the stabilities of hydrogen bonded complexes of these conformations and the corresponding partners? Finally, the combination of experimental and theoretical data can be used to explain the observed absence of intermolecular hydrogen bonding here, and provide deeper insight in the phenomenon of multiple hydrogen bonding. The reported calculations below were performed by Dr. D. Guo and Dr. H. Zuilhof.

Previously, extensive theoretical investigations have been reported on hydrogen bonded dimers.⁴⁹ More recently, multiple hydrogen bonded systems, including DNA base pairs,^{50,51} have also been studied theoretically, in order to rationalize relative stabilities.^{8,52-54} Validation of studies of electronic energies and free energies in solution showed that quantum mechanical techniques could be used to perform calculations on molecular systems of practical significance. More specifically, density functional B3LYP calculations recently confirmed the strong homodimerization of ureido-pyrimidinone (UPy) molecules in the keto tautomer and enol tautomer. For the keto tautomer, experimental hydrogen bond distances $r(\text{N-N})$ and $r(\text{N-O})$ are 2.97 and 2.76 Å,¹² respectively, while the B3LYP/6-311G(d,p)-computed values are 3.01 and 2.78 Å, respectively.⁵³ The ΔG° value of dimerization 'in solution' (mimicked by a polarized dielectric medium) was calculated to be -11.29 kcal/mol, which is in close agreement

with the experimental value of -12.1 kcal/mol in chloroform.¹³ Since in those cases agreement within experimental error was found for these parameters, the same methods were used to evaluate differences in the possible conformations of **1** and stabilities of the hydrogen-bonded complexes of **1** with complementary compound **4a** and 2,6-diaminopyridine (dap).

2.2.3.1 Geometry optimization

The calculated energy difference between **1a** and **1b** using specific methods and basis sets is displayed in Table 2.2. The calculated energy differences between **1a** and **1b** is only 1 kcal/mol at the B3LYP/6-311G(d,p) level (entry 1). Further stepwise increase of the basis set size up to B3LYP/6-311+G(2df,2p) (entry 2) shows no changes, suggesting that the basis set at the B3LYP/6-311G(d,p) level is appropriate. Thus the set of data primarily implies that the stabilities of **1a** and **1b** are close. At the B3LYP/6-311G(d,p) level, the free energy of **1a** is slightly lower than that of **1b** (~ 0.70 kcal/mol) which means that the equilibrium between the two conformations favors **1a**. Furthermore, the energy difference between the 2 conformations at the LMP2/6-311G(d,p)//B3LYP/6-311G(d,p) level is 0.90 kcal/mol and at the LMP2/6-311+G(d,p)//B3LYP/6-311G(d,p) level **1a** is favored by 0.44 kcal/mol (entries 3 and 4). These data, obtained with several totally different high-level methods, all suggest that the two conformations of **1** display similar stabilities, with a slightly lower energy for **1a**. In addition, the energy difference in CHCl₃ was calculated via a polarized continuum model⁵⁵ to be 1.07 kcal/mol (entry 5). The dipole moments were calculated to be 6.16 and 4.51 Debye, respectively for **1a** and **1b** at the B3LYP/6-311G(d,p) level. The fact that the dipole moment of **1a** is slightly higher than that of **1b** may be the reason why **1a** is slightly more stabilized than **1b** in solution. In summary, the two conformations of **1**, which differ in the site of intramolecular hydrogen bonding, have little difference in stabilities in either gas or solution phase. Although NOE NMR experiments show that conformer **1a** is present in solution, the small calculated energy differences suggests that conformations **1a** and **1b** exist in roughly equal amounts in solution ($K_a \sim 0.2$).

Table 2.2 Energy differences between **1a** and **1b** from different methods and basis sets.

entry	Method and basis set	ΔE^0 (kcal/mol)
1	B3LYP/6-311G(d,p)	0.67
2	B3LYP/6-311+G(2df,2p)//B3LYP/6-311G(d, p)	1.01
3	LMP2/6-311G(d,p) //B3LYP/6-311G(d,p)	0.90
4	LMP2/6-311+G(d,p)//B3LYP/6-311G(d,p)	0.44
5	B3LYP/6-11+G(d,p), Sol//B3LYP/6-311G(d,p)	1.07

Notes: 1) At B3LYP/6-311G(d,p) level, $\Delta H^{298} = 0.66$ kcal/mol; $\Delta G^{298} = 0.50$ kcal/mol; 2) According to $\Delta G^{298, \text{sol}} = \Delta G^{298} - \Delta(\Delta E^{\text{sol-gas}})$, $\Delta G^{298, \text{sol}} = 0.95$ kcal/mol where $\Delta(\Delta E^{\text{sol-gas}}) = \Delta E^{\text{gas}} - \Delta E^{\text{sol}}$, in which ΔE was taken at B3LYP/6-311+G(d,p), CHCl₃//B3LYP/6-311G(d,p).

2.2.3.2 Hydrogen bonding abilities with complementary motifs

The hydrogen bonding combinations of **1a** and **1b** with both **4a** and 2,6-diaminopyridine have been fully optimized to obtain information about the structure and stability of the corresponding heterodimers. The calculated results are collected in Table 2.3. Remarkably, the free energies in CHCl₃ solution ($\Delta G^{298, \text{sol}}$) in all complexes of **1a** and **1b** are all significantly positive, indicating that complexes of **1** are less stable in solution than the corresponding set of monomers. This is unlike the situation reported earlier for the self-complexation of quadruple hydrogen-bonded UPy units, which display strong hydrogen-bonding that is also computed. Therefore, the current data strongly suggest that little to no complex formation can be expected, as was indeed experimentally observed. Furthermore, the stability of the complexes decreases in the following order: **1a** – **dap** > **1a** – **4a** > **1b** – **4a** > **1b** – **dap**. This trend was mimicked when more sophistication was added in the computations, e.g. by going from total energies to free energies i.e. inclusion of vibrational energy, and intrinsic entropy effects, apart from those involved in solvation (results not included in Table 2.3). Especially the free energies computed in dielectric medium mimicking CHCl₃ ($\Delta G^{298, \text{sol}}$) were found to increase in the same order as in the gas phase. Therefore, the decrease in stabilization is not due to solvation effects. The calculated dipole moments of the complexes (Table 2.3) are larger than in UPy dimers (~ 0.2 Debye), which implies significant solvent stabilization of the dipole. However, the complexation energies are positive. Therefore, the effects are believed to be truly intrinsic. Although the differences are small, the computed data indicate that complexes of **1a** are slightly more stable than those of **1b**. As found experimentally, binding to a DAD array is more favorable than to a DADD array.

Table 2.3 Comparison of binding abilities between molecules (kcal/mol).

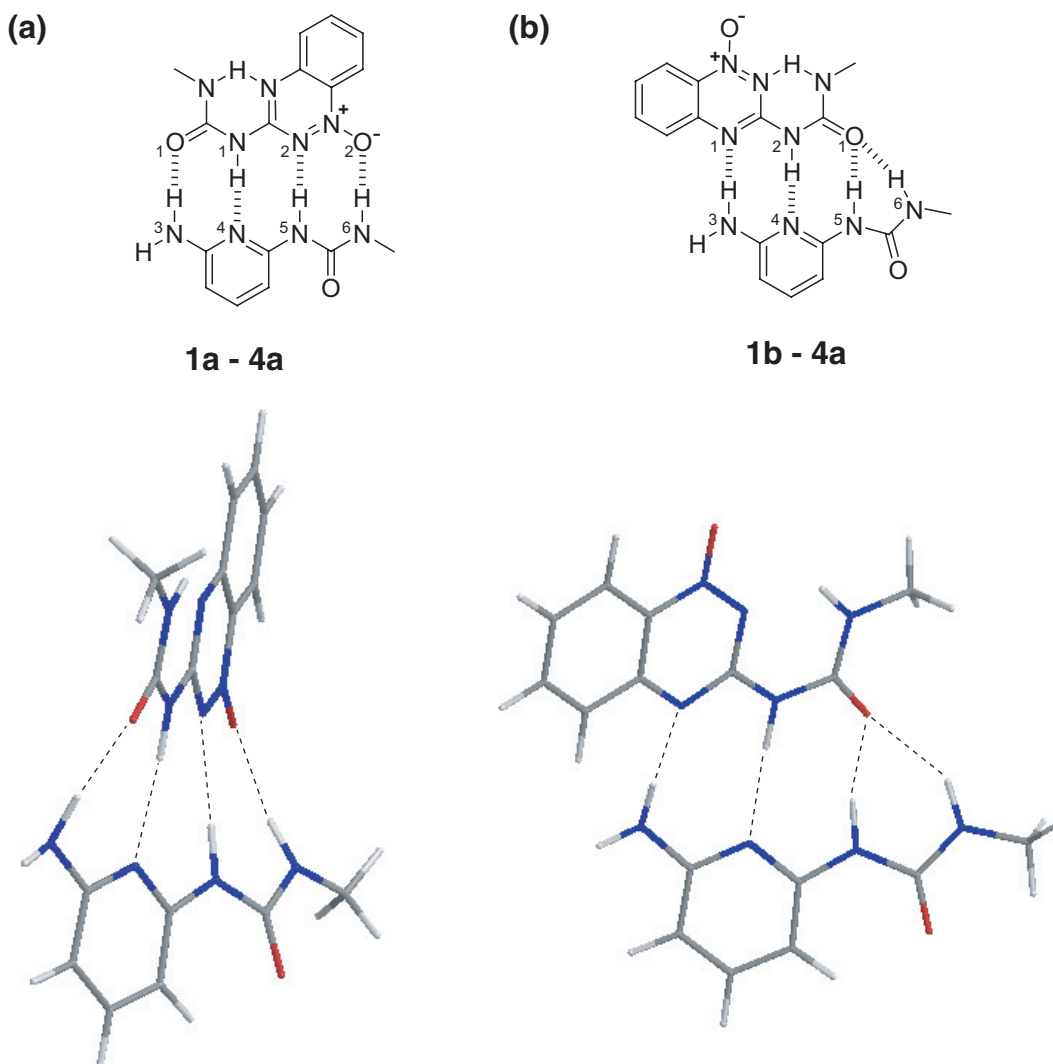
entry	complex	ΔE^o ^a	ΔH^{298} ^a	ΔG^{298} ^a	$\Delta G^{298, \text{sol}}$ ^b	Dipole (Debye) ^c
1	1a – 4a	-16.5102	-15.0483	-2.3350	5.7230	13.8022
2	1a – dap	-16.8883	-15.3117	-2.4935	5.5358	11.5170
3	1b – 4a	-14.8924	-13.1326	-0.1497	6.8127	8.0693
4	1b – dap	-13.5272	-12.8727	1.0285	6.9352	5.4843

^a Optimized at the B3LYP/6-311G(d,p) level; ^b $\Delta G^{298, \text{sol}} = \Delta G^{298} - \Delta(\Delta E^{\text{sol-gas}})$, where $\Delta(\Delta E^{\text{sol-gas}}) = \Delta E^{\text{gas}} - \Delta E^{\text{sol}}$, in which ΔE was taken at B3LYP/6-311+G(d,p), CHCl₃//B3LYP/6-311G(d,p); ^c Optimized at the 6-311+G(d,p), CHCl₃//6-311G(d, p).

To compare the differences in structure, the hydrogen bond lengths of heterodimers **1a-4a** and **1b-4a** have been collected in Table 2.4. A two and three dimensional picture of the optimized structures of the heterodimers is given in Scheme 2.6. The computed hydrogen bonding lengths of complex **1a-4a** are between 2.91 and 3.20 Å. These lengths are significantly longer than distances found by both X-ray determination as well as computational methods for strong multiple hydrogen bonded motif which are between 2.70 and 3.00 Å. An additional feature indicating weak association of the individual molecules is the significantly longer distances of the two middle hydrogen bonds. In this way, a concave molecule is formed which is not capable of strong binding to the more linear pyridylurea **4a**. A similar explanation can be given for weak binding of **1b** to **4a**. Even though the carbonyl group of **1b** is involved in a bifurcated hydrogen bond to the urea of **4a**, hydrogen bond lengths do not indicate strong binding. Furthermore, geometry optimization clearly shows that the individual molecules in the heterocomplexes are not planar. In fact, the angles between the two π -planes are 28.5° and 26.9° for complex **1a-4a** and **1b-4a**, respectively. These findings suggest that the electronic fine structure of **1** prevents the formation of ADAA – DADD complexes. Apparently, triazine-N-oxides are weaker hydrogen bond acceptors than pyridine-N-oxides. In addition, upon formation of the hydrogen bond dimer, the structures of **1a** and **4a** need to be deformed with respect to their (planar) structure prior to dimerization, and this deformation energy amounts to almost 2 kcal/mol.

Table 2.4 Calculated hydrogen bond lengths in **1-4b** complexes.

atom pair 1a – 4a	O1-N3	N1-N4	N2-N5	O2-N6
bond length (Å)	2.907	3.150	3.195	3.041
atom pair 1b – 4a	N1-N3	N2-N4	O1-N5	O1-N6
bond length (Å)	3.131	3.159	2.866	3.131

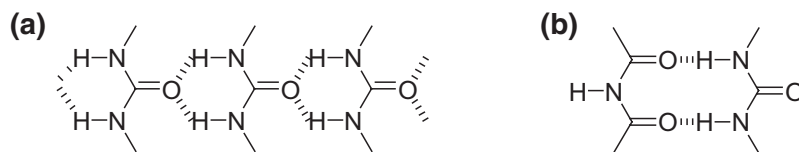


Scheme 2.6 Optimized structures of complexes **1a-4a** and **1b-4a**.

2.3 Hydrogen bonding based on an imide motif

Although the urea group has been studied extensively as a double hydrogen bonding donor module, the complementary array is often the single carbonyl group of a second urea molecule (Scheme 2.7a). Therefore, the formed bifurcated hydrogen bond lacks directionality due to self-complementarity of the urea and is not very strong as compared to multiple hydrogen bond motifs (as urea association is a cooperative process, $K_{\text{dim}} \sim 10^2 \text{ M}^{-1}$ while $K \sim 10^3 \text{ M}^{-1}$).^{56,57} Directionality can be accomplished by employing the two carbonyl groups of an imide functionality as a double hydrogen bonding acceptor (Scheme 2.7b). However, in literature single AA binding motifs are hardly explored. Etter *et al.* were the first to report the use of acyclic imides in hydrogen bond directed cocrystallization.⁵⁸ In order to display two hydrogen bond acceptor sites, the imide should be pre-organized into the *Z,Z* conformation in solution. A

successful procedure to pre-organize benzoyl amides based on three-center hydrogen bonding system, consisting of an S(6) type⁵⁹ hydrogen bonded ring was reported previously by Gong *et al.*⁶⁰ It not only persisted in the solid state and CHCl₃ solution but also in the highly polar solvent DMSO.^{61,62}

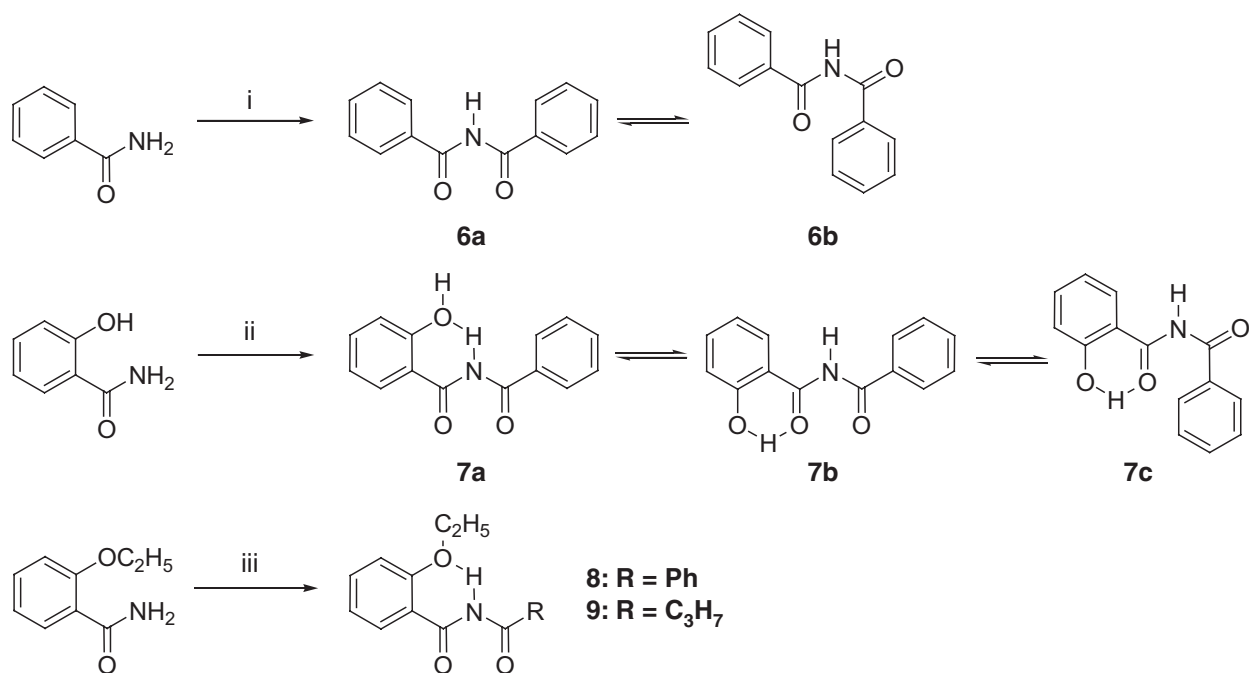


Scheme 2.7 (a) Bifurcated hydrogen bonds between urea groups. (b) Complementary double hydrogen bonding based on urea and imide groups.

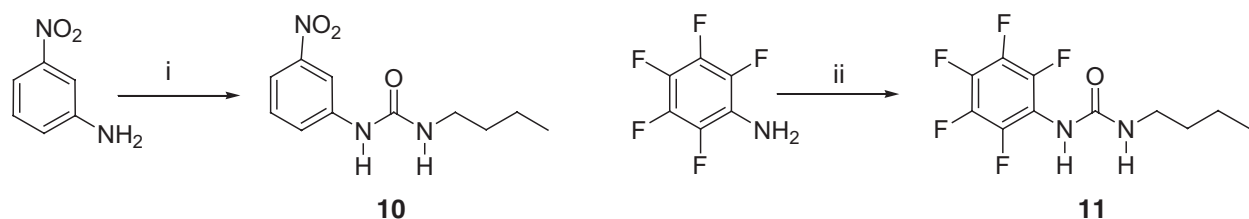
2.3.1 Synthesis and characterization

In general, imides are obtained by acylation of amides with acid chlorides in the presence of a base catalyst depending on the nucleophilicity of the amide used. Dibenzamide **6** was obtained from a pyridine catalyzed condensation of benzamide and benzoyl chloride. Recrystallization from diethyl ether gave colorless needles (30%).⁶³ Similarly, N-benzoyl-salicylamide **7** was obtained by condensation of salicylamide with benzoyl chloride. Crystals were obtained by crystallization from 1/1 v/v% EtOH/toluene (77%). Elevated temperatures were needed for the reaction of 2-ethoxybenzamide with benzoyl chloride and butyryl chloride. The desired products **8** and **9** were obtained after recrystallization from diisopropyl ether (24%) and purification by column chromatography (20%), respectively. A pronounced difference in reactivity between the amides and benzoyl chloride was observed: salicylicamide > benzamide >> 2-ethoxybenzamide. This has been explained by a higher reactivity of the hydroxy group of the salicyl amide towards acylation, thus forming O-benzoylsalicylamide which rearranges to the imide N-benzoylsalicylamide.⁶⁴⁻⁶⁶ Moreover, the amide group in 2-ethoxybenzamide is less nucleophilic due to intramolecular hydrogen bonding.

As a complementary motif, used for complexation studies with imides **6-9**, 1-butyl-3(3-nitrophenyl)-urea **10** and 1-butyl-3(2,3,4,5,6-pentafluorophenyl)-urea **11** were synthesized by a DMAP-catalyzed reaction of the appropriate aniline and *n*-butylisocyanate (Scheme 2.9). Phenyl urea derivatives with strongly electron accepting substituents on the meta position have been reported to adopt a conformation in which the phenyl and urea groups are coplanar, masking the acceptor character of the carbonyl group for self-association.^{67,68}



Scheme 2.8 Synthesis of acyclic imides **6-9**; i: benzoyl chloride, pyridine, 16 h, CH₂Cl₂, RT; ii: benzoyl chloride, pyridine, 2 h, CH₂Cl₂, RT; iii: benzoyl chloride or butyryl chloride, 16 h, pyridine, 80 °C.



Scheme 2.9 Synthesis of activated urea **10-11**; i: DMAP, *n*-butylisocyanate, 20 h, CHCl₃, reflux; ii: DMAP, *n*-butylisocyanate, 20 h, pyridine, reflux.

Studies of derivatives **6** and **7** in the solid state have been reported and revealed that these imides are in the *Z,Z* conformation (**6a** and **7a**).^{58,69} In organic solvents like chloroform and dioxane, however, conformation **6b** and a mixture of **7b** and **7c** is reported.^{70,71} Factors such as dipole-dipole interaction and steric effects are the main cause that acyclic imides are found in the *E,Z* conformation in solution.⁷² A clear indication of the pre-organization in CDCl₃ solution of **8** and **9** can be seen in the ¹H NMR spectrum which reveals the presence of a broad signal at 11.2 and 10.4 ppm for **8** and **9**, respectively. This signal does not shift upon dilution indicating the presence of an intramolecular hydrogen bond between the imide N-H and the oxygen atom of the ethyl ether. The presence of the *Z,Z* conformation in **8** and **9** will have to be confirmed by complexation data since the data presented is also valid for the *E,Z* conformation.

By single X-ray structure determination of **8**, several hydrogen bonds are observed while the required *Z,Z*-conformation is present (Figure 2.2). An intramolecular hydrogen bond is formed between the imide N-H and the oxygen atom of the ether functionality (Figure 2.2a). The $N_{\text{imide}} - O_{\text{ether}}$ distance of 2.65 Å is indicative of a strong hydrogen bond. Also three C-H...O interactions are observed of which two ensure the molecules to orient in the [0, 1, -1] direction as a double ribbon and one orienting the molecules in the [0, 1, 0] direction (Figure 2.2b and c). Furthermore, the molecule is not fully planar. Although the imide group is in plane with the 2-ethoxybenzene ring, the other ring is at an angle of 40.6°. Since both carbonyl groups are involved in intermolecular hydrogen bonding in the solid state, interaction with hydrogen bond donors in solution is expected.

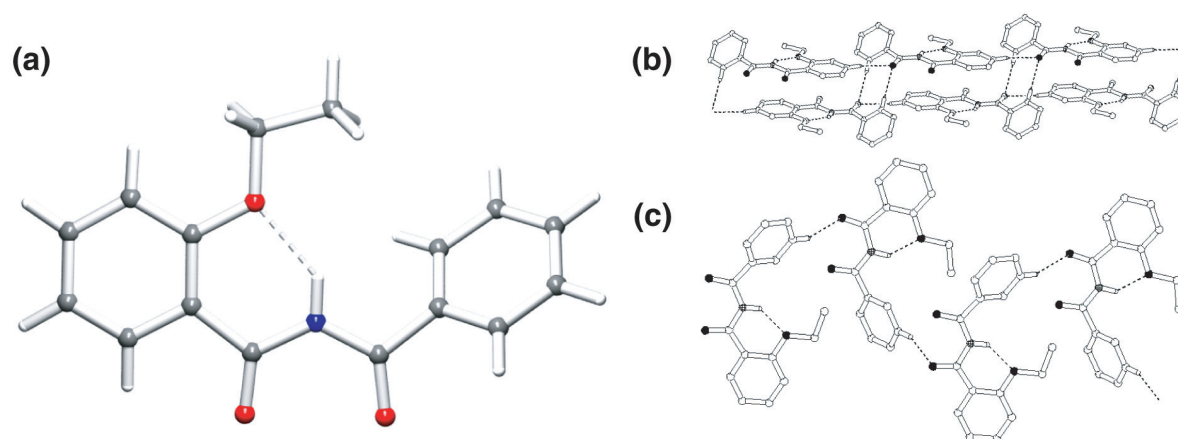


Figure 2.2 Pluton representation of single-crystal X-ray structure of compound **8**.

2.3.2 Binding studies

The formation of hydrogen bonded complexes was substantiated by ^1H NMR spectroscopy. Titrations of urea **10-11** to **6-9** were performed in CDCl_3 at 298 K in which the downfield shift of urea NHCH_2 was used as a probe to determine the association constants (K_a). Dilution of ureas **10** and **11** in the concentration range of interest monitored by ^1H NMR revealed an almost concentration independent chemical shift for **10**, while for **11** a dimerization of 18 M^{-1} was observed. Apparently, the hydrogen bond acceptor character of the carbonyl group for self-association is blocked more effectively in **10** than in **11**. In determination of K_a values, however, dimerization of the urea compounds was ignored. Similarly, imides are known to form intermolecular hydrogen bonds in solution but at the concentrations used in this study, K_a values were negligibly affected. The association constants are collected in Table 2.5.

Table 2.5 Association constants in M^{-1} determined in $CDCl_3$ at 25 °C.

entry	imide	urea	K_a , M^{-1} ^a
1	6	10	38 ± 6.8 (1.8)
2	7	10	< 10
3	8	10	260 ± 3.0 (1.9) ^b
4	8	11	97 ± 3 (1.8) ^b
5	9	10	65 ± 2 (1.4)
6	9	11	20 ± 4 (1.6)

^a CIS values (ppm) given in parentheses. ^b average value of 2 measurements

A significant difference can already be seen between the association of **6** and **7** with **10** (entries 1 and 2). Although a low K_a value of $38 M^{-1}$ was determined for complex **6-10**, no complexation was observed when **7** was used. This is in line with the presence of an intramolecular hydrogen bond from the hydroxy group to one of the imide carbonyl groups (conformation **7b**). The higher degree of pre-organization in the desired *Z,Z* conformation in imide **8** is expressed in the high K_a values with ureas **10** and **11** of 260 and $100 M^{-1}$, respectively (entries 3 and 4). The K_a value of $260 M^{-1}$ corresponds to a free energy of association (ΔG°) of $-3.3 \text{ kcal/mol}^{-1}$ which equals $-1.65 \text{ kcal/mol}^{-1}$ for a single hydrogen bond. When two imides are incorporated in a similar pre-organized fashion, a theoretical K_a value for binding with complementary bis-urea motifs of $7 \cdot 10^4 M^{-1}$ is obtained. The fact that decreased association occurs when the benzoyl group of **8** is replaced by a butyryl group (entries 5 and 6), can be rationalized by a loss of pre-organization. The smaller butyryl group will cause a decrease in the rotational barrier. Therefore, the imide will exist preferentially in its *E,Z* conformation in solution. Additional evidence for the AA-DD mode of association for complexes **8-10** and **8-11** in solution was obtained by 2D-NOESY NMR experiments.⁷³ The presence of the *Z,Z* conformation in $CDCl_3$ was indeed confirmed by observation of the intramolecular NOE contacts indicated by double headed arrows in Figure 2.3. The contacts indicate formation of the complex with a specific relative orientation which is probably due to electronic properties of the individual components.

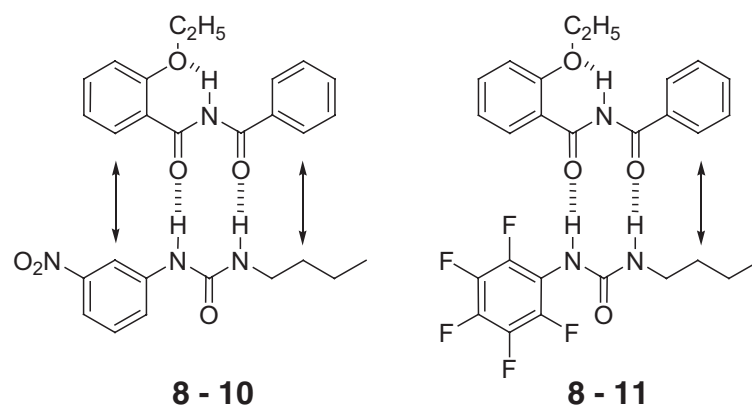


Figure 2.3 Intermolecular NOE contacts in chloroform solution of complexes **8-10** and **8-11** (indicated with a double headed arrow).

2.4 Conclusions

It was shown that 3-butylureido-benzo-1,2,4-triazine- $\text{N}-1$ -oxide **1**, which is readily available by condensation of an isocyanate with 3-aminobenzo-1,2,4-triazine- $\text{N}-1$ -oxide **2**, displays an ADAA hydrogen bonding motif. Although significant binding to a complementary DAD array is observed in chloroform solution, very weak association was reported for seemingly complementary DADD arrays. Geometry analysis of conformations **1a** and **1b** by *ab initio* methods at DFT levels of theory indicated no significant differences in free energy levels in solution. These results were confirmed by calculations at local MP2 level. Significant positive free energies of association of **1** with a ureidopyridine and diaminopyridine in the gas phase as well as in solution confirmed the experimental observation that little or no complex formation can be expected. The ineffectiveness of this ureido-benzotriazine- N -oxide derivative in the complexation of ureidopyridines is not yet fully understood, but may be related to a low hydrogen bond basicity of the N -oxide oxygen atom in this particular system.

The rational design of pre-organized acyclic imides to display an AA hydrogen bonding array was reported. Pre-organization of the imide into its Z,Z conformation was achieved by means of formation of an intramolecular hydrogen bond between the imide $\text{N}-\text{H}$ and the oxygen atom from the ether functionality *ortho* to the imide. This was confirmed in the solid state by X-ray structure analysis and 2D-NOESY NMR in chloroform solution. Significant increase in binding to ureas was observed for the imides compared to reference imides without pre-organization. An important factor in the association of these imides and ureas could be the limited acceptor character of the urea carbonyl, thereby limiting self-association of the urea molecules. The pre-organized AA array based on Z,Z imides seems eminently suitable as a modular building block in the synthesis of supramolecular architectures where complementary multiple hydrogen binding is important. Furthermore, due to the large spacing between the

hydrogen bonds, repulsive secondary interactions are minimized. A modular approach can now be envisioned towards extending the pre-organization strategy in order to generate complementary quadruple hydrogen bonding arrays using bis-imides and bis-urea molecules.

2.5 Experimental procedures

General methods. All synthetic procedures were performed under inert atmosphere of dry nitrogen unless stated otherwise. Commercial solvents and reagents were used without purification unless stated otherwise. Pyridine was dried over 4 Å molecular sieves prior to use. ^1H NMR and ^{13}C NMR spectra were recorded on a Varian Gemini 300, Varian Mercury 400 or Varian Inova 500 spectrometer. Chemical shifts are reported in ppm relative to tetramethylsilane (TMS) and multiplicities as singlet (s), doublet (d), triplet (t), quartet (q) and multiplet (m). Matrix assisted laser desorption/ionization mass-time of flight (MALDI-TOF) were obtained using a PerSeptive Biosystems Voyager-DE PRO spectrometer using an acid α -cyanohydroxycinnamic acid (CHCA) or a neutral 2-[(2E)-3-(4-*t*-butylphenyl)-2-methylprop-2-enylidene]malononitrile (DCTB) matrix. Electrospray ionization mass spectrometry (ESI-MS) was carried out on a PE-Sciex API 300 LC/MS/MS System mass spectrometer with a mass range of 3000. Infrared (IR) spectra were recorded on a Perkin Elmer Spectrum One FT-IR spectrometer with a Universal ATR sampling Accessory. Elemental analysis was performed on a Perkin Elmer 2400 series II CHNS/O Analyzer. Melting points were determined on a Büchi Melting Point B-540 apparatus.

Single crystal X-ray structure determination for compound 1: $\text{C}_{12}\text{H}_{15}\text{N}_5\text{O}_2$, $M_r = 261.29$, yellow block-shaped crystal (0.2 x 0.3 x 0.3 mm), monoclinic, space group $P2_1/c$ (no. 14) with $a = 10.917(10)$, $b = 19.4699(10)$, $c = 12.785(3)$ Å, $\beta = 110.518(10)^\circ$, $V = 2545.0(7)$ Å³, $Z = 8$, $D_x = 1.364$ g cm⁻³, $F(000) = 1104$, Mo $K\alpha = 0.098$ mm⁻¹. 69404 Reflections measured, 5814 independent reflections, $R_{\text{int}} = 0.0529$, $R_\sigma = 0.0263$, $1.00^\circ < \theta < 27.48^\circ$, $T = 150$ K, Mo $K\alpha$ radiation, graphite monochromator, $\lambda = 0.71073$ Å. Data were collected on an Nonius KappaCCD area detector on rotating anode. The structure was solved by direct methods (shelxs86) and refined on F^2 using shelxl-97-2. The NHBu moiety of one of the two independent molecules is disordered over two positions. A disorder model was introduced; the occupancy of the major component refined to 0.800(2). Positional parameters of the ordered N-H hydrogen atoms were refined, all other hydrogen atoms were included in the refinement on calculated positions riding on their carrier atoms. The non-H atoms of the minor disorder component were included in the refinement with a fixed isotropic displacement parameter, set equal to the equivalent isotropic displacement parameter of the corresponding atom in the major disorder component. All other non-hydrogen atoms were refined with anisotropic displacement parameters. Hydrogen atoms were refined with a fixed isotropic displacement parameter linked to the value of the equivalent isotropic displacement parameter of their carrier atoms. Final $wR2 = 0.1131$, $w = 1/[\sigma^2(F^2) + (0.0618P)^2 + 0.28P]$, where $P = (\max(F_o^2, 0) + 2F^2)/3$, $R1 = 0.0409$ (for 4205 $I > 2\sigma(I)$), $S = 1.030$, 370 refined parameters, $-0.23 < \Delta\rho < 0.22$ e Å⁻³.

Single crystal X-ray structure determination for compound 8: C₁₆H₁₅NO₃, $M_r = 269.29$, colorless needles (0.1 x 0.1 x 0.3 mm), monoclinic, space group C21/c (no. 15) with $a = 17.439(3)$, $b = 11.812(3)$, $c = 13.649(3)$ Å, $\beta = 103.515(9)^\circ$, $V = 2733.7(10)$ Å³, $Z = 8$, $D_x = 1.309$ g cm⁻³, $F(000) = 1136$, $\mu(\text{Mo K}\alpha) = 0.091$ mm⁻¹. 29329 Reflections measured, 3132 independent reflections, $R_{\text{int}} = 0.0698$, $R_\sigma = 0.0481$, $1.00^\circ < \theta < 27.48^\circ$, $T = 150$ K, Mo K α radiation, graphite monochromator, $\lambda = 0.71073$ Å. Data were collected on an Nonius KappaCCD area detector on rotating anode. The structure was solved by direct methods (shelxs86) and refined on F^2 using shelxl-97-2. Positional parameters of all hydrogen atoms were refined. Non-hydrogen atoms were refined with anisotropic displacement parameters. Hydrogen atoms were refined with a fixed isotropic displacement parameter linked to the value of the equivalent isotropic displacement parameter of their carrier atoms. Final $wR2 = 0.1104$, $w = 1/[\sigma^2(F^2) + (0.0598P)^2]$, where $P = (\max(F_o^2, 0) + 2F_c^2)/3$, $R1 = 0.0428$ (for 2044 $I > 2\sigma(I)$), $S = 1.021$, 226 refined parameters, $-0.21 < \Delta\rho < 0.22$ e Å⁻³.

Binding experiments: For the ¹H NMR titrations, CDCl₃ (Cambridge Isotope Laboratories) was dried and de-acidified over activated alumina (type I) and stored on 4 Å molsieves. DMSO-*d*₆ was dried over 4 Å molsieves. At least 8 data points in the 20-80% saturation range were measured using temperature control at 25 °C unless stated otherwise. The association constants were evaluated by non-linear least-squares computer fitting of the concentration dependence of the chemical shifts of NH protons to a 1:1 binding isotherm ignoring dimerization of the individual components using standard methods.⁷⁴

Computational methods: The molecular geometries of **1a** and **1b** and hydrogen-bonded complexes have been fully optimized using density functional theory (DFT) with the B3LYP functional as implemented in Gaussian03.⁷⁵ To obtain the single point energies with diffuse functions, **1a** and **1b** have also been calculated at 6-311+G(d,p), 6-311+G(2d,2p), and 6-311+G(2df,2p) basis sets. In addition, the total energy in chloroform solution has been calculated via a Polarized Continuum model (PCM model), in which the solution is represented as a continuum. Free energies in solution were determined as follows after deciding the geometries of the monomers or complexes: $\Delta G^{298, \text{sol}} = \Delta G^{298} - \Delta(\Delta E^{\text{sol-gas}})$ where $\Delta(\Delta E^{\text{sol-gas}}) = \Delta E^{\text{gas}} - \Delta E^{\text{sol}}$ in which ΔE was taken at B3LYP/6-311+G(d,p)//B3LYP/6-311G(d,p) or B3LYP/6-311+G(d,p), CHCl₃//B3LYP/6-311G(d,p). The geometry was thus optimized at the B3LYP/6-311G(d,p) level of theory, and diffuse functions were added in subsequent single point calculations. Diffuse functions are frequently useful in the description of long-distance interactions, which include the interaction of lone pairs with other entities.

Synthesis. 2,4-Diamino-6-(3,4,5-tri(dodecyloxy)phenyl)-s-triazine **3a** was synthesized according to Beijer *et al.*¹¹ 2,6-Di(hexanoylamino)pyridine **3b** was synthesized according to Bernstein *et al.*⁷⁶ Hexanoic acid (6-amino-pyridin-2-yl)-amide **4a** and hexanoic acid[6-(3-butylureido)-pyridin-2-yl]-amide **4b** were synthesized according to Söntjens *et al.*²³

3-Butylureido-1,2,4-benzotriazine-1-N-oxide 1 To a mixture of 3-amino-1,2,4-benzotriazine-1-oxide **2** (0.26 g, 1.6 mmol) in dry pyridine (4 ml) was added *n*-butylisocyanate (1.58 g, 16 mmol) dropwise. The

suspension was stirred at 110 °C for 16 h. The pyridine was evaporated in vacuo before chloroform was added and the solution was washed with 1M HCl, water, brine and dried. The product could be obtained as yellow block crystals by crystallization from chloroform (0.13 g, 31%). M.P. 140-144 °C; ¹H NMR (CDCl₃): δ = 8.91 (br, 1H, NH), 8.40 (dd, 1H, *J* = 8.0, 0.7 Hz), 7.92 (dt, 1H, *J* = 7.1, 0.8 Hz), 7.80 (dd, 1H, *J* = 8.3, 0.7 Hz), 7.61 (dt, 1H, *J* = 7.0, 0.8 Hz), 7.30 (br, 1H, NH), 3.48 (q, 2H, *J* = 6 Hz), 1.70 (m, 2H), 1.53 (m, 2H), 1.04 (t, 3H, *J* = 7 Hz) ppm. ¹³C NMR (CDCl₃): δ = 154.9, 152.9, 145.9, 136.3, 132.2, 127.8, 126.7, 120.4, 39.9, 31.6, 30.1, 13.6. ppm; ESI-MS: (*m/z*) calcd. 261.29; observed: 262.19 (M+H⁺), 284.17 (M+Na⁺), 545.35 (2M+Na⁺), 806.51 (3M+Na⁺), 1067.70 (4M+Na⁺); FTR-IR (ATR): ν = 3251, 3096, 2931, 2869, 1678, 1579, 1518, 1490, 1419, 1357, 1303, 1280, 1198, 1135, 1050, 962, 840 cm⁻¹; Anal. Calcd. for C₁₂H₁₅N₅O₂: C 55.16, H 5.79, N 26.80; found: C 54.97, H 5.53, N 27.06.

3-Amino-1,2,4-benzotriazine-1-N-oxide 2 Synthesis according to a modified literature procedure:⁴¹ Guanidine hydrochloride (5.74 g, 60 mmol) was passed through an ion exchange column (120 g, DOWEX 550A OH) and the eluate was evaporated in vacuo to yield the free guanidine base as a colorless oil (3.50 g, 59 mmol). To the guanidine, THF (60 mL) and *o*-fluoronitrobenzene (0.70 g, 5.0 mmol) was added and the mixture was stirred at 70 °C for 4 h. KO-*t*-Bu (0.60 g, 5.3 mmol) was subsequently added to the orange mixture followed by an additional 2 hours of stirring at 70 °C. Upon addition of ethyl acetate (40 mL) to the cooled mixture, more yellow precipitate was formed which was isolated by filtration. The crude product was dissolved in hot ethyl acetate and washed with water. The resulting solid was washed with acetone and dried in vacuo to obtain the pure title compound (0.78 g, 96%). Characterization data for the compound corresponded with those reported previously.⁷⁷

Dibenzamide 6 Preparation according to a slightly modified literature procedure.⁶³ To a mixture of benzamide (0.42 g, 3.5 mmol) and pyridine (0.32 g, 4.0 mmol) in dry CH₂Cl₂ (5 mL) cooled on an ice bath was added benzoyl chloride (0.49 g, 3.5 mmol) dropwise. The mixture was allowed to stir at 0 °C for 30 minutes before warming to room temperature for 16 hours under a nitrogen atmosphere. The crude product precipitated from the reaction mixture and was isolated by filtration followed by purification by crystallization from diethyl ether to obtain the title compound as small colorless needles (0.24 g, 30%). Characterization data for the compound corresponded to those reported previously.⁵⁸

N-Benzoyl-salicylamide 7 Preparation according to a slightly modified literature procedure.⁶⁴ To a mixture of salicylamide (0.50 g, 3.6 mmol) and pyridine (0.32 g, 4.0 mmol) in dry CH₂Cl₂ (10 mL) cooled on an ice bath was added benzoyl chloride (0.51 g, 3.6 mmol) dropwise. The mixture was allowed to stir at 0 °C for 1 h and allowed to warm to room temperature for 2 h under a nitrogen atmosphere. The crude product could be isolated after washing the crude reaction mixture with 1M HCl, water, brine and drying with MgSO₄. The title compound was obtained as colorless/white needles by crystallization from 1/1 v/v% EtOH/toluene and subsequent washing with cold EtOH (0.48 g, 77%). ¹H NMR (CDCl₃): δ = 8.24 (d, 2H, *J* = 7 Hz), 7.96 (d, 1H, *J* = 8 Hz), 7.71 (t, 1H, *J* = 8 Hz), 7.59-7.46 (m, 3H), 7.42 (t, 1H, *J* = 8 Hz), 7.25 (d, 1H, *J* = 8 Hz), 6.38 (br, 1H, NH), 5.77 (br, 1H, NH) ppm; ¹³C NMR (CDCl₃): δ = 167.3, 164.7, 148.2, 134.0, 132.3, 130.3, 130.1, 128.8, 128.7, 127.4, 126.3, 123.2 ppm; IR-Characterization of the compound was similar as reported previously.⁶⁵

N-Benzoyl-2-ethoxybenzamide 8 To a mixture of 2-ethoxybenzamide (0.58 g, 3.5 mmol) in dry pyridine (4 ml) cooled on an ice bath was added benzoyl chloride (0.49 g, 3.5 mmol) dropwise. The mixture was allowed to stir at 0 °C for 30 minutes before heating to 80 °C for 16 h under a nitrogen atmosphere. The pyridine was removed *in vacuo* and chloroform (10 ml) was added before washing with 1M HCl, water, brine and drying. The product was obtained as colorless needles by crystallization from diisopropyl ether (0.23 g, 24%). M.P. 139-141 °C; ¹H NMR (CDCl₃): δ = 11.2 (br, 1H, NH), 8.32 (d, 1H), 7.94 (d, 2H), 7.62 (t, 1H), 7.57-7.50 (m, 3H), 7.14 (t, 1H), 7.06 (d, 1H), 4.32 (q, 2H), 1.52 (t, 3H) ppm; ¹³C NMR (CDCl₃): δ = 165.5, 163.1, 156.8, 134.4, 134.3, 133.3, 132.7, 128.7, 127.7, 121.9, 120.8, 112.6, 65.6, 15.2 ppm; ESI-MS: (m/z) calcd. 269.29; observed: 292.11 (M+Na⁺), 561.30 (2M+Na⁺), 830.48 (3M+Na⁺); FT-IR (ATR): ν 3317, 2976, 1727, 1598, 1501, 1473, 1456, 1391, 1369, 1261, 1261, 1206, 1174, 1131, 1113, 1033, 924, 805 cm⁻¹; Anal. Calcd. for C₁₆H₁₅NO₃: C 71.36, H 5.61, N 5.20; found: C 71.50, H 5.40, N 4.95.

N-Butyryl-2-ethoxybenzamide 9 To a mixture of 2-ethoxybenzamide (1.67 g, 10.1 mmol) in dry pyridine (10 ml) cooled on an ice bath was added butyryl chloride (0.72 g, 6.8 mmol) dropwise. The mixture was allowed to stir at 0 °C for 30 min before heating to 80 °C for 16 h under a nitrogen atmosphere. The pyridine was removed *in vacuo* and chloroform (25 ml) was added before washing with 1M HCl, water, brine and drying over MgSO₄. The crude product was purified by column chromatography (SiO₂, ethyl acetate/*n*-hexane 2:1 v/v) followed by crystallization from *n*-heptane to give the title compound as colorless needles (0.20 g, 12%). M.P. 52 °C; ¹H NMR (CDCl₃): δ = 10.4 (br, 1H, NH), 8.12 (d, 1H), 7.54 (t, 1H), 7.03 (t, 1H), 6.88 (d, 1H), 4.22 (q, 2H), 2.79 (t, 2H), 1.65 (m, 2H), 1.52 (t, 3H), 1.03 (t, 3H) ppm; ¹³C NMR (CDCl₃): δ = 175.7, 163.6, 157.0, 132.7, 132.7, 121.5, 120.3, 112.5, 65.1, 40.0, 17.5, 14.5, 13.7 ppm; MALDI-ToF-MS: (m/z) calcd. 235.12; observed: 236.28 (M+H⁺), 258.28 (M+Na⁺); FT-IR (ATR): ν 3309, 1705, 1685 cm⁻¹; Anal. Calcd. for C₁₃H₁₇NO₃: C 66.36, H 7.28, N 5.95; found: C 66.24, H 7.23, N 5.92.

1-Butyl-3(3-nitrophenyl)-urea 10 To a solution of *m*-nitroaniline (0.69 g, 5.0 mmol) and 4-dimethylaminopyridine (0.030 g, 0.25 mmol) in chloroform (5 ml) was added *n*-butylisocyanate (0.49 g, 5.0 mmol) dropwise. The solution was stirred and refluxed under nitrogen atmosphere for 20 hours. The product was purified by extensive washing with 6 M HCl followed by crystallization from ethanol/water (1/1) to give colorless microneedles (0.92 g, 77%). M.P. 126 °C; ¹H NMR (CDCl₃): 8.15 (s, 1H), 7.86 (d, 1H), 7.84 (d, 1H), 7.42 (t, 1H), 6.64 (br, 1H, NH), 4.75 (br, 1H, NH), 3.28 (q, 2H), 1.54 (m, 2H), 1.38 (m, 2H), 0.94 (t, 3H) ppm; ¹³C NMR (CDCl₃): 155.6, 148.4, 140.3, 129.6, 124.9, 117.1, 113.6, 40.0, 31.9, 19.9, 13.6 ppm; ESI-MS: (m/z) calcd. 237.26; observed: 260.16 (M+Na⁺), 497.31 (2M+Na⁺), 734.48 (3M+Na⁺), 971.63 (4M+Na⁺); FT-IR (ATR): ν = 3349, 3288, 2922, 2862, 1640, 1594, 1563, 1525, 1471, 1344, 1312, 1244, 1080, 890.6 cm⁻¹; Anal. Calcd. for C₁₁H₁₅N₃O₃: C 55.69, H 6.37, N 17.71; found: C 55.60, H 6.15, N 17.52.

1-Butyl-3-(2,3,4,5,6-pentafluorophenyl)-urea 11 To a solution of 2,3,4,5,6-pentafluoroaniline (1.01 g, 5.5 mmol) and 4-dimethylaminopyridine (0.035 g, 0.28 mmol) in pyridine (5 ml) was added *n*-butylisocyanate (0.47 g, 5.0 mmol) dropwise. The solution was stirred and heated at 115 °C under nitrogen atmosphere for 20 hours. The reaction mixture was evaporated *in vacuo* followed by purification by column chromatography (SiO₂, 3 % methanol/chloroform) to yield the title compound (0.97 g, 70%). An analytically pure sample was obtained after recrystallization from *n*-hexane. M.P. 146-147 °C; ¹H NMR (CDCl₃): 5.86 (br, 1H, NH), 4.81 (br, 1H, NH), 3.32 (q, 2H), 1.54 (q, 2H), 1.44 (m, 4H), 0.9

(t, 3H) ppm; ^{13}C NMR (CDCl_3): 154.5, 144.1, 141.7, 138.8, 136.5, 40.7, 32.0, 19.9, 13.7 ppm; MALDI-ToF-MS: (m/z) calcd. 282.08; observed: 283.01 ($\text{M}+\text{H}^+$); FT-IR (ATR): ν = 3329, 3280, 2959, 2865, 2877, 1662, 1646, 1501 cm^{-1} ; Anal. Calcd. for $\text{C}_{11}\text{H}_{11}\text{F}_5\text{N}_2\text{O}$: C 46.82, H 3.93, N 9.93; found: C 46.43, H 3.49, N 9.52.

2.6 References

- (1) Hamilton, A. D. *Advances in Supramolecular Chemistry* **1990**, 1, 1-64.
- (2) Vögtle, F. *Supramolecular Chemistry*; J. Wiley & Sons: Chichester, 1991.
- (3) Lehn, J.-M. *Supramolecular Chemistry*; Wiley-VCH, 1995.
- (4) Taft, R. W.; Gurka, D.; Joris, L.; Schleyer, P. v. R.; Rakshys, J. W. *J. Am. Chem. Soc.* **1969**, 91, 4801-8.
- (5) Taft, R. W.; Berthelot, M.; Laurence, C.; Leo, A. J. *Chemtech* **1996**, 26, 20-29.
- (6) Abraham, M. H. *J. Phys. Org. Chem.* **1993**, 6, 660-84.
- (7) Platts, J. A. *Phys. Chem. Chem. Phys.* **2000**, 2, 3115-3120.
- (8) Jorgensen, W. L.; Pranata, J. *J. Am. Chem. Soc.* **1990**, 112, 2008-10.
- (9) Pranata, J.; Wierschke, S. G.; Jorgensen, W. L. *J. Am. Chem. Soc.* **1991**, 113, 2810-19.
- (10) Zimmerman, S. C.; Corbin, P. S. *Struct. Bonding (Berlin)* **2000**, 96, 63-94.
- (11) Beijer, F. H.; Kooijman, H.; Spek, A. L.; Sijbesma, R. P.; Meijer, E. W. *Angew. Chem. Int. Ed.* **1998**, 37, 75-78.
- (12) Beijer, F. H.; Sijbesma, R. P.; Kooijman, H.; Spek, A. L.; Meijer, E. W. *J. Am. Chem. Soc.* **1998**, 120, 6761-6769.
- (13) Söntjens, S. H. M.; Sijbesma, R. P.; van Genderen, M. H. P.; Meijer, E. W. *J. Am. Chem. Soc.* **2000**, 122, 7487-7493.
- (14) Chang, S. K.; Hamilton, A. D. *J. Am. Chem. Soc.* **1988**, 110, 1318-19.
- (15) Zeng, H.; Miller, R. S.; Flowers, R. A., II; Gong, B. J. *J. Am. Chem. Soc.* **2000**, 122, 2635-2644.
- (16) Wyler, R.; de Mendoza, J.; Rebek, J., Jr. *Angew. Chem.* **1993**, 105, 1820-1 (See also *Angew Chem*, Int Ed Engl, 1993, 32(12), 1699-701).
- (17) Ghadiri, M. R.; Granja, J. R.; Milligan, R. A.; McRee, D. E.; Khazanovich, N. *Nature* **1993**, 366, 324-7.
- (18) Hirschberg, J. H. K. K.; Brunsveld, L.; Ramzi, A.; Vekemans, J. A. J. M.; Sijbesma, R. P.; Meijer, E. W. *Nature* **2000**, 407, 167-170.
- (19) Hirschberg, J. H. K. K.; Koevoets, R. A.; Sijbesma, R. P.; Meijer, E. W. *Chem. Eur. J.* **2003**, 9, 4222-4231.
- (20) Sijbesma, R. P.; Beijer, F. H.; Brunsveld, L.; Folmer, B. J. B.; Hirschberg, J. H. K. K.; Lange, R. F. M.; Lowe, J. K. L.; Meijer, E. W. *Science* **1997**, 278, 1601-1604.
- (21) Ky Hirschberg, J. H. K.; Beijer, F. H.; van Aert, H. A.; Magusin, P. C. M. M.; Sijbesma, R. P.; Meijer, E. W. *Macromolecules* **1999**, 32, 2696-2705.
- (22) Folmer, B. J. B.; Sijbesma, R. P.; Versteegen, R. M.; van der Rijt, J. A. J.; Meijer, E. W. *Adv. Mater.* **2000**, 12, 874-878.
- (23) Söntjens, S. H. M.; Meijer, J. T.; Kooijman, H.; Spek, A. L.; van Genderen, M. H. P.; Sijbesma, R. P.; Meijer, E. W. *Org. Lett.* **2001**, 3, 3887-3889.
- (24) Brammer, S.; Luning, U.; Kuhl, C. *Eur. J. Org. Chem.* **2002**, 4054-4062.
- (25) Corbin, P. S.; Zimmerman, S. C.; Thiessen, P. A.; Hawryluk, N. A.; Murray, T. J. *J. Am. Chem. Soc.* **2001**, 123, 10475-10488.
- (26) Mayer, M. F.; Nakashima, S.; Zimmerman, S. C. *Org. Lett.* **2005**, 7, 3005-3008.
- (27) Yang, X.; Martinovic, S.; Smith, R. D.; Gong, B. J. *J. Am. Chem. Soc.* **2003**, 125, 9932-9933.
- (28) Gong, B. *Synlett.* **2001**, 582-589.
- (29) Kulevsky, N.; Lewis, L. J. *Phys. Chem.* **1972**, 76, 3502-3.

- (30) Dega-Szafran, Z.; Kania, A.; Grundwald-Wyspianska, M.; Szafran, M.; Tykarska, E. *J. Mol. Struct.* **1996**, 381, 107-125.
- (31) Prezhdo, V. V.; Vashchenko, E. V.; Prezhdo, O. V. *Russian Journal of General Chemistry (Translation of Zhurnal Obshchei Khimii)* **2000**, 70, 121-129.
- (32) Moreno-Fuquen, R.; De Castro, E. V. R.; Moreno, M.; De Almeida Santos, R. H.; Montano, A. M. *Acta Cryst.* **2000**, C56, 206-207.
- (33) Goswami, S.; Ghosh, K.; Mukherjee, R. *Supramol. Chem.* **2000**, 11, 191-199.
- (34) Noe, E. A.; Raban, M. J. *Am. Chem. Soc.* **1974**, 96, 1598-9.
- (35) Kozhevnikov, D. N.; Rusinov, V. L.; Chupakhin, O. N. *Advances in Heterocyclic Chemistry* **2002**, 82, 261-305.
- (36) Birincioglu, M.; Jaruga, P.; Chowdhury, G.; Rodriguez, H.; Dizdaroglu, M.; Gates, K. S. *J. Am. Chem. Soc.* **2003**, 125, 11607-11615.
- (37) Junnotula, V.; Sarkar, U.; Sinha, S.; Inman, C.; Barnes, C. L.; Gates, K. S. *Abstracts of Papers, 230th ACS National Meeting, Washington, DC, United States, Aug. 28-Sept. 1, 2005* **2005**, TOXI-075.
- (38) Arndt, F. *Ber.* **1913**, 46, 3522-3532.
- (39) Wolf, F. J.; Pfister, K., III; Wilson, R. M., Jr.; Robinson, C. A. *J. Am. Chem. Soc.* **1954**, 76, 3551-3.
- (40) Wolf, F. J.; Wilson, R. M., Jr.; Pfister, K., 3rd; Tishler, M. J. *Am. Chem. Soc.* **1954**, 76, 4611-13.
- (41) Suzuki, H.; Kawakami, T. *Synthesis* **1997**, 855-857.
- (42) Suzuki, H.; Kawakami, T. *J. Org. Chem.* **1999**, 64, 3361-3363.
- (43) Stott, K.; Keeler, J.; Van, Q. N.; Shaka, A. J. *J. Magn. Reson.* **1997**, 125, 302-324.
- (44) Beijer, F. H., Eindhoven University of Technology, Thesis, 1998.
- (45) Sudha, L. V.; Sathyanarayana, D. N. *J. Mol. Struct.* **1984**, 125, 89-96.
- (46) Corbin, P. S.; Zimmerman, S. C. *J. Am. Chem. Soc.* **2000**, 122, 3779-3780.
- (47) Luning, U.; Kuhl, C.; Uphoff, A. *Eur. J. Org. Chem.* **2002**, 4063-4070.
- (48) Quinn, J. R.; Zimmerman, S. C. *Org. Lett.* **2004**, 6, 1649-1652.
- (49) Hadzi, D. *Theoretical Treatments of Hydrogen Bonding*; Wiley: New York, 1997.
- (50) Guerra, C. F.; Bickelhaupt, F. M. *Angew. Chem. Int. Ed.* **2002**, 41, 2092-2095.
- (51) Asensio, A.; Kobko, N.; Dannenberg, J. J. *J. Phys. Chem. A* **2003**, 107, 6441-6443.
- (52) Lukin, O.; Leszczynski, J. *J. Phys. Chem. A* **2002**, 106, 6775-6782.
- (53) Guo, D.; Sijbesma, R. P.; Zuilhof, H. *Org. Lett.* **2004**, 6, 3667-3670.
- (54) Kobko, N.; Dannenberg, J. J. *J. Phys. Chem. A* **2003**, 107, 10389-10395.
- (55) Cossi, M.; Scalmani, G.; Rega, N.; Barone, V. *J. Chem. Phys.* **2002**, 117, 43-54.
- (56) Jadzyn, J.; Stockhausen, M.; Zywucki, B. *J. Phys. Chem.* **1987**, 91, 754-7.
- (57) De Loos, M.; Van Esch, J.; Kellogg, R. M.; Feringa, B. L. *Angew. Chem. Int. Ed.* **2001**, 40, 613-616.
- (58) Etter, M. C.; Reutzel, S. M. *J. Am. Chem. Soc.* **1991**, 113, 2586-98.
- (59) Bernstein, J.; Davis, R. E.; Shimon, L.; Chang, N.-L. *Angew. Chem. Int. Ed.* **1995**, 34, 1555-73.
- (60) Gong, B.; Yan, Y.; Zeng, H.; Skrzypczak-Jankun, E.; Kim, Y. W.; Zhu, J.; Ickes, H. *J. Am. Chem. Soc.* **1999**, 121, 5607-5608.
- (61) Parra, R. D.; Gong, B.; Zeng, X. C. *J. Chem. Phys.* **2001**, 115, 6036-6041.
- (62) Parra, R. D.; Zeng, H.; Zhu, J.; Zheng, C.; Zeng, X. C.; Gong, B. *Chem. Eur. J.* **2001**, 7, 4352-4357.
- (63) Titherley, A. W. *J. Chem. Soc.* **1904**, 85, 1673-1691.
- (64) McConnan, J.; Titherley, A. W. *J. Chem. Soc.* **1906**, 89(II), 1318-1339.
- (65) Topping, R. M.; Russell, P. L.; Tutt, D. E. *J. Chem. Soc. section B* **1971**, 657-61.
- (66) Vyas, K.; Rao, V. M.; Manohar, H. *Acta Cryst.* **1987**, C43, 1197-200.
- (67) Etter, M. C.; Panunto, T. W. *J. Am. Chem. Soc.* **1988**, 110, 5896-7.
- (68) Etter, M. C.; Urbanczyk-Lipkowska, Z.; Zia-Ebrahimi, M.; Panunto, T. W. *J. Am. Chem. Soc.* **1990**, 112, 8415-26.
- (69) Vyas, K.; Rao, V. M.; Manohar, H. *Acta Cryst.* **1987**, C43, 1201-4.
- (70) Slavinskaya, R. A.; Gabdrakipov, V. Z.; Nurakhynova, M.; Sumarokova, T. N. *Zh. Obshch. Khim.* **1981**, 51, 2779-87.

- (71) Uflyand, I. E.; Ryabukhin, Y. I.; Sorbunova, M. O.; Kovaleva, T. V.; Starikov, A. G.; Dimukhamedov, A. I.; Sheinker, V. N. *Zh. Obshch. Khim.* **1990**, 60, 1643-50.
- (72) Reutzel, S. M.; Etter, M. C. *J. Phys. Org. Chem.* **1992**, 5, 44-54.
- (73) Macura, S.; Huang, Y.; Suter, D.; Ernst, R. R. *J. Magn. Reson.* **1981**, 43, 259-81.
- (74) Schneider, H.-J.; Yatsimirsky, A. *Principles and Methods in Supramolecular Chemistry*; J. Wiley & Sons Ltd.: Chichester, 2000.
- (75) Gaussian 03: Revision C02; Frisch, M. J.; Trucks, G. W.; Schlegel, H. B.; Scuseria, G. E.; Robb, M. A.; Cheeseman, J. R.; Montgomery, J., J. A.; Vreven, T.; Kudin, K. N.; Burant, J. C.; Millam, J. M.; Iyengar, S. S.; Tomasi, J.; Barone, V.; Mennucci, B.; Cossi, M.; Scalmani, G.; Rega, N.; Petersson, G. A.; Nakatsuji, H.; Hada, M.; Ehara, M.; Toyota, K.; Fukuda, R.; Hasegawa, J.; Ishida, M.; Nakajima, T.; Honda, Y.; Kitao, O.; Nakai, H.; Klene, M.; Li, X.; Knox, J. E.; Hratchian, H. P.; Cross, J. B.; Bakken, V.; Adamo, C.; Jaramillo, J.; Gomperts, R.; Stratmann, R. E.; Yazyev, O.; Austin, A. J.; Cammi, R.; Pomelli, C.; Ochterski, J. W.; Ayala, P. Y.; Morokuma, K.; Voth, G. A.; Salvador, P.; Dannenberg, J. J.; Zakrzewski, V. G.; Dapprich, S.; Daniels, A. D.; Strain, M. C.; Farkas, O.; Malick, D. K.; Rabuck, A. D.; Raghavachari, K.; Foresman, J. B.; Ortiz, J. V.; Cui, Q.; Baboul, A. G.; Clifford, S.; Cioslowski, J.; Stefanov, B. B.; Liu, G.; Liashenko, A.; Piskorz, P.; Komaromi, I.; Martin, R. L.; Fox, D. J.; Keith, T.; Al-Laham, M. A.; Peng, C. Y.; Nanayakkara, A.; Challacombe, M.; Gill, P. M. W.; Johnson, B.; Chen, W.; Wong, M. W.; Gonzalez, C.; Pople, J. A.; Gaussian, Inc.: Wallingford CT, 2004.
- (76) Bernstein, J.; Stearns, B.; Dexter, M.; Lott, W. A. *J. Am. Chem. Soc.* **1947**, 69, 1147-50.
- (77) Fuchs, T.; Chowdhury, G.; Barnes, C. L.; Gates, K. S. *J. Org. Chem.* **2001**, 66, 107-114.

3

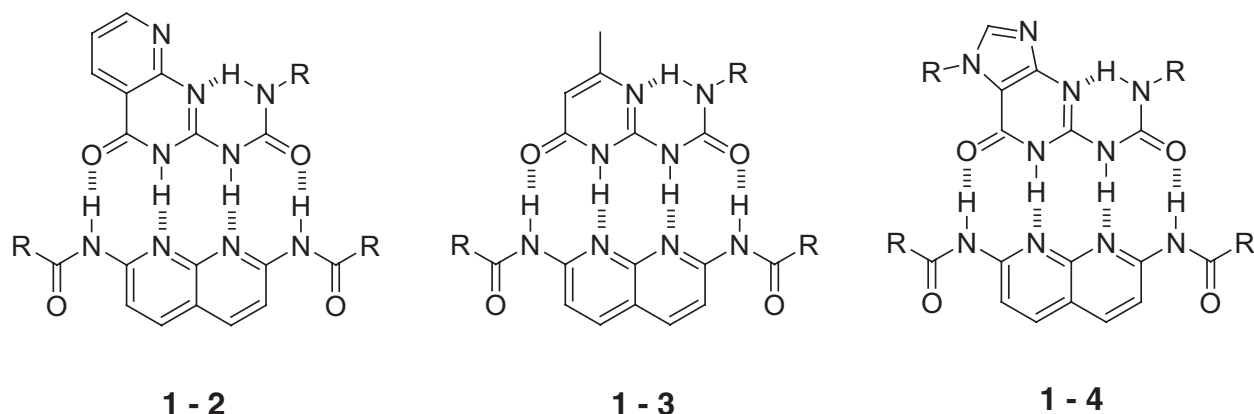
Pd-catalyzed amidation of 2-chloro- and 2,7-dichloro-1,8-naphthyridines

Abstract

A general catalytic amidation of 2-chloro- and 2,7-dichloro-1,8-naphthyridines with primary amides bearing functional groups is reported. Using Pd(OAc)₂, Xantphos and K₂CO₃ symmetric as well as non-symmetric 2,7-diamido-1,8-naphthyridines were obtained in 50-90% yield with good functional group compatibility. Mono-amidation of 2,7-dichloro-1,8-naphthyridine using 0.9 equivalents of amide proceeded with good selectivity compared to formation of the diamide. Although supramolecular chemistry could be used to isolate the mono-amidated product from the diamide, isolated yields were poor to moderate (22 to 42%). A quantitative study of the hydrolysis of four Napy derivatives reveals an enhanced stability of 2-alkyl substituted diamides.

3.1 Introduction

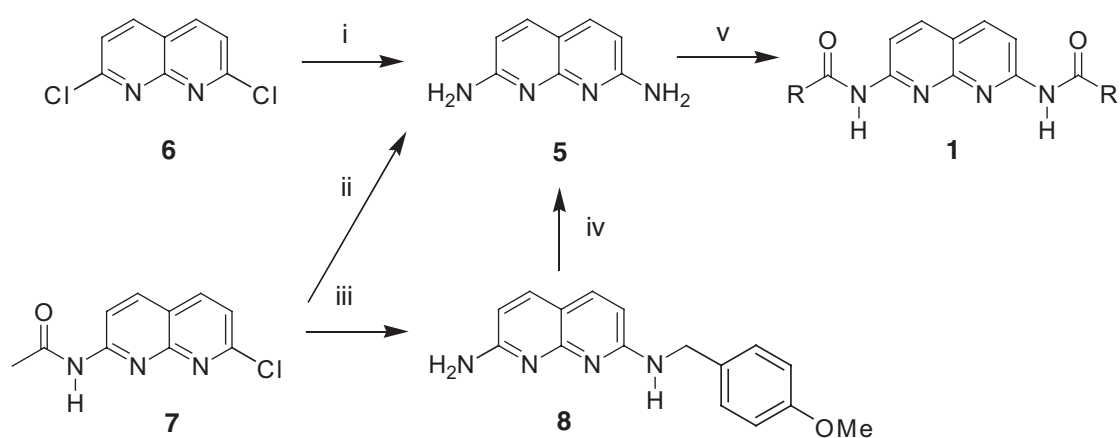
The use of intermolecular interactions to organize two- or three-dimensional structures from synthetic molecules through a spontaneous and reversible process is termed self-assembly.¹ Among several non-covalent interactions, multiple hydrogen bonding has received much attention for its use in self-assembly processes.²⁻⁵ Especially quadruple hydrogen bonding⁶⁻⁸ units have been demonstrated to be very useful in supramolecular polymer chemistry due to their strength and directionality.^{9,10} Although self-complementary quadruple hydrogen bonding motifs have been available since 1997, developing complementary quadruple hydrogen bonding units has been much more challenging.^{11,12} Zimmerman *et al.* were the first to report a complementary quadruple hydrogen bonding motif based on a 2,7-diamido-1,8-naphthyridine **1** (Napy) derivative with 2-ureido-[3H]-pyrido-(2,3-d)pyrimidin-4-one **2**.⁸ Li and coworkers reported the strong and selective complementary complexation of the 6[1H] tautomeric form of a ureido-pyrimidinone **3** (UPy) with **1** via quadruple hydrogen bonds between ADDA and DAAD arrays (Scheme 3.1).¹³ More recently, Zimmerman *et al.* reported the use of the highly stable heterocomplex of guanosine urea **4** with **1** for supramolecular copolymer blends.¹⁴ In addition, our group showed that the UPy-Napy heterocomplex formation exhibits a concentration dependent selectivity with $K_a(\text{UPy-Napy}) = > 10^6 \text{ M}^{-1}$ and is very suitable for the construction of supramolecular copolymers.¹⁵ The high selectivity and strength of all these heterocomplexes render Napy derivatives very attractive for constructing supramolecular architectures using quadruple hydrogen bonding.



Scheme 3.1 Quadruple hydrogen bond arrays based on 2,7-diamido-1,8-naphthyridine derivatives **1**.

The literature procedure to synthesize diamido-naphthyridines **1** uses 2,7-diamino-1,8-naphthyridine **5** obtained by aminolysis of either the symmetric 2,7-chloro-1,8-naphthyridine¹⁶ **6** or the non-symmetric 7-acetamido-2-chloro-1,8-naphthyridine **7**.¹⁷ The aminolysis requires

high pressures and temperatures, thus creating a potential safety hazard. Only recently, Park *et al.* reported the two-step conversion of **7** to **5** via a nucleophilic aromatic substitution with 4-methoxybenzylamine to crude **8** and subsequent deprotection.¹⁸ Due to its low solubility in commonly used organic solvents, the isolated diamino product **5** is often of low purity. Furthermore, due to the low nucleophilicity of the aromatic amines, subsequent reaction with an acid chloride yields diamido derivatives in low to moderate yields (Scheme 3.2).^{17,19} Therefore, improving the synthetic route towards functionalized Napy derivatives is a key issue in the development of complementary quadruple hydrogen bonding units for self-assembly.



Scheme 3.2 Synthetic routes to 2,7-diamido-1,8-naphthyridine derivatives **1**. i: PhOH, NH₃ (g), 170 °C, 20 h, 20–94%^{20,21} or NH₄OH, 180 °C, 24 h, 70%¹⁷; ii: NH₃/EtOH, 180 °C, 24 h, 74%¹⁷; iii: 4-methoxybenzylamine, pyridine, 120 °C, 83%¹⁸; iv: conc HCl, 100 °C, 95%¹⁸; v: acid chloride, Et₃N, CHCl₃, 30–60%^{17,19}

A general palladium-catalyzed methodology to 2,7-diamido-1,8-naphthyridines displaying DAAD quadruple hydrogen bond motifs is investigated in this chapter. The scope and limitations of this synthetic approach are examined and the synthesis of a variety of Napy derivatives including functional groups is described using optimized conditions. Since it is expected that the first amidation reaction will proceed faster, a systematic study of the mono-amidation of 2,7-dichloro-1,8-naphthyridine is presented. Finally, alkaline and acid hydrolysis of a number of Napy compounds is quantified.

3.2 Pd-catalyzed amidation of arylhalides

Over the past decade, palladium-catalyzed aromatic C-N forming reactions by the cross-coupling of aryl halides and amines have been extensively studied by the groups of Hartwig and Buchwald.^{22,23} Although a wide range of aryl halides could be aminated with various amines, attempts to perform the analogous coupling reactions using primary amides as the nitrogen nucleophile were less successful. Recently, the group of Buchwald reported the successful Pd-catalyzed amidation of various aryl halides, tosylates and triflates^{24,25} as well as a Cu-catalyzed cross-coupling of aryl bromides and iodides with primary amides.²⁶⁻²⁸ These results prompted us to explore the application of these catalytic amidations on compounds **6** and **7**.

3.2.1 Optimization of Pd-catalyzed amidation of 2,7-dichloro-1,8-naphthyridine

In order to establish the most effective conditions for a general amidation route to derivatives of **1**, the reaction between **6** and dodecanoyl amide to diamido-naphthyridine **1a** was examined first (Table 3.1). With Xantphos²⁹ as the ligand and Cs₂CO₃ as a base, the reaction went smoothly (entry 1). In contrast, replacing Cs₂CO₃ by the strong base KO-*t*-Bu decreased the yield significantly (entry 2). This can be rationalized by hydrolysis of the weak Napy amide bond to a primary amine upon workup of the basic reaction mixture.^{19,30} In addition to Xantphos, bidentate phosphine ligands BINAP and DPPF were also tested (entries 3 and 4). However, conversions as well as isolated yields were lower. Reducing the amount of palladium(0) or replacing it by a palladium(II) source, Pd(OAc)₂, did not prevent the reaction going to completion (entries 5 and 6). It was reported earlier by Buchwald et al. that Pd(OAc)₂ is the Pd source of choice in reactions involving electron-deficient aryl halides. Since **6** is an electron-deficient aryl dihalide, the reaction was complete within 5 hours. Addition of a catalytic amount of phenyl boronic acid to ensure complete conversion of the Pd(II) precatalyst to Pd(0) did not improve the yield further (entry 7).²⁸ From an industrial point of view, 1,4-dioxane has often been replaced by toluene as a solvent, however, due to poor solubility of compound **6**, 1,4-dioxane was selected.

Table 3.1 Optimization of conditions^a

entry	%Pd ^b	ligand	base	conv (%) ^c	yield (%) ^d
1	8	Xantphos	Cs ₂ CO ₃	>99	82
2	8	Xantphos	KO- <i>t</i> -Bu	<25	0
3	8	BINAP	Cs ₂ CO ₃	56	25
4	8	DPPF	Cs ₂ CO ₃	36	15
5	4	Xantphos	Cs ₂ CO ₃	>99	78
6	4 ^e	Xantphos	K ₂ CO ₃	>99 ^f	85
7	4 ^{e, g}	Xantphos	K ₂ CO ₃	>99 ^f	80

^a Reaction conditions: 0.5 mmol of **6**, 1.0 mmol dodecanoyl amide, L/Pd = 2.0, 2.1 equivalents of base, 3–5 mL of 1,4-dioxane, 100 °C, 24 h. ^b 1 mol % Pd refers to 0.5 mol % Pd₂(dba)₃. ^c as determined by ¹H NMR. ^d isolated yields. ^e Pd(OAc)₂ was used. ^f reaction time 5 h. ^g 0.05 mmol of PhB(OH)₂ was added.

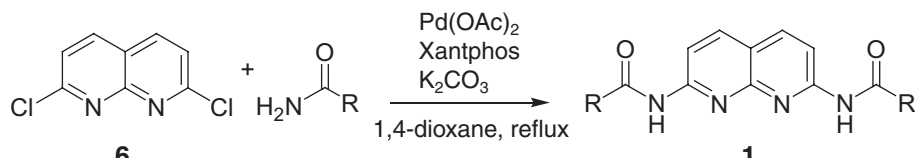
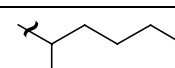

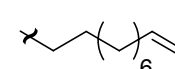
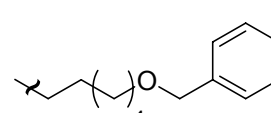
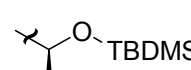
3.2.2 Symmetric bisamidation of 2,7-dichloro-1,8-naphthyridine

Using the optimized conditions, i.e. Xantphos as the ligand, K₂CO₃ as the base, and dioxane as the solvent, several primary amides were reacted with 2,7-dichloro-1,8-naphthyridine **6**. As demonstrated in Table 3.2, symmetric Napy derivatives were obtained in moderate to high yields in 4–20 hours. By amidation with 2-methylhexanoic amide derivative **1b** was obtained in moderate yield. A bulky primary amide like adamantyl-1-carboxylic amide (**1c**) required a longer reaction time. It was previously reported that the use of a base such as Cs₂CO₃ or K₂CO₃ is compatible with the presence of functional groups.^{31–33} Amidation with 10-undecenoic amide went very rapidly and derivative **1d** was isolated in high yield. The terminal double bond of the amide was partially isomerized to an internal double bond during the reaction when 4 mol % Pd(OAc)₂ was used. Increasing the amount of palladium up to 10 mol % also increased the amount of isomerized product, which is difficult to separate from the desired compound (see Experimental procedures; compound **1d isomer**).

Useful derivatives would be the bis-hydroxy-terminated bisamido-naphthyridines. Unfortunately, 6-hydroxy-hexanoic amide did not react under the aforementioned conditions to yield the desired product. However, when the reaction was performed with 6-benzyloxy-protected hexanoic amide **9**, symmetric product **1e** was obtained in moderate yield. A second protected hydroxy amide, which was readily synthesized from commercially available ethyl-*S*-lactate, also reacted with **6** to give **1f** in high yield. A strong advantage of the catalytic route,

next to the high amidation yield, is that purification by column chromatography of the crystallizable products (**1d** and **1f**) is not necessary.

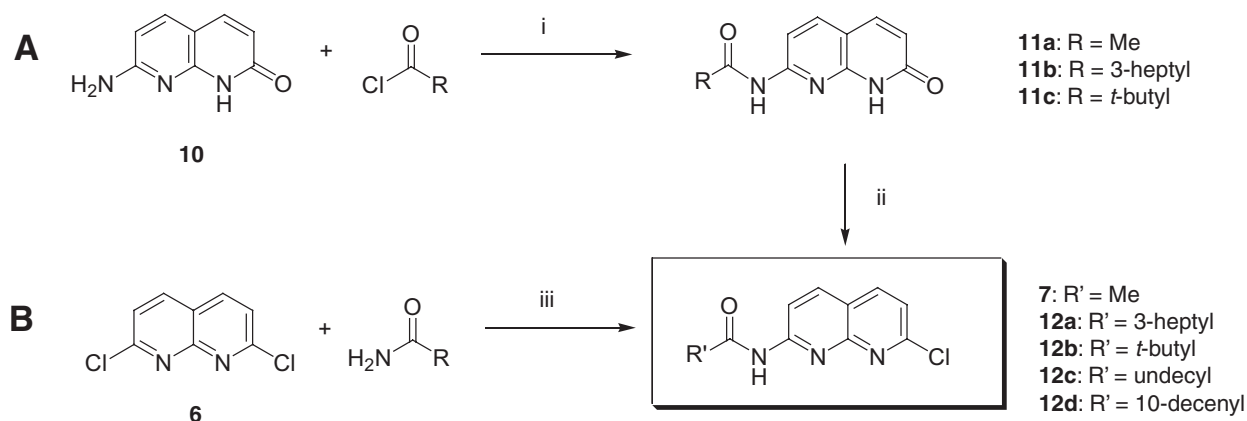
Table 3.2 Pd-catalyzed amidation of 2,7-dichloro-1,8-naphthyridine^a

				
product	R-group	mol% Pd	time(h)	yield(%)
1b		5	12	44
1c		10	20	82
1d		4.5	4	90
1e		8.6 ^b	10	60
1f		4.7	10	82

^a Reaction conditions: **6** (1 equiv), amide (2 equiv), L/Pd = 2.5 - 3.0, K₂CO₃ (2.0-2.1 equiv) in refluxing 1,4-dioxane (0.15-0.25 M). ^b Pd₂(dba)₃ was used as the palladium source.

3.2.3 Mono-amidation of 2,7-dichloro-1,8-naphthyridine

Next, the synthesis of non-symmetric naphthyridines was examined. Introduction of functional groups at one side of the compound would open the possibility of functionalizing various other organic compounds with Napy groups. Non-symmetric naphthyridines have been prepared previously by non-symmetric hydrolysis of 2,7-diamido-1,8-naphthyridine **1a** to a 7-amino-2-amido-1,8-naphthyridine derivative.¹⁹ Subsequent reaction with an acid chloride yields a non-symmetric diamide derivative in moderate yield.³⁴ We decided to pursue two alternative approaches to the synthesis of non-symmetric Napy derivatives (Scheme 3.3).



Scheme 3.3 Two approaches to non-symmetric 1,8-naphthyridines. i: acid chloride, pyridine, 110 °C, 16 h, 20-85%; ii: POCl₃, 95 °C, 3 h, 60-91%; iii: Pd-catalyst, ligand, base.

Strategy A was reported previously for the synthesis of 7-acetamido-2-chloro-1,8-naphthyridine **7** via 7-acetamido-[1H]-2-oxo-1,8-naphthyridine **11a**.¹⁷ In this approach an R-group of choice is introduced by reaction of 7-amino-[1H]-2-oxo-1,8-naphthyridine¹⁶ **10** with the appropriate acid chloride followed by conversion of the oxo group to the chloride using POCl₃. Using this strategy, 2-chloro-1,8-naphthyridines **12a** and **12b** could be synthesized via chlorination of their precursors **11b** and **11c**, respectively. Although **12a** could be obtained in 59% over-all yield, the 16% yield of **12b** can be rationalized by steric hindrance of the pivaloyl chloride in the first reaction step. Strategy B which also applies mono-amidation of **6** requires the least number of synthetic steps. Since it is reasonable to assume that the first amidation of **6** is faster than the second, catalytic amidation of **6** with 2-ethylhexanoyl amide to derivative **12a** was examined (Table 3.3).

Although conversion is complete within six hours when 1.0 equivalent of amide is used, it is evident that the second amidation competes with the first. This is expressed in the mono- to diamido ratio being quite small (entry 1). A decrease in temperature results in an increase of this ratio, however, it also results in a decrease in conversion (entries 2 and 3). In contrast, the use of THF and DMF at 60 °C to ensure high selectivity increased conversion slightly (entries 4 and 5). Due to the difficulty of removing DMF from the reaction mixture, 1,4-dioxane is the preferred solvent at 80 °C. Finally, a good product to side-product ratio was obtained by reducing the amount of primary amide to 0.9 equivalent and reducing reaction time to 8 hours.

Table 3.3 Optimization of conditions ^a

entry	T (°C)	solvent	time (h)	conv (%) ^b	m/d ratio ^c
1	100	1,4-dioxane	6	>99	3.3
2	80	1,4-dioxane	20	>99	3.8
3	60	1,4-dioxane	20	20	>20
4	60	THF	16	55	7.1
5	60	DMF	16	65	18
6 ^d	80	1,4-dioxane	8	>92	6.8

^a Reaction conditions: 0.25 mmol of **6**, 2 mol% Pd(OAc)₂, 4 mol% Xantphos, 0.7 mmol K₂CO₃, 1.0 equivalent of 2-ethyl-hexanoyl amide, 1.0 mL of solvent. ^b based on amide consumption as determined by ¹H NMR. ^c mono-amido/diamido ratio. ^d 0.9 equivalent of 2-ethyl-hexanoyl amide was used.

Using the optimized conditions three non-symmetric chloro-naphthyridines were synthesized and isolated (Table 3.4, compounds **12a**, **c**, and **d**). In contrast to the synthesis of symmetric diamido-naphthyridines, these non-symmetric compounds could not be purified by crystallization. Even though diamido-naphthyridines formed as by-products in the synthesis of **12c** and **12d** can be crystallized from ethanol or toluene, it was not possible to purify the desired mono-amides by regular column chromatography on silica gel, due to similar retention behavior of the amidation products. However, the isolation of the non-symmetric product could be achieved by employing supramolecular chemistry. Due to the formation of strong heterocomplexes of UPy **3** (R = *n*-butyl) with 2,7-diamido-1,8-naphthyridines, the R_f factor of the latter compounds was reduced, allowing their separation from the non-binding monoamides. The desired compounds were eventually obtained in low to moderate yield by addition of **3** to the product mixture before chromatography. Although Ullmann-Goldberg type catalytic mono-amidations have been reported before for aryl bromides with secondary amides,^{35,36} this is the first time a Buchwald-Hartwig mono-amidation with primary amides is reported.

Table 3.4 Pd-catalyzed mono-amidation of 2,7-dichloro-1,8-naphthyridine ^a

product	R-group	conv (%) ^b	m/d ratio ^c	yield (%) ^d
12a		92	6.8	42
12c		94	7.0	25
12d		91	6.2	22

^a Reaction conditions: 0.25 mmol of **6**, 2 mol% Pd(OAc)₂, 4 mol% Xantphos, 0.7 mmol K₂CO₃, 0.9 equivalent of amide, 1.0 mL 1,4-dioxane, 8 hours, 80 °C. ^b based on amide consumption as determined by ¹H NMR. ^c mono-amido/diamido ratio. ^d isolated in > 99 % purity after UPy-assisted column chromatography.

3.2.4 Amidation of 7-amido-2-chloro-1,8-naphthyridine

Due to higher yields of strategy A outlined in scheme 3.3, non-symmetric Napy derivatives **13** bearing one acetamidido side chain were synthesized by catalytic amidation of **7** (Table 3.5). Although the non-symmetric products required purification by column chromatography, isolated yields were moderate to good. Introduction of bulky side groups, however, led to a decrease in yield and more catalyst had to be used (compounds **13a-13c**). As found previously, functional groups could be introduced in good yields (compounds **13d-13f**). Furthermore, synthesis of **13d** was not accompanied by olefin isomerization at catalyst loadings below 2 mol %.

Table 3.5 Pd-catalyzed amidation of 7-acetamido-2-chloro-1,8-naphthyridine^a

product	R-group	mol% Pd	time (h)	yield (%)
13a		1.4	18	66
13b		4.0 ^b	20	51
13c		10	20	35
13d		1.0	20	88
13e		4.0 ^b	18	80
13f		4.0 ^b	24	76

^a Reaction conditions: **7** (1 equiv), amide (1.2 equiv), L/Pd = 2.0, K₂CO₃ (1.4 equiv) in refluxing 1,4-dioxane (0.20-0.25 M). ^b Pd₂(dba)₃ was used in combination with Cs₂CO₃ (1.4 equiv).

Unfortunately, all of these compounds are quite prone to acidic or basic hydrolysis (see paragraph 3.3). Therefore, a 2-ethylpentyl or a *t*-butyl side-chain was introduced to decrease the sensitivity to hydrolysis. In addition, these side chains also enhanced the solubility of the derivatives. Pd-catalyzed amidation reactions on these 2-chloro-1,8-naphthyridine derivatives are summarized in Table 3.6. Slightly higher yields were obtained when 7-(2-ethyl)-hexanamido-2-chloro-1,8-naphthyridine **12a** was used as the halide instead of the acetamido derivative **7** (leading to compounds **14a** and **14b**). This can be rationalized by either its greater solubility or by partial decomposition of the acetamido derivatives on silica gel. The asymmetric TBDMS-protected alcohol-containing naphthyridine **14c** was obtained in good yield and, in contrast to its symmetric analogue (**14a**), it was readily soluble in apolar solvents like diethyl ether and pentane. In contrast to all previously isolated compounds which were solids, the benzyl-carbamate-protected 6-amino-hexanoic-amido-naphthyridine **14d** was isolated as an oil. Finally, 2-ethyl-hexanoic amide reacted with **12b** to give **15** in moderate yield.

Table 3.6 Pd-catalyzed amidation of 7-amido-2-chloro-1,8-naphthyridines^a

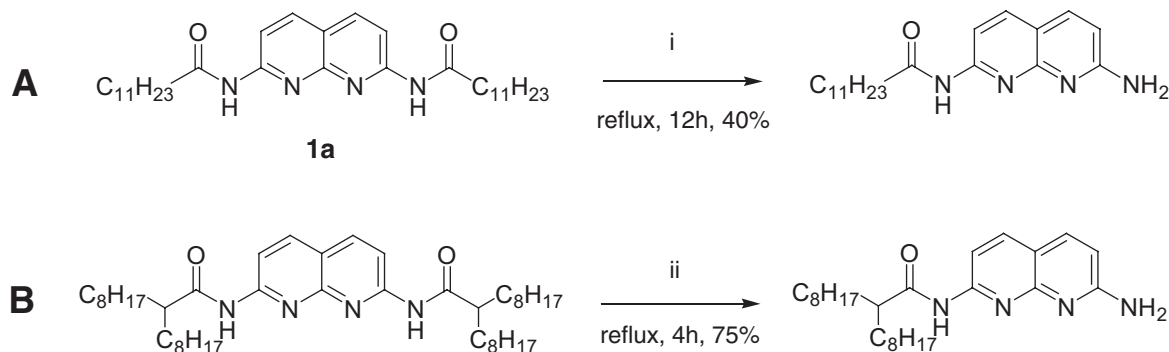
product	R-group	R'-group	mol% Pd	time (h)	yield (%)
14a			4.0	16	89
14b			10	20	47
14c			1.1	10	85
14d			1.1	20	65
15			1.3	20	54

^a Reaction conditions: **12a** or **12b** (1 equiv), amide (1.2 equiv), L/Pd = 2.0, K₂CO₃ (1.4 equiv) in refluxing 1,4-dioxane (0.20-0.25 M).

3.3 Hydrolysis of 2,7-diamido-1,8-naphthyridines

In the previous paragraphs, the synthesis of various Napy derivatives was described. Although products could be obtained in moderate to high yields, it was observed that some diamido-naphthyridine derivatives degraded during column chromatography, resulting in significantly lower isolated yields than suggested by NMR spectroscopy of the crude reaction mixture. NMR analysis of the by-products indicated hydrolysis of the amide bonds to primary naphthyridine amines. This phenomenon is most probably due to the electron-deficiency of the naphthyridine core which renders the carbon in the amide carbonyl more electrophilic. Additionally, protonation of the nitrogen atoms in the naphthyridine core facilitates nucleophilic attack of water on to the carbon in the amide carbonyl. Indeed, alkaline hydrolysis of diamido-naphthyridine derivatives has been reported previously.^{19,30,34} Li *et al.* reported the non-symmetric hydrolysis of **1a** to 7-amino-2-dodecanoylamino-1,8-naphthyridine (Scheme 3.4A). Similarly, they reported hydrolysis of bis(2-octyl-decanoylamino)-1,8-naphthyridine to the mono-amine (Scheme 3.4B). Furthermore, the group of Nakatani reported a study on the

thermal and alkaline stability of 2-amido-7-methyl-1,8-naphthyridine. Although no quantitative information was reported before, the presence of branched side chains next to the amide carbonyl was thought to increase hydrolytic stability.



Scheme 3.4 Non-symmetric hydrolysis of 2,7-diamido-1,8-naphthyridines. i: 20 mM NaOH, 20 mM **1a** in 1:1 v/v% THF/H₂O; ii: 310 mM NaOH, 75 mM Napy in 5:1 v/v% EtOH/H₂O.

To gain insight into the degradation pathway and to quantify hydrolysis of several Napy derivatives, we first examined the hydrolysis of 15 mM **13a** at 25 °C in 150 mM KOH in 1:1 v/v% THF/H₂O (Figure 3.1). Samples were analyzed with LC-MS and followed with MS and UV-detection. Quantification was done on the corresponding precursor ion in the MS-MS-mode. The major product was identified as 7-amino-2-(2-ethylhexanoyl)amino-1,8-naphthyridine **16** (Figure 3.1a). The small peak present in the MS-trace at 1.5 min was not present in the UV-trace (not shown) and could be assigned to small amounts of 2-ethylhexanoic amide present in **13a** and N-acylated 2-ethylhexanoic amide. When following the reaction in time, a decrease in concentration of **13a** was observed. The rate of hydrolysis in this case will be given by equation 3.1:

$$-d[\mathbf{13a}]/dt = k \cdot [\mathbf{13a}] \cdot [\text{OH}^-] \quad (3.1)$$

However, when assuming pseudo first order reaction kinetics due to the excess of base used in the experiment, equation 3.2 is obtained:

$$-d[\mathbf{13a}]/dt = k' \cdot [\mathbf{13a}] \quad \text{where } k' = k \cdot [\text{OH}^-] \quad (3.2)$$

Integration of 3.2 yields equation 3.3 which is a linear relation between $\ln[\mathbf{13a}]$ and t . In this relation constant A corresponds to $[\mathbf{13a}]$ at $t = 0$ h and slope k' is the pseudo first order reaction rate constant.

$$\ln[\mathbf{13a}] = -k' \cdot t + A \quad (3.3)$$

This relation can also be rewritten to display the relative decrease of $[\mathbf{13a}]$ as a function of time, obtaining equation 3.4:

$$\ln([\mathbf{13a}]_t / [\mathbf{13a}]_0) = -k' \cdot t \quad (3.4)$$

In order to quantify the pseudo first order reaction rate constants of hydrolysis of **13a**, experiments were run at three temperatures with 15 mM **13a** and 150 mM KOH in 1:1 v/v% THF/H₂O. Quantification was done by LC-MS in MS-MS mode. A linear relation is then subsequently found between $\ln([13a]_t/[13a]_0)$ and time (Figure 3.1b). Using standard fitting procedures, k' values were determined (Table 3.7). A dramatic increase in rate constant is observed when temperature is increased emphasizing the hydrolytic instability of the acetamide functionality in **13a**. Remarkably, no hydrolysis of the 2-ethylhexanoic amide group was observed at temperatures up to 80 °C.

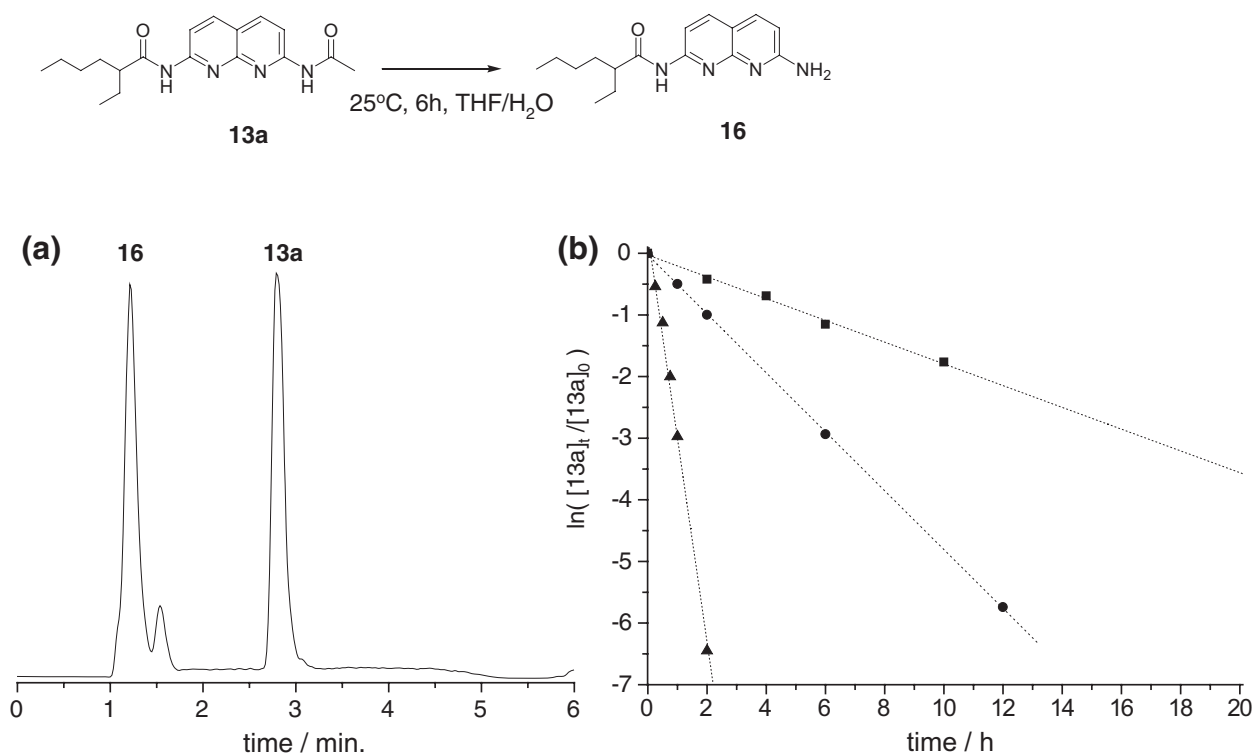


Figure 3.1 Hydrolysis of **13a** to **16**; (a): LC-MS mass profile for the hydrolysis of **13a** at 25 °C in 1/1 v/v% THF/H₂O after 6 hours; (b): Hydrolysis of **13a** over time at 25 (■), 40 (●) and 60 (▲) °C in 1:1 v/v% THF/H₂O; dotted lines indicate fitted data according to a linear relation.

Table 3.7 Evaluation of k' for hydrolysis of **13a**.

entry	T / °C	r^2	k' / h^{-1}
1	25	0.995	0.176 ± 0.007
2	40	0.999	0.478 ± 0.003
3	60	0.993	3.302 ± 0.139

Changing the physical environment next to a reactive site has been used for a long time to increase or decrease reaction rates. Therefore, introduction of branched side-chains next to the amide carbonyl was thought to suppress hydrolysis of the naphthyridine amide linkages. In order to validate this hypothesis, compounds **1b**, **13a**, **14a** and **15** were subjected to alkaline as well as acidic hydrolysis at 60 °C (Figure 3.2). Due to a lower solubility of **1b** and **14a** in THF/H₂O, mixtures of dioxane/H₂O were chosen as the solvent.

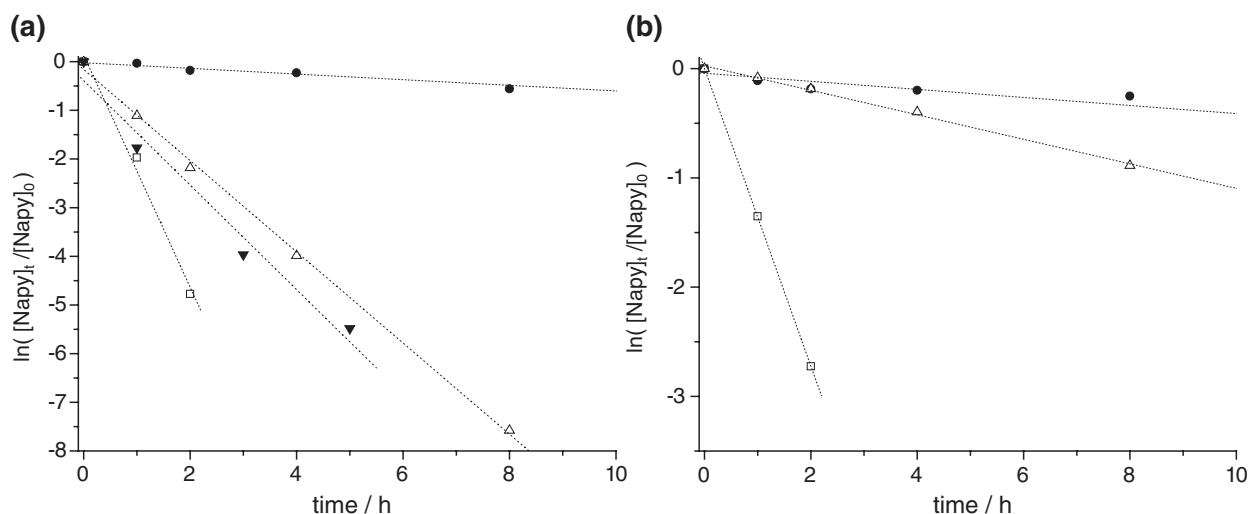


Figure 3.2 (a): Alkaline hydrolysis of 10 mM **1b** (▼), **13a** (□), **14a** (●) and **15** (△). (b): Acid hydrolysis of 10 mM, **13a** (□), **14a** (●) and **15** (△).

In all cases, major hydrolysis products were identified with LC-MS. Compound **1b** was found to be hydrolyzed to 7-amino-2-(2-methylhexanoyl)amino-1,8-naphthyridine. Hydrolysis of **13a** and **14a** resulted in the formation of **16**. Surprisingly, the major hydrolysis product of derivative **15** was **16** and not 7-amino-2-pivaloylamino-1,8-naphthyridine as expected. The k' values could be obtained by fitting procedures as described previously in this paragraph (Table 3.8). Although almost complete hydrolysis is observed for **13a** under alkaline as well acidic conditions within 2 hours (entries 2 and 5), derivatives **1b** and **15** require somewhat longer reaction times under alkaline conditions (entries 1 and 4). However, a significant difference is found for **14a** of which 50 and 75% remains unreacted after 10 hours under alkaline and acidic conditions respectively (entries 3 and 6). A noteworthy difference is also observed between alkaline and acidic hydrolysis of **15** (entries 4 and 7). It is clear that the presence of an ethyl group next to the amide carbonyl has a large stabilizing effect compared to two α -methyl substituents. A possible explanation of this increased stability compared to the pivaloyl group could be an increased hydrophobic effect of the 3-heptyl group, therefore decreasing the rate of nucleophilic attack of the hydroxide anion on the carbonyl carbon of the amide.

Table 3.8 Evaluation of k' for hydrolysis of Napy derivatives at 60 °C.

entry	conditions ^a	compound	r^2	k' / h^{-1}
1	A	1b	0.974	1.074 ± 0.123
2	A	13a	0.990	2.386 ± 0.240
3	A	14a	0.993	0.058 ± 0.0024
4	A	15	0.998	0.937 ± 0.022
5	B	13a	0.999	1.363 ± 0.006
6	B	14a	0.977	0.0369 ± 0.0028
7	B	15	0.996	0.112 ± 0.004

^a Reaction conditions: A: 10 mM Napy, 100 mM KOH in 2/1 v/v% dioxane/H₂O at 60 °C; B: 10 mM Napy, 320 mM KOH in 4:1 v/v% dioxane/H₂O at 60 °C.

3.4 Conclusions

In conclusion, a generally applicable palladium catalyzed amidation of 2-chloro- and 2,7-dichloro-1,8-naphthyridines was developed using Pd(OAc)₂ as the catalyst, Xantphos as the ligand, K₂CO₃ as the base and 1,4-dioxane as the solvent. Using a weak base in this procedure, functional groups are incorporated easily. Furthermore, introducing branched side chains not only increases stability towards hydrolysis but also enhances solubility of the naphthyridine derivatives. The simplicity and functional group tolerance makes this an attractive method for synthesizing Napy-functionalized molecules that may be useful in many aspects of both self-assembly of discrete structures as well as supramolecular copolymers.

Significant differences in reactivity between 2-chloro-7-amido- and 2,7-dichloro-1,8-naphthyridines allow the synthesis of mono-amidonaphthyridines with good selectivity. However, due to similar chromatographic behavior of mono-amido and diamidonaphthyridines, isolated yields of the mono-amido derivatives are poor to moderate. Besides, a key step in their isolation proved to be utilization of the binding ability of UPy to Napy to decrease elution time of the latter. Furthermore, Napy derivatives have been shown to be prone to both alkaline as well as acidic hydrolysis. Although acetamides and 2-methylhexanoylamino groups could be hydrolyzed rapidly, 2-ethylhexanoylamino substituents were significantly more stable.

3.5 Experimental procedures

General methods. See General methods Chapter 2. Liquid Chromatography – Mass Spectroscopy (LC-MS) was performed on a system consisting of the following components: Shimadzu SCL-10A VP system controller with Shimadzu LC-10AD VP liquid chromatography pumps (with an Alltima C18 3u (50 mm x 2.1 mm) reversed phase column and gradients of water-acetonitrile supplemented with 0.1% formic acid), a Shimadzu DGU-14A degasser, a Thermo Finnigan surveyor autosampler, a Thermo Finnigan surveyor PDA detector and a Finnigan LCQ Deca XP Max.

Liquid Chromatography – Mass Spectroscopy. Linear calibration curves of derivatives **1b**, **13a**, **14a** and **15** were obtained by injection of 0.1 – 2.0 μ L 1.0 mM solutions in acetonitrile and measurement in MS-MS mode. The measured signal was integrated using a Gaussian curve fitting procedure. Curves from at least 5 data points were obtained for all compounds ($r^2 > 0.99$). Compounds were hydrolyzed by charging a 40 mL Radley Carousel Reaction Tube with 0.010 mM Napy followed by addition of 1.0 mL of the appropriate solvent and heating the solutions at the temperature of choice in a Radley Carousel with applied cooling under temperature control. 50 μ L Samples were taken at specific time intervals and diluted to 1.0 mL acetonitrile. Subsequent measurement by injection of 3.0 μ L was performed in MS-MS mode by MS and UV detection followed by integration of the signal gave the desired concentrations. Data acquired by UV as well as MS detection were in good agreement. Data depicted in figures 3.1 and 3.2 were obtained from the MS-trace.

Synthesis. 2-*n*-Butylureido-6-methyl-4[1H]-pyrimidinone (**3**) was prepared as reported by Beijer *et al.*⁷ 2,7-dichloro-1,8-naphthyridine (**6**) and 7-amino-[1H]-2-oxo-1,8-naphthyridine (**10**) were prepared as reported by Newkome *et al.*¹⁶ 7-Acetamido-[1H]-2-oxo-1,8-naphthyridine (**11a**) and 7-acetamido-2-chloro-1,8-naphthyridine (**7**) were prepared as reported by Corbin *et al.*¹⁷ Primary amides were synthesized according to literature procedures except the synthesis of 6-benzyloxyhexanoic amide which is described below.

General procedure for the symmetric Pd-catalyzed amidation of 2,7-dichloro-1,8-naphthyridine (6**) with primary amides (Table 3.1 and 3.2):** A Schlenk tube was charged with Pd-catalyst, ligand (L/Pd = 2.0-3.0), inorganic base (2 equiv), **6** (1 equiv), primary amide (2 equiv) and 1,4-dioxane. The Schlenk was capped, evacuated and back-filled with Ar three times. Still under Ar, it was immersed into a 100 °C oil bath. After stirring for 4 - 24 h, the mixture was cooled, filtered over diatomaceous earth and evaporated in vacuo.

General procedure for the non-symmetric Pd-catalyzed amidation of 2,7-dichloro-1,8-naphthyridine (6**) with primary amides (Table 3.4):** A Schlenk tube was charged with Pd-catalyst, ligand (L/Pd = 2.0-3.0), inorganic base (1.4 equiv), **6** (1 equiv), primary amide (0.9 equiv) and 1,4-dioxane. The Schlenk was capped, evacuated and back-filled with Ar three times and was immersed into a 80 °C oil bath. After stirring for 8 h, the mixture was cooled, filtered over diatomaceous earth and evaporated in vacuo.

General procedure for the Pd-catalyzed amidation of 7-amido-2-chloro-1,8-naphthyridine with primary amides (Table 3.5 and 3.6): A Schlenk tube was charged with Pd-catalyst, ligand (L/Pd = 2.0), K₂CO₃ (1.4 equiv), corresponding **7** (1 equiv), primary amide (1.2 equiv) and 1,4-dioxane (0.20-0.25 M). The Schlenk was capped, evacuated and back-filled with Ar three times. Still under Ar, it was immersed into a 100 °C oil bath. After stirring for 10 – 24 h, the mixture was cooled, filtered over diatomaceous and evaporated in vacuo.

2,7-Bis-(dodecanoylamino)-1,8-naphthyridine, 1a (Table 3.1): Following the general procedure with 1.0 mmol **6** using a ligand to base ratio of 2.0-2.1 gave a red residue. This residue was recrystallized from EtOH, dried and recrystallized from toluene to yield the title compound as long white needles. Characterization of the compound was reported previously.¹³

2,7-Bis-(2-methylhexanoylamino)-1,8-naphthyridine, 1b (Table 3.2): To a Schlenk flask charged with **6** (100 mg, 0.502 mmol), 2-methylhexanoic acid amide (130 mg, 1.00 mmol), K₂CO₃ (146 mg, 1.06 mmol), Pd(OAc)₂ (5.6 mg, 25 μmol), and Xantphos (44.0 mg, 76 μmol) 5 mL of distilled dioxane was added. The resulting dispersion was immediately frozen by liquid-nitrogen, deoxygenated by two freeze-pump-thaw cycles, and finally backfilled with argon. The dispersion was stirred at reflux temperature (100 °C) for 12 h. After evaporation in vacuo, the brownish residue was dissolved in chloroform. The solution was filtered and evaporated. Purification by column chromatography (silica gel, chloroform, then chloroform/acetone 20:1 v/v), 88 mg (46 %) of a yellowish powder was obtained, which is pure according to the NMR spectrum. An analytical sample was prepared by precipitation in heptane to give a white powder. M.P. 95-100 °C; ¹H NMR (CDCl₃): δ = 8.42 (d, 2H, J = 9 Hz), 8.33 (br, 2H), 8.11 (d, 2H, J = 9 Hz), 2.22 (m, 2H), 1.62 (m, 2H), 1.40 (m, 2H), 1.31 (m, 8H), 1.15 (d, 6H, J = 7 Hz), 0.89 (t, 6H, J = 8 Hz) ppm; ¹³C NMR (CDCl₃): δ = 175.9, 153.9, 153.5, 138.8, 118.1, 113.4, 42.5, 33.8, 29.3, 22.5, 17.4, 13.7 ppm; MALDI-TOF-MS: (m/z) calcd. 384.53; observed: 385.32 (M+H⁺), 407.28 (M+Na⁺); FTR-IR (ATR): ν = 2960, 2928, 2860, 1684 (C=O stretch), 1608, 1537, 1500, 1460, 1392, 1377, 1310, 1282, 1169, 1134, 1116, 854, 803 cm⁻¹; Anal. Calcd. for C₂₂H₃₂N₄O₂: C 68.72, H 8.39, N 14.57; found: C 69.02, H 8.39, N 14.42.

2,7-Bis-(1-adamantanecarbonylamino)-1,8-naphthyridine, 1c (Table 3.2): Following the general procedure with 0.5 mmol **6** the resulting brownish residue was dissolved in chloroform followed by filtration. The title compound was purified by chromatography (SiO₂, chloroform / acetone 20:1 v/v) as a white powder (200 mg, 82%). M.P. 177-182 °C; ¹H NMR (CDCl₃): δ = 8.45 (d, 2H), 8.31 (br, 2H), 8.11 (d, 2H), 2.12 (m, 6H), 2.00 (m, 12H), 1.72- 1.81 (m, 12H) ppm; ¹³C NMR (CDCl₃): δ = 177.0, 154.0, 153.7, 138.8, 118.3, 138.9, 113.4, 42.0, 39.1, 36.3, 28.0 ppm; MALDI-TOF-MS: (m/z) calcd. 484.65; observed: 485.37 (M+H⁺), 507.35 (M+Na⁺), 523.33 (M+K⁺); FTR-IR (ATR): ν = 2905, 2852, 1690, 1609, 1529, 1498, 1454, 1378, 1308, 1284, 1260, 1206, 1177, 1133, 1079, 976, 930, 867, 855, 802 cm⁻¹; Anal. Calcd. for C₃₀H₃₆N₄O₂: C 74.35, H 7.49, N 11.56; found: C 74.62, H 7.61, N 11.20.

2,7-Bis-(10-undecenoylamino)-1,8-naphthyridine, 1d (Table 3.2): Following the general procedure with 10 mmol **6** the resulting red-brown residue was washed with *n*-heptane, filtered, dissolved in chloroform and filtered again. Evaporation gave an orange-colored crude product, which was recrystallized twice from ethanol to give the title compound as a fine white powder (4.38 g, 89%). M.P. 124-127 °C; ¹H NMR (CDCl₃): δ = 8.64 (br, 2H), 8.44 (d, 2H, J = 9 Hz), 8.11 (d, 2H, J = 9 Hz), 5.82-5.78 (m, 2H), 5.00-4.90 (m, 4H),

2.44 (t, 4H, $J = 9$ Hz), 2.01 (m, 4H), 1.70 (m, 4H), 1.35-1.26 (m, 20H) ppm; ^{13}C NMR (CDCl_3): $\delta = 172.4$, 154.0, 153.6, 139.1, 139.0, 118.3, 114.2, 113.5, 37.9, 33.7, 29.3–28.9 (multiple peaks), 25.2 ppm; MALDI-TOF-MS: (m/z) calcd. 492.35; observed: 493.31 ($\text{M}+\text{H}^+$), 515.29 ($\text{M}+\text{Na}^+$), 531.27 ($\text{M}+\text{K}^+$); FTR-IR (ATR): $\nu = 3327$, 2920, 2850, 1673, 1614, 1547, 1507, 1469, 1399, 1317, 1293, 1177, 1145, 994, 968, 910, 851, 803 cm^{-1} ; Anal. Calcd. for $\text{C}_{30}\text{H}_{44}\text{N}_4\text{O}_2$: C 73.13, H 9.02, N 11.37; found: C 73.12, H 9.06, N 11.58.

2,7-Bis-(9-undecenoylamino)-1,8-naphthyridine, 1d isomer 20 mL of distilled toluene was added to 200 mL of Schlenk flask charged with **6** (200 mg, 1.00 mmol), 10-undecenoic acid amide (369 mg, 2.00 mmol), K_2CO_3 (276 mg, 2.00 mmol), $\text{Pd}(\text{OAc})_2$ (30.3 mg, 0.136 mmol), and Xantphos (237 mg, 0.405 mmol). The resulting dispersion was immediately frozen by liquid-nitrogen, deoxygenated by a freeze-pump-thaw cycle, and backfilled with argon. The dispersion was stirred at reflux temperature for 32 hours. After evaporation in vacuo, the brownish residue was washed with *n*-heptane and dissolved in chloroform. Insoluble matter was removed by silica-gel filtration, followed by a second evaporation. The orange-colored crude product was recrystallized twice from hot ethanol to give the almost fully isomerized compound as a fine pale-yellowish powder (82 mg, 17 %). M.P. 117–119 °C; ^1H NMR (CDCl_3): $\delta = 8.44$ (d, 2H, $J = 9$ Hz), 8.39 (br, 2H), 8.12 (d, 2H, $J = 9$ Hz), 5.40 (m, 4H), 2.44 (t, 4H, $J = 7$ Hz), 2.04–1.95 (m, 4H), 1.72 (m, 4H), 1.63–1.58 (dd, 6H), 1.36–1.29 (m, 16H) ppm; ^{13}C NMR (CDCl_3): $\delta = 172.3$, 153.9, 153.7, 139.0, 131.5, 130.7, 124.7, 123.7, 118.3, 113.4, 38.0, 32.5, 29.5, 29.4, 29.2, 29.2, 29.1, 29.0, 28.9, 26.8, 25.2, 17.9 ppm; MALDI-TOF-MS: (m/z) calcd. 492.35; observed: 493.33 ($\text{M}+\text{H}^+$), 515.31 ($\text{M}+\text{Na}^+$), 531.28 ($\text{M}+\text{K}^+$); FTR-IR (ATR): $\nu = 3325$, 3009, 2920, 2850, 1672, 1614, 1546, 1507, 1467, 1398, 1291, 1176, 1145, 963, 851, 818 cm^{-1} .

2,7-Bis-(6-benzyloxyhexanoylamino)-1,8-naphthyridine, 1e (Table 3.2): Following the general procedure with 0.5 mmol **6**, 21.6 μmol of $\text{Pd}_2(\text{dba})_3$ and 121 μmol of Xantphos gave a red-brown residue which was dissolved in chloroform and filtered. Evaporation gave a red-colored crude product, which was purified by chromatography (SiO_2 , chloroform / acetone 8:1 v/v) to yield the title compound as a yellowish gum (168 mg, 59 %). No reaction was observed when $\text{Pd}(\text{OAc})_2$ was used as a palladium source. ^1H NMR (CDCl_3): $\delta = 8.99$ (br, 2H), 8.42 (d, 2H, $J = 9$ Hz), 8.09 (d, 2H, $J = 9$ Hz), 7.35–7.23 (m, 10H), 4.48 (s, 4H), 3.44 (t, 4H, $J = 6$ Hz), 2.42 (t, 4H, $J = 8$ Hz), 1.72–1.57 (m, 8H), 1.39 (m, 4H) ppm; ^{13}C NMR (CDCl_3): $\delta = 172.8$, 154.1, 153.5, 139.0, 138.5, 128.4, 127.6, 127.5, 118.3, 113.5, 72.5, 70.9, 37.9, 29.4, 25.8, 25.2 ppm; MALDI-TOF-MS: (m/z) calcd. 568.30; observed: 569.18 ($\text{M}+\text{H}^+$), 591.16 ($\text{M}+\text{Na}^+$), 607.13 ($\text{M}+\text{K}^+$); FTR-IR (ATR): $\nu = 3327$, 2925, 2852, 1669, 1618, 1547, 1507, 1469, 1399, 1317, 1293, 1177, 1145, 1102, 1024, 968, 910, 851 cm^{-1} .

2,7-Bis-[2-(*t*-butyldimethylsilyloxy)propanoylamino]-1,8-naphthyridine, 1f (Table 3.2): Following the general procedure with 10 mmol **6** the resulting red-brown residue was dissolved in dichloromethane and filtered. Evaporation gave a red-colored crude product, which was recrystallized twice from MeOH and finally from heptane to give the title compound as fine white needles (4.36 g, 82%). M.P. 110–111 °C; ^1H NMR (CDCl_3): $\delta = 9.32$ (br, 2H), 8.49 (d, 2H, $J = 9$ Hz), 8.14 (d, 2H, $J = 9$ Hz), 4.40 (q, 2H, $J = 7$ Hz), 1.47 (d, 6H, $J = 7$ Hz), 0.97 (s, 18H), 0.17 (s, 12H) ppm; ^{13}C NMR (CDCl_3): $\delta = 174.2$, 153.7, 139.2, 119.0, 113.8, 70.9, 26.2, 22.5, 18.5, -4.4, -4.7 ppm; MALDI-TOF-MS: (m/z) calcd. 532.29; observed: 533.28 ($\text{M}+\text{H}^+$), 555.27 ($\text{M}+\text{Na}^+$), 571.24 ($\text{M}+\text{K}^+$); FTR-IR (ATR): $\nu = 3388$, 2957, 2928, 2857, 1697, 1612, 1528, 1506, 1463, 1390, 1312, 1292, 1255, 1120, 1070, 957, 925, 908, 830, 800 cm^{-1} ; Anal. Calcd. for $\text{C}_{26}\text{H}_{44}\text{N}_4\text{O}_4\text{Si}_2$: C 58.61, H 8.32, N 10.52; found: C 58.41, H 8.29, N 10.36.

6-Benzyloxy-hexanoic amide, 9: 6-Benzyloxy-hexanoic acid (4.5 g, 20.2 mmol) was converted to the acid chloride by oxalyl chloride (5 mL) with two drops of dimethylformamide (DMF) as a catalyst, followed by a dropwise addition into a large excess of concentrated ammonia solution (20 mL) to give a white precipitate. The precipitate was collected by filtration and washed with concentrated ammonia solution and water. The product was dried in vacuo overnight at 60 °C to yield the title compound as a white powder (4.15 g, 93%). M.P. 76-79 °C; ^1H NMR (CDCl_3): δ = 7.38-7.27 (m, 5H), 5.46 (br, 2H), 4.49 (s, 2H), 3.47 (t, 2H, J = 6 Hz), 2.22 (t, 2H, J = 8 Hz), 1.64 (m, 4H), 1.45 (m, 2H) ppm; ^{13}C NMR (CDCl_3): δ = 175.4, 138.6, 128.4, 127.6, 127.5, 72.9, 70.1, 35.8, 29.4, 25.8, 25.2 ppm; MALDI-TOF-MS: (m/z) calcd. 492.3; observed 493.3 ($M+1$), 515.3 ($M+\text{Na}^+$), 531.3 ($M+\text{K}^+$); FTR-IR (ATR): ν = 3357, 3180, 2942, 2856, 1659, 1630, 1464, 1453, 1414, 1359, 1345, 1102, 1050, 967 cm^{-1} .

7-(2-Ethyl-hexanoylamino)-[1H]-2-oxo-1,8-naphthyridine, 11b: A mixture of **10** (11.0 g, 68.3 mmol) and 2-ethylhexanoyl chloride (19.0 g, 116.8 mmol) in 100 mL pyridine was heated to 110 °C and stirred for 18 h. The reaction mixture was evaporated to dryness followed by co-evaporation with toluene. The black residue was dissolved in 20 mL hot CHCl_3 and 250 mL *n*-pentane was added under vigorous stirring to precipitate the crude product. Further purification by column chromatography (silica gel, EtOAc/*n*-hexane 1:1) gave 12.5 g (64%) of white product. M.P. = 172 °C; ^1H NMR (CDCl_3): δ = 12.89 (s, 1H), 11.79 (s, 1H), 8.45 (d, 1H), 7.93 (d, 1H), 7.75 (d, 1H), 6.64 (d, 1H), 2.84 (m, 1H), 1.73-1.42 (m, 4H), 1.41-1.25 (m, 4H), 0.97 (t, 3H), 0.86 (t, 3H) ppm; ^{13}C NMR (CDCl_3): δ = 177.7, 165.0, 154.0, 148.6, 139.6, 138.9, 119.8, 111.1, 110.8, 48.4, 32.4, 29.6, 26.1, 22.8, 13.8, 11.8 ppm; MALDI-TOF-MS: (m/z) calcd. 287.16; observed: 288.31 ($M+\text{H}^+$), 310.29 ($M+\text{Na}^+$); FTR-IR (ATR): ν = 3107, 2958, 2872, 1701, 1662, 1622, 1578, 1522, 1462, 1398, 1343, 1306, 1287, 1256, 1246, 1184, 1137, 1020, 935, 839, 817, 784, 669 cm^{-1} . Anal. Calcd. for: $\text{C}_{16}\text{H}_{21}\text{N}_3\text{O}_2$: C 66.88, H 7.37, N 14.62 found: C 66.82, H 7.46, N 14.69.

7-Pivaloylamino-[1H]-2-oxo-1,8-naphthyridine, 11c: A mixture of **10** (5.07 g, 31.5 mmol) and pivaloyl chloride (6.03 g, 50.0 mmol) in 50 mL pyridine was heated to 110 °C and stirred for 20 hours. The reaction mixture was evaporated to dryness followed by co-evaporation with toluene. The black residue was dissolved in 200 mL hot ethyl acetate and filtered. Multiple crystallizations from ethyl acetate gave the title compound as white needles (1.55 g, 20 %). M.P. = 261 °C; ^1H NMR (CDCl_3): δ = 11.32 (br, 1H), 9.74 (br, 1H), 8.22 (d, 1H, J = 9 Hz), 7.91 (d, 1H, J = 9 Hz), 7.71 (d, 1H, J = 9 Hz), 6.62 (d, 1H, J = 9 Hz), 1.39 (s, 9H) ppm. ^{13}C NMR (CDCl_3): δ = 179.0, 164.5, 154.0, 148.5, 139.5, 138.6, 120.4, 111.5, 111.3, 40.4, 27.1 ppm. MALDI-TOF-MS: (m/z) calcd. 245.12; observed: 246.27 ($M+\text{H}^+$); FTR-IR (ATR): ν = 3177, 2976, 2910, 1687, 1659, 1617, 1574, 1511, 1476, 1461, 1398, 1374, 1339, 1304, 1282, 1246, 1153, 1141, 995, 939, 918, 847, 828, 801 cm^{-1} ; Anal. Calcd. for: $\text{C}_{16}\text{H}_{21}\text{N}_3\text{O}_2$: C 63.66, H 6.16, N 17.13; found: C 63.66, H 6.20, N 17.09.

7-(2-Ethyl-hexanoylamino)-7-chloro-1,8-naphthyridine, 12a A solution of **11b** (12.5 g, 43.5 mmol) in 100 mL POCl_3 was stirred at 95 °C for 3 hours. The solution was allowed to cool to room temperature and some excess of POCl_3 was evaporated in vacuo. The remaining solution was slowly poured into 500 mL iced water under vigorous stirring followed by neutralization with concentrated aqueous NH_3 solution to pH = 8. Subsequently, the crude product was extracted by CH_2Cl_2 (2 x 150 mL) followed by washing the combined organic layers with saturated NaHCO_3 solution (2 x 100 mL), H_2O (2 x 100 mL), brine (1 x 100 mL) and dried with Na_2SO_4 . By column chromatography (silica gel, EtOAc/*n*-hexane 1:1) 12.1 g (91%) of

white product was obtained. M.P. = 108-112 °C; ^1H NMR (CDCl_3): δ = 9.34 (s, 1H), 8.55 (d, 1H), 8.15 (d, 1H), 8.02 (d, 1H), 7.32 (d, 1H), 2.26 (m, 1H), 1.65-1.43 (m, 4H), 1.22-1.15 (m, 4H), 0.85 (t, 3H), 0.75 (t, 3H) ppm; ^{13}C NMR (CDCl_3): δ = 176.0, 154.6, 154.2, 154.1, 139.0, 138.7, 121.9, 119.0, 115.8, 50.1, 32.1, 29.5, 25.7, 22.6, 13.7, 11.7 ppm; MALDI-TOF-MS: (m/z) calcd. 305.13; observed: 306.25 ($\text{M}+\text{H}^+$), 328.23 ($\text{M}+\text{Na}^+$); FTR-IR (ATR): ν = 3182, 3127, 3054, 2962, 2930, 2857, 1694, 1609, 1593, 1489, 1400, 1321, 1279, 1259, 1176, 1133, 1107, 1002, 940, 850, 796; Anal. Calcd. for: $\text{C}_{16}\text{H}_{20}\text{ClN}_3\text{O}$: C 62.84, H 6.59, N 13.74; found: C 62.54, H 6.80, N 13.43.

7-Pivaloylamino-[1H]-2-chloro-1,8-naphthyridine, 12b A mixture of **11c** (1.55 g, 6.31 mmol) in 20 mL POCl_3 was stirred at 95 °C for 4 hours. The solution was allowed to cool to room temperature and some excess of POCl_3 was evaporated in vacuo. The remaining solution was slowly poured into 250 mL iced water under vigorous stirring followed by neutralization with concentrated aqueous NH_3 solution to pH = 8. The title compound was isolated as a white powder by filtration of the precipitate (1.34 g, 80 %). M.P. 174 °C; ^1H NMR (CDCl_3): δ = 8.59 (d, 1H, J = 9 Hz), 8.44 (br, 1H), 8.19 (d, 1H, J = 9 Hz), 8.07 (d, 1H, J = 9 Hz), 7.40 (d, 1H, J = 9 Hz), 1.36 (s, 9H) ppm; ^{13}C NMR (CDCl_3): δ = 177.6, 154.4, 154.3, 139.0, 138.6, 121.9, 119.0, 115.1, 40.0, 27.3 ppm; MALDI-TOF-MS: (m/z) calcd. 263.08; observed: 264.24 ($\text{M}+\text{H}^+$), 286.22 ($\text{M}+\text{Na}^+$). FTR-IR (ATR): ν = 3435, 3048, 2970, 1693, 1609, 1568, 1557, 1505, 1486, 1392, 1366, 1321, 1276, 1256, 1230, 1131, 988, 941, 906, 851, 792, 782 cm^{-1} ; Anal. Calcd. for $\text{C}_{16}\text{H}_{20}\text{ClN}_3\text{O}$: C 59.21, H 5.35, N 15.93 found: C 59.23, H 5.45, N 16.17.

7-(2-Ethylhexanoylamino)-2-chloro-1,8-naphthyridine, 12a (Table 3.4): Following the general procedure with 0.5 mmol **6** the resulting red residue was dissolved in chloroform and 2-*n*-butylureido-6-methyl-4[1H]-pyrimidinone (7.0 mg, 0.031 mmol) was added. The title compound was obtained as a white solid after purification by chromatography (SiO_2 , 2 % acetone / chloroform) as a white powder (50 mg, 42 %). Characterization of the compound indicated > 99% purity.

7-Dodecanoylamino-2-chloro-1,8-naphthyridine, 12c (Table 3.4): Following the general procedure with 0.5 mmol **6** the resulting brownish residue was dissolved in chloroform and 2-*n*-butylureido-6-methyl-4[1H]-pyrimidinone (7.2 mg, 0.032 mmol) was added. The title compound was obtained as a white solid after purification by chromatography (SiO_2 , 2 % acetone / chloroform) as a white powder (40 mg, 25 %). M.P. 147-149 °C; ^1H NMR (CDCl_3): δ = 9.12 (s, 1H), 8.58 (d, 1H), 8.20 (d, 1H), 8.05 (d, 1H), 7.28 (d, 1H), 2.45-2.49 (t, 2H), 1.75-1.86 (q, 2H), 1.18-1.43 (m, 16H), 0.87-0.92 (t, 3H) ppm; ^{13}C NMR (CDCl_3): δ = 176.2, 154.6, 154.2, 154.1, 139.0, 138.7, 121.9, 119.0, 115.8, 38.0, 31.2, 29.0-28.8 (multiple peaks), 25.0, 22.1, 13.7 ppm; MALDI-TOF-MS: (m/z) calcd. 361.92; observed: 362.52 ($\text{M}+\text{H}^+$), 384.48 ($\text{M}+\text{Na}^+$); FTR-IR (ATR): ν = 3182, 3131, 3062, 2961, 2922, 2870, 2850, 1685, 1610, 1597, 1490, 1400, 1345, 1265, 1185, 1154, 1142, 1007, 940, 853, 801; Anal. Calcd. for $\text{C}_{20}\text{H}_{28}\text{ClN}_3\text{O}$: C 66.37, H 7.80, N 11.61; found: C 66.10, H 7.63, 11.78.

7-(10-undecenoylamino)-2-chloro-1,8-naphthyridine, 12d (Table 3.4): Following the general procedure with 0.5 mmol **6** the resulting brownish residue dissolved in chloroform and 2-*n*-butylureido-6-methyl-4[1H]-pyrimidinone (7.6 mg, 0.034 mmol) was added. The title compound was obtained as a white solid after purification by chromatography (SiO_2 , 2 % acetone / chloroform) as a white powder (35 mg, 22 %). M.P. 137-141 °C; ^1H NMR (CDCl_3): δ = 9.12 (s, 1H), 8.58 (d, 1H), 8.20 (d, 1H), 8.05 (d, 1H), 7.28 (d, 1H), 5.80-5.77 (m, 1H), 5.03-4.94 (m, 2H), 2.41 (t, 2H, J = 9 Hz), 2.04 (m, 2H), 1.68 (m, 2H), 1.40-1.28 (m, 10H)

ppm; ^{13}C NMR (CDCl_3): δ = 175.8, 154.7, 154.3, 154.1, 140.3, 139.0, 138.7, 121.9, 118.8, 115.2, 114.4, 38.0, 33.9, 29.4–28.8 (multiple peaks), 25.0 ppm; MALDI-TOF-MS: (m/z) calcd. 345.88; observed: 346.62 ($\text{M}+\text{H}^+$), 368.57 ($\text{M}+\text{Na}^+$); FTR-IR (ATR): ν = 3156, 3115, 3051, 2932, 2863, 1691, 1612, 1594, 1470, 1401, 1351, 1265, 1187, 1162, 1143, 999, 971, 912, 857, 804; Anal. Calcd. for $\text{C}_{19}\text{H}_{24}\text{ClN}_3\text{O}$: C 65.98, H 6.99, N 12.15; found: C 65.75, H 6.79, 12.19.

2-(2-Ethylhexanoylamino)-7-acetylamino-1,8-naphthyridine, 13a (Table 3.5): Following the general procedure with 1.0 mmol **7** the resulting red residue was dissolved in chloroform and n-hexane was added to precipitate. The crude product was filtered and purified by chromatography (SiO_2 , ethyl acetate / hexane 2:1 v/v) to yield the title compound as a white powder (220 mg, 66 %). M.P. 117–122 °C; ^1H NMR (CDCl_3): δ = 9.80 (br, 1H), 8.98 (br, 1H), 8.49 (d, 2H, J = 9 Hz), 8.43 (d, 2H, J = 9 Hz), 8.10 (dd, 2H, J = 9 Hz), 2.25 (m, 1H), 2.21 (s, 3H), 1.75–1.48 (m, 4H), 1.28–1.26 (m, 4H), 0.96–0.82 (m, 6H) ppm; ^{13}C NMR (CDCl_3): δ = 175.6, 169.8, 154.3, 154.0, 153.4, 139.0, 138.9, 118.1, 113.8, 113.7, 50.4, 32.2, 29.6, 25.8, 24.8, 22.6, 13.8, 11.9 ppm; MALDI-TOF-MS: (m/z) calcd. 328.19; observed: 329.31 ($\text{M}+\text{H}^+$), 351.29 ($\text{M}+\text{Na}^+$); FTR-IR (ATR): ν = 3212, 2959, 2929, 2860, 1689, 1607, 1542, 1498, 1436, 1378, 1312, 1283, 1231, 1170, 1134, 1118, 852, 802 cm^{-1} ; Anal. Calcd. for $\text{C}_{18}\text{H}_{24}\text{N}_4\text{O}_2$: C 65.83, H 7.37, N 17.06; found: C 65.50, H 6.99, 16.75.

2-(Benzoylamino)-7-acetylamino-1,8-naphthyridine, 13b (Table 3.5): Following the general procedure with 1.0 mmol **7** the resulting red residue was purified by chromatography (SiO_2 , 5 % methanol / chloroform) to yield the title compound as a yellow powder (157 mg, 51 %). M.P. 125–128 °C; ^1H NMR (CDCl_3): δ = 9.16 (br, 1H), 9.00 (br, 1H), 8.61 (d, 1H, J = 9 Hz), 8.43 (d, 2H, J = 9 Hz), 8.17 (dd, 2H, J = 9 Hz), 7.93 (d, 2H, J = 9 Hz), 7.57 (t, 1H, J = 6 Hz), 7.47 (t, 2H, J = 8 Hz), 2.26 (s, 3H) ppm; ^{13}C NMR (CDCl_3): δ = 169.6, 166.2, 154.2, 153.6, 139.1, 133.9, 132.6, 128.9, 127.4, 118.4, 113.7, 25.0 ppm; MALDI-TOF-MS: (m/z) calcd. 306.11; observed: 307.27 ($\text{M}+\text{H}^+$), 329.25 ($\text{M}+\text{Na}^+$); FTR-IR (ATR): ν = 3213, 3057, 1682, 1606, 1539, 1496, 1376, 1282, 1246, 1135, 955, 894, 853, 801 cm^{-1} ; Anal. Calcd. for $\text{C}_{17}\text{H}_{14}\text{N}_4\text{O}_2$: C 66.66, H 4.61, N 18.29; found: C 66.78, H 4.60, N 16.95.

2-(1-Adamantanoylamino)-7-acetylamino-1,8-naphthyridine, 13c (Table 3.5): Following the general procedure with 0.5 mmol **7** the resulting red-brown residue was dissolved in chloroform and filtered. Evaporation yielded an orange-red product which was purified further by chromatography (SiO_2 , chloroform / acetone 8:1 v/v) followed by trituration with heptane to yield the title compound as a white powder (58 mg, 35 %). M.P. 152–155 °C; ^1H NMR (CDCl_3): δ = 8.46 (d, 1H, J = 9 Hz), 8.41 (d, 1H, J = 9 Hz), 8.33 (br, 1H), 8.15 (br, 1H), 8.13 (d, 2H, J = 9 Hz), 2.27 (s, 3H), 2.12 (m, 3H), 2.00 (m, 6H), 1.76 (m, 6H) ppm; ^{13}C NMR (CDCl_3): δ = 177.0, 169.0, 154.2, 153.7, 153.6, 139.0, 138.9, 118.4, 113.6, 113.1, 42.0, 39.1, 36.3, 28.0, 25.1 ppm; MALDI-TOF-MS: (m/z) calcd. 364.45; observed: 365.24 ($\text{M}+\text{H}^+$), 387.23 ($\text{M}+\text{Na}^+$); FTR-IR (ATR): ν = 3307, 2904, 2851, 1691, 1608, 1535, 1500, 1378, 1311, 1283, 1231, 1211, 1178, 1136, 1082, 1040, 982, 853, 802 cm^{-1} ; Anal. Calcd. for $\text{C}_{21}\text{H}_{24}\text{N}_4\text{O}_2$: C 69.21, H 6.64, N 15.37; found: C 69.23, H 6.48, N 15.33.

2-(10-Undecenoylamino)-7-acetylamino-1,8-naphthyridine, 13d (Table 3.5): Following the general procedure with 5.0 mmol **7** the resulting red residue was purified by chromatography (SiO_2 , 3 % methanol/chloroform). Trituration with pentane gave the title compound as a white powder (1.62 mg, 88 %). M.P. 133–135 °C; ^1H NMR (CDCl_3): δ = 8.43 (dd, 2H, J = 9 Hz), 8.13 (d, 2H, J = 9 Hz), 8.10 (br, 2H), 5.80 (m, 1H), 4.92 (m, 2H), 2.46 (t, 2H, J = 7 Hz), 2.28 (s, 3H), 2.03 (m, 2H), 1.75 (t, 2H), 1.35–1.25 (m, 10H) ppm;

^{13}C NMR (CDCl_3): δ = 172.2, 169.1, 153.7, 153.6, 153.5, 139.1, 139.0, 138.9, 118.3, 114.1, 113.3, 113.2, 38.0, 33.7, 29.2, 29.0, 28.9, 28.8, 25.4, 25.1, 25.0 ppm; MALDI-TOF-MS: (m/z) calcd. 369.22; observed: 369.41 ($\text{M}+\text{H}^+$), 391.40 ($\text{M}+\text{Na}^+$); FTR-IR (ATR): ν = 3303, 2925, 2854, 1689, 1607, 1545, 1498, 1435, 1384, 1282, 1232, 1134, 1118, 990, 908, 854, 802 cm^{-1} ; Anal. Calcd. for $\text{C}_{21}\text{H}_{28}\text{N}_4\text{O}_2$: C 68.45, H 7.66, N 15.20; found: C 68.53, H 8.01, N 14.96.

2-(6-Benzyloxyhexanoylamino)-7-acetylamino-1,8-naphthyridine, 13e (Table 3.5): Following the general procedure with 2.0 mmol **7** and using $\text{Pd}_2(\text{dba})_3$ as the catalyst and Cs_2CO_3 as a base, the resulting red-brown residue was purified by chromatography (SiO_2 , 2 % ethanol / chloroform) to yield the title compound as a yellow powder (653 mg, 80 %). M.P. 146 °C; ^1H NMR (CDCl_3): δ = 10.0 (br, 1H), 9.69 (br, 1H), 8.42 (d, 1H, J = 9 Hz), 8.41 (d, 1H, J = 9 Hz), 8.06 (d, 2H, J = 9 Hz), 4.46 (s, 2H), 3.41 (t, 2H, J = 6 Hz), 2.40 (t, 2H, J = 7 Hz), 2.17 (s, 3H), 1.64-1.50 (m, 4H), 1.38-1.30 (m, 2H) ppm; ^{13}C NMR (CDCl_3): δ = 172.7, 169.9, 154.4, 153.3, 139.0, 138.9, 138.4, 128.2, 127.5, 127.4, 118.0, 113.7, 113.6, 72.8, 69.9, 29.3, 25.6, 24.8, 24.7 ppm; MALDI-TOF-MS: (m/z) calcd. 406.20; observed: 407.40 ($\text{M}+\text{H}^+$), 429.38 ($\text{M}+\text{Na}^+$), 445.35 ($\text{M}+\text{K}^+$); FTR-IR (ATR): ν = 3213, 3032, 2933, 2857, 1694, 1606, 1542, 1496, 1454, 1379, 1312, 1282, 1232, 1134, 1115, 1090, 852, 802 cm^{-1} ; Anal. Calcd. for $\text{C}_{23}\text{H}_{26}\text{N}_4\text{O}_2$: C 67.96, H 6.45, N 13.78; found: C 67.78, H 6.22, N 13.69.

2-(5-Methoxycarbonyl-hexanoylamino)-7-acetylamino-1,8-naphthyridine, 13f (Table 3.5): Following the general procedure with 5.0 mmol **7** and using $\text{Pd}_2(\text{dba})_3$ as the catalyst and Cs_2CO_3 as a base, the resulting red-brown residue was purified by chromatography (SiO_2 , 3 % methanol / chloroform) to yield the title compound as a white powder (1.32 g, 76 %). M.P. 93-95 °C; ^1H NMR (CDCl_3): δ = 8.41 (d, 2H, J = 8 Hz), 8.32 (br, 2H), 8.14 (d, 2H, J = 9 Hz), 3.68 (s, 3H), 2.48 (t, 2H, J = 7 Hz), 2.37 (t, 2H, J = 6 Hz), 2.27 (s, 3H), 1.75 (m, 4H); ^{13}C NMR (CDCl_3): δ = 173.7, 171.7, 169.2, 153.8, 153.5, 139.0, 118.3, 113.4, 113.3, 51.5, 37.3, 33.5, 25.0, 23.4, 24.2 ppm; MALDI-TOF-MS: (m/z) calcd. 344.15; observed: 345.32 ($\text{M}+\text{H}^+$), 367.31 ($\text{M}+\text{Na}^+$); FTR-IR (ATR): ν = 3241, 2950, 1739, 1705, 1614, 1548, 1507, 1418, 1376, 1314, 1290, 1258, 1234, 1198, 1155, 1132, 1118, 985, 884, 850 cm^{-1} ; Anal. Calcd. for $\text{C}_{17}\text{H}_{20}\text{N}_4\text{O}_4$: C 59.29, H 5.85, N 16.27; found: C 58.95, H 5.63, N 18.31.

2,7-Bis-(2-ethylhexanoylamino)-1,8-naphthyridine, 14a (Table 3.6): Following the general procedure with 1.0 mmol **12a** the resulting red residue was dissolved in heptane and filtered. Purification by chromatography (SiO_2 , chloroform / acetone 8:1 v/v) gave the title compound as a white powder (360 mg, 89 %). M.P. 87-92 °C; ^1H NMR (CDCl_3): δ = 8.46 (d, 2H, J = 9 Hz), 8.35 (br, 2H), 8.13 (d, 2H, J = 9 Hz), 2.21 (m, 2H), 1.74-1.49 (m, 8H), 1.29 (m, 8H), 0.97-0.83 (m, 12H) ppm; ^{13}C NMR (CDCl_3): δ = 175.4, 153.8, 153.3, 139.0, 118.4, 113.5, 50.9, 32.4, 29.7, 26.0, 22.7, 13.9, 12.0 ppm; MALDI-TOF-MS: (m/z) calcd. 412.58; observed: 413.35 ($\text{M}+\text{H}^+$), 435.34 ($\text{M}+\text{Na}^+$); FTR-IR (ATR): ν = 2959, 2929, 2860, 1684, 1608, 1537, 1500, 1460, 1392, 1377, 1310, 1282, 1169, 1134, 1116, 854, 803 cm^{-1} ; Anal. Calcd. for $\text{C}_{24}\text{H}_{36}\text{N}_4\text{O}_2$: C 69.87, H 8.80, N 13.58; found: C 69.27, H 8.39, N 13.42.

2-(1-Adamantanoylamino)-7-(2-ethylhexanoylamino)-1,8-naphthyridine, 14b (Table 3.6): Following the general procedure with 0.3 mmol **12a** the resulting red-brown residue was dissolved in chloroform and filtered. Evaporation yielded an orange-red product, which was purified further by chromatography (SiO_2 , chloroform / acetone 20:1 v/v) followed by precipitation from heptane to yield the title compound as a white powder (68 mg, 47 %). M.P. 113-116 °C; ^1H NMR (CDCl_3): δ = 8.45 (d, 2H, J = 9 Hz), 8.31 (br,

1H), 8.13 (d, 2H, $J = 9$ Hz), 8.08 (br, 1H), 2.23 (m, 1H), 2.13 (m, 3H), 2.00 (m, 6H), 1.82-1.57 (m, 10H), 1.33 (m, 4H), 1.00-0.87 (m, 6H) ppm; ^{13}C NMR (CDCl_3): $\delta = 177.0, 175.3, 154.1, 153.8, 153.7, 139.0, 138.9, 118.3, 113.5, 113.4, 50.9, 41.9, 39.0, 36.3, 32.4, 29.7, 28.0, 26.0, 22.7, 14.1, 13.9, 12.0$ ppm; MALDI-TOF-MS: (m/z) calcd. 448.61; observed: 449.35 ($\text{M}+\text{H}^+$), 471.33 ($\text{M}+\text{Na}^+$); FTR-IR (ATR): $\nu = 2906, 2852, 1693, 1608, 1535, 1500, 1378, 1311, 1283, 1175, 1135, 1082, 854, 802\text{ cm}^{-1}$; Anal. Calcd. for $\text{C}_{27}\text{H}_{36}\text{N}_4\text{O}_2$: C 72.29, H 8.09, N 12.49; found: C 72.27, H 7.75, N 11.97.

7-[2-(*t*-Butyldimethylsilyloxy)propanoylamino]-2-(2-ethylhexanoylamino)-1,8-naphthyridine, 14c (Table 3.6): Following the general procedure with 10.0 mmol **12a** the resulting red residue was further purified by chromatography (SiO_2 , 10 % ethyl acetate / hexane) to yield the title compound as a white powder (4.02 g, 85 %). M.P. 84 °C; ^1H NMR (CDCl_3): $\delta = 9.33$ (br, 1H), 9.18 (br, 1H), 8.37 (dd, 2H, $J = 9$ Hz), 8.02 (dd, 2H, $J = 9$ Hz), 4.25 (q, 1H), 2.15 (m, 1H), 1.63-1.37 (m, 4H), 1.34 (d, 3H, $J = 7$ Hz), 1.15-1.04 (m, 4H), 0.83-0.63 (m, 15H) ppm; ^{13}C NMR (CDCl_3): $\delta = 175.6, 175.4, 173.4, 154.2, 154.1, 153.6, 153.1, 153.0, 138.8, 138.7, 118.3, 113.7, 113.0, 70.2, 50.1, 50.0, 32.0, 31.8, 29.4, 29.3, 25.7, 25.6, 25.9, 25.5, 22.5, 23.8, 21.8, 17.9, 13.7, 13.6, 11.8, 11.6$ ppm; MALDI-TOF-MS: (m/z) calcd. 472.29; observed: 473.21 ($\text{M}+\text{H}^+$), 495.19 ($\text{M}+\text{Na}^+$), 511.16 ($\text{M}+\text{K}^+$); FTR-IR (ATR): $\nu = 3380, 2931, 2859, 1703, 1608, 1530, 1500, 1380, 1311, 1283, 1253, 1172, 1134, 1118, 1061, 948, 910, 831, 803\text{ cm}^{-1}$; Anal. Calcd. for $\text{C}_{25}\text{H}_{40}\text{N}_4\text{O}_3\text{Si}$: C 63.52, H 8.53, N 11.85; found: C 63.32, H 8.58, N 11.82.

7-[6-(Benzyloxycarbonylamino)-hexanoylamino]-2-(2-ethylhexanoylamino)-1,8-naphthyridine, 14d (Table 3.6): Following the general procedure with 1.0 mmol **12a** the resulting red-brown residue was purified by chromatography (SiO_2 , ethyl acetate / hexane 1:1 v/v) to yield the title compound as a yellow oil (330 mg, 65 %). ^1H NMR (CDCl_3): $\delta = 8.58$ (br, 1H), 8.47 (d, 2H, $J = 9$ Hz), 8.41 (br, 1H), 8.16 (dd, 2H, $J = 9$ Hz), 5.10 (s, 1H), 4.93 (s, 1H), 3.21 (q, 2H), 2.43 (t, 2H), 2.24 (m, 1H), 1.82-1.25 (m, 14H), 0.98-0.84 (m, 6H) ppm; ^{13}C NMR (CDCl_3): $\delta = 176.1, 172.7, 156.3, 154.5, 154.3, 139.0, 138.9, 136.6, 128.3, 127.9, 118.0, 113.9, 66.4, 49.8, 40.6, 36.9, 32.0, 29.5, 29.2, 25.9, 25.7, 24.3, 22.6, 13.8, 11.8$ ppm; MALDI-TOF-MS: (m/z) calcd. 533.26; observed: 534.26 ($\text{M}+\text{H}^+$), 556.25 ($\text{M}+\text{Na}^+$); FTR-IR (ATR): $\nu = 3301, 3035, 2930, 2860, 1684, 1607, 1537, 1498, 1456, 1380, 1311, 1282, 1166, 1134, 1027, 910, 853, 803\text{ cm}^{-1}$.

7-(Pivaloylamino)-2-(2-ethylhexanoylamino)-1,8-naphthyridine, 15 (Table 3.6): Following the general procedure with 0.5 mmol **12b** the resulting red residue was further purified by chromatography (SiO_2 , 1 % methanol / chloroform) to yield the title compound as a white powder (100 mg, 54 %). M.P. 99-101 °C; ^1H NMR (CDCl_3): $\delta = 8.47$ (dd, 2H, $J = 9$ Hz), 8.36 (br, 1H), 8.33 (br, 1H), 8.14 (dd, 2H, $J = 9$ Hz), 2.23 (m, 1H), 1.75-1.58 (m, 4H), 1.36 (s, 12H), 1.35-1.32 (m, 4H), 0.98-0.86 (m, 6H) ppm; ^{13}C NMR (CDCl_3): $\delta = 177.4, 175.2, 153.9, 153.6, 153.5, 138.9, 138.8, 118.2, 113.4, 113.2, 50.8, 39.9, 32.3, 29.6, 27.2, 25.9, 22.6, 13.8, 11.8$ ppm; MALDI-TOF-MS: (m/z) calcd. 370.24; observed: 371.20 ($\text{M}+\text{H}^+$), 393.18 ($\text{M}+\text{Na}^+$), 413.23 ($\text{M}+\text{K}^+$); FTR-IR (ATR): $\nu = 3314, 2960, 2931, 2873, 1700, 1676, 1606, 1538, 1499, 1376, 1309, 1283, 1166, 1135, 854, 801\text{ cm}^{-1}$; Anal. Calcd. for $\text{C}_{21}\text{H}_{30}\text{N}_4\text{O}_2$: C 68.08, H 8.16, N 15.12; found: C 67.96, H 7.90, N 14.89.

3.6 References

- (1) Lawrence, D. S.; Jiang, T.; Levett, M. *Chem. Rev.* **1995**, *95*, 2229-60.

- (2) Prins, L. J.; Reinhoudt, D. N.; Timmerman, P. *Angew. Chem. Int. Ed.* **2001**, 40, 2382-2426.
- (3) Zimmerman, S. C.; Corbin, P. S. *Struct. Bonding (Berlin)* **2000**, 96, 63-94.
- (4) Sherrington, D. C.; Taskinen, K. A. *Chem. Soc. Rev.* **2001**, 30, 83-93.
- (5) Sijbesma, R. P.; Meijer, E. W. *Chem. Commun.* **2003**, 5-16.
- (6) Sijbesma, R. P.; Beijer, F. H.; Brunsveld, L.; Folmer, B. J. B.; Hirschberg, J. H. K. K.; Lange, R. F. M.; Lowe, J. K. L.; Meijer, E. W. *Science* **1997**, 278, 1601-1604.
- (7) Beijer, F. H.; Sijbesma, R. P.; Kooijman, H.; Spek, A. L.; Meijer, E. W. *J. Am. Chem. Soc.* **1998**, 120, 6761-6769.
- (8) Corbin, P. S.; Zimmerman, S. C. *J. Am. Chem. Soc.* **1998**, 120, 9710-9711.
- (9) Ciferri, A. *Supramolecular Polymers*; Marcel Dekker: New York, 2000.
- (10) Brunsveld, L.; Folmer, B. J. B.; Meijer, E. W.; Sijbesma, R. P. *Chem. Rev.* **2001**, 101, 4071-4097.
- (11) Söntjens, S. H. M.; Meijer, J. T.; Kooijman, H.; Spek, A. L.; van Genderen, M. H. P.; Sijbesma, R. P.; Meijer, E. W. *Org. Lett.* **2001**, 3, 3887-3889.
- (12) Brammer, S.; Luning, U.; Kuhl, C. *Eur. J. Org. Chem.* **2002**, 4054-4062.
- (13) Wang, X.-Z.; Li, X.-Q.; Shao, X.-B.; Zhao, X.; Deng, P.; Jiang, X.-K.; Li, Z.-T.; Chen, Y.-Q. *Chem. Eur. J.* **2003**, 9, 2904-2913.
- (14) Park, T.; Zimmerman, S. C.; Nakashima, S. *J. Am. Chem. Soc.* **2005**, 127, 6520-6521.
- (15) Ligthart, G. B. W. L.; Ohkawa, H.; Sijbesma, R. P.; Meijer, E. W. *J. Am. Chem. Soc.* **2005**, 127, 810-811.
- (16) Newkome, G. R.; Garbis, S. J.; Majestic, V. K.; Fronczek, F. R.; Chiari, G. *J. Org. Chem.* **1981**, 46, 833-9.
- (17) Corbin, P. S.; Zimmerman, S. C.; Thiessen, P. A.; Hawryluk, N. A.; Murray, T. J. *J. Am. Chem. Soc.* **2001**, 123, 10475-10488.
- (18) Park, T.; Mayer, M. F.; Nakashima, S.; Zimmerman, S. C. *Synlett.* **2005**, 1435-1436.
- (19) Li, X.-Q.; Jiang, X.-K.; Wang, X.-Z.; Li, Z.-T. *Tetrahedron* **2004**, 60, 2063-2069.
- (20) Collin, J. P.; Youinou, M. T. *Inorg. Chim. Acta* **1992**, 201, 29-34.
- (21) Boelrijk, A. E. M.; Neenan, T. X.; Reedijk, J. *J. Chem. Soc., Dalton Trans.* **1997**, 4561-4570.
- (22) Hartwig, J. F. *Angew. Chem. Int. Ed.* **1998**, 37, 2046-2067.
- (23) Wolfe, J. P.; Wagaw, S.; Marcoux, J.-F.; Buchwald, S. L. *Acc. Chem. Res.* **1998**, 31, 805-818.
- (24) Yin, J.; Buchwald, S. L. *Org. Lett.* **2000**, 2, 1101-1104.
- (25) Yin, J.; Buchwald, S. L. *J. Am. Chem. Soc.* **2002**, 124, 6043-6048.
- (26) Klapars, A.; Antilla, J. C.; Huang, X.; Buchwald, S. L. *J. Am. Chem. Soc.* **2001**, 123, 7727-7729.
- (27) Klapars, A.; Huang, X.; Buchwald, S. L. *J. Am. Chem. Soc.* **2002**, 124, 7421-7428.
- (28) Huang, X.; Anderson, K. W.; Zim, D.; Jiang, L.; Klapars, A.; Buchwald, S. L. *J. Am. Chem. Soc.* **2003**, 125, 6653-6655.
- (29) Kranenburg, M.; van der Burgt, Y. E. M.; Kamer, P. C. J.; van Leeuwen, P. W. N. M.; Goubitz, K.; Fraanje, J. *Organomet.* **1995**, 14, 3081-9.
- (30) Peng, T.; Murase, T.; Goto, Y.; Kobori, A.; Nakatani, K. *Bioorgan. Med. Chem. Lett.* **2005**, 15, 259-262.
- (31) Wolfe, J. P.; Rennels, R. A.; Buchwald, S. L. *Tetrahedron* **1996**, 52, 7525-7546.
- (32) Wolfe, J. P.; Buchwald, S. L. *Tetrahedron Lett.* **1997**, 38, 6359-6362.
- (33) Yang, B. H.; Buchwald, S. L. *Org. Lett.* **1999**, 1, 35-37.
- (34) Li, X.-Q.; Feng, D.-J.; Jiang, X.-K.; Li, Z.-T. *Tetrahedron* **2004**, 60, 8275-8284.
- (35) Raposo, M. M. M.; Oliveira-Campos, A. M. F.; Shannon, P. V. R. *J. Chem. Res., Synopses* **1997**, 354-355.
- (36) Raposo, M. M. M.; Pereira, A. M. B.; Oliveira-Campos, A. M. F.; Shannon, P. V. R. *J. Chem. Res., Synopses* **2000**, 156-158, 528-558.

4

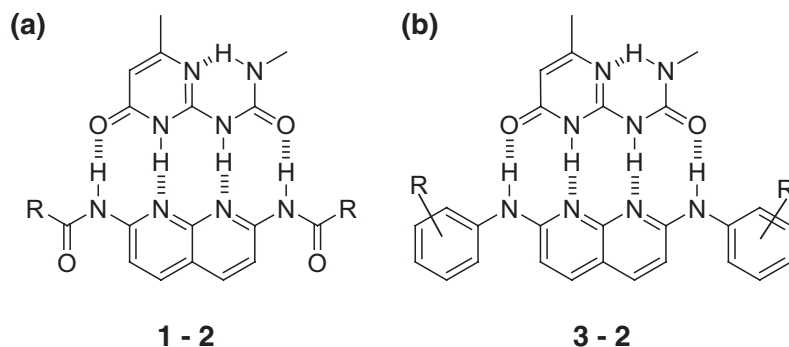
Pd-catalyzed amination to 2-amino- and 2,7-diamino-1,8-naphthyridines

Abstract

2,7-Di(arylamino)-1,8-naphthyridines and 7-amido-2-arylamino-1,8-naphthyridines are presented as a new class of donor-acceptor-acceptor-donor (DAAD) hydrogen bonding molecules. The synthetic accessibility by palladium catalyzed amination of 2-chloro- and 2,7-dichloro-1,8-naphthyridines is explored. Although catalytic amination of 2,7-dichloro-1,8-naphthyridines proved unsuccessful, a general catalytic amination of 7-amido-2-chloro-1,8-naphthyridines with a number of electron-rich and electron-deficient anilines using Pd(OAc)₂, Xantphos and K₂CO₃ or Cs₂CO₃ in dioxane was developed. Purification was performed by automated semi-preparative RP-HPLC. An asymmetric route to 2,7-di(arylamino)-1,8-naphthyridines was established by palladium catalyzed arylation of 7-amino-2-phenylamino-1,8-naphthyridine with aryl bromides. After optimization of reaction conditions, derivatives with electron-rich and electron-deficient aryl groups were synthesized and purified with automated semi-preparative RP-HPLC. Moderate yields are obtained and considerable biarylation of the naphthyridinamine group is observed. A study to the alkaline degradation of a di(arylamino), arylamino-carbamate and arylamino-amido derivatives showed no degradation of the arylamine group up to 120 °C. Additionally, the branched amide functionality displayed remarkable stability up to 60 °C.

4.1 Introduction

In the construction of supramolecular polymers as well as in the self-assembly of supramolecular architectures, there is an obvious need for strong complementary hydrogen bonding motifs. A promising binding motif for use in supramolecular engineering displaying strong and selective complementary binding is the DAAD – ADDA binding array of 2,7-diamido-1,8-naphthyridines **1** (Napy) with the 6[1H] tautomeric form of ureido-pyrimidinones **2** (UPy) (Scheme 4.1a).¹⁻⁶ In the previous chapter, a generally applicable palladium catalyzed amidation to 2,7-diamido-1,8-naphthyridine derivatives was reported.⁷ Thanks to the use of a weak base, functional groups could be incorporated. However, because of the electron-deficiency of the naphthyridine core, 2-amino-1,8-naphthyridine is a good leaving group upon nucleophilic attack at the carbonyl and in addition, the carbon of the amide carbonyl is presumably quite electrophilic. These effects result in a decreased hydrolytic stability of the amide functionality.^{3,4,8} An increased stability towards hydrolysis was observed when branched side-chains were introduced next to the carbonyl. When the amide functionalities are replaced by amino groups, increased stability under hydrolytic conditions can be expected. Therefore, the development of 2,7-diamino-1,8-naphthyridines **3** as complementary binding agent to the UPy seems interesting. However, to ensure sufficient hydrogen bond donor capability of the amino protons, the electron withdrawing character of the phenyl rings is essential (Scheme 4.1b).⁹

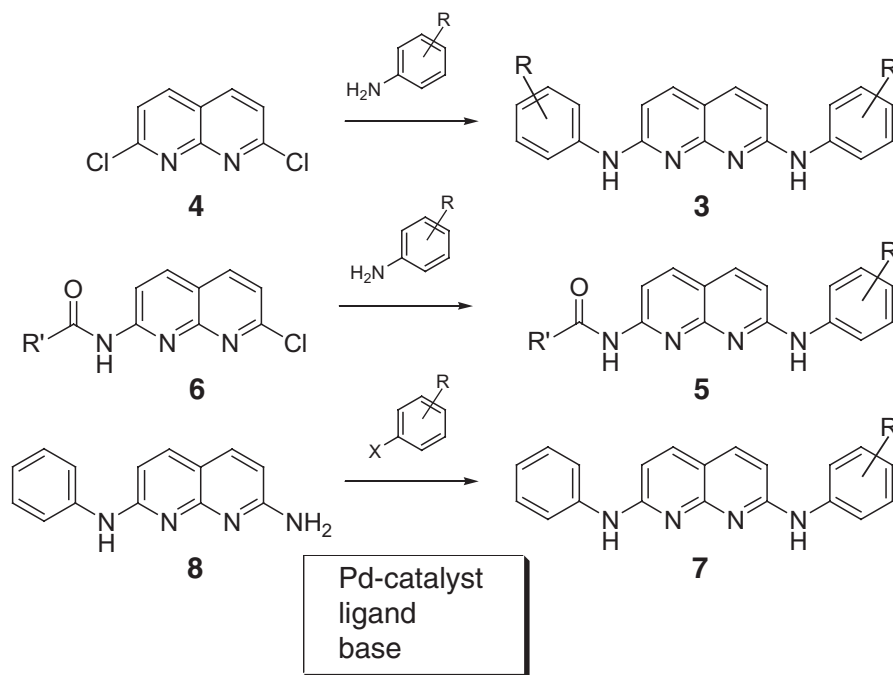


Scheme 4.1 Quadruple hydrogen bonding array based on ureido-pyrimidinone **2** with (a) 2,7-diamido-1,8-naphthyridines and (b) 2,7-diamino-1,8-naphthyridines.

Traditionally, preparation of diarylamines was performed by reductive elimination of aniline derivatives or arene nitration/reduction protocols.¹⁰ Over the last two decades, however, a number of cleverly designed and extremely useful methods for aryl-C-N bond formation have been reported.¹¹⁻¹³ These catalytic aminations of aryl halides with primary and secondary amines are numerous in literature and allow access to a large variety of di(arylamino)

compounds including functional groups. Although nickel^{14,15} and copper^{16,17} catalyzed aminations have been reported, palladium catalyzed aminations feature higher reactivity over a larger range of substrates and excellent functional group compatibility. Especially, the development of new and more electron rich phosphine ligands accelerated progress in this field. However, due to the fact that heteroaromatic halides such as chloropyridines are possible binding ligands for late transition metals,¹⁸ Pd-catalyzed amination of these derivatives was not possible until the advent of chelating diphosphine ligands like DPPP, DPPF and BINAP.^{19,20} Even though several papers have reported the successful amination of heteroaromatic halides containing one or multiple nitrogen atoms,²¹⁻²⁷ amination with anilines remains challenging due to their reduced nucleophilicity as compared to secondary or primary alkyl amines.

Starting from either the symmetric 2,7-dichloro-1,8-naphthyridine²⁸ **4** or an asymmetric 7-amido-2-chloro-1,8-naphthyridine **6**,^{6,7,29} a synthetic strategy to obtain 2,7-di(arylamino)- and 7-arylamino-2-amido-1,8-naphthyridines (**3** and **5**, respectively) was envisioned as indicated in Scheme 4.2. Monofunctional 2,7-di(arylamino)-1,8-naphthyridine derivatives **7** can be obtained by catalytic arylation of 7-amino-2-phenylamino-1,8-naphthyridine **8**.



Scheme 4.2 Synthetic strategy towards amino-amido and diamino-naphthyridines.

In this chapter, the synthetic accessibility by palladium catalyzed amination reactions leading to 2,7-di(arylamino)-1,8-naphthyridine derivatives **3** and **7** and 7-arylamino-2-amido-1,8-naphthyridines **5** is explored. When optimal reaction conditions are established, a number of derivatives bearing functional groups are synthesized and purified by automated semi-

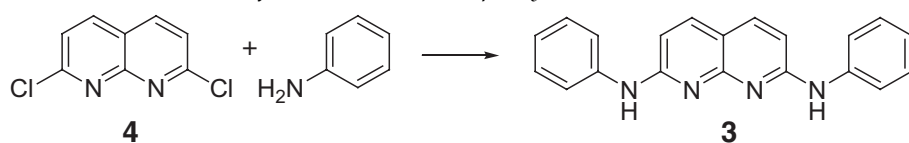
preparative RP-HPLC. Finally, the stability towards hydrolysis of a number of these Napy derivatives is evaluated.

4.2 Pd-catalyzed amination to 2-amino and 2,7-diamino-1,8-naphthyridine

4.2.1 Pd-catalyzed amination of 2,7-dichloro-1,8-naphthyridine

The reaction between 2,7-dichloro-1,8-naphthyridine **4** and aniline to give 2,7-diphenylamino-1,8-naphthyridine **3** was first examined to establish the most effective reaction conditions (Table 4.1). Without the use of a catalyst and with aniline as the solvent, **3** could be obtained as a yellow solid in 26% yield (entry 1). However, a catalytic route is preferred in which aniline is not used as the solvent and reaction temperatures can be decreased. Under mild conditions with dCHPB²¹ (2-(dicyclohexylphosphino)biphenyl) as the ligand and Cs₂CO₃ as a base, the product was observed in the reaction mixture. However, purification by column chromatography resulted in the isolation of N,N-bis-7-(2-chloro-1,8-naphthyridine)-phenylamine **9** (entry 2). Therefore, use of TMS-protected aniline was thought likely to increase conversion to the desired product. Furthermore, since there is no functional group, the weak base Cs₂CO₃ was replaced by the strong base KO-*t*-Bu. Although **3** could be isolated from the reaction mixture, the yield was low (entry 3). Additionally, combinations of other electron rich ligands such as DPPF (1,1'-bis(diphenyl-phosphino)ferrocene), BINAP (2,2'-bis(diphenyl-phosphino)-1,1'-binaphthyl) and Xantphos^{30,31} (9,9'-dimethyl-4,5-bis(diphenylphosphino)-xanthene) with bases did not result in high isolated yields (entries 4 – 7). Recently, a very successful combination of palladium catalyst and JOSIPHOS ligand ((*R*)-di-*t*-butyl- -phosphine) for aminations of aryl chlorides with primary nitrogen nucleophiles has been reported by the group of Hartwig.²⁵ However, this catalyst/ligand combination turned out to be inactive for the amination of **4** with aniline (entry 8) as well as dodecylamine. In general, crude reaction mixtures contained amounts of insoluble 2,7-dichloro-1,8-naphthyridine and by-products which could not be identified by GC-MS or MALDI-ToF-MS.

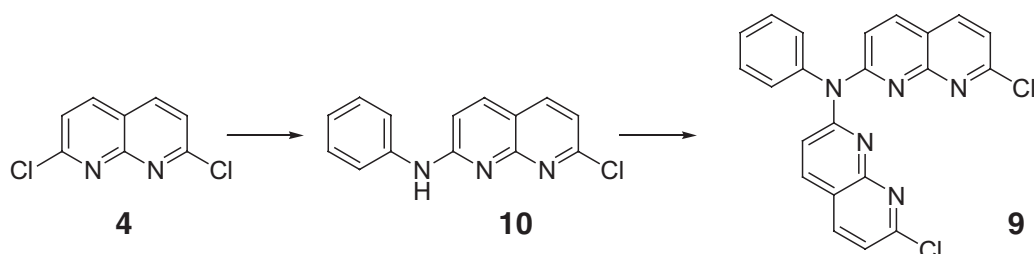
In addition to these results, attempts to apply microwave irradiation to the amination of **4** in order to decrease reaction time and prevent the formation of unwanted by-products were unsuccessful; even though successful synthetic routes leading to N-aryl derivatives using similar substrates have been reported using microwave chemistry.³²⁻³⁴ Concluding, the catalytic amination of 2,7-dichloro-1,8-naphthyridine **4** is problematic. Possible explanations involve low solubility of the substrate and formation of various by-products which are difficult to isolate

Table 4.1 Amination of 2,7-dichloro-1,8-naphthyridine.^a

entry	%Pd ^b	ligand	base	yield (%)
1 ^c	-	-	K ₂ CO ₃	26
2 ^d	2	dCHPB	Cs ₂ CO ₃	25 ^f
3 ^e	2.5	dCHPB	KO- <i>t</i> -Bu	25
4	2	DPPF	Cs ₂ CO ₃	0
5	2	BINAP	Cs ₂ CO ₃	0
6	2	Xantphos	KO- <i>t</i> -Bu	0
7	4	Xantphos	K ₂ CO ₃	< 10
8 ^g	1	JOSIPHOS	NaO- <i>t</i> -Bu	< 5

^a Reaction conditions: 0.5 mmol **4**, 1.4 mmol aniline, L/Pd = 2.0, 1.4 mmol base, 2 mL 1,4-dioxane, 100 °C, 20 h; ^b 1 mol % Pd refers to 1.0 mol % Pd(OAc)₂; ^c 2.0 mmol **4**, 4.0 mmol base, 8 mL aniline, 180 °C, 6 h; ^d 0.5 mmol aniline was used; ^e 1.4 mmol TMS-aniline was used; ^f isolated product was N,N-bis-7-(2-chloro-1,8-naphthyridine)-phenylamine **9**; ^g 0.25 mmol **4**, 0.6 mmol aniline, L/Pd = 1.0, 0.7 mmol base, 2.5 mL 1,2-dimethoxyethane, 100 °C, 20 h.

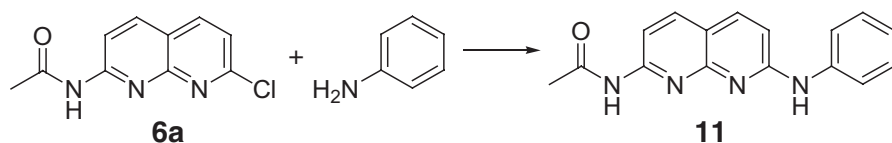
and identify. The formation of **9** indicated that the secondary amine formed in mono-amination of **4** with aniline has higher reactivity than aniline in nucleophilic aromatic substitution. Coordination and deprotonation of intermediate **10** will therefore be more likely, followed by reductive elimination with a coordinated 2,7-dichloro-1,8-naphthyridine to form **9** (Scheme 4.3). Alternatively, the higher solubility of **10** compared to **4** also offers a partial explanation. Furthermore, since coordination to the metal center of two nitrogen atoms in these naphthyridines is likely to occur, several by-products may be formed. The ¹H NMR and ¹³C NMR of **3** were completely assigned with help of 1D and 2D NMR techniques and used as a reference for other compounds.

**Scheme 4.3** By-product formation in the amination of **4**.

4.2.2 Pd-catalyzed mono-amination of 2-chloro-1,8-naphthyridine

Due to its good solubility, 7-acetamido-2-chloro-1,8-naphthyridine **6** was investigated as the substrate in the palladium catalyzed amination with aniline to give 2-acetamido-7-phenylamino-1,8-naphthyridine **11**. The results are collected in Table 4.2. With dTBPB²¹ (2-(di-*t*-butylphosphino)biphenyl) and dCHPB as the ligand and a weak base, the reaction proceeded to moderate and high conversions (entries 1-4). The use of Cs₂CO₃ gave slightly higher conversions (entries 2 and 4). Although these monophosphines do not differ much in electron richness, use of the more sterically hindered dCHPB leads to almost complete conversion (entries 3 and 4). Replacing dCHPB by the bidentate phosphine ligand BINAP decreased the yield (entry 5). However, using Xantphos as a bidentate ligand resulted in nearly complete conversion (entry 6). A significant decrease between conversion and isolated yield is observed for the purification of 2-acetamido-7-phenylamino-1,8-naphthyridine **11**. This can be rationalized by hydrolysis of the weak Napy amide bond to a primary amine upon workup of the basic reaction mixture by column chromatography.^{3,8}

Table 4.2 Pd-catalyzed amination of 7-acetamido-2-chloro-1,8-naphthyridine.^a

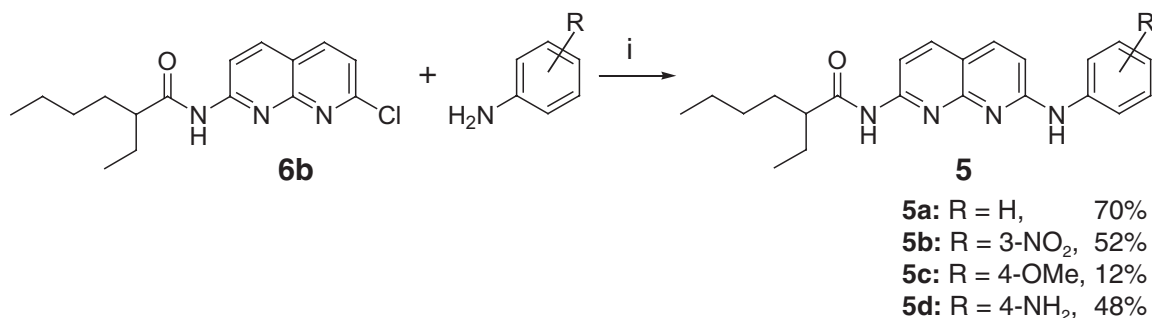


entry	ligand	base	conv (%) ^b	yield (%)
1	dTBPB	K ₂ CO ₃	52	30
2	dTBPB	Cs ₂ CO ₃	75	61
3	dCHPB	K ₂ CO ₃	91	68
4	dCHPB	Cs ₂ CO ₃	95	75
5	BINAP	Cs ₂ CO ₃	48	26
6	Xantphos	Cs ₂ CO ₃	> 99	81

^a Reaction conditions: 1.0 mmol **6a**, 1.2 mmol aniline, 2.0 mol % Pd(OAc)₂, L/Pd = 2.0, 1.4 mmol base, 5 mL 1,4-dioxane, 100 °C, 18 h; ^b determined by ¹H NMR on crude reaction mixture.

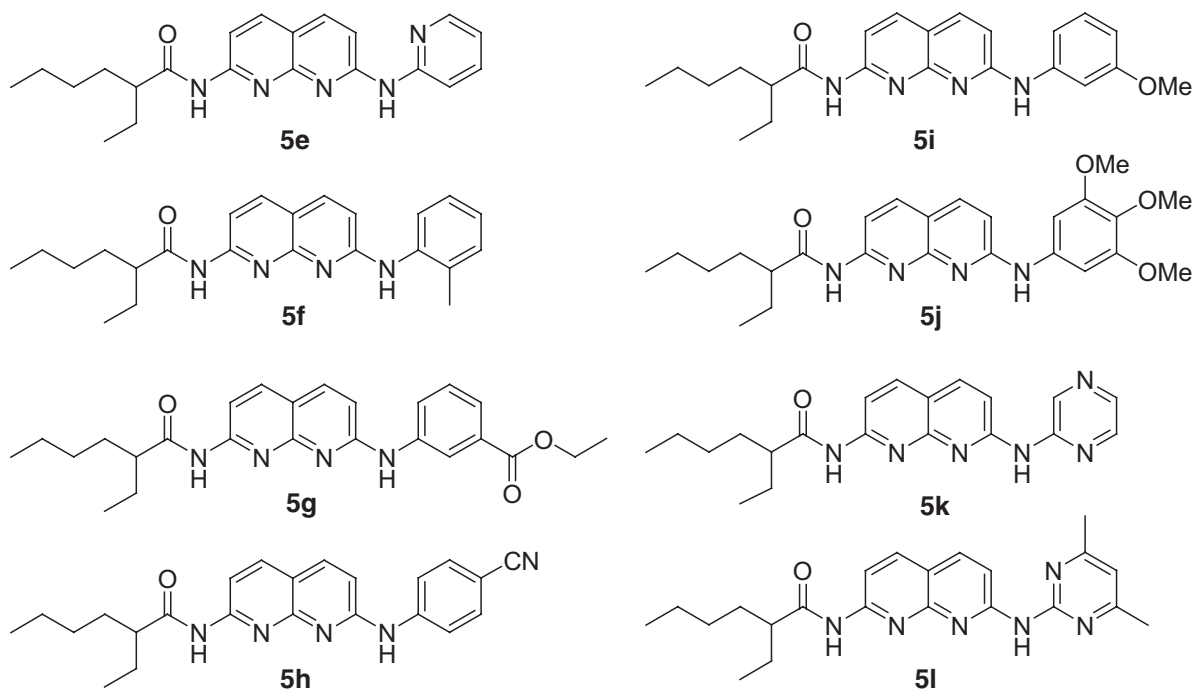
Using the optimized conditions, three anilines were reacted with 7-(2-ethylhexanoylamino)-2-chloro-1,8-naphthyridine **6b** to give derivatives **5a-d** (Scheme 4.4). The ¹H NMR and ¹³C NMR spectra of **5a** and **5b** were completely assigned from the results of 1D and 2D NMR techniques and act as references for other compounds in this class of naphthyridines. The branched alkyl chain next to the amide carbonyl not only ensures high solubility but also significantly enhances hydrolytic stability of the amide functionality (see Chapter 3). Since

dCHPB is not air-stable, Xantphos was preferred as the ligand. Reaction of **6b** with aniline went smoothly and the product **5a** was obtained in 70% yield. Amination with the weaker nucleophile 3-nitroaniline resulted in the isolation of **5b** in 52% yield. Although 4-anisidine is a stronger nucleophile, **5c** could only be obtained in 12% yield due to losses during extensive purification. In contrast, when 1,4-phenylenediamine was used, **5d** could be isolated in 48% yield. In this way, a synthetic handle is provided on the DAAD hydrogen bonding motif in one step from the 2-chloro-naphthyridine. Noteworthy is the fact that diarylated product was detected by MALDI-ToF-MS analysis in all cases. This indicates that diarylation of the anilines with 2-chloro-1,8-naphthyridines is an important competing side-reaction.



Scheme 4.4 Route to 7-(2-ethyl-hexanoylamino)-2-phenylamino-1,8-naphthyridines **5** and isolated yields; *i*: Pd(OAc)₂, Xantphos, Cs₂CO₃, dioxane, 18 h, 100 °C.

Additionally, the scope of the mono-amination was investigated by parallel synthesis of a number of derivatives **5e-l** (Scheme 4.5). These compounds could be prepared on mg-scale

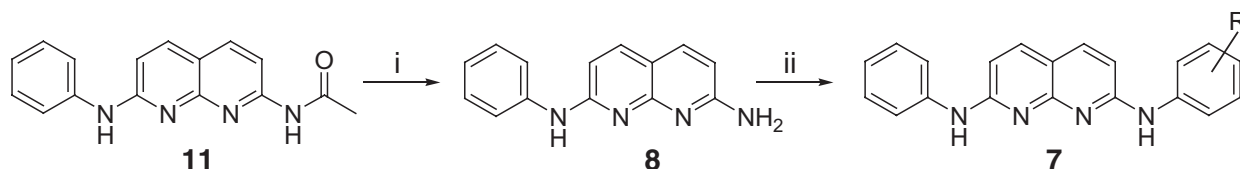


Scheme 4.5 7-(2-Ethyl-hexanoylamino)-2-phenylamino-1,8-naphthyridines **5e-l**.

and purified by automated semi-prep-RP-HPLC using UV or LC-MS detection. Although both electron-rich as well as electron-deficient anilines reacted with **6b**, no product formation was observed when 2,6-dimethylaniline was used. This can be rationalized by the great steric hindrance caused by the two *o*-methyl groups. Likewise, no reaction was observed when 4-nitro- or 3,5-dinitroaniline were used due to their reduced nucleophilicity. Although the main interest in synthesizing these derivatives was related to determination of the association constants with UPy **2**, yields were generally determined to be 25-50%.

4.2.3 Synthetic strategy to 2,7-diamino-1,8-naphthyridines

Few examples of Pd-catalyzed N-arylation of heteroarylamines have been reported.^{19,35} Pd-catalyzed arylation of aminopyridines has been achieved previously using DPPP, BINAP, DPPF or P(*t*-Bu)₃ as a ligand. However, the use of NaO-*t*-Bu as the base limited the scope of these reactions. More recently, the arylation of 2-aminopyridines and analogues using Xantphos or BINAP and a weak base such as K₂CO₃ or Cs₂CO₃ was reported.^{20,36} Inspired by these results, the N-arylation of 7-amino-2-phenylamino-1,8-naphthyridine **8** to asymmetric 2,7-diphenylamino-1,8-naphthyridines **7** was examined (Scheme 4.6). As reported in Chapter 3, the acetamide functionality can be rapidly hydrolyzed. Using this feature, **8** was obtained in 44% yield by alkaline hydrolysis of 2-acetamido-7-phenylamino-1,8-naphthyridine **11** which was used without purification.

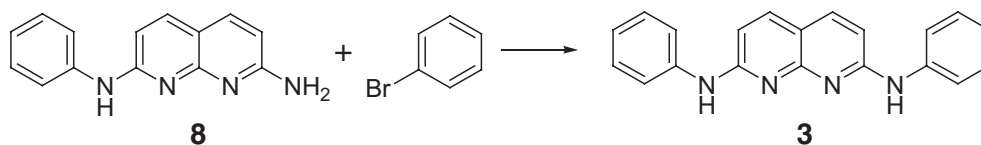


Scheme 4.6 Synthetic approach towards 2,7-diphenylamino-1,8-naphthyridines **7**; i: 6% NaOMe/MeOH, 10 h, 60 °C, 44%; ii: aryl halide, Pd-catalyst, ligand, base, dioxane, 100 °C, 20 h.

In order to establish the most effective conditions for this arylation route to derivatives **7**, the reaction between **8** and bromobenzene was first examined (Table 4.3). With Pd₂(dba)₃ as the palladium source, BINAP as the ligand and Cs₂CO₃ as a base, the reaction proceeded to 40% conversion (entry 1). Due to the absence of a functional group, it was believed that a strong base could also be used. However, when Cs₂CO₃ was replaced by KO-*t*-Bu, no product was observed (entry 2). When Xantphos was applied as the ligand, moderate to high conversions were observed (entries 3-5). Similarly to when BINAP was used, a decrease in conversion was observed when a strong base was used (entry 4). Although Pd₂(dba)₃ is often the catalyst of choice in the amination of aryl bromides,^{19,21,36} the dba ligand can interfere with the oxidative

addition step of the aryl halide.³⁷ However, choosing Pd(OAc)₂ as the palladium source only led to a slightly increased conversion (entry 5). These results suggest that KO-*t*-Bu either deactivates the catalyst or the substrate. Due to its increased acidity the anilino N-H of **8** might be deprotonated with such a strong base leading to by-product formation. A weak base, however, will only assist in deprotonation after coordination of the primary amine and oxidative addition of the aryl halide to the transition metal center have taken place.^{38,39} Subsequently, the product is released by reductive elimination. Previous mechanistic studies on palladium catalyzed amination reactions applying bidentate phosphine ligands confirmed the independence of base by showing that rates were clearly zero order in base for aryl halide aminations catalyzed by palladium complexes of BINAP and DPPF.^{39,40} As observed before in the synthesis of 7-(2-ethyl-hexanoylamino)-2-phenylamino-1,8-naphthyridines **5** (paragraph 4.2.2), diarylated product was detected by MALDI-ToF-MS analysis in entries 1,2 and 4. Furthermore, replacing Cs₂CO₃ with K₂CO₃ as the base did not influence conversion.

Table 4.3 Pd-catalyzed arylation of 7-amino-2-phenylamino-1,8-naphthyridine (**8**).^a



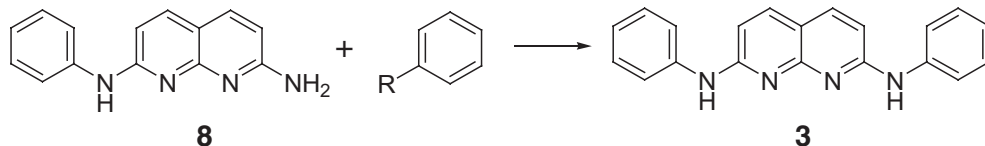
entry	catalyst ^b	ligand	base	conv (%) ^c
1	Pd ₂ (dba) ₃	BINAP	Cs ₂ CO ₃	40
2	Pd ₂ (dba) ₃	BINAP	KO- <i>t</i> -Bu	0
3	Pd ₂ (dba) ₃	Xantphos	Cs ₂ CO ₃	85
4	Pd ₂ (dba) ₃	Xantphos	KO- <i>t</i> -Bu	48
5	Pd(OAc) ₂	Xantphos	Cs ₂ CO ₃	91

^a Reaction conditions: 0.17 mmol **8**, 0.19 mmol bromobenzene, 4.0 mol % Pd, L/Pd = 1.0, 0.24 mmol base, 1.0 mL 1,4-dioxane, 100 °C, 18 h; ^c determined by ¹H NMR on crude reaction mixture.

The oxidative addition of aryl halides is generally the first step in most palladium-catalyzed coupling reactions.⁴¹ Although this addition is considered to be the rate-limiting step in many cases,^{42,43} several results are inconsistent with this proposal. In order to evaluate reactivity of four aryl halides, the arylation of **8** was investigated (Table 4.4). While reaction with iodobenzene resulted in complete conversion of **8**, reaction with chlorobenzene gave only 15% conversion. Apparently, the rate of oxidative addition follows the trend: PhI > PhBr > PhCl >> PhF. These results seem to be in agreement with previous mechanistic studies on catalytic aminations using bis-phosphine complexes with steric ligands which reported that addition of iodobenzene occurs by associative phosphine displacement. Whereas bromobenzene is added

by rate-limiting dissociation of phosphine while addition of chlorobenzene occurs by reversible dissociation of phosphine, followed by rate-limiting oxidative addition.⁴⁴ No further mechanistic studies were performed on the arylation of **8** to elucidate the catalytic pathway. Although iodobenzene displayed a higher reactivity in the catalytic amination, arylbromides were used in subsequent reactions due to their commercial availability.

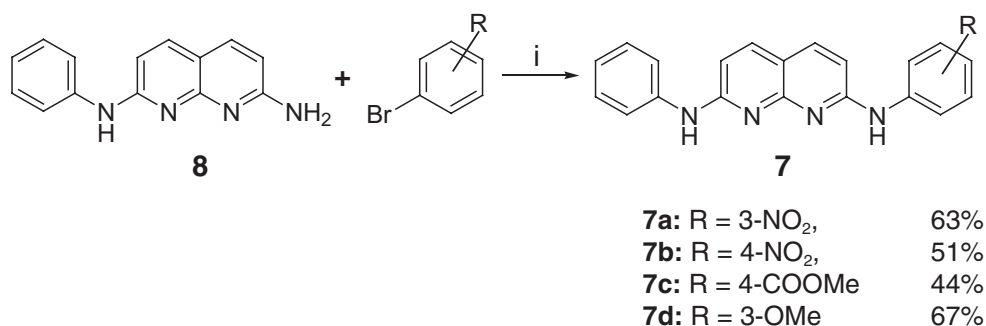
Table 4.4 Pd-catalyzed arylation of 7-amino-2-phenylamino-1,8-naphthyridine (**II**).^a



entry	aryl halide	conv (%) ^b
1	R = I	> 99
2	R = Br	87
3	R = Cl	15
4	R = F	0

^a Reaction conditions: 0.2 mmol **8**, 1.1 mmol aryl halide, 2.0 mol % Pd(OAc)₂, 4.0 mol % Xantphos, 1.4 mmol Cs₂CO₃, 1.0 mL 1,4-dioxane, 100 °C, 20 h; ^b determined by ¹H NMR on crude reaction mixture.

Using the optimized conditions, i.e. Pd(OAc)₂ as the palladium source, Xantphos as the ligand and K₂CO₃ as the base, four aryl bromides were reacted with 7-amino-2-phenylamino-1,8-naphthyridine **8** (Scheme 4.7). Arylation with electron-deficient 1-bromo-3-nitrobenzene and 1-bromo-4-nitrobenzene which are activated for catalytic amination, yielded derivatives **7a** and **7b** in 63% and 51%, respectively. Similarly, a bromobenzene containing a methyl ester functionality at the *para*-position was coupled to **8** affording product **7c** in 44% yield. No hydrolysis of the ester functionality was observed under these conditions. The electron-rich substrate 3-bromoanisole was effectively coupled with the amino-naphthyridine and gave **7d** in 67% yield.



Scheme 4.7 Route to 2,7-diphenylamino-1,8-naphthyridines **7** and isolated yields; i: Pd(OAc)₂, Xantphos, K₂CO₃, dioxane, 18 h, 100 °C.

Similar to previously described observations, arylated by-products were observed in these reactions. The crude reaction mixture of **7b** was purified by column chromatography. Product **7b** and by-products **12** and **13** were obtained in 51%, 31% and 3%, respectively. Although ^1H NMR is not conclusive about the precise position of the second PhNO_2 group (on N(2) PhNO_2 or N(7) Ph), ^{13}C NMR results indicated arylation on N(7) Ph based on the asymmetry of the spectrum. Due to the more nucleophilic character of $\text{NH}(7)\text{Ph}$, arylation of this secondary amine is more probable. Full assignment of the ^1H NMR and ^{13}C NMR of **7b** was based on the results of 1D and 2D NMR data and used as a reference for other asymmetric compounds in this class of naphthyridines. Analogous to this, purification of **7c** gave the product and biarylated by-product in 44% and 25% yield, respectively. These results indicate the relatively strong nucleophilic character of the secondary amine in 2-anilino-1,8-naphthyridine derivatives and therefore stress the necessity of using a weak base in these reactions.

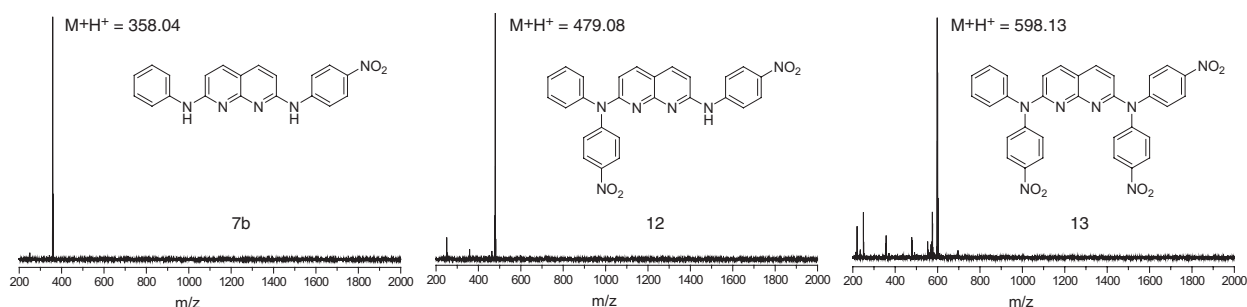
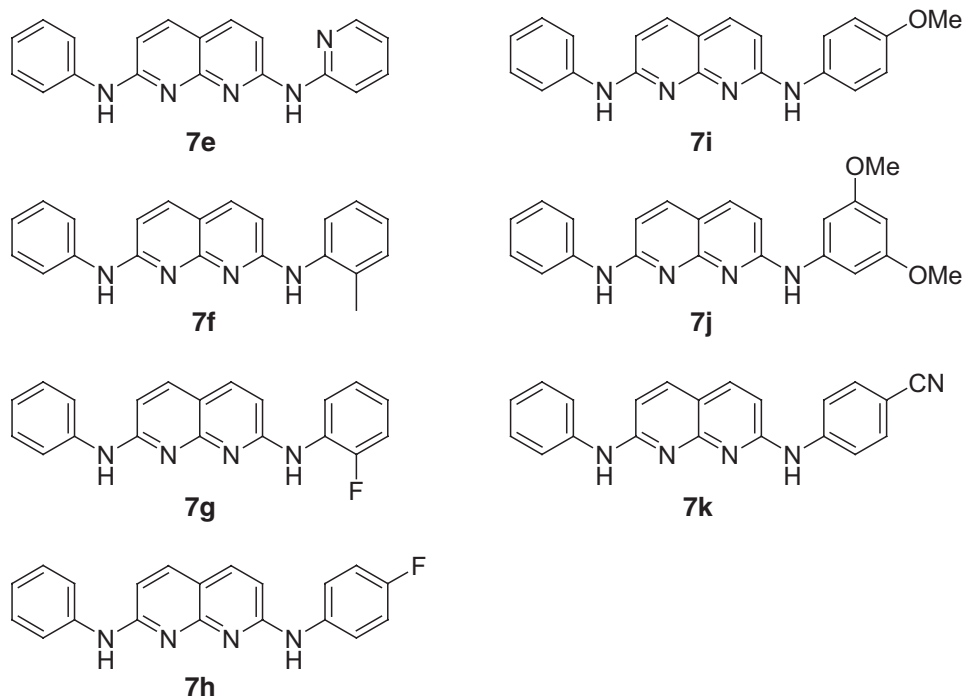


Figure 4.1 MALDI-ToF-MS spectra of N-arylated product **7b** and by-products **12** and **13** from the palladium catalyzed amination of 1-bromo-4-nitrobenzene with **8**.

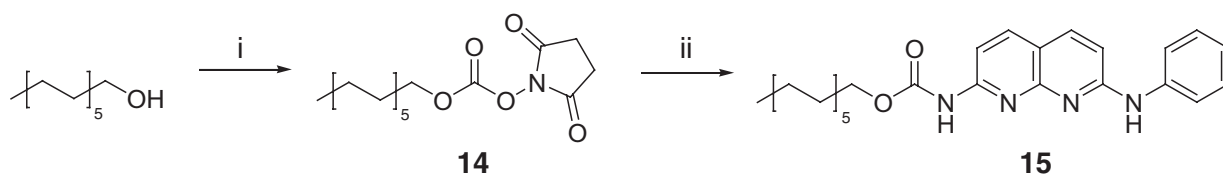
Finally, the scope of this catalytic arylation was examined by parallel synthesis and automated semi-preparative RP-HPLC yielding mg quantities of a number of derivatives **7e-k** analogous to 7-(2-ethyl-hexanoylamino)-2-phenylamino-1,8-naphthyridines **5e-l** (Scheme 4.8). As can be seen from Schemes 4.7 and 4.8, the scope is quite broad. Reactions of both electron-deficient and electron-rich aryl bromides with the electron-deficient amino-naphthyridine resulted in product formation. Not surprisingly, reaction of bromo-fluorobenzenes with **8** showed selectivity to displacement of the bromide over the fluoride affording derivatives **7g** and **7h**. In general, yields were determined to be 35-70%.



Scheme 4.8 2,7-Diphenylamino-1,8-naphthyridines **7e-k**.

4.3 Degradation of 2-amido-7-arylamino- and 2,7-di(arylamino)-1,8-naphthyridines

In the previous paragraphs, the synthesis of a number of amido-arylamino- and di(arylamino)-Napy derivatives was described. One of the key goals to synthesize these derivatives was to increase stability under hydrolytic conditions compared to the diamido-naphthyridines discussed in Chapter 3. As expected, no degradation to amino-naphthyridines was observed upon purification of the crude reaction mixtures. Previously, increased thermal and alkaline stability was observed for 2-carbamato-7-methyl-1,8-naphthyridine compared to 2-amido-7-methyl-1,8-naphthyridine by the group of Nakatani.⁸ In order to evaluate the relative stability to alkaline hydrolysis of di(arylamino)- and amido-arylamino-Napy derivatives **3** and **5a**, respectively, carbamate Napy **15** was synthesized. The synthesis of **15** is outlined in Scheme 4.9. Dodecyl alcohol was reacted with *N,N'*-disuccinimidyl carbonate (DSC) to produce carbonate **14**,⁴⁵ which was then reacted with 7-amino-2-phenylamino-1,8-naphthyridine **8** to afford carbamate **15**.



Scheme 4.9 Synthesis of Napy-carbamate **15** from carbonate **14**; i: *N,N'*-disuccinimidyl carbonate, acetonitrile, triethylamine, RT, 5 h, 92%; ii: **8**, triethylamine, dichloromethane, 40 °C, 12 h, 20%.

Similar to the procedure described in the previous chapter, the degradation of **3**, **5a** and **15** was investigated under alkaline conditions. In order to quantify the pseudo first order reaction rate constants of hydrolysis of Napy derivatives **3**, **5a** and **15**, experiments were run at 60 °C with 10 mM Napy derivative in 100 mM KOH in 2:1 v/v% 1,4-dioxane/H₂O. Samples were analyzed with LC-MS and followed with MS and UV-detection. Quantification was done on the corresponding precursor ion in the MS-MS-mode. The major hydrolysis product for the degradation of **5a** and **15** was amino Napy derivative **8** as determined with LC-MS. A linear relation was found between $\ln([Napy]_t/[Napy]_0)$ and time according to: $\ln([Napy]_t/[Napy]_0) = -k' \cdot t$ (equation 3.4) (Figure 4.2). Values of k' were determined using standard fitting procedures and are collected in Table 4.5.

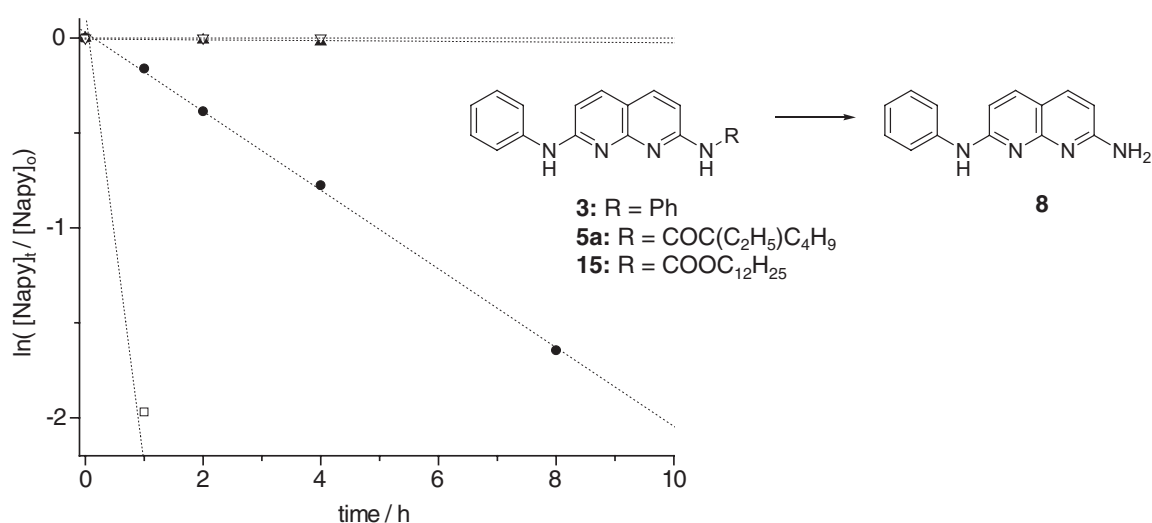


Figure 4.2 Alkaline hydrolysis of 10 mM **3** (∇), **5a** (\blacktriangle), **15** (\bullet) and 2-(2-ethylhexanoylamino)-7-acetylamino-1,8-naphthyridine (\square).

Table 4.5 Evaluation of k' for hydrolysis of Napy derivatives at 60 °C.^a

entry	compound	r^2	k' / h^{-1}
1	3	1	0
2	5a	0.947	0.00194 ± 0.00033
3	15	0.999	0.207 ± 0.004
4	ref ^b	0.990	2.386 ± 0.240

^a Reaction conditions: 10 mM Napy, 100 mM KOH in 2:1 v/v% dioxane/H₂O at 60 °C; ^b 2-(2-ethylhexanoylamino)-7-acetylamino-1,8-naphthyridine was used as a reference.

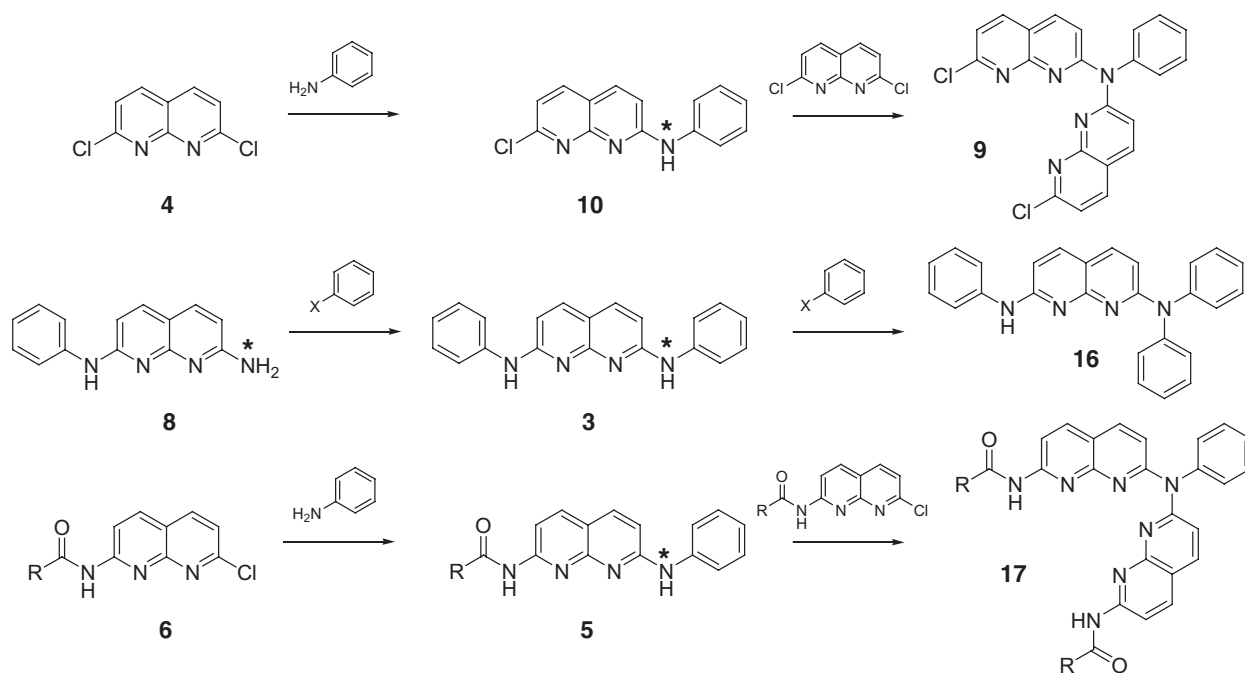
As expected, no degradation was observed for 2,7-diphenylamino-1,8-naphthyridine **3** (entry 1). While **5a** was hydrolyzed to an extent less than 5% after 24 hours, it took 26 hours to hydrolyze carbamate **15** to the extent of 95% (entries 2 and 3). In contrast, complete hydrolysis was observed for reference compound 2-(2-ethylhexanoylamino)-7-acetylamino-1,8-

naphthyridine under these conditions within 2 hours (entry 4). A noteworthy difference of three orders of magnitude was thus observed between k' values of hydrolysis of **5a** and the reference. The observed increase in hydrolytic stability of **15** compared to the reference is in fair agreement with results reported in literature.⁸ Furthermore, the k' value of **5a** is about 25 times lower than for its diamido analogue with two 2-ethylhexanoyl groups (compound **30** in Chapter 3). Additional experiments indicated no significant degradation of **3** and **5a** within 10 hours up to 120 °C with 10 mM **5a** in 500 mM KOH in 2:1 v/v% N,N'-dimethylacetamide/H₂O. Possible explanations of this remarkable increase in stability of **5a** involve increased hydrophobicity of the molecule in combination with a difference in electronic structure of the naphthyridine ring due to the replacement of an amide group with an arylamine functionality.

4.4 Reactivity of naphthyridine substrates in Pd-catalyzed aminations and arylations

In the palladium catalyzed amination and arylation of 1,8-naphthyridine substrates, significant by-product formation was observed. These reactions are depicted in Scheme 4.10. Direct palladium catalyzed amination of 2,7-dichloro-1,8-naphthyridine **4** to symmetric 2,7-di(arylamino)-1,8-naphthyridines **3** proved to be difficult. Although initial amination of **4** to 7-arylamino-2-chloro-1,8-naphthyridine **10** with aniline is probably fast due to a high electrophilicity of the dichloro-naphthyridine, subsequent amination by aniline to give product **3** is in competition with arylation of the secondary amine (N indicated with *). This secondary amine is considerably more acidic than the primary amine of aniline and is therefore likely to be deprotonated by a weak base such as K₂CO₃ or Cs₂CO₃ yielding a very reactive anion. Subsequent reaction with a second dichloro-naphthyridine will therefore take place giving compound **9** as a major product. In addition to this effect, the presence of a secondary amine on position 7 of the naphthyridine ring has an electron-donating effect therefore decreasing electrophilicity of the mono chloride.

In contrast, 2,7-di(arylamino)-1,8-naphthyridines **3** were synthesized by catalytic arylation of 7-amino-2-phenylamino-1,8-naphthyridine **8**. Although the secondary amine in **8** will be the most acidic (however, acidity is decreased compared to its analogue in **10**, due to an electron-donating effect of the primary amine), the primary amine is more nucleophilic. Coordination of the neutral primary amine to the catalytic centre followed by deprotonation will therefore be faster than direct deprotonation of the secondary amine. Subsequent arylation of **3** to derivatives **16** will occur when the concentration of **8** decreases and the aryl bromide is used in small excess. This is in full agreement with the results described in section 4.2.3.



Scheme 4.10 Evaluation of possible side-reactions in the palladium catalyzed amination and arylation of 1,8-naphthyridines; * indicates the most nucleophilic nitrogen centers.

A similar rationale can be used to explain by-product formation like derivatives **17** in the catalytic amination of 7-amido-2-chloro-1,8-naphthyridines **6**. First, amination of **6** with aniline will afford product **5**. This compound contains two nucleophilic nitrogen atoms of which the arylamine is more nucleophilic and the amide nitrogen is more acidic. In this case, the amide nitrogen will now be deprotonated faster but the resulting anion will be stabilized by the carbonyl ensuring fast reaction of the deprotonated arylamine with **6** to give derivatives **17** as the major by-product. Although MALDI-ToF-MS results obtained from crude product mixtures indicated the presence of masses identical to **17**, the exact structure is not proved conclusively due to the absence of NMR-data.

The results described in this chapter and the previous chapter suggest a different role for the weak base in the catalytic cycle of the reactions. In the catalytic amidations, deprotonation of the neutral primary amide by the base will be followed by coordination of the anion to the palladium centre. Subsequent reactions will afford the amidated product. In contrast, in the catalytic aminations, the weak base is unable to deprotonate a primary amine. Therefore, a neutral primary amine will first coordinate to the metal centre giving a more acidic NH proton, which can be removed by a weak base. By reductive elimination, an arylamino derivative will be formed. At this moment unwanted side-reactions can now occur since the arylamine on the naphthyridine ring is acidic enough to be deprotonated by the base. The resulting anion will compete for coordination with a neutral primary amine.

4.5 Conclusions

In conclusion, although palladium catalyzed amination of 2,7-dichloro-1,8-naphthyridine to symmetric 2,7-di(arylamino)-1,8-naphthyridines is not successful, asymmetric derivatives can be synthesized by catalytic arylation of 7-amino-2-phenylamino-1,8-naphthyridine. Optimum reaction conditions for this arylation were found to employ Pd(OAc)₂ as the palladium source, Xantphos as the ligand and K₂CO₃ or Cs₂CO₃ as a base in dioxane. The scope of the catalytic reaction is shown to be broad since electron-deficient as well as electron-rich aryl bromides react with the less nucleophilic amine of the naphthyridine. Although moderate yields are obtained, considerable bi-arylation of the arylamine group is observed. This can be rationalized due to a difference in nucleophilicity between the secondary arylamine and the primary amino group on the naphthyridine ring. An improved catalytic system would therefore have to display a higher selectivity towards coordinating the primary amine. Moreover, a general palladium catalyzed amination of 7-amido-2-chloro-1,8-naphthyridines with anilines bearing various electron-rich and electron-deficient groups is established. Even though unwanted arylation reactions also occur, yields are moderate. Due to the use of a weak base, functional groups like a primary amine can be introduced opening the way for further functionalization. Furthermore, parallel synthesis and automated purification by semi-preparative RP-HPLC of a large number of crude reaction mixtures proved to be a successful approach to obtain a large number of Napy derivatives on a mg scale. A quantitative study of the rate of alkaline degradation of di(arylamino) and amino-amido derivative shows no degradation of the arylamine group up to 120 °C in DMA/H₂O mixtures. No significant hydrolysis of the branched amide functionality is observed up to 60 °C in 1,4-dioxane/H₂O mixtures. These naphthyridines present a previously unexplored class of donor-acceptor-acceptor-donor (DAAD) hydrogen bonding molecules which display increased hydrolytic stability compared to the diamido derivatives discussed in Chapter 3.

4.6 Experimental procedures

General methods. See General methods Chapter 3. Analytical HPLC analysis and purification by semi-prep-HPLC using UV detection were performed on a Waters 1525 system equipped with a binary HPLC pump, a Waters 996 PDA detector and a Gilson 215 injectcollect. The mobile phases are 0.05% TFA in H₂O and 0.05% TFA in 9/1 v/v% acetonitrile/H₂O. Spectra were acquired using MassLynx 4.0 SP4 software. Analytical runs were carried out using a Waters XTerra® MS C18 (4.6x20 mm) column with a particle size of 3.5 µm. Semi-preparative runs were carried out using a Waters XTerra® PrepMS C18 (10x50mm) column with a particle size of 5 µm. Analytical HPLC analysis and purification by semi-prep-

HPLC using LC-MS detection were performed on a Waters 600 controller system equipped with a binary HPLC pump, a Gilson 215 injectcollect, a Waters 996 PDA detector and a Micromass ZMD LC-MS. The mobile phases are 0.05% TFA in H₂O and 0.05% TFA in 9/1 v/v% acetonitrile/H₂O. Spectra were acquired using MassLynx 4.0 SP4 software. Analytical runs were carried out using a Waters XTerra® MS C18 (4.6x20 mm) column with a particle size of 3.5 µm. Semi-preparative runs were carried out using a Phenomenex Luna C18 (21.2x60mm) column with a particle size of 10 µm.

Liquid chromatography – mass spectroscopy. Linear calibration curves of derivatives **3**, **5a** and **9** were obtained by injection of 0.1 – 2.0 µL 1.0 mM solutions in acetonitrile and measurement in MS-MS mode. The measured signal was integrated using a Gaussian curve fitting procedure. Curves from at least 5 data points were obtained for all compounds ($r^2 > 0.99$). Compounds were hydrolyzed by charging a 40 mL Radley Carousel Reaction Tube with 0.010 mM Napy followed by addition of 1.0 mL of the appropriate solvent and heating the solutions at the temperature of choice in a Radley Carousel with applied cooling under temperature control. 50 µL Samples were taken at specific time intervals and diluted to 1.0 mL acetonitrile. Subsequent measurement by injection of 3.0 µL was performed in MS-MS mode by MS and UV detection followed by integration of the signal gave the desired concentrations. Data acquired by UV as well as MS detection were in good agreement. Data depicted in figures 4.2 were obtained from the MS-trace.

Synthesis. 2,7-Dichloro-1,8-naphthyridine **4** was prepared as reported by Newkome *et al.*²⁸ 7-Acetamido-2-chloro-1,8-naphthyridine **6a** was prepared according to Corbin *et al.*²⁹ 7-(2-Ethylhexanoylamino)-2-chloro-1,8-naphthyridine **6b** was synthesized as reported by Lighthart *et al.*⁶ 2-n-Butylureido-6-methyl-4[1H]-pyrimidinone **2** was prepared as reported by Beijer *et al.*⁴⁶

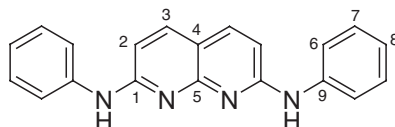
General procedure for the Pd-catalyzed amination of 7-(2-ethylhexanoyl)amino-2-chloro-1,8-naphthyridine with anilines (Scheme 4.5): A 40 mL Radley Carousel Reaction Tube was charged with Pd(OAc)₂ (2 mol%), Xantphos (L/Pd = 2.0), Cs₂CO₃ (0.14 mmol), 7-(2-ethylhexanoyl)amino-2-chloro-1,8-naphthyridine (0.10 mmol), aniline (0.11 mmol) and 1,4-dioxane (1.0 mL). The reaction vessel was capped, evacuated and back-filled with N₂ three times. Still under N₂, it was immersed into a 100 °C oil bath. After stirring for 20 h, the mixture was cooled, filtered over diatomaceous earth and evaporated.

General procedure for the Pd-catalyzed arylation of 7-amino-2-phenylamino-1,8-naphthyridine with aryl halides (Scheme 4.8): A 40 mL Radley Carousel Reaction Tube was charged with Pd(OAc)₂ (2 mol%), Xantphos (L/Pd = 2.0), Cs₂CO₃ (0.14 mmol), 7-amino-2-(phenylamino)-1,8-naphthyridine (0.10 mmol), aryl halide (0.11 mmol) and 1,4-dioxane (1.0 mL). The reaction vessel was capped, evacuated and back-filled with N₂ three times. Still under N₂, it was immersed into a 100 °C oil bath. After stirring for 20 h, the mixture was cooled, filtered over diatomaceous earth and evaporated.

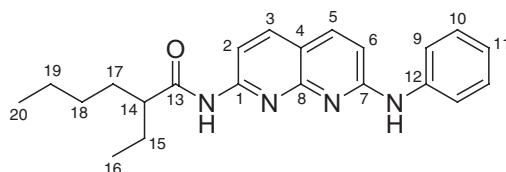
Purification of compounds 5e-l and 7e-k by semi-prep-HPLC using UV or LC-MS detection: The crude product was dissolved in 1.2 mL 1,4-dioxane of which 450 µL was injected on the column when UV detection was used and 900 µL when LC-MS detection was applied. The product fractions were collected

and TFA was neutralized by addition of 0.5 mL saturated aqueous Na_2CO_3 solution. Evaporation to dryness was performed using a GeneVac HT-4 series II apparatus. The product was dissolved in 2.0 mL dichloromethane and washed with 1.0 mL H_2O followed by removal of the organic layer and drying with Na_2SO_4 . After filtration over a cotton plug, the solutions were concentrated and *n*-hexane was added to precipitate the compounds. By careful evaporation, the derivatives were obtained as powders.

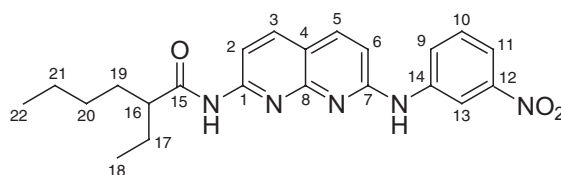
2,7-Bis-(phenylamino)-1,8-naphthyridine 3: A mixture of 2,7-dichloro-1,8-naphthyridine **4** (400 mg, 2.0 mmol) and K_2CO_3 (0.55 g, 4.0 mmol) in aniline (8 mL) was stirred at 180 °C for 6 h. The crude product was precipitated in *n*-hexane followed by purification by column chromatography (SiO_2 , 5 % methanol in dichloromethane) to yield the title compound as a yellow solid (160 mg, 26 %). Full assignment was done based on ^1H NMR, apt ^{13}C NMR, gCOSY, gHMQC and gHMBC measurements. ^1H NMR (CDCl_3): δ = 7.62 (d, 2H, J = 9 Hz, 3), 7.56 (br, 2H, NH), 7.45 (d, 4H, J = 7 Hz, 6), 7.30 (t, 4H, J = 7 Hz, 7), 7.05 (t, 2H, J = 7 Hz, 8), 6.82 (d, 2H, J = 9 Hz, 2) ppm; ^{13}C NMR (CDCl_3): δ = 157.4 (1), 156.4 (5), 139.8 (9), 137.5 (3), 129.1 (7), 123.5 (8), 121.6 (6), 112.8 (4), 107.3 (2) ppm; MALDI-TOF-MS: (m/z) calcd. 312.14; observed: 313.35 ($\text{M}+\text{H}^+$); FTR-IR (ATR): ν = 3395, 3030, 1589, 1569, 1510, 1490, 1445, 1434, 1423, 1336, 1246, 1142, 1077, 1028, 998, 972, 896, 829 cm^{-1} ; Anal. Calcd. for $\text{C}_{20}\text{H}_{16}\text{N}_4$: C 76.90, H 5.16, N 17.94; found: C 75.02, H 4.89, N 17.44.



2-(2-Ethylhexanoyl)amino-7-phenylamino-1,8-naphthyridine 5a: A Schlenck tube was charged with $\text{Pd}(\text{OAc})_2$ (1.23 mg, 5.5 μmol), Xantphos (5.83 mg, 10.1 μmol), Cs_2CO_3 (105 mg, 0.32 mmol), 7-(2-ethylhexanoyl)amino-2-chloro-1,8-naphthyridine **6b** (73.1 mg, 0.24 mmol), aniline (28 mg, 0.30 mmol) and 1,4-dioxane (1.0 mL). The reaction vessel was capped, evacuated and back-filled with N_2 three times. Subsequently, the reaction mixture was stirred at 100 °C for 16 h. The mixture was cooled, filtered over diatomaceous earth and evaporated in vacuo. The title compound could be obtained as a yellow solid after purification by column chromatography (SiO_2 , 3 % acetone in chloroform) and precipitation in *n*-hexane (87 mg, 70 %). Full assignment was done based on ^1H NMR, apt ^{13}C NMR, gCOSY, gHMQC and gHMBC measurements. ^1H NMR (CDCl_3): δ = 8.29 (d, 1H, J = 9 Hz, 2), 8.19 (br, 1H, NH), 7.97 (d, 1H, J = 9 Hz, 3), 7.83 (d, 1H, J = 9 Hz, 5), 7.56 (d, 2H, J = 7 Hz, 9), 7.38 (t, 2H, J = 9 Hz, 10), 7.28 (br, 1H), 7.13 (t, 1H, J = 6 Hz, 11), 6.93 (d, 1H, J = 9 Hz, 6), 2.21 (m, 1H, 14), 1.75-1.48 (m, 4H, 15,17), 1.28-1.26 (m, 4H, 20,21), 0.96-0.82 (m, 6H, 16,20) ppm; ^{13}C NMR (CDCl_3): δ = 175.3 (13), 157.7 (7), 155.3 (8), 153.2 (1), 139.6 (12), 138.7 (3), 137.6 (5), 129.4 (10), 129.3 (10), 124.0 (11), 121.9 (9), 121.8 (9), 115.8 (4), 110.7 (2), 110.6 (6), 50.6 (14), 32.4 (15), 29.8 (18), 26.0 (17), 22.7 (19), 13.9 (16), 12.0 (20) ppm; MALDI-TOF-MS: (m/z) calcd. 362.11; observed: 363.16 ($\text{M}+\text{H}^+$); Anal. Calcd. for $\text{C}_{22}\text{H}_{26}\text{N}_4\text{O}$: C 72.90, H 7.23, N 15.46; found: C 70.83, H 6.94, N 14.60.



2-(2-Ethylhexanoyl)amino-7-(3-nitrophenyl)amino-1,8-naphthyridine 5b: A Schlenck tube was charged with Pd(OAc)₂ (2.94 mg, 13 μmol), Xantphos (15.4 mg, 26.6 μmol), Cs₂CO₃ (300 mg, 0.92 mmol), 7-(2-ethylhexanoyl)amino-2-chloro-1,8-naphthyridine **6b** (200.5 mg, 0.66 mmol), 3-nitroaniline (99.5 mg, 0.72 mmol) and 1,4-dioxane (10 mL). The reaction vessel was capped, evacuated and back-filled with N₂ three times. The reaction mixture was stirred at 100 °C for 20 h followed by cooling to room temperature and filtration over diatomaceous earth. Evaporation in vacuo gave a dark yellow residue from which the title compound could be obtained as a brightly yellow powder after purification by column chromatography (SiO₂, 3 % acetone in chloroform) and precipitation in n-hexane (140 mg, 52 %). Full assignment was done based on ¹H NMR, apt ¹³C NMR, gCOSY, gHMQC and gHMBC measurements. ¹H NMR (CDCl₃): δ = 8.60 (s, 1H, 13), 8.56 (br, 1H, NH), 8.36 (d, 1H, *J* = 9 Hz, 2), 8.12 (d, 1H, *J* = 8 Hz, 11), 8.07 (br, 1H, NH), 8.02 (d, 1H, *J* = 9 Hz, 3), 7.91 (d, 1H, *J* = 9 Hz, 5), 7.83 (d, 1H, *J* = 8 Hz, 9), 7.43 (t, 1H, *J* = 8 Hz, 10), 6.94 (d, 1H, *J* = 9 Hz, 6), 2.23 (m, 1H, 16), 1.72-1.47 (m, 4H, 17,19), 1.30-1.27 (m, 4H, 20,21), 0.98-0.84 (m, 6H, 18,22) ppm; ¹³C NMR (CDCl₃): δ = 175.5 (15), 156.2 (7), 154.7 (8), 153.6 (1), 148.8 (12), 140.8 (14), 138.9 (3), 138.2 (5), 129.9 (10), 125.7 (11), 117.6 (9), 116.2 (4), 114.8 (13), 111.8 (2), 111.6 (6), 50.6 (16), 32.4 (17), 29.8 (20), 26.0 (19), 22.7 (21), 13.9 (18), 12.0 (22) ppm; MALDI-TOF-MS: (*m/z*) calcd. 407.20; observed: 408.13 (M+H⁺); Anal. Calcd. for C₂₂H₂₅N₅O₃: C 64.85, H 6.18, N 17.19; found: C 62.68, H 6.02, N 16.43.



2-(2-Ethylhexanoyl)amino-7-(4-methoxyphenyl)amino-1,8-naphthyridine 5c: A Schlenck tube was charged with Pd(OAc)₂ (1.54 mg, 6.9 μmol), Xantphos (7.82 mg, 13.5 μmol), Cs₂CO₃ (159 mg, 0.49 mmol), 7-(2-ethylhexanoyl)amino-2-chloro-1,8-naphthyridine **6b** (102.1 mg, 0.33 mmol), 4-anisidine (46.7 mg, 0.38 mmol) and 1,4-dioxane (2.0 mL). The reaction vessel was capped, evacuated and back-filled with N₂ three times followed by heating at 100 °C for 20 h. The mixture was cooled to room temperature, filtered over diatomaceous earth and evaporated in vacuo. Extensive purification by column chromatography (SiO₂, 1:3 v/v% ethylacetate/n-hexane) and precipitation in n-hexane gave the title compound as a light yellow solid (15 mg, 12 %). ¹H NMR (CDCl₃): δ = 8.26 (d, 1H, *J* = 9 Hz), 8.19 (br, 1H), 7.98 (d, 1H, *J* = 9 Hz), 7.78 (d, 1H, *J* = 9 Hz), 7.52 (br, 1H, NH), 7.42 (d, 2H, *J* = 7 Hz), 6.96 (d, 2H, *J* = 7 Hz), 6.81 (d, 1H, *J* = 8 Hz), 2.21 (m, 1H), 1.75-1.48 (m, 4H), 1.28-1.26 (m, 4H), 0.96-0.82 (m, 6H) ppm; ¹³C NMR (CDCl₃): δ = 175.3, 160.4, 156.8, 154.4, 153.2, 132.9, 131.4, 128.5, 124.2, 116.9, 114.4, 111.1, 110.6, 55.4, 51.2, 32.6, 30.0, 26.2, 22.9, 14.1, 12.2 ppm; MALDI-TOF-MS: (*m/z*) calcd. 392.23; observed: 393.19 (M+H⁺).

2-(2-Ethylhexanoyl)amino-7-(4-aminophenyl)amino-1,8-naphthyridine 5d: A Schlenck tube was charged with Pd(OAc)₂ (5.3 mg, 24 μmol), dCHPB (15.5 mg, 44 μmol), Cs₂CO₃ (456.3 mg, 1.40 mmol), 7-(2-ethylhexanoyl)amino-2-chloro-1,8-naphthyridine **6b** (306.0 mg, 1.00 mmol), 1,4-phenylenediamine (217.1 mg, 2.00 mmol) and 1,4-dioxane (5.0 mL). The reaction vessel was capped, evacuated and back-filled with N₂ three times followed by heating at 100 °C for 20 h. The reaction mixture was filtered and evaporated in vacuo followed by purification by column chromatography (SiO₂, 3 % ethanol in chloroform). The product was obtained as a yellow solid (180 mg, 48 %). ¹H NMR (CDCl₃): δ = 8.26 (d,

1H, $J = 9$ Hz), 8.20 (br, 1H, NH), 7.98 (d, 1H, $J = 9$ Hz), 7.80 (d, 1H, $J = 9$ Hz), 7.21 (d, 2H, $J = 7$ Hz & br, 3H, NH), 6.72 (m, 3H), 2.21 (m, 1H), 1.75-1.48 (m, 4H), 1.28-1.26 (m, 4H), 0.96-0.82 (m, 6H) ppm; ^{13}C NMR (CDCl_3): $\delta = 175.4, 159.0, 155.1, 153.3, 144.5, 138.9, 138.0, 129.6, 126.0, 116.0, 115.5, 110.5, 109.8, 51.2, 32.7, 29.9, 26.3, 22.9, 14.1, 12.2$ ppm; MALDI-TOF-MS: (m/z) calcd. 377.22; observed: 378.17 ($\text{M}+\text{H}^+$), 400.15 ($\text{M}+\text{Na}^+$); FTR-IR (ATR): $\nu = 3288, 2958, 2929, 2858, 1682, 1598, 1505, 1456, 1429, 1378, 1316, 1249, 1276, 1249, 1174, 1140, 1116, 839, 800\text{ cm}^{-1}$.

2-(2-Ethylhexanoyl)amino-7-(2-pyridyl)amino-1,8-naphthyridine 5e: Following the general procedure and purification by semi-prep-HPLC using UV detection, the title compound was obtained as a dark yellow powder (10.2 mg). ^1H NMR (CDCl_3): $\delta = 8.67$ (br, 1H), 8.55 (br, 1H), 8.34 (d, 1H, $J = 9$ Hz), 8.28 (d, 1H, $J = 6$ Hz), 8.21 (d, 1H, $J = 6$ Hz), 8.03 (d, 1H, $J = 9$ Hz), 7.89 (d, 1H, $J = 9$ Hz), 7.67 (t, 1H, $J = 6$ Hz), 7.34 (d, 1H, $J = 9$ Hz), 6.94 (t, 1H, $J = 6$ Hz), 2.21 (m, 1H), 1.75-1.48 (m, 4H), 1.28-1.26 (m, 4H), 0.96-0.82 (m, 6H) ppm; ^{13}C NMR (CDCl_3): $\delta = 175.6, 156.1, 153.6, 153.3, 147.4, 138.8, 138.2, 137.4, 117.7, 116.2, 114.0, 113.4, 111.9, 50.6, 32.4, 29.8, 26.0, 22.7, 13.9, 12.0$ ppm; MALDI-TOF-MS: (m/z) calcd. 363.21; observed: 364.12 ($\text{M}+\text{H}^+$).

2-(2-Ethylhexanoyl)amino-7-(2-tolyl)amino-1,8-naphthyridine 5f: Following the general procedure and purification by semi-prep-HPLC using LC-MS detection, the title compound was obtained as a yellow powder (2.4 mg). ^1H NMR (CDCl_3): $\delta = 8.28$ (d, 1H, $J = 8$ Hz), 8.08 (br, 1H), 7.98 (d, 1H, $J = 8$ Hz), 7.82 (d, 1H, $J = 8$ Hz), 7.56 (d, 1H, $J = 6$ Hz), 7.29 (t, 2H, $J = 6$ Hz), 7.21 (d, 1H, $J = 6$ Hz), 6.83 (br, 1H), 6.80 (d, 1H, $J = 8$ Hz), 2.32 (s, 3H), 2.21 (m, 1H), 1.76-1.50 (m, 4H), 1.28-1.26 (m, 4H), 0.96-0.82 (m, 6H) ppm; ^{13}C NMR (CDCl_3): $\delta =$ ppm; MALDI-TOF-MS: (m/z) calcd. 376.23; observed: 377.14 ($\text{M}+\text{H}^+$), 399.13 ($\text{M}+\text{Na}^+$).

2-(2-Ethylhexanoyl)amino-7-(3-ethoxycarbonylphenyl)amino-1,8-naphthyridine 5g: Following the general procedure and purification by semi-prep-HPLC using UV detection, the title compound was obtained as a yellow powder (4.4 mg). ^1H NMR (CDCl_3): $\delta = 8.34$ (d, 1H, $J = 9$ Hz), 8.26 (br, 1H), 8.07 (d, 1H, $J = 8$ Hz), 8.04 (br, 1H), 8.02 (d, 1H, $J = 9$ Hz), 7.88 (d, 1H, $J = 9$ Hz), 7.78 (d, 1H, $J = 8$ Hz), 7.47 (t, 1H, $J = 8$ Hz), 7.27 (s, 1H), 7.17 (br, 1H), 6.92 (d, 1H, $J = 9$ Hz), 4.40 (q, 2H, $J = 6$ Hz), 2.23 (m, 1H), 1.75-1.48 (m, 4H), 1.40 (t, 3H, $J = 5$ Hz), 1.28-1.26 (m, 4H), 0.97-0.84 (m, 6H) ppm; ^{13}C NMR (CDCl_3): $\delta = 175.5, 166.5, 157.2, 155.3, 153.5, 139.8, 138.9, 131.7, 129.6, 125.7, 124.8, 122.1, 116.2, 111.4, 111.0, 61.3, 51.2, 32.6, 29.9, 26.2, 22.9, 14.5, 14.1, 12.2$ ppm; MALDI-TOF-MS: (m/z) calcd. 434.23; observed 435.23 ($\text{M}+\text{H}^+$).

2-(2-Ethylhexanoyl)amino-7-(4-cyanophenyl)amino-1,8-naphthyridine 5h: Following the general procedure and purification by semi-prep-HPLC using LC-MS detection, the title compound was obtained as a yellow powder (17.6 mg). ^1H NMR (CDCl_3): $\delta = 8.35$ (br, 1H), 8.38 (d, 1H, $J = 8$ Hz), 8.02 (d, 1H, $J = 8$ Hz), 7.93 (d, 1H, $J = 8$ Hz), 7.91 (d, 2H, $J = 9$ Hz), 7.71 (br, 1H), 7.58 (d, 2H, $J = 8$ Hz), 6.93 (d, 1H, $J = 9$ Hz), 2.22 (m, 1H), 1.76-1.49 (m, 4H), 1.28-1.23 (m, 4H), 0.97-0.85 (m, 6H) ppm; ^{13}C NMR (CDCl_3): $\delta = 175.7, 156.1, 154.8, 153.7, 144.1, 139.1, 138.1, 133.5, 119.6, 119.3, 116.5, 112.6, 112.1, 105.0, 51.2, 32.5, 29.9, 26.2, 22.8, 14.0, 12.1$ ppm; MALDI-TOF-MS: (m/z) calcd. 387.21; observed: 388.19 ($\text{M}+\text{H}^+$).

2-(2-Ethylhexanoyl)amino-7-(3-methoxyphenyl)amino-1,8-naphthyridine 5i: Following the general procedure and purification by semi-prep-HPLC using LC-MS detection, the title compound was obtained as a light yellow powder (11.2 mg). ^1H NMR (CDCl_3): $\delta = 8.35$ (d, 1H, $J = 8$ Hz), 8.27 (br, 1H), 7.97 (d, 1H, $J = 8$ Hz), 7.84 (d, 1H, $J = 8$ Hz), 7.28 (t, 1H, $J = 6$ Hz), 7.18 (d, 1H, $J = 6$ Hz), 7.07 (s, 1H), 7.01 (d,

1H, $J = 8$ Hz), 6.72 (d, 1H, $J = 6$ Hz), 3.81 (s, 3H), 2.19 (m, 1H), 1.74-1.46 (m, 4H), 1.29-1.24 (m, 4H), 0.93-0.81 (m, 6H) ppm; ^{13}C NMR (CDCl_3): $\delta = 175.5, 160.6, 157.7, 155.4, 153.4, 138.9, 137.9, 130.3, 116.0, 114.4, 111.1, 110.6, 109.7, 55.5, 51.2, 32.6, 30.0, 26.2, 22.9, 14.1, 12.2$ ppm; MALDI-TOF-MS: (m/z) calcd. 392.22; observed: 393.20 ($\text{M}+\text{H}^+$).

2-(2-Ethylhexanoyl)amino-7-(3,4,5-trimethoxyphenyl)amino-1,8-naphthyridine 5j: Following the general procedure and purification by semi-prep-HPLC using UV detection, the title compound was obtained as a yellow powder (5.8 mg). ^1H NMR (CDCl_3): $\delta = 8.29$ (d, 1H, $J = 9$ Hz), 8.26 (br, 1H), 7.97 (d, 1H, $J = 9$ Hz), 7.85 (d, 1H, $J = 9$ Hz), 7.10 (br, 1H), 6.93 (d, 1H, $J = 9$ Hz), 6.71 (s, 2H), 3.88 (s, 9H), 2.20 (s, 1H), 1.76-1.49 (m, 4H), 1.30-1.24 (m, 4H), 0.96-0.84 (m, 6H) ppm; ^{13}C NMR (CDCl_3): $\delta = 175.5, 158.2, 155.4, 153.9, 153.5, 138.9, 135.5, 135.1, 116.0, 111.0, 110.2, 100.9, 61.1, 56.4, 51.2, 32.6, 29.9, 26.2, 22.9, 14.1, 12.2$ ppm; MALDI-TOF-MS: (m/z) calcd. 452.24; observed: 452.20 ($\text{M}+\text{H}^+$).

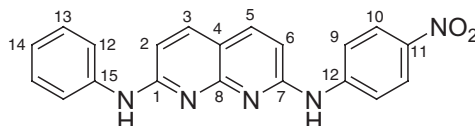
2-(2-Ethylhexanoyl)amino-7-(2-pyrazinyl)amino-1,8-naphthyridine 5k: Following the general procedure and purification by semi-prep-HPLC using UV detection, the title compound was obtained as a light yellow powder (7.1 mg). ^1H NMR (CDCl_3): $\delta = 9.38$ (br, 1H), 8.64 (br, 1H), 8.55 (br, 1H), 8.39 (d, 1H, $J = 8$ Hz), 8.19 (d, 2H, $J = 7$ Hz), 8.06 (d, 1H, $J = 8$ Hz), 8.00 (d, 1H, $J = 8$ Hz), 7.64 (br, 1H), 2.23 (m, 1H), 1.75-1.48 (m, 4H), 1.29-1.26 (m, 4H), 0.98-0.85 (m, 6H) ppm; ^{13}C NMR (CDCl_3): $\delta = 175.7, 155.3, 153.9, 150.0, 141.5, 139.0, 138.4, 137.0, 112.6, 51.0, 32.5, 29.9, 26.1, 22.9, 14.0, 12.2$ ppm; MALDI-TOF-MS: (m/z) calcd. 364.20; observed: 365.15 ($\text{M}+\text{H}^+$), 387.14 ($\text{M}+\text{Na}^+$), 403.12 ($\text{M}+\text{K}^+$).

2-(2-Ethylhexanoyl)amino-7-[2-(4,6-dimethyl)pyrimidyl]amino-1,8-naphthyridine 5l: Following the general procedure and purification by semi-prep-HPLC using LC-MS detection, the title compound was obtained as a yellow powder (12.8 mg). ^1H NMR (CDCl_3): $\delta = 8.81$ (d, 1H, $J = 9$ Hz), 8.38 (d, 1H, $J = 9$ Hz), 8.26 (br, 1H), 8.08 (d, 1H, $J = 9$ Hz), 8.06 (d, 1H, $J = 9$ Hz), 8.03 (br, 1H), 6.63 (s, 1H), 2.42 (s, 6H), 2.20 (m, 1H), 1.77-1.50 (m, 4H), 1.32-1.26 (m, 4H), 0.98-0.86 (m, 6H) ppm; ^{13}C NMR (CDCl_3): $\delta = 175.4, 167.9, 158.6, 155.6, 154.4, 153.5, 138.9, 138.2, 117.4, 113.6, 113.2, 112.3, 51.2, 32.6, 29.9, 26.2, 24.1, 22.9, 14.0, 12.2$ ppm; MALDI-TOF-MS: (m/z) calcd. 392.23; observed: 393.17 ($\text{M}+\text{H}^+$).

2-(3-Nitrophenyl)amino-7-phenylamino-1,8-naphthyridine 7a: A 10 mL Schlenck vessel was charged with $\text{Pd}(\text{OAc})_2$ (1.92 mg, 8.6 μmol), Xantphos (5.22 mg, 9.0 μmol), K_2CO_3 (38.6 mg, 0.28 mmol), 7-amino-2-(phenylamino)-1,8-naphthyridine **8** (48.1 mg, 0.20 mmol), 1-bromo-3-nitrobenzene (40.6 mg, 0.20 mmol) and 1,4-dioxane (1.0 mL). The reaction vessel was capped, evacuated and back-filled with N_2 three times before stirring at 100 $^\circ\text{C}$ for 20 h. Subsequently, the mixture was cooled, filtered over diatomaceous earth and evaporated in vacuo. The crude reaction product could be purified by column chromatography (SiO_2 , 6 % acetone in chloroform) to yield the title compound as a yellow solid (45 mg, 63 %). ^1H NMR (CDCl_3): $\delta = 8.51$ (s, 1H), 8.07 (d, 1H, $J = 8$ Hz), 7.71 (d, 3H, $J = 7$ Hz), 7.40 (d, 2H, $J = 8$ Hz), 7.30 (t, 3H, $J = 7$ Hz), 7.06 (t, 1H, $J = 7$ Hz), 6.90 (d, 1H, $J = 8$ Hz), 6.86 (d, 1H, $J = 8$ Hz) ppm; ^{13}C NMR (CDCl_3): $\delta = 157.6, 156.6, 155.9, 148.7, 141.6, 139.5, 138.2, 138.0, 129.7, 129.4, 125.8, 124.2, 122.0, 116.9, 114.6, 11.5, 109.1, 108.1$ ppm; MALDI-TOF-MS: (m/z) calcd. 357.12; observed: 358.04 ($\text{M}+\text{H}^+$); Anal. Calcd. for $\text{C}_{20}\text{H}_{15}\text{N}_5\text{O}_2$: C 67.22, H 4.23, N 19.60; found: C 65.00, H 3.90, N 18.17.

2-(4-Nitrophenyl)amino-7-phenylamino-1,8-naphthyridine 7b: A 10 mL Schlenck vessel was charged with $\text{Pd}(\text{OAc})_2$ (2.1 mg, 9.3 μmol), Xantphos (5.1 mg, 8.9 μmol), K_2CO_3 (44.2 mg, 0.32 mmol), 7-amino-2-

(phenylamino)-1,8-naphthyridine **8** (51.7 mg, 0.22 mmol), 1-bromo-4-nitrobenzene (48.7 mg, 0.24 mmol) and 1,4-dioxane (2.0 mL). The reaction vessel was capped, evacuated and back-filled with N₂ three times before stirring at 100 °C for 20 h. The mixture was cooled, filtered over diatomaceous earth and evaporated in vacuo. Purification by column chromatography (SiO₂, 5 % acetone in chloroform) gave the title compound (R_f = 0.05) as a yellow solid (40 mg, 51 %). By-products **12** and **13** had R_f values 0.4 and 0.65 respectively. Full assignment was done based on ¹H NMR, apt ¹³C NMR, gCOSY, gHMQC and gHMBC measurements. ¹H NMR (CDCl₃): δ = 8.04 (d, 2H, *J* = 9 Hz, 10), 7.82 (d, 2H, *J* = 8 Hz, 3,5), 7.77 (d, 2H, *J* = 8 Hz, 9), 7.44 (d, 2H, *J* = 7 Hz, 12), 7.33 (t, 2H, *J* = 7 Hz, 13), 7.10 (t, 1H, *J* = 7 Hz, 14), 6.95 (d, 1H, *J* = 9 Hz, 2), 6.88 (d, 1H, *J* = 9 Hz, 6), ppm; ¹³C NMR (CDCl₃): δ = 158.0 (1), 156.1 (15), 155.5 (8), 146.5 (12), 141.5 (11), 139.3 (15), 138.0 (3), 137.9 (5), 129.5 (13), 129.4 (13), 125.3 (10), 124.2 (14), 122.0 (12), 121.9 (12), 118.1 (9), 118.0 (9), 113.8 (4), 109.4 (6), 108.6 (2) ppm; MALDI-TOF-MS: (*m/z*) calcd. 357.37; observed: 358.04 (M+H⁺); FTR-IR (ATR): ν = 3364, 3036, 1591, 1576, 1543, 1493, 1441, 1352, 1317, 1300, 1253, 1219, 1178, 1143, 1109, 902, 831 cm⁻¹; Anal. Calcd. for C₂₀H₁₅N₅O₂: C 67.22, H 4.23, N 19.60; found: C 65.61, H 4.61, N 18.44.



2-(4-Methoxycarbonylphenyl)amino-7-phenylamino-1,8-naphthyridine 7c: A 10 mL Schlenck vessel was charged with Pd(OAc)₂ (1.9 mg, 8.5 μmol), Xantphos (5.7 mg, 9.9 μmol), K₂CO₃ (43.0 mg, 0.31 mmol), 7-amino-2-(phenylamino)-1,8-naphthyridine **8** (50.2 mg, 0.21 mmol), methyl 4-bromobenzoate (50.3 mg, 0.23 mmol) and 1,4-dioxane (2.0 mL). The reaction vessel was capped, evacuated and back-filled with N₂ three times before stirring at 100 °C for 20 h. After cooling, the mixture was filtered over diatomaceous earth and evaporated in vacuo. Purification by column chromatography (SiO₂, 10 % acetone in chloroform) afforded the title compound (R_f = 0.05) as a yellow solid (35 mg, 44 %). The biarylated by-products had an R_f value of 0.3. ¹H NMR (CDCl₃): δ = 8.02 (d, 2H, *J* = 9 Hz), 7.79 (d, 2H, *J* = 8 Hz), 7.68 (d, 2H, *J* = 8 Hz), 7.47 (d, 2H, *J* = 9 Hz), 7.39 (t, 2H, *J* = 8 Hz), 7.18 (br, 2H), 7.14 (t, 1H, *J* = 7 Hz), 6.90 (d, 2H, *J* = 9 Hz), 3.84 (s, 3H) ppm; ¹³C NMR (CDCl₃): δ = 167.0, 157.8, 156.5, 156.2, 144.5, 139.6, 138.0, 137.9, 131.3, 129.5, 124.2, 123.9, 122.0, 118.7, 113.7, 108.8, 108.1, 52.0 ppm; MALDI-TOF-MS: (*m/z*) calcd. 370.14; observed: 371.08 (M+H⁺); FTR-IR (ATR): ν = 3346, 3028, 2950, 1698, 1588, 1506, 1494, 1433, 1408, 1339, 1275, 1253, 1173, 1142, 1106, 967, 898, 832 cm⁻¹.

2-(3-Methoxyphenyl)amino-7-phenylamino-1,8-naphthyridine 7d: A 10 mL Schlenck vessel was charged with Pd(OAc)₂ (0.91 mg, 4.1 μmol), Xantphos (5.32 mg, 9.2 μmol), K₂CO₃ (58.0 mg, 0.42 mmol), 7-amino-2-(phenylamino)-1,8-naphthyridine **8** (50.8 mg, 0.21 mmol), 1-bromo-3-methoxybenzene (42.7 mg, 0.23 mmol) and 1,4-dioxane (1.0 mL). The reaction vessel was capped, evacuated and back-filled with N₂ three times before stirring at 100 °C for 18 h. The red reaction mixture was cooled, filtered over diatomaceous earth and evaporated in vacuo. The title compound could be obtained as a yellow powder after purification by column chromatography (SiO₂, 5 % methanol in chloroform) followed by precipitation in *n*-heptane (48 mg, 67 %). ¹H NMR (CDCl₃): δ = 7.68 (d, 2H, *J* = 8 Hz), 7.50 (d, 2H, *J* = 7 Hz), 7.42 (br, 2H), 7.34 (t, 2H, *J* = 7 Hz), 7.22 (t, 1H, *J* = 7 Hz), 7.11 (s, 1H), 7.08 (t, 1H, *J* = 7 Hz), 7.06 (t, 1H,

$J = 7$ Hz), 6.89 (d, 1H, $J = 8$ Hz), 6.73 (d, 1H, $J = 8$ Hz), 6.65 (d, 1H, $J = 7$ Hz), 3.80 (s, 3H) ppm; ^{13}C NMR (CDCl_3): $\delta = 160.1, 157.2, 157.1, 156.3, 140.9, 139.6, 137.3, 137.2, 129.6, 128.8, 123.2, 121.4, 121.3, 113.6, 112.7, 108.8, 107.1, 55.0$ ppm; MALDI-TOF-MS: (m/z) calcd. 342.15; observed: 343.05 ($\text{M}+\text{H}^+$); Anal. Calcd. for $\text{C}_{21}\text{H}_{18}\text{N}_4\text{O}$: C 73.67, H 5.30, N 16.36; found: C 72.67, H 5.02, N 16.36.

2-(2-Pyridyl)amino-7-phenylamino-1,8-naphthyridine 7e: Following the general procedure and purification by semi-prep-HPLC using UV detection, the title compound was obtained as a dark yellow powder (6.3 mg). ^1H NMR (CDCl_3): $\delta = 8.29$ (d, 1H, $J = 7$ Hz), 8.17 (br, 1H), 7.97 (br, 1H), 7.80 (d, 1H, $J = 8$ Hz), 7.77 (d, 1H, $J = 8$ Hz), 7.68 (t, 1H, $J = 7$ Hz), 7.46 (d, 2H, $J = 7$ Hz), 7.40-7.28 (m, 4H), 7.13 (t, 1H, $J = 7$ Hz), 6.94-6.89 (m, 2H) ppm; ^{13}C NMR (CDCl_3): $\delta = 157.7, 155.7, 153.6, 147.7, 139.8, 138.3, 138.0, 137.8, 129.5, 124.1, 121.9, 117.5, 113.7, 113.4, 110.4, 108.0$ ppm; MALDI-TOF-MS: (m/z) calcd. 313.13; observed: 314.03 ($\text{M}+\text{H}^+$).

2-(2-Tolyl)amino-7-phenylamino-1,8-naphthyridine 7f: Following the general procedure and purification by semi-prep-HPLC using LC-MS detection, the title compound was obtained as a yellow powder (13.4 mg). ^1H NMR (CDCl_3): $\delta = 7.70$ (d, 1H, $J = 8$ Hz), 7.62 (d, 1H, $J = 8$ Hz), 7.50 (d, 1H, $J = 7$ Hz), 7.47 (d, 2H, $J = 6$ Hz), 7.36 (t, 2H, $J = 7$ Hz), 7.28 (d, 1H, $J = 7$ Hz), 7.24 (t, 1H, $J = 7$ Hz), 7.14 (t, 1H, $J = 7$ Hz), 7.10 (t, 1H, $J = 6$ Hz), 7.03 (br, 2H), 6.81 (d, 1H, $J = 9$ Hz), 6.61 (d, 1H, $J = 9$ Hz), 2.32 (s, 3H) ppm; ^{13}C NMR (CDCl_3): $\delta = 158.6, 157.5, 156.9, 139.9, 137.9, 137.7, 133.0, 131.2, 129.4, 127.0, 125.5, 124.9, 123.7, 121.8, 121.6, 113.0, 107.3, 106.3, 18.2$ ppm; MALDI-TOF-MS: (m/z) calcd. 326.15; observed: 327.07 ($\text{M}+\text{H}^+$).

2-(2-Fluorophenyl)amino-7-phenylamino-1,8-naphthyridine 7g: Following the general procedure and purification by semi-prep-HPLC using LC-MS detection, the title compound was obtained as a yellow powder (12.1 mg). ^1H NMR (CDCl_3): $\delta = 8.42$ (t, 1H, $J = 7$ Hz), 7.75 (d, 1H, $J = 9$ Hz), 7.72 (d, 1H, $J = 9$ Hz), 7.46 (d, 2H, $J = 7$ Hz), 7.39 (t, 2H, $J = 7$ Hz), 7.18-7.08 (m, 5H), 7.02 (t, 1H, $J = 7$ Hz), 6.84 (d, 1H, $J = 8$ Hz), 6.70 (d, 1H, $J = 8$ Hz) ppm; ^{13}C NMR (CDCl_3): $\delta = 157.7, 156.7, 156.6, 139.8, 137.9, 137.8, 129.5, 124.8, 124.7, 123.3, 123.2, 122.3, 121.9, 115.3, 115.1, 113.3, 108.6, 107.6$ ppm; MALDI-TOF-MS: (m/z) calcd. 330.13; observed: 331.10 ($\text{M}+\text{H}^+$).

2-(4-Fluorophenyl)amino-7-phenylamino-1,8-naphthyridine 7h: Following the general procedure and purification by semi-prep-HPLC using LC-MS detection, the title compound was obtained as a yellow powder (10.2 mg). ^1H NMR (CDCl_3): $\delta = 7.71$ (d, 2H, $J = 9$ Hz), 7.47 (m, 4H), 7.36 (t, 2H, $J = 7$ Hz), 7.07 (m, 5H), 6.84 (d, 1H, $J = 8$ Hz), 6.70 (d, 1H, $J = 8$ Hz) ppm; ^{13}C NMR (CDCl_3): $\delta = 161.1, 157.8, 157.7, 156.7, 139.8, 137.8, 135.9, 129.4, 124.1, 124.0, 123.9, 121.8, 116.2, 115.9, 113.1, 107.3$ ppm; MALDI-TOF-MS: (m/z) calcd. 330.13; observed: 331.10 ($\text{M}+\text{H}^+$).

2-(4-Methoxyphenyl)amino-7-phenylamino-1,8-naphthyridine 7i: Following the general procedure and purification by semi-prep-HPLC using UV detection, the title compound was obtained as a dark yellow powder (6.4 mg). ^1H NMR (CDCl_3): $\delta = 7.74$ -7.65 (m, 2H), 7.47 (d, 2H, $J = 8$ Hz), 7.39-7.33 (m, 5H), 7.11 (t, 1H, $J = 7$ Hz), 7.10 (br, 2H), 6.92 (d, 1H, $J = 8$ Hz), 6.82 (d, 1H, $J = 8$ Hz), 6.77 (d, 1H, $J = 8$ Hz), 3.83 (s, 3H) ppm; ^{13}C NMR (CDCl_3): $\delta = 158.7, 157.6, 157.5, 157.0, 139.9, 137.8, 132.6, 129.5, 125.2, 123.9, 123.7, 121.8, 121.7, 114.7, 112.9, 107.4, 107.1, 106.8, 55.7$ ppm; MALDI-TOF-MS: (m/z) calcd. 342.15; observed: 343.11 ($\text{M}+\text{H}^+$).

2-(3,5-Dimethoxyphenyl)amino-7-phenylamino-1,8-naphthyridine 7j: Following the general procedure and purification by semi-prep-HPLC using UV detection, the title compound was obtained as a yellow powder (5.8 mg). ^1H NMR (CDCl_3): δ = 7.74 (d, 1H, J = 9 Hz), 7.71 (d, 1H, J = 9 Hz), 7.54 (d, 2H, J = 7 Hz), 7.38 (t, 2H, J = 7 Hz), 7.08 (br, 2H), 6.95 (d, 1H, J = 8 Hz), 6.84 (t, 1H, J = 8 Hz), 6.65 (s, 2H), 6.23 (s, 1H), 3.82 (s, 6H) ppm; ^{13}C NMR (CDCl_3): δ = 161.5, 157.5, 141.8, 139.9, 137.9, 129.4, 123.7, 121.8, 121.6, 113.2, 107.8, 107.6, 107.4, 100.0, 96.0, 55.5 ppm; MALDI-TOF-MS: (m/z) calcd. 372.16; observed: 373.00 ($\text{M}+\text{H}^+$).

2-(4-Cyanophenyl)amino-7-phenylamino-1,8-naphthyridine 7k: Following the general procedure and purification by semi-prep-HPLC using UV detection, the title compound was obtained as a yellow powder (5.2 mg). ^1H NMR (CDCl_3): δ = 7.91-7.79 (m, 5H), 7.61 (d, 2H, J = 9 Hz), 7.49-7.38 (m, 5H), 7.17 (t, 1H, J = 7 Hz), 6.96 (d, 1H, J = 9 Hz), 6.82 (d, 1H, J = 9 Hz) ppm; ^{13}C NMR (CDCl_3): δ = 158.0, 156.3, 155.8, 144.4, 139.4, 138.1, 138.0, 133.4, 129.6, 124.4, 122.1, 119.7, 119.0, 113.8, 108.3, 104.5 ppm; MALDI-TOF-MS: (m/z) calcd. 337.13; observed: 338.10 ($\text{M}+\text{H}^+$).

7-Amino-2-phenylamino-1,8-naphthyridine 8: A clear solution of crude 2-acetamido-7-phenylamino-1,8-naphthyridine **11** (2.66 g, 9.5 mmol) in 6% NaOMe/MeOH (20 mL) was stirred at 60 °C for 10 h. The solution was cooled to RT followed by evaporation in vacuo to yield a dark red oil. The product was purified by column chromatography (SiO_2 , THF) and obtained as a bright yellow solid (1.00 g, 44 %). ^1H NMR (CDCl_3): δ = 7.69 (d, 2H, J = 8 Hz), 7.50 (d, 2H, J = 8 Hz), 7.36 (t, 2H, J = 7 Hz), 7.10 (t, 1H, J = 6 Hz), 6.80 (br, 1H), 6.77 (d, 1H, J = 8 Hz), 6.52 (d, 1H, J = 8 Hz), 4.86 (br, 2H) ppm; ^{13}C NMR (CDCl_3): δ = 160.1, 157.2, 156.7, 140.0, 137.7, 137.5, 129.1, 125.5, 123.2, 121.2, 112.1, 108.0, 107.2 ppm; MALDI-TOF-MS: (m/z) calcd. 236.11; observed: 237.04 ($\text{M}+\text{H}^+$); FTR-IR (ATR): ν = 3435, 3385, 3298, 3028, 1589, 1567, 1511, 1494, 1447, 1428, 1353, 1331, 1307, 1251, 1141, 896, 830, 798 cm^{-1} . Anal. Calcd. for $\text{C}_{14}\text{H}_{12}\text{N}_4$: C 71.17, H 5.12, N 23.71; found: C 71.28, H 5.01, N 23.55.

2-Acetamido-7-phenylamino-1,8-naphthyridine 11: A 100 mL Schlenck tube was charged with $\text{Pd}(\text{OAc})_2$ (50 mg, 0.22 mmol), Xantphos (150 mg, 0.43 mmol), Cs_2CO_3 (6.06 g, 18.6 mmol), 7-acetamido-2-chloro-1,8-naphthyridine **6a** (2.95 g, 13.3 mmol), aniline (1.44 g, 15.5 mmol) and 1,4-dioxane (44 mL). The reaction vessel was capped, evacuated and back-filled with N_2 three times. Subsequently, the reaction mixture was stirred at 100 °C for 16 h. The mixture was cooled, filtered over diatomaceous earth and evaporated in vacuo to obtain the crude product as a red oil (3.0 g). The product was used without further purification. An analytical sample was made by trituration with diisopropylether to yield the title compound as a yellow solid. ^1H NMR (CDCl_3): δ = 9.41 (br, 1H, NH), 8.20 (d, 1H, J = 9 Hz), 7.93 (d, 1H, J = 9 Hz), 7.80 (d, 1H, J = 9 Hz), 7.72 (br, 1H), 7.58 (d, 2H, J = 7 Hz), 7.37 (t, 2H, J = 7 Hz), 7.13 (t, 1H, J = 7 Hz), 6.92 (d, 1H, J = 9 Hz), 2.18 (s, 3H) ppm; ^{13}C NMR (CDCl_3): δ = 157.6, 155.1, 153.5, 139.4, 138.6, 137.5, 129.1, 123.8, 121.6, 115.6, 110.9, 110.7, 24.8 ppm; MALDI-TOF-MS: (m/z) calcd. 236.11; observed: 237.04 ($\text{M}+\text{H}^+$); Anal. Calcd. for $\text{C}_{16}\text{H}_{14}\text{N}_4\text{O}$: C 69.05, H 5.07, N 20.13; found: C 69.28, H 5.21, N 20.55.

7-(4-Nitrophenyl)amino-2-(N-4-nitrophenyl-N-phenyl)amino-1,8-naphthyridine 12: The title compound was isolated as a yellow solid by column chromatography from the crude reaction mixture of **7b** and had an R_f value of 0.4 (24 mg, 31 %). ^1H NMR ($\text{CDCl}_3+\text{DMSO}$): δ = 9.68 (br, 1H, NH), 8.12 (m, 5H), 7.88 (d, 2H), 7.49 (m, 3H), 7.39-7.28 (m, 5H), 7.08 (d, 1H), 6.76 (d, 1H) ppm; ^{13}C NMR ($\text{CDCl}_3+\text{DMSO}$): δ =

158.3, 156.0, 154.6, 150.9, 146.7, 143.6, 141.8, 140.5, 137.6, 136.7, 130.0, 127.7, 126.8, 124.5, 124.5, 124.1, 122.7, 117.6, 114.9, 113.3, 112.8 ppm; MALDI-TOF-MS: (m/z) calcd. 478.14; observed: 479.08 (M+H⁺);

(N-Succinimidyl)-(dodecyl) carbonate 14: To a stirred solution of dodecyl alcohol (0.185 g, 1.0 mmol) in dry acetonitrile (5.0 mL) were added triethyl amine (303 mg, 3.0 mmol) and N,N'-succinimidyl carbonate (DSC) (384 mg, 1.5 mmol). The mixture was stirred at room temperature for 5 h followed by concentration in vacuo to 1 mL. Saturated NaHCO₃ solution was added (10 mL) followed by extraction of the product with dichloromethane (2 x 10 mL). The combined organic layers were washed with brine (10 mL) and dried over MgSO₄. Evaporation to dryness afforded the title compound as an oil (300 mg, 92 %). ¹H NMR (CDCl₃): δ = 4.24 (t, 2H), 2.75 (s, 4H), 1.65 (m, 2H), 1.35-1.21 (m, 18H), 0.81 (t, 3H) ppm; ¹³C NMR (CDCl₃): δ = 168.9, 151.5, 71.6, 31.9, 29.6, 29.5, 29.4, 29.3, 29.0, 28.3, 25.4 (2), 22.6, 14.1 ppm; MALDI-TOF-MS: (m/z) calcd. 327.43; observed: 328.46 (M+H⁺).

2-(Dodecyloxy-carbonylamino)-7-phenylamino-1,8-naphthyridine 15: To a stirred solution of **8** (115 mg, 0.487 mmol) and triethylamine (73 mg, 0.72 mmol) in dry dichloromethane (4.0 mL) was added a solution of mixed carbamate **14** (144 mg, 0.44 mmol) in dry dichloromethane (1.0 mL). The solution was stirred at 40 °C for 12 h. The crude product was obtained by purification by column chromatography (SiO₂, 1:3 v/v% ethylacetate/n-hexane) as a white solid. The title compound was obtained as colorless needles by crystallization from ethylacetate/n-hexane (1:3 v/v%, 10 mL) and dried in vacuo (40 mg, 20 %). ¹H NMR (CDCl₃): δ = 8.00 (d, 1H, J = 9 Hz), 7.93 (d, 1H, J = 9 Hz), 7.81 (d, 1H, J = 9 Hz), 7.47 (d, 2H, J = 6 Hz), 7.39 (t, 2H, J = 6 Hz), 7.15 (t, 1H, J = 6 Hz), 6.91 (d, 1H, J = 9 Hz), 4.20 (t, 2H, J = 6 Hz), 1.71 (m, 2H), 1.36-1.25 (m, 18H), 0.88 (t, 3H) ppm; ¹³C NMR (CDCl₃): δ = 157.9, 155.6, 153.4, 153.5, 139.5, 138.7, 137.8, 129.5, 124.3, 122.2, 115.3, 110.2, 109.3, 66.0, 32.1, 29.8 (2), 29.7 (2), 29.5, 29.4, 28.9, 26.0, 22.8, 14.3 ppm; MALDI-TOF-MS: (m/z) calcd. 448.28; observed: 449.27 (M+H⁺); FTR-IR (ATR): ν = 3376, 3153, 2956, 2921, 2850, 1737, 1622, 1605, 1595, 1520, 1472, 1425, 1383, 1364, 1324, 1299, 1193, 1136, 1084, 1020, 836 cm⁻¹.

4.7 References

- (1) Wang, X.-Z.; Li, X.-Q.; Shao, X.-B.; Zhao, X.; Deng, P.; Jiang, X.-K.; Li, Z.-T.; Chen, Y.-Q. *Chem. Eur. J.* **2003**, *9*, 2904-2913.
- (2) Zhao, X.; Wang, X.-Z.; Jiang, X.-K.; Chen, Y.-Q.; Li, Z.-T.; Chen, G.-J. *J. Am. Chem. Soc.* **2003**, *125*, 15128-15139.
- (3) Li, X.-Q.; Jiang, X.-K.; Wang, X.-Z.; Li, Z.-T. *Tetrahedron* **2004**, *60*, 2063-2069.
- (4) Li, X.-Q.; Feng, D.-J.; Jiang, X.-K.; Li, Z.-T. *Tetrahedron* **2004**, *60*, 8275-8284.
- (5) Li, X.-Q.; Jia, M.-X.; Wang, X.-Z.; Jiang, X.-K.; Li, Z.-T.; Chen, G.-J.; Yu, Y.-H. *Tetrahedron* **2005**, *61*, 9600-9610.
- (6) Ligthart, G. B. W. L.; Ohkawa, H.; Sijbesma, R. P.; Meijer, E. W. *J. Am. Chem. Soc.* **2005**, *127*, 810-811.
- (7) Ligthart, G. B. W. L.; Ohkawa, H.; Sijbesma, R. P.; Meijer, E. W. *manuscript submitted*.
- (8) Peng, T.; Murase, T.; Goto, Y.; Kobori, A.; Nakatani, K. *Bioorgan. Med. Chem. Lett.* **2005**, *15*, 259-262.
- (9) see Chapter 5 of this Thesis.
- (10) Smith, M. B.; March, J. *March's Advanced Organic Chemistry: Reactions, Mechanisms and Structure*; 5th ed.; Wiley-Interscience: New York, 2001.

- (11) Wolfe, J. P.; Wagaw, S.; Marcoux, J.-F.; Buchwald, S. L. *Acc. Chem. Res.* **1998**, *31*, 805-818.
- (12) Hartwig, J. F. *Angew. Chem. Int. Ed.* **1998**, *37*, 2046-2067.
- (13) Muci, A. R.; Buchwald, S. L. *Top. Curr. Chem.* **2002**, *219*, 131-209.
- (14) Wolfe, J. P.; Buchwald, S. L. *J. Am. Chem. Soc.* **1997**, *119*, 6054-6058.
- (15) Lipshutz, B. H.; Ueda, H. *Angew. Chem. Int. Ed.* **2000**, *39*, 4492-4494.
- (16) Kelkar, A. A.; Patil, N. M.; Chaudhari, R. V. *Tetrahedron Lett.* **2002**, *43*, 7143-7146.
- (17) Kwong, F. Y.; Buchwald, S. L. *Org. Lett.* **2003**, *5*, 793-796.
- (18) Paul, F.; Patt, J.; Hartwig, J. F. *Organometallics* **1995**, *14*, 3030-9.
- (19) Wagaw, S.; Buchwald, S. L. *J. Org. Chem.* **1996**, *61*, 7240-7241.
- (20) Jonckers, T. H. M.; Maes, B. U. W.; Lemiere, G. L. F.; Dommissie, R. *Tetrahedron* **2001**, *57*, 7027-7034.
- (21) Wolfe, J. P.; Tomori, H.; Sadighi, J. P.; Yin, J.; Buchwald, S. L. *J. Org. Chem.* **2000**, *65*, 1158-1174.
- (22) Viciu, M. S.; Kelly, R. A., III; Stevens, E. D.; Naud, F.; Studer, M.; Nolan, S. P. *Org. Lett.* **2003**, *5*, 1479-1482.
- (23) Urgaonkar, S.; Nagarajan, M.; Verkade, J. G. *Org. Lett.* **2003**, *5*, 815-818.
- (24) Urgaonkar, S.; Verkade, J. G. *J. Org. Chem.* **2004**, *69*, 9135-9142.
- (25) Shen, Q.; Shekhar, S.; Stambuli, J. P.; Hartwig, J. F. *Angew. Chem. Int. Ed.* **2005**, *44*, 1371-1375, S1371/1-S1371/79.
- (26) Wang, H.; Rizzo, C. J. *Org. Lett.* **2001**, *3*, 3603-5.
- (27) Schoffers, E.; Olsen, P. D.; Means, J. C. *Org. Lett.* **2001**, *3*, 4221-4223.
- (28) Newkome, G. R.; Garbis, S. J.; Majestic, V. K.; Fronczek, F. R.; Chiari, G. J. *Org. Chem.* **1981**, *46*, 833-9.
- (29) Corbin, P. S.; Zimmerman, S. C.; Thiessen, P. A.; Hawryluk, N. A.; Murray, T. J. *J. Am. Chem. Soc.* **2001**, *123*, 10475-10488.
- (30) Kranenburg, M.; van der Burgt, Y. E. M.; Kamer, P. C. J.; van Leeuwen, P. W. N. M.; Goubitz, K.; Fraanje, J. *Organometallics* **1995**, *14*, 3081-9.
- (31) Guari, Y.; Van Es, D. S.; Reek, J. N. H.; Kamer, P. C. J.; Van Leeuwen, P. W. N. M. *Tetrahedron Lett.* **1999**, *40*, 3789-3790.
- (32) Lidstrom, P.; Tierney, J.; Wathey, B.; Westman, J. *Tetrahedron* **2001**, *57*, 9225-9283.
- (33) Loones, K. T. J.; Maes, B. U. W.; Rombouts, G.; Hostyn, S.; Diels, G. *Tetrahedron* **2005**, *61*, 10338-10348.
- (34) Mogilaiah, K.; Reddy, N. V. *Indian J. Chem., Sect. B* **2003**, *42B*, 2124-2125.
- (35) Iwaki, T.; Yasuhara, A.; Sakamoto, T. *J. Chem. Soc., Perkin Trans. 1* **1999**, 1505-1510.
- (36) Yin, J.; Zhao, M. M.; Huffman, M. A.; McNamara, J. M. *Org. Lett.* **2002**, *4*, 3481-3484.
- (37) Amatore, C.; Broeker, G.; Jutand, A.; Khalil, F. J. *Am. Chem. Soc.* **1997**, *119*, 5176-5185.
- (38) Wolfe, J. P.; Buchwald, S. L. *Tetrahedron Lett.* **1997**, *38*, 6359-6362.
- (39) Singh, U. K.; Strieter, E. R.; Blackmond, D. G.; Buchwald, S. L. *J. Am. Chem. Soc.* **2002**, *124*, 14104-14114.
- (40) Alcazar-Roman, L. M.; Hartwig, J. F.; Rheingold, A. L.; Liable-Sands, L. M.; Guzei, I. A. *J. Am. Chem. Soc.* **2000**, *122*, 4618-4630.
- (41) Negishi, E. I. *Handbook of Organopalladium Chemistry for Organic Synthesis*; Wiley-Interscience: New York, 2002.
- (42) Hamann, B. C.; Hartwig, J. F. *J. Am. Chem. Soc.* **1998**, *120*, 7369-7370.
- (43) Espinet, P.; Echavarren, A. M. *Angew. Chem. Int. Ed.* **2004**, *43*, 4704-4734.
- (44) Barrios-Landeros, F.; Hartwig, J. F. *J. Am. Chem. Soc.* **2005**, *127*, 6944-6945.
- (45) Ghosh, A. K.; Duong, T. T.; McKee, S. P.; Thompson, W. J. *Tetrahedron Lett.* **1992**, *33*, 2781-4.
- (46) Beijer, F. H.; Sijbesma, R. P.; Kooijman, H.; Spek, A. L.; Meijer, E. W. *J. Am. Chem. Soc.* **1998**, *120*, 6761-6769.

5

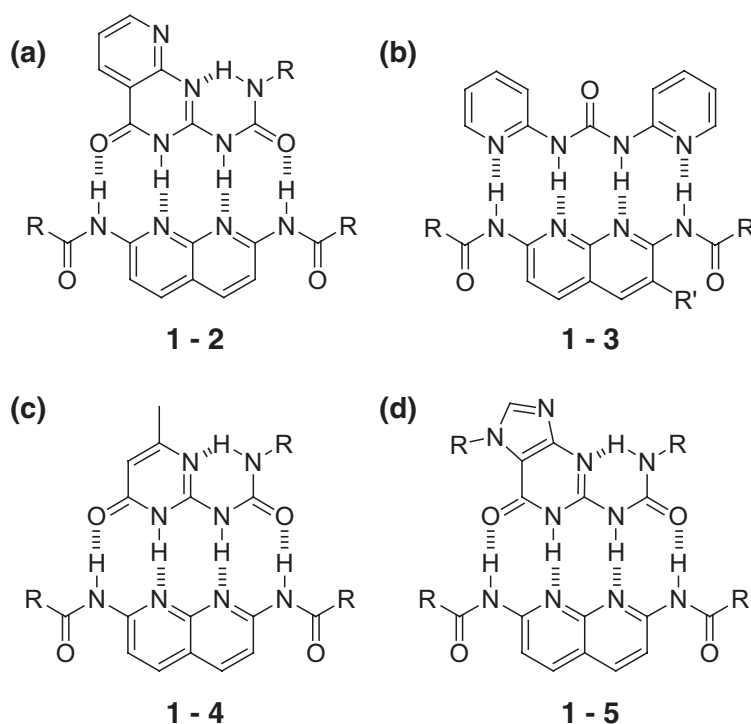
Complementary quadruple hydrogen bonding based on the UPy - Napy binding motif

Abstract

A strong complementary quadruple hydrogen bonded complex is formed between 2,7-diamido-1,8-naphthyridine and 2-ureido-6[1H]-pyrimidinone in organic solvents. The ureido-pyrimidinone undergoes a complexation-induced tautomeric shift from the 4[1H] to the 6[1H] tautomeric form as indicated by NMR spectroscopy. The equilibrium between ureido-pyrimidinone homodimers and ureido-pyrimidinone - 2,7-diamido-1,8-naphthyridine heterodimers displays a concentration dependent selectivity with higher selectivity at higher concentrations. The association constant ($K_a = 5 (\pm 2) \times 10^6 \text{ M}^{-1}$ in CDCl_3) of the heterocomplex was determined by ^1H NMR, UV/Vis and fluorescence spectroscopy. For a large number of complexes of naphthyridines bearing various substituents with a 2-ureido-pyrimidinone derivative, association constants were determined using a single point ^1H NMR method. Whereas arylamino-substituted naphthyridines form heterodimers with a ureido-pyrimidinone with high selectivity, alkylamino substituents do not provide the required acidity of the amino protons for sufficiently strong hydrogen bonding. Sterically demanding substituents have a dramatic effect on the selectivity of heterocomplex formation while electron-withdrawing and donating substituents induce small deviations in the association constant. Finally, kinetic parameters for the exchange between ureido-pyrimidinone homodimers and ureido-pyrimidinone - 2,7-diamido-1,8-naphthyridine heterodimers were determined by dynamic NMR.

5.1 Introduction

The assembly of functional supramolecular structures with a precision analogous to that found in nature requires an understanding and control of non-covalent interactions, such as hydrogen bonding and metal-ligand coordination as well as π - π stacking, hydrophobic, Coulombic and Van der Waals forces. All these interactions have different characteristics, which can be applied to fine-tune the properties of the self-assembly process or the properties of the supramolecular material. In supramolecular association, where many processes are in competition, the association constant (K_a) determines the energetically most favourable state. The association constant of hydrogen-bonded systems is closely linked to the number of hydrogen bonds and their physical arrangement.¹⁻⁴ The binding energy can vary from 4 up to 120 kJ·mol⁻¹, approaching that of a weak covalent bond.⁵ The development of complementary quadruple hydrogen bonding arrays displaying high binding constants is of major importance for the introduction of directionality in supramolecular architectures. Of the four types of complementary quadruple hydrogen bond couples that are possible, the binding properties of four DAAD – ADDA couples have been reported (Scheme 5.1).⁶⁻¹¹



Scheme 5.1 Heterocomplexes based on the DAAD – ADDA binding motif, (a) Napy **1** – 2-ureido-[3H]-pyrido-(2,3-d)pyrimidin-4-one **2** complex, $K_a = 3300 \text{ M}^{-1}$ in 5% DMSO/chloroform;⁶ (b) Napy **1** – *N,N'*-di-2-pyridylurea **3**, $R = \text{CN}$, $K_a = 2000 \text{ M}^{-1}$ in chloroform;^{7,9} $R = \text{H}$, $K_a = 1200 \text{ M}^{-1}$ in chloroform;⁸ (c) Napy **1** – UPy **4**, $K_a = 1.5 \times 10^9 \text{ M}^{-1}$ in chloroform;¹⁰ (d) Napy **1** – 2-ureido-guanosine **5**, $K_a = 5 \times 10^7 \text{ M}^{-1}$ in chloroform.^{11,12}

As can be seen from Scheme 5.1, 2,7-diamido-1,8-naphthyridine **1** (Napy) derivatives have been used in all examples as the DAAD array. Two of the tautomeric forms of **2** contain an ADDA array (one shown), and its very high association constant with **1** was determined by ^1H NMR titration.⁶ The importance of the intramolecular hydrogen bond present in **2** is evident when **2** is replaced by N,N'-di-2-pyridylurea **3**. The latter derivatives are capable of forming inter- and intramolecular hydrogen bonds in solution,¹³ therefore increasing the energetic barrier to form heterocomplexes **1** – **3** resulting in lower K_a values. During the course of the investigation described in this chapter, Li and coworkers reported the selective complexation of the 6[1H] tautomeric form of a ureido-pyrimidinone **4** (UPy) with Napy **1**.¹⁴ An association constant of $1.5 \times 10^9 \text{ M}^{-1}$ was indirectly determined by a competitive binding experiment.¹⁰ More recently, Zimmerman *et al.* determined a K_a value of $5 \times 10^7 \text{ M}^{-1}$ for the highly stable heterocomplex of guanosine urea **5** with **1** using fluorescence resonance energy transfer.^{11,12}

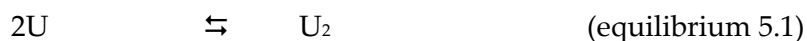
A second important parameter that governs the process of error-correction in self-assembly is the lifetime of a supramolecular complex. It can extend from the nanosecond timescale up to many years (for metal – ligand coordination complexes), depending on the type of non-covalent interaction. The lifetime of a non-covalent interaction is directly related to the activation energy for exchange. In hydrogen bonded complexes, it is mostly dependent on the cooperative effect or number of simultaneous hydrogen bonds present in the complex. A system having two hydrogen bonds like in the hetero- and homo-association of 1-cyclohexyluracil and 9-ethyladenine in chloroform, the lifetime τ of the associated species is in the nanosecond regime at room temperature ($\tau < 28 \text{ ns}$).¹⁵ In contrast, the lifetime can increase to several seconds¹⁶⁻¹⁸ or even many minutes^{19,20} when a multiple hydrogen bond motif is applied. While associated states with long lifetimes promote stable supramolecular structures, the rate of error-correction is low. Complexes with short lifetimes on the other hand, promote fast error-correction, but result in a complex with limited stability which is quickly fluctuating between different states. Recently, Craig and co-workers have shown that slow dynamics result in strong materials regardless of the equilibrium constant for supramolecular networks based on metal-ligand interactions.^{21,22} Therefore, both association constant and lifetime are clearly important parameters in any supramolecular system and will determine the material properties of supramolecular materials to a large extent.

In this chapter, the binding properties of 2,7-diamido-1,8-naphthyridine with 2-ureido-6-[1H]-pyrimidinone are reported and evaluated with ^1H and ^{13}C NMR as well as UV/Vis and fluorescence spectroscopy. The full scope of hetero-dimerization was investigated with a range of 1,8-naphthyridines bearing various substituents. The lifetime of the heterodimer was studied in toluene and chloroform with dynamic NMR spectroscopy.

5.2 The association constant of the 2-ureido-6-[1H]-pyrimidinone – 2,7-diamido-1,8-naphthyridine dimer

5.2.1 Introduction

Direct information on the thermodynamic stability of a given state is obtained from the association constant (K_a). Usually, the K_a value is determined by a titration where the ratio between host and guest is varied. This titration technique is probed by a suitable spectroscopic technique such as NMR,^{23,24} UV/Vis or fluorescence that allows the concentration of the individual components to be determined. The system under study here is governed by three equilibria when the self-association of the Napy unit is ignored²⁵:



where U, U_2 , N and NU represent free UPy, UPy homodimer, free Napy and UPy – Napy heterodimer respectively. The appearance of the NMR spectrum of a mixture of N and U primarily depends on the equilibrium constants (K) and on the rate of the reactions. The equilibrium constants in this system are defined in the following equations (eq. 5.1-3):

$$K_{\text{dim}} = [U_2]/[U]^2 \quad (\text{eq. 5.1})$$

$$K_d = [NU]^2/([U_2] \times [N]^2) \quad (\text{eq. 5.2})$$

$$K_a = [NU]/([N] \times [U]) \quad (\text{eq. 5.3})$$

where K_{dim} , K_d and K_a are the dimerization constant of U, the disproportionation constant of N with U_2 and the association constant of N with U, respectively. When the rate of reaction is high on the NMR time scale, time average signals will be observed and the reaction constants can be derived from the shift of a probe proton. In case of slow exchange, distinct sets of signals are observed that can be integrated to determine the equilibrium concentrations of the species and hence the reaction constants. Previously, Söntjens *et al.* have determined a K_{dim} value of 6×10^7 and $6 \times 10^8 \text{ M}^{-1}$ in chloroform and toluene, respectively, by excimer fluorescence spectroscopy.¹⁸ In this section, the investigation of the UPy – Napy heterodimer is described using NMR, UV/Vis and fluorescence spectroscopy.

5.2.2 NMR measurements

The formation of the UPy – Napy complex was readily observed by ^1H NMR spectroscopy in CDCl_3 . As seen in Figure 5.1, the NH resonances of a 1:1 mixture of UPy **4a** ($R = n$ -butyl) and Napy **1a** ($R' = n$ -propyl) appeared as four sharp signals which are significantly downfield from their original position in the individual components UPy₂ and Napy. Addition of 0.5 equivalent of **1a** to a solution of **4a** gives rise to a distinct set of new peaks in the down-

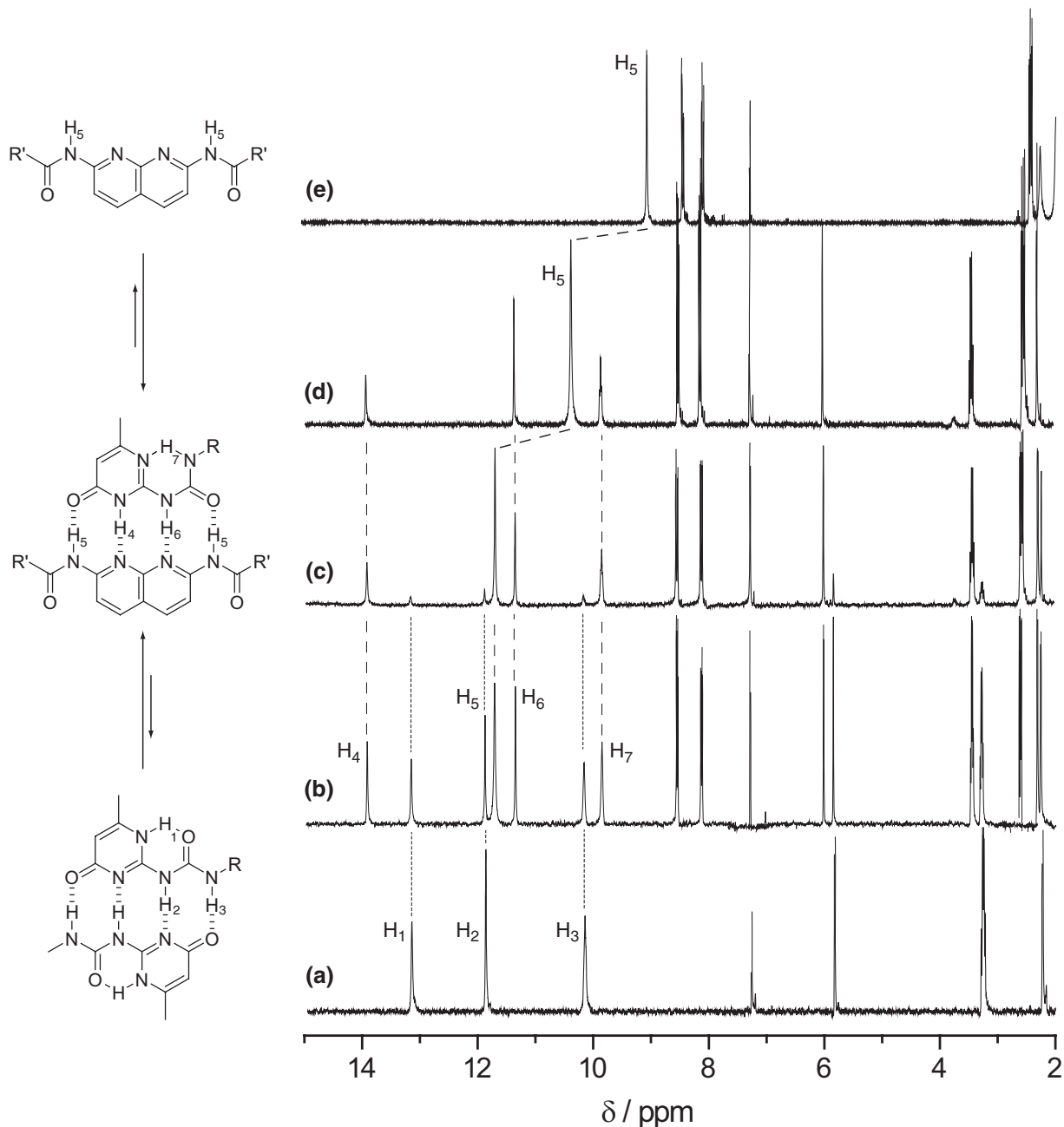


Figure 5.1 ^1H NMR in CDCl_3 for UPy **4a** – Napy **1a**; (a) 10 mM **4a**; (b) 10 – 5 mM **4a** – **1a**; (c) 10 – 10 mM **4a** – **1a**; (d) 5 – 10 mM **4a** – **1a**; (e) 10 mM **1a**.

field region at 13.9, 11.7, 11.3 and 9.8 ppm (Figure 5.1b). These resonances are attributed to 4 different NH protons which exist in the heterodimer **1a** – **4a**. Furthermore, upon complexation new signals appear downfield at 6.0, 3.4, and 2.3 ppm for the alkylidene, ureido-methylene, and methyl-pyrimidone, respectively. These observations are characteristic of an exchange rate that is low on the NMR time scale between **4a** – **4a** and **1a** and suggests the existence of the 6[1H]-pyrimidinone tautomer. At a ratio of 1:1, nearly selective generation of the heterocomplex is observed indicating the very selective disruption of UPy dimers by free Napy molecules (Figure 5.1c). A further decrease in the UPy to Napy ratio now results in an upfield shift of the Napy NH resonance (Figure 5.1d), while the NH signals of the UPy tautomer stay at their original downfield position. From this observation, it can be concluded that there is fast exchange between heterodimerized and free Napy and simultaneous slow exchange between hetero- and homodimerized UPy. Upon heating to 60 °C, the NH signals of an equimolar mixture of **1a** and **4a** broadened to some extent but did not shift dramatically ($\delta < 0.15$ ppm), in contrast to shifts reported in literature.²⁶ This indicates strong and selective binding in combination with slow exchange kinetics even at elevated temperatures. In summary, these ¹H NMR data corroborate that the UPy undergoes a complexation induced tautomeric shift from the AADD to the ADDA form.²⁷

The kinetic stability of the UPy – Napy heterodimer is remarkable; when a 2:1 mixture UPy **4a** /Napy **1a** was heated to 60 °C in CDCl₃ or to 100 °C in toluene-*d*₈ the ¹H NMR spectrum still showed separate signals for both independent assemblies. Although some line broadening was observed, the ratio between UPy in the heterodimer and UPy in the homodimer did not change significantly. Moreover, the downfield NH resonances did not shift which indicates that the exchange between the UPy homodimer and the UPy – Napy heterodimer remains slow.

The ADDA geometry of the 6[1H]-pyrimidinone tautomer of **4a** in solution was confirmed by 2D Nuclear Overhauser Effect (NOE) spectroscopy,²⁸ used to assign the NH proton signals. Pronounced NOE contacts were observed as indicated in Figure 5.2. Moderate NOE-effects were observed at 9.8 and 6.0 ppm for the CH₃ signal of the UPy. Since the signal at 6.0 ppm can be attributed to the UPy alkylidene, the resonance at 9.8 ppm therefore corresponds to the intramolecularly hydrogen bonded NH proton H7 as can also be concluded from the small splitting in the signal which is due to coupling with the neighboring methylene protons. Analogous reasoning led to the assignment of as given in Figure 5.1.

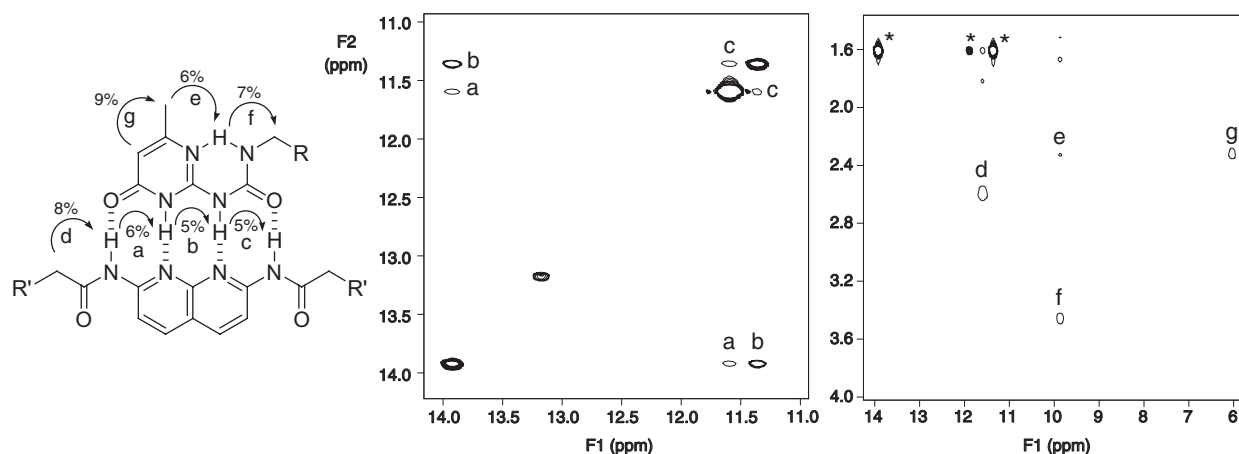
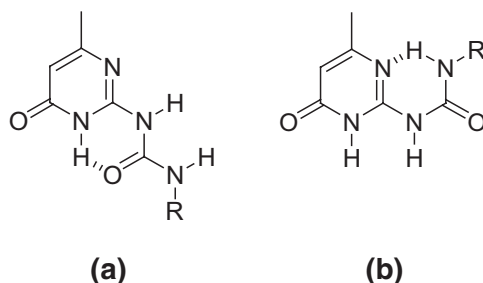


Figure 5.2 Partial Nuclear Overhauser Effect spectra in CDCl_3 for a 1:1 mixture of UPy **4a** – Napy **1a**. Nuclear Overhauser effects between protons (in %) are indicated with letters and arrows in the structure. Chemical exchange with H_2O is indicated with asterisks.

Pioneering work by Beijer *et al.* on the dimerization of UPy derivatives suggested the existence of conformation (a) of the 6[1H]-pyrimidinone tautomer in $\text{CDCl}_3/\text{DMSO}-d_6$ mixtures (Scheme 5.2, $\text{R} = n\text{-butyl}$).^{29,30} However, the exact geometry was not unequivocally determined. Very recently, Park *et al.* indeed calculated a slightly lower energy level for conformation (a).¹² This was supported by 2D-NOE NMR measurements that revealed a strong NOE effect between the ureido-methylene and the NH resonance at 7.2 ppm. In contrast, the other two NH signals are found at 11.4 and 9.4 ppm. For the UPy **4a** – Napy **1b** ($\text{R}' = 3\text{-heptyl}$) heterodimer, a similar ^{13}C NMR spectrum was obtained. Full assignment of the ADDA conformation in **4a** – **1b**, as depicted in Figure 5.3, was achieved based on gHMBC NMR and comparison with the ^{13}C NMR spectrum of UPy₂. Particularly noteworthy is the chemical shift of the pyrimidinone carbonyl (C3) which shifts from 173.0 ppm in the homodimer to 165.2 ppm in the heterodimer. This shift is indicative for the 6[1H]-pyrimidinone keto tautomer.



Scheme 5.2 Two geometries of the 6[1H]-pyrimidinone tautomer.

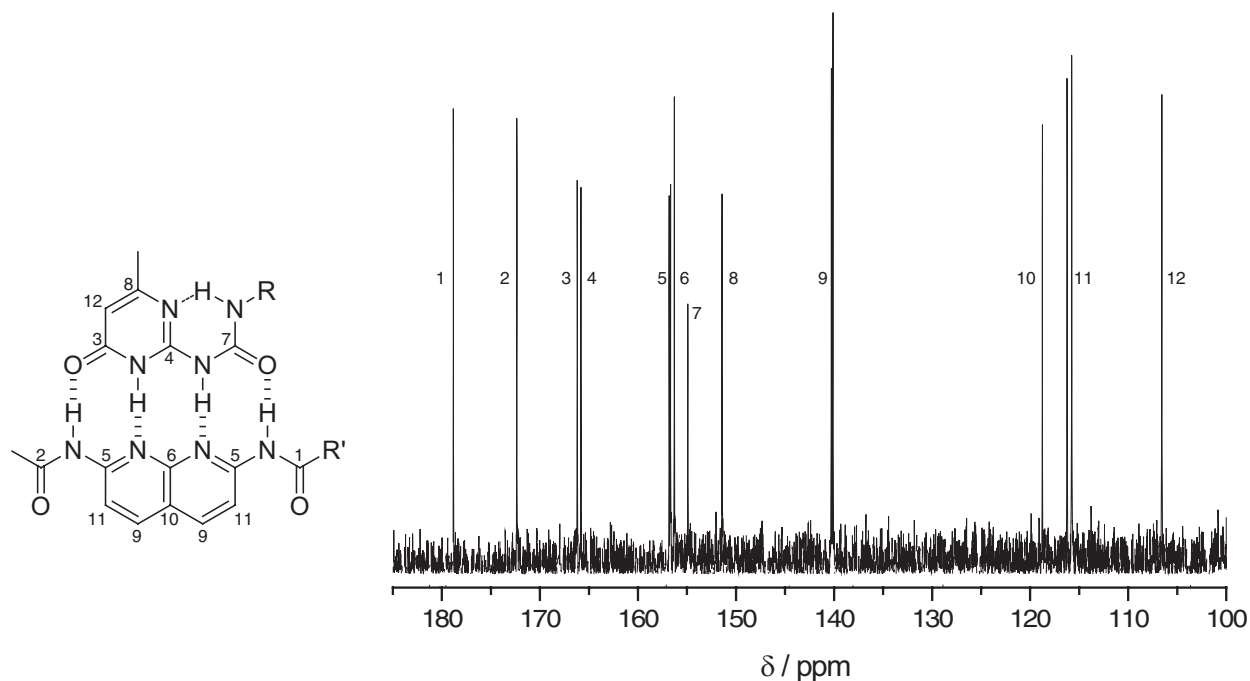


Figure 5.3 ^{13}C NMR in CDCl_3 for a 1:1 mixture of UPy **4a** – Napy **1b** ($R = n\text{-butyl}$; $R' = n\text{-heptyl}$).

Single-point method to determine the UPy - Napy association constant

The ^1H NMR spectrum of a 2:1 UPy – Napy mixture exhibits two sets of resonances which are attributed to the UPy homodimer and the UPy – Napy heterodimer. Slow exchange phenomena have been observed previously in supramolecular host-guest systems and this kinetic effect permits the calculation of the absolute concentrations of all the components from the initial concentrations and the relative intensities of the corresponding ^1H NMR signals. Therefore, K_a values along with their associated free energies of association ($-\Delta G_a^0$) can be estimated using the so-called single-point method.³¹ This method has been used previously as a fast way to determine thermodynamic parameters in supramolecular host-guest systems displaying fast^{31,32} or slow³³ exchange kinetics. However, these systems were based on 1:1 binding. The UPy – Napy complex formation under study here is a 1:2 binding system which is governed by equilibria 5.1-3. Since equilibrium 5.2 can directly be studied by ^1H NMR spectroscopy, the K_a value can be determined from K_d by single-point ^1H NMR measurements. K_a is related to K_d according to equation 5.4:

$$K_a = (K_{\text{dim}} \times K_d)^{1/2} \quad (\text{eq. 5.4})$$

Using equations 5.5-7, the absolute concentrations of UPy_2 , UPy – Napy, UPy and Napy can be calculated:

$$[U_2]_0 = [U_2] + 2 [NU] \quad (\text{eq. 5.5})$$

$$[N]_0 = [N] + [NU] \quad (\text{eq. 5.6})$$

$$[U_2] = [U_2]_0 \times I(U_2) / (I(U_2) + I(NU)) \quad (\text{eq. 5.7})$$

where $[U_2]_0$ and $[N]_0$ are the initial concentrations of UPy and Napy; $[U_2]$, $[N]$ and $[NU]$ are the concentrations of UPy₂, Napy and UPy – Napy, respectively, and $I(U_2)$ and $I(NU)$ are the integrals of UPy homodimer and UPy – Napy heterodimer as determined by ¹H NMR. Substitution of equations 5.5-7 in equation 5.2 and subsequent use of equation 5.4, affords a K_a value for each data point. It is evident from the spectra in Figure 5.1 that well-resolved, baseline separated signals are observed corresponding to the UPy in the homodimer and the heterodimer. The downfield shift is 0.17, 0.16 and 0.06 ppm for the signals attributed to the alkylidene, ureido-methylene and pyrimidinone-methyl, respectively. By evaluation of 8 data points corresponding to UPy **4a** – Napy **1c** (Figure 5.1, R' = undecyl) ratios between 10 and 0.5 with a fixed Napy concentration of 5.0 mM, the K_a value can be estimated to be between 10^6 and 10^7 M⁻¹. However, since the statistical error is smaller when the integrals are equal in intensity, a more accurate estimate of K_a in CDCl₃ is 5×10^6 M⁻¹. A similar procedure in toluene-*d*₈ using 2-hexylureido-6-(3-heptyl)-4[1H]-pyrimidinone **4b** and Napy **1b**, affords an estimate of K_a of 1×10^7 M⁻¹. The corresponding Gibbs free energy of association in chloroform is determined to be -38.2 kJ·mol⁻¹ NU.

Selectivity in dilute CDCl₃ solutions

The position of equilibrium 5.2 and hence the selectivity of heterocomplexation are expected to be concentration dependent due to mass-action. This was confirmed previously by ¹H NMR spectroscopy which indicated the presence of UPy homodimers in a 1:1 mixture of **4a** – **1a** at 10 mM. The selectivity of heterocomplexation was measured with ¹H NMR of CDCl₃ solutions of a 1:1 mixture of UPy **4a** and Napy **1c**. Since the dimers are in slow exchange on the NMR time scale, separate signals are observed for the UPy homodimer and the UPy-Napy heterodimer. At concentrations as low as 2×10^{-5} M the resonances corresponding to the alkylidene, ureido-methylene protons in 1:1 mixtures of **4a** and **1c** could be integrated (Figure 5.4a).³⁴ The ratios of these integrals were calculated and averaged over a concentration range from 5×10^{-2} M to 2×10^{-5} M. As indicated in Figure 5.4b, dilution resulted in decreased selectivity from 93% to 56% heterocomplexation.

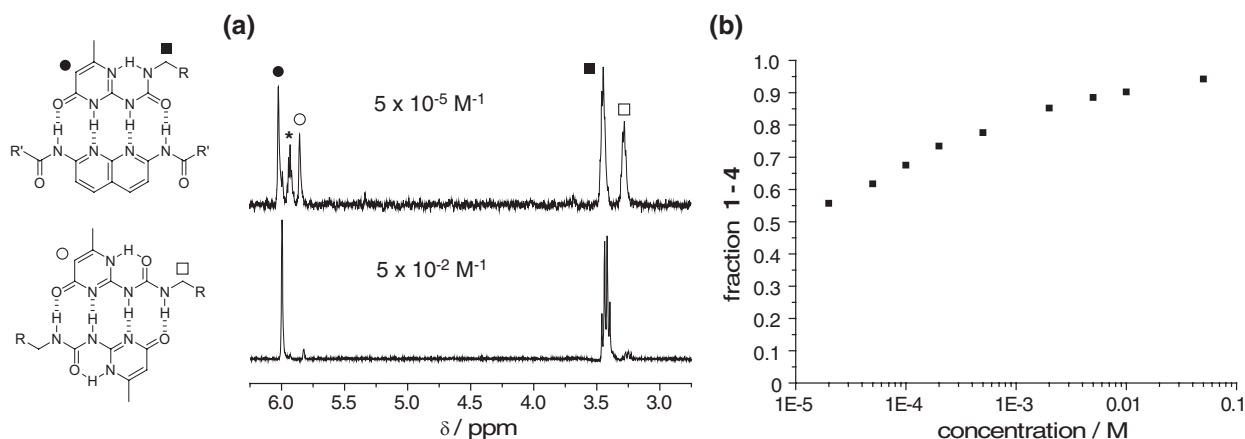
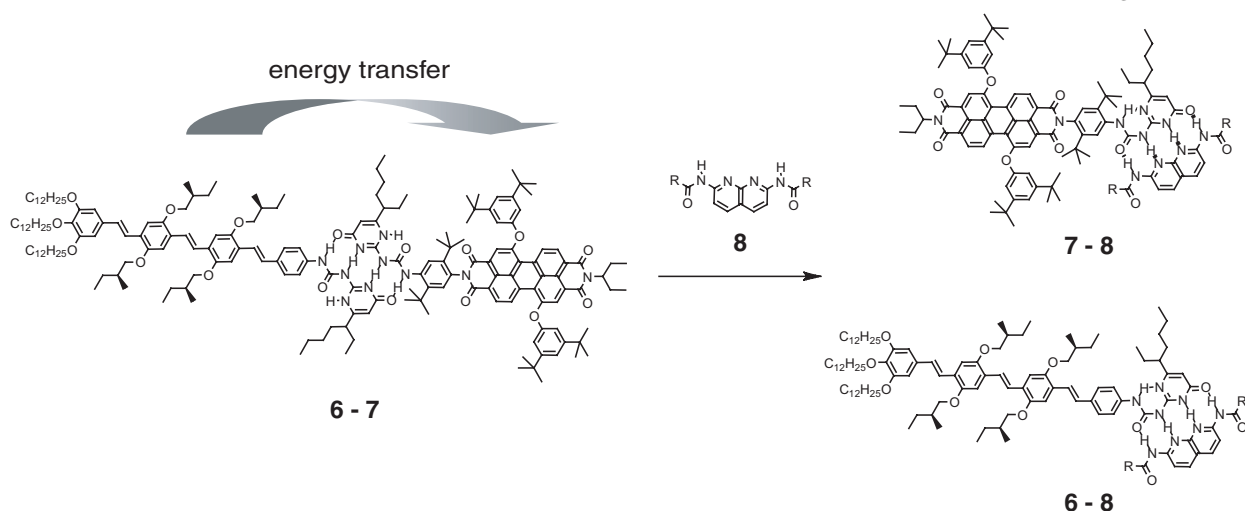


Figure 5.4 (a) Partial ^1H NMR spectra of 1:1 mixtures **4a** – **1a** at 5×10^{-2} M and 5×10^{-5} M; * indicates a solvent impurity; (b) concentration dependent selectivity of **4a** – **1a** heterocomplexation in 1:1 mixtures.

5.2.3 Fluorescence measurements

In order to evaluate the selectivity in heterodimerization below concentrations of 10^{-5} M, fluorescence spectroscopy was performed using UPy derivatives **6** and **7**. It has been reported previously that heterodimerization via quadruple hydrogen bonds between tetra(phenylene-vinylene) derivative **6** (UPy-OPV-4) and perylenebisimide derivative **7** (UPy-PERY) allows efficient energy transfer from the donor OPV to the acceptor perylenebisimide, while between two dyes without UPy, no energy transfer can be observed.³⁵ However, upon addition of Napy **8** (R = 9-undecenyl), partial quenching of the energy transfer occurs due to disruption of donor-acceptor aggregate **6** – **7** (Scheme 5.3). Therefore, selectivity of heterodimerization can be evaluated in terms of the decrease of the fluorescence of **7** as a function of added **8** (Figure 5.5).



Scheme 5.3 Quenching of energy transfer of aggregate **6** – **7** by addition of **8**.

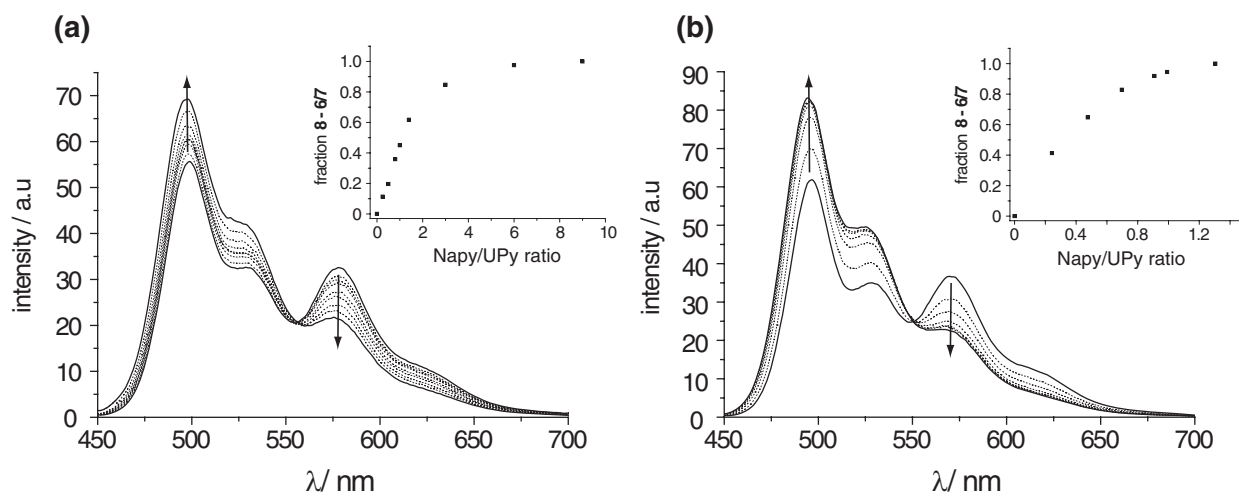


Figure 5.5 (a) Fluorescence spectra of a 1:1 mixture of **6** – **7** in chloroform 4×10^{-6} M upon addition of $10 \times$ **8**, $\lambda_{ex} = 440$ nm; inset shows fraction in heterodimer as a function of Napy / UPy ratio; (b) fluorescence spectra of a 1:1 mixture of **6** – **7** in toluene 2×10^{-6} M upon of $1.5 \times$ **8**, $\lambda_{ex} = 440$ nm; inset shows fraction in heterodimer as a function of Napy / UPy ratio.

As shown in Figure 5.5, a steady decrease in perylene emission at 570 nm and hence energy transfer is observed in chloroform as well as in toluene upon addition of **8** to a 1:1 mixture of **6** and **7**. The presence of an isobestic point in both solvents indicates that the disruption process is molecular in nature and no aggregates due to π - π stacking are formed. A tremendous difference in selectivity in these solvents is observed when the fraction UPy – Napy heterodimer is plotted as a function of the Napy (see insets). In chloroform at 4×10^{-6} M UPy, 45% selectivity is observed for a 1:1 ratio Napy/UPy, while at 2×10^{-6} M in toluene the selectivity is almost 95%. This is in qualitative agreement with the difference in association constants determined by ^1H NMR described in the previous section. As expected, performing a second titration at a decreased UPy concentration of 1×10^{-6} M in chloroform showed a decrease in selectivity to 29%.

5.2.4 Theoretical model of concentration dependent UPy-Napy association

To assess the validity of the single-point method and to fit the results on selectivity obtained in the previous section, selectivities of UPy-Napy heterocomplexation in 1:1 mixtures of UPy and Napy in chloroform were calculated as a function of concentration. The calculation of selectivities requires an explicit expression for the concentration of free UPy (U), UPy homodimer (U₂), and UPy - Napy heterodimer (NU) in terms of the analytical concentrations N₀, U₀, and the binding constants K_{dim} and K_a . The following expressions were all derived using Maple 9, © Maplesoft inc. 2003. The value of K_{dim} was kept at the reported value of 6×10^7

M^{-1} , while the value of the association constant for heterocomplexation was varied to reproduce the experimental data in Figure 5.4b to which two data points were added that were obtained by fluorescence titrations.

The total analytical concentrations of N0 and U0 of Napy and UPy, respectively are described by the mass balance equations 5.8 and 5.9 (similar to equations 5.5 and 5.6):

$$N0 = N + NU \quad (\text{eq. 5.8})$$

$$U0 = U + 2 \times U2 + NU \quad (\text{eq. 5.9})$$

The dimerization and association constant are defined in equations 5.1 and 5.3, respectively leading to equations 5.10, 5.11 and 5.12 which give explicit expressions for N, NU, and U2, respectively:

$$N = N0 - NU \quad (\text{eq. 5.10})$$

$$NU = U0 - U - 2 \times U2 \quad (\text{eq. 5.11})$$

$$U2 = K_{\text{dim}} \times U^2 \quad (\text{eq. 5.12})$$

For the experiments in Figure 5.4(b), the analytical concentrations of N and U are equal:

$$N0 = U0 \quad (\text{eq. 5.13})$$

Successive substitution of equations 5.10 to 5.13 in equation 5.3 gives an expression for K_a in terms of U and the known values of U0 and K_{dim}

$$K_a = \frac{U0 - U - 2 \times K_{\text{dim}} \times U^2}{(U + 2 \times K_{\text{dim}} \times U^2) \times U} \quad (\text{eq. 5.14})$$

Finally, solving the third order polynomial of equation 5.14 results in a lengthy, but nevertheless unambiguous expression for U in terms of K_a , K_{dim} and U0. U2 can now be calculated from U using equation 5.12. Subsequently, NU can be calculated using mass balance equation 5.8.

Using these equations, simulated curves were generated for different values of K_a and a constant value for the UPy dimerization constant of $6 \times 10^7 \text{ M}^{-1}$ (Figure 5.6). The value of the association constant for heterocomplexation that best reproduces the experimental data is $K_a =$

$5 \times 10^6 \text{ M}^{-1}$ (Figure 5.6a). As can be seen from the figure, heterodimer selectivity decreases upon dilution due to mass-action law. Noteworthy is the fact that a maximum was calculated for the fraction UPy in its homodimer around $3 \mu\text{M}$. At such low concentrations equilibria 5.1-3 are in competition and monomeric UPy is being formed in significant amounts.

Error analysis is based on the fact that with K_a values of $3 \times 10^6 \text{ M}^{-1}$ and $7 \times 10^6 \text{ M}^{-1}$, all data points lie above and below the simulated line ($K_a = 5 \times 10^6 \text{ M}^{-1}$), respectively (Figure 5.6b). A very conservative estimate of the error would therefore give a binding constant of $5 (\pm 2) \times 10^6 \text{ M}^{-1}$. Because this is in good agreement with the single-point data obtained from ^1H NMR experiments, the single-point method is believed to be an accurate method to determine the association constants for UPy – Napy heterocomplexes.

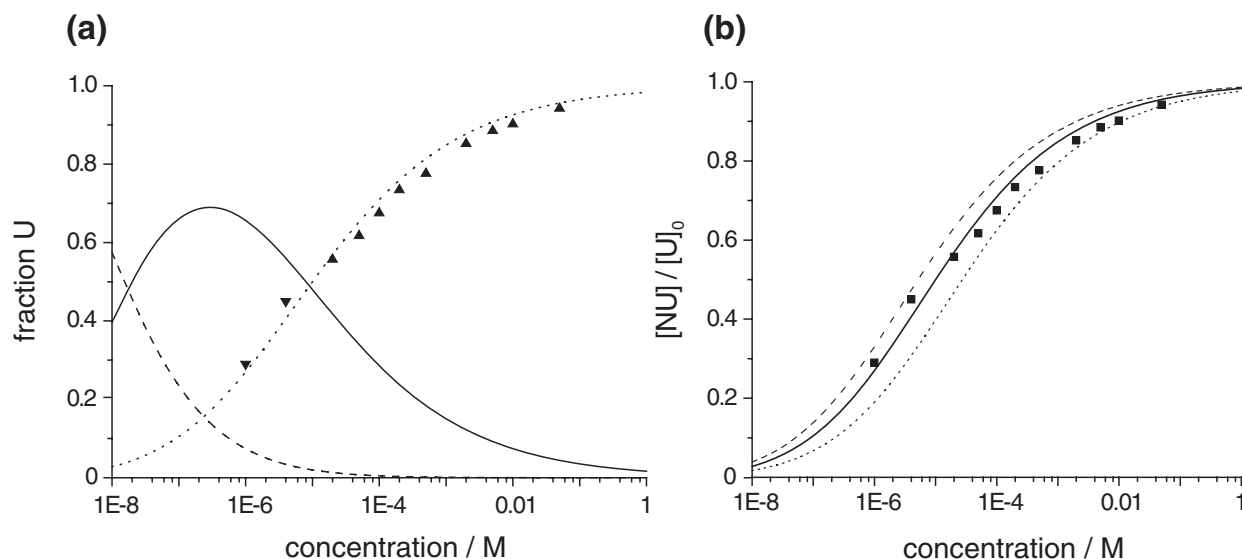


Figure 5.6 (a) Measured fractions of UPy present in UPy-Napy heterodimer determined by NMR (▲) and fluorescence (▼); Calculated fractions of UPy in UPy – Napy (dotted), UPy – UPy (straight), and free UPy (dashed) as a function of concentration (M) in a 1:1 mixture of UPy and Napy; $K_{dim} = 6 \times 10^7 \text{ M}^{-1}$, $K_a = 5 \times 10^6 \text{ M}^{-1}$; (b) experimental (■) and simulated heterocomplexation selectivities as a function of concentration (M) in 1:1 mixtures of UPy and Napy; $K_a = 7 \times 10^6 \text{ M}^{-1}$ (dashed), $K_a = 5 \times 10^6 \text{ M}^{-1}$ (straight), $K_a = 3 \times 10^6 \text{ M}^{-1}$ (dotted).

5.2.5 UV/Vis measurements

In order to evaluate the complexation at low concentrations, UV/Vis is an often employed spectrophotometric method. The UPy unit displays an absorption maximum at 260 nm indicative of the 4[1H]-pyrimidinone tautomer and has no significant absorption above 300 nm.^{36,37} In contrast, the Napy unit gives rise to absorption spectra with vibrational fine structure between 300 and 350 nm with a maximum at $\lambda = 346 \text{ nm}$. Upon addition of Napy **1b** to UPy **4b**,

a new absorption at $\lambda = 355$ nm is observed in chloroform as well as in toluene ($\lambda = 357$ nm) (Figure 5.7). In addition a shoulder arises at 285 nm which can be attributed to the 6[1H]-pyrimidinone tautomer of the UPy. A similar observation has been reported for the interaction of the 6[1H] tautomer of isocytosine with creatinine (AAD type array).³⁸ The presence of four isobestic points in Figure 5.7 indicate that no aggregates are formed and the monitored processes are molecular in nature. The bathochromic shift of the Napy chromophore indicates a significant change in its electronic fine structure upon formation of the quadruple hydrogen bonded complex with a UPy molecule. The shift is presumably caused by strong electron donation to the naphthyridine core due to hydrogen bonding which raises the HOMO level and hence reduces the band gap of the chromophore. Apparently, the electron-deficient core is not affected much by hydrogen bond formation of the two amide substituents.

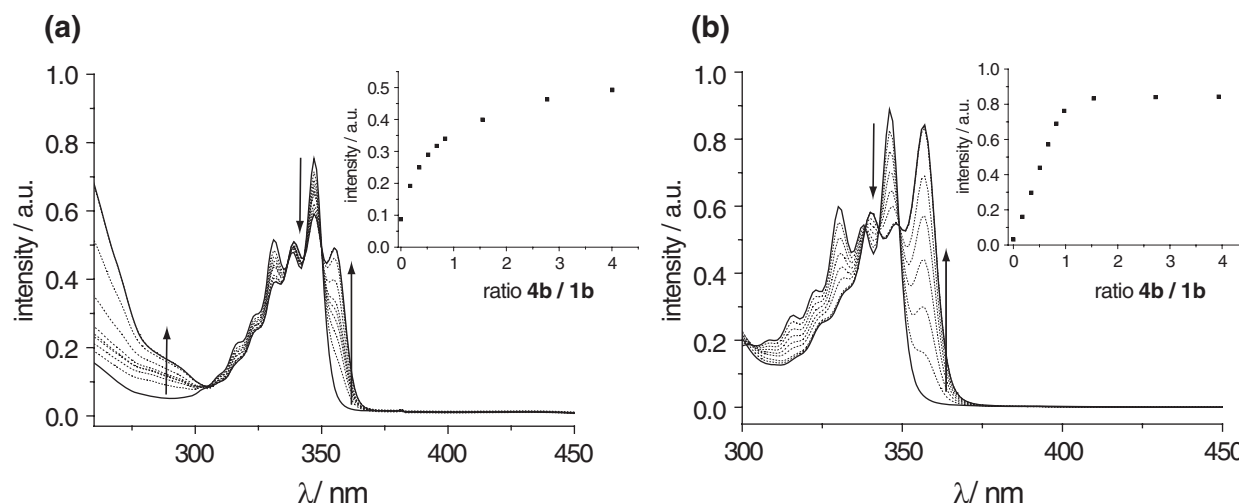


Figure 5.7 (a) UV-visible spectra of 2.5×10^{-5} M **1b** upon addition of **4b** in chloroform, inset shows change in absorbance at $\lambda = 355$ nm as function of the ratio **4b/1b**; (b) UV-visible spectra of 2.5×10^{-5} M **1b** upon addition of **4b** in toluene, inset shows change in absorbance at $\lambda = 357$ nm as function of the ratio **4b/1b**.

The UV/Vis data was fitted to a model derived from the binding model described in the previous section. In this method model K_a and the extinction coefficient of the UPy – Napy heterodimer at the new absorption maximum (ϵ_{NU}) are calculated from a dataset containing K_{dim} (5.7×10^7 M⁻¹ in chloroform and 5.9×10^8 M⁻¹ in toluene), the intensity as a function of UPy and Napy concentration as well as the extinction coefficient of the Napy at the absorption maximum (determined to be 3500 and 1200 L·mol⁻¹·cm⁻¹ in chloroform and toluene, respectively). The data obtained is depicted in Table 5.1. The data obtained for chloroform match nicely with the single-point data obtained from ¹H NMR experiments. The calculated value of ϵ_{NU} is lower than ϵ_N determined for $\lambda = 346$ nm (39.8×10^3) causing a less intense signal at 355 nm than the signal at 346 nm at complete heterodimerization. The calculated K_a values in

toluene are high compared to the results obtained with ^1H NMR. This is explained by an increasingly difficult fit around the equivalence point. A measurement at lower concentration (2.5×10^{-6} M) reduced the K_a value to $7.0 (\pm 3.5) \times 10^7 \text{ M}^{-1}$. A conservative estimate of the K_a value in toluene is therefore $> 10^7 \text{ M}^{-1}$ but given the difficulty in obtaining reproducible data at such high dilution, it could be an order of magnitude higher.

Table 5.1 Association constants and extinction coefficients UPy – Napy in chloroform and toluene determined by UV/Vis titration.

parameter	chloroform	toluene
K_a (M)	$2.13 (\pm 0.48) \times 10^6$	$2.48 (\pm 0.98) \times 10^8$
ϵ ($\text{L}\cdot\text{mol}^{-1}\cdot\text{cm}^{-1}$)	$28.9 (\pm 2.32) \times 10^3$	$33.1 (\pm 0.40) \times 10^3$

5.3 Evaluation of substituent effects on binding strengths

5.3.1 Association of substituted 2,7-diamino-1,8-naphthyridines

One of the driving forces of strong binding between 2,7-diamido-1,8-naphthyridines and 2-ureido-6[1H]-pyrimidinones is the strong electron-withdrawing nature of the amide carbonyl group. The amido protons are, therefore, expected to be considerably more acidic than normal amides and hence better hydrogen bond donors. As shown in Chapter 3, these amide bonds are indeed quite prone to acidic and alkaline hydrolysis due to the electron-poor character of the naphthyridine core which enhances the electrophilicity of the carbon in the amide carbonyl group.³⁹ The stability under hydrolytic conditions can be increased by substitution of the carbonyl group with phenyl rings as demonstrated in Chapter 4. However, substitution with phenyl or alkyl groups is anticipated to decrease the association constant with UPy derivatives due to a lower acidity of the amine NH. In order to investigate this hypothesis, the association constants of compounds **9** – **13** with UPy **4a** were determined using the single-point method described in section 5.2.2. The values of K_a depicted in Figure 5.8 are average values obtained from three data points.

Relative to **1c**, all other Napy derivatives show decreased binding with UPy **4a**. However, whereas arylamino substituents still provide sufficient acidity to the NH protons to give significant complexation ($K_a = 2.3 \times 10^6$ and $1.1 \times 10^6 \text{ M}^{-1}$ for **9** and **10**, respectively), the significant decrease in acidity of NH protons of alkylamino substituents results in a dramatic decrease in association ($K_a = 8.2 \times 10^4$ and $2.0 \times 10^4 \text{ M}^{-1}$ for **12** and **13**, respectively).

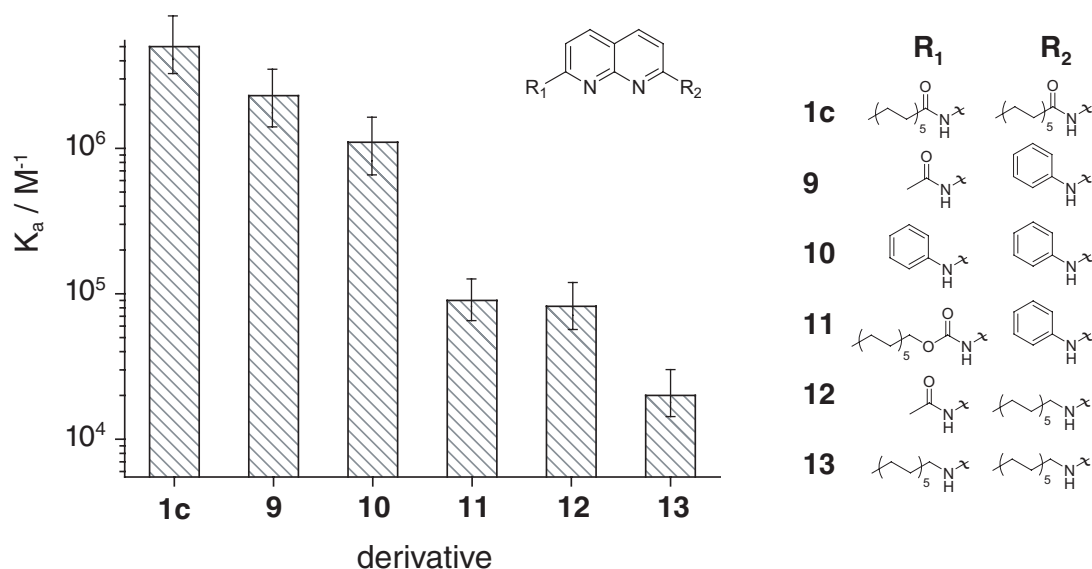


Figure 5.8 Graphic representation of association constants with systematic errors of UPy **4a** with Napy derivatives **1c**, **9** - **13** in CDCl_3 at 298 K (K_a for **4a** - **1c** is included for comparison).

Compound **11** shows low affinity for binding UPy **4a** ($K_a = 9.0 \times 10^4 \text{ M}^{-1}$), although a similar derivative to carbamate Napy **11** was reported to bind to a guanosine featuring an ADD array.⁴⁰ An explanation for such weak binding despite the electron-withdrawing character of the carbamate might involve two causes: i) steric repulsion between the oxygen atom of the carbamate and the UPy carbonyl oxygen binding to the NH of the carbamate and ii) steric repulsion between the oxygen atoms of the carbamate causing the NH proton to move to the naphthyridine core which results in a decreased perfect fit of the UPy featuring the ADDA array. In summary, 1,8-naphthyridines substituted on the 2 and/or 7 position with arylamino groups are able to form a heterodimer with a UPy derivative with $K_a > 10^6 \text{ M}^{-1}$ while a significant decrease in binding is observed for alkylamino or carbamate substituents.

5.3.2 Influence of bulky substituents

In order to gain insight into the influence of bulky substituents on the ability of 2,7-amido-1,8-naphthyridine derivatives to bind UPy derivatives, the K_a values of Napy derivatives **14** - **22** with UPy **4a** were determined in a single ^1H NMR experiment. A graphic representation of K_a values is presented in Figure 5.9.

A clear trend is observed when more sterically demanding side chains are introduced. Introduction of a methyl or ethyl group on the α -position next to the carbonyl group decreases the association constant to 1.8×10^6 and $6.9 \times 10^5 \text{ M}^{-1}$ for **14** and **15**, respectively. A much larger

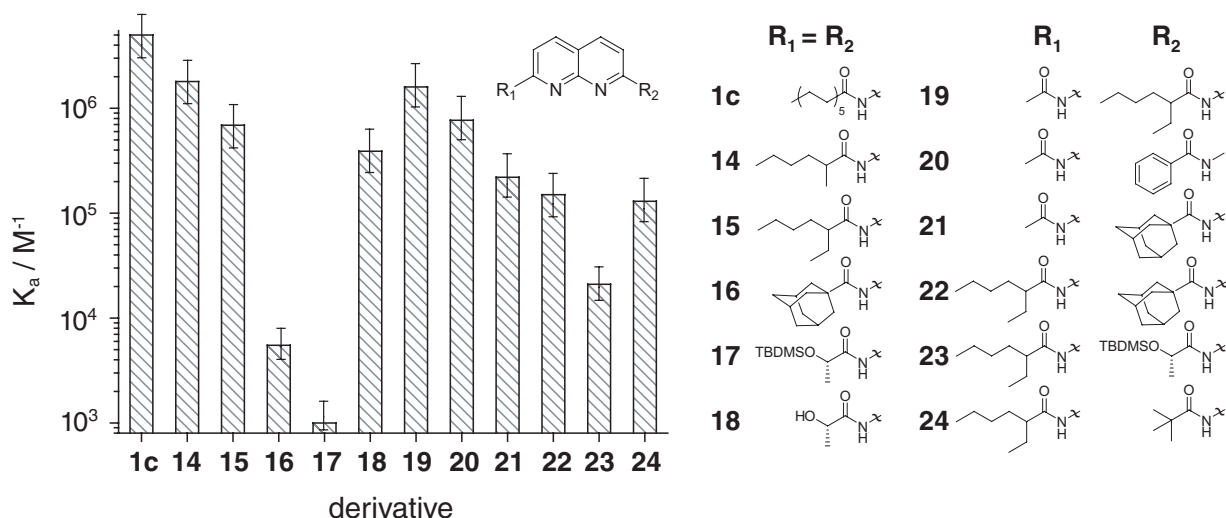


Figure 5.9 Graphic representation of association constants with systematic errors of UPy **4a** with Napy derivatives **14** - **24** in $CDCl_3$ at 298 K (K_a for **4a** – **1c** is included for comparison).

substituent such as adamantyl decreases K_a value with 2 orders of magnitude (K_a (**4a** – **16**) = $5500 M^{-1}$). However, binding is not fully determined by steric influences. The bulky TBDMS group is located farther from the naphthyridine core in compound **17**. However, the association constant is less than $10^3 M^{-1}$. A possible rationale for this observation would be a combination of increased repulsion between the oxygen atoms in the *S*-lactate fragment and a steric effect of the TBDMS group. In this way, the methyl group on the α -position next to the carbonyl is pushed towards the NH protons causing increased steric hindrance. Deprotection of the TBDMS groups with triethylamine tri-hydrofluoride gave the dihydroxy derivative **18** in excellent yield (95%). Although the K_a value of this compound with UPy **4a** ($K_a = 3.9 \times 10^5 M^{-1}$) was considerably higher than for **17**, this value is lower than derivative **14** due to repulsion between the two oxygen atoms in the lactate fragment. A similar trend as described for symmetric compounds **14** – **18** is observed for non-symmetric derivatives **19** – **24**. A stepwise increase in size of the substituent in derivatives **19** – **21** shows a steady decrease in association constant with UPy **4a** ($K_a = 1.6 \times 10^6$, 7.7×10^5 and $2.2 \times 10^5 M^{-1}$ for **19**, **20** and **21**, respectively). The decrease is continued when an acetamido group is replaced by a 2-ethylhexanoylamino group for derivatives **22** – **24**. Noteworthy is the fact that a *t*-butyl group has a similar influence on K_a value as the adamantyl group ($K_a = 1.5 \times 10^5$ and $1.3 \times 10^5 M^{-1}$ for **22** and **24**, respectively). Analogous to compound **17**, a decrease of two orders of magnitude in K_a was determined for derivative **23** which contains only one TBDMS-protected lactate amide ($K_a = 2.1 \times 10^4 M^{-1}$).

5.3.3 Electronic effects on binding strength

Although correlations between substitution and reactivity have been accepted in the context of the covalent bond for decades,⁴¹⁻⁴⁴ reports on this phenomenon in supramolecular systems are not that abundant^{33,45-47} and almost non-existent in the case of multiple hydrogen bonds. In this section, the influence of electronic substituents on the binding strength of the UPy – Napy heterodimer is investigated by means of changing the electronic or steric character of one or more substituents on one phenyl ring in 2-amido-7-arylmino-1,8-naphthyridines **25** – **36** and 2,7-di(arylmino)-1,8-naphthyridine derivatives **37** – **48**. The K_a values of the heterodimers using UPy **4a** were determined by the single-point ^1H NMR method as described in previous sections. The results are presented in Figure 5.10.

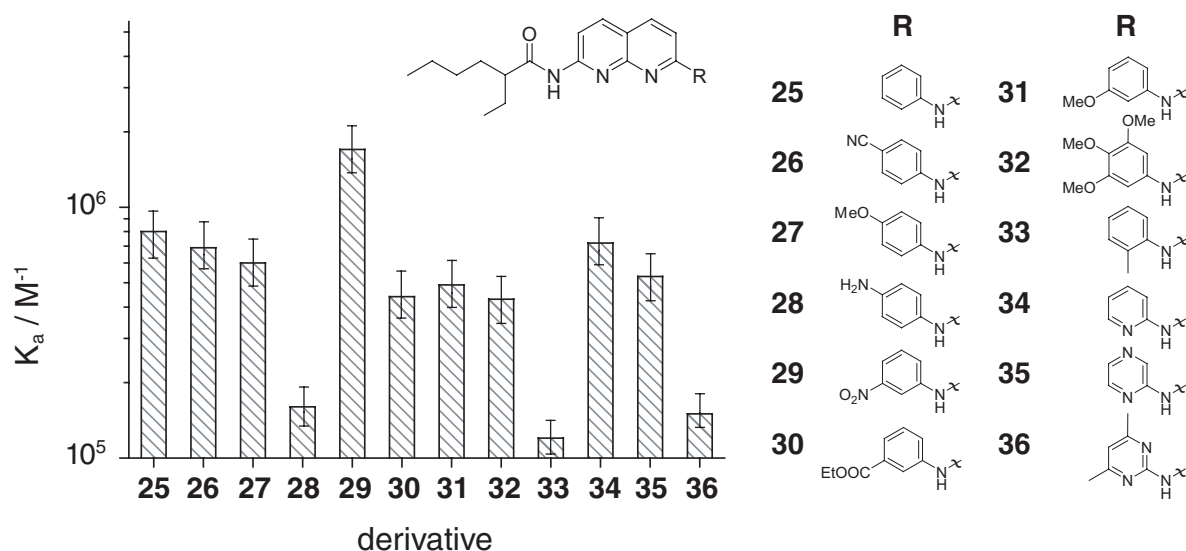


Figure 5.10 Graphic representations of association constants with systematic errors of UPy **4a** with Napy derivatives **25** – **36** in CDCl_3 at 298 K.

Due to steric hindrance of the branched alkyl chain on the amide, an association constant of $8.0 \times 10^5 \text{ M}^{-1}$ is determined for derivative **25**. This value is similar to the K_a value determined for 2,7-bis-(2-ethylhexanoylamino)-1,8-naphthyridine **15**. An increase in acidity of the amino NH proton and hence an increase in K_a value is expected upon introduction of electron-withdrawing substituents on the phenyl ring in **25**. The opposite is expected for electron-donating groups. While a small decrease is observed for derivatives **27** and **28** ($K_a = 6.0 \times 10^5$ and $1.5 \times 10^5 \text{ M}^{-1}$, respectively) with a methoxy or an amine on the *para*-position of the phenyl ring, an unexpected decrease in binding ($K_a = 6.9 \times 10^5 \text{ M}^{-1}$) is observed for **26** containing an electron-withdrawing nitrile substituent on the *para*-position. While the electronic influence of a *meta*-nitro group in derivative **29** on the acidity of the NH proton is not expected to be

significant, strong binding was observed ($K_a = 1.7 \times 10^6 \text{ M}^{-1}$). In contrast, weaker association was observed for compounds **30** to **32** ($K_a = 4.4 \times 10^5$, 4.9×10^5 , $4.3 \times 10^5 \text{ M}^{-1}$, respectively), which all have an overall electron-withdrawing inductive effect. A dramatic decrease in K_a value ($K_a = 1.5 \times 10^5 \text{ M}^{-1}$) was determined for compound **33** containing a methyl group on the *ortho*-position. Although the methyl has a small electron-donating effect, the large decrease in binding is attributed to steric hindrance. Finally, K_a values for binding of UPy **1** with compounds **34** to **36**, showed a steady decrease ($K_a = 7.2 \times 10^5$, 5.3×10^5 and $1.5 \times 10^5 \text{ M}^{-1}$ for **34**, **35** and **36**, respectively). Although the electron-withdrawing character increases upon going from **34** to **36**, an electronic repulsion may arise between the nitrogen lone pairs in the arylamino substituents and one of both UPy carbonyl group. Apparently, inductive effects do not solely determine the strength of binding in these naphthyridines. Overall, it should be mentioned that most of the determined association constants are within one order of magnitude difference.

The association constants for 2,7-di(arylamino)-1,8-naphthyridine derivatives **37** – **48** with UPy **4a** are displayed in Figure 5.11. The K_a value of $1.1 (\pm 0.3) \times 10^6 \text{ M}^{-1}$ in CDCl_3 for 2,7-di(phenylamino)-1,8-naphthyridine **37** with a UPy was not only determined by the single-point method but also by dilution experiments and the fitting procedure described in section 5.2. Surprisingly weak binding was found for compounds **38** to **40** (2.4×10^4 , 1.3×10^5 and $4.4 \times 10^4 \text{ M}^{-1}$, respectively) all of which feature strong electron-attracting substituents on the *para*-position. Similar values for K_a were subsequently determined for derivatives **41** to **43** (8.5×10^5 , 7.3×10^5 and $7.4 \times 10^5 \text{ M}^{-1}$, respectively) which contain electronically different substituents. In contrast, *meta*-substituted derivative **44** displays a slight increase in association constant ($1.9 \times 10^6 \text{ M}^{-1}$) compared to its di(phenylamino) analogue **37** even though its inductive effect is small and there is no resonance effect on the NH proton. Whereas, a relatively weak association is observed for **45** ($K_a = 3.4 \times 10^5 \text{ M}^{-1}$), no dramatic decrease in K_a value is determined for compounds **46** and **47** (7.0×10^5 and $9.8 \times 10^5 \text{ M}^{-1}$). The former could be explained by repulsive interactions as described for compounds **34** to **36**. The latter effect could be due to a larger deviation from coplanarity of the phenyl rings for these 2,7-di(arylamino)-1,8-naphthyridines as compared to 2-amido-7-arylamino-1,8-naphthyridines. Finally, a similar K_a value was found for dimethoxy substituted derivative **48** ($K_a = 1.9 \times 10^6 \text{ M}^{-1}$) as for its monomethoxy analogue **44**. Except for derivatives **38** to **40**, most of the determined association constants are within one order of magnitude difference which illustrates that electronic substituent effects are small.

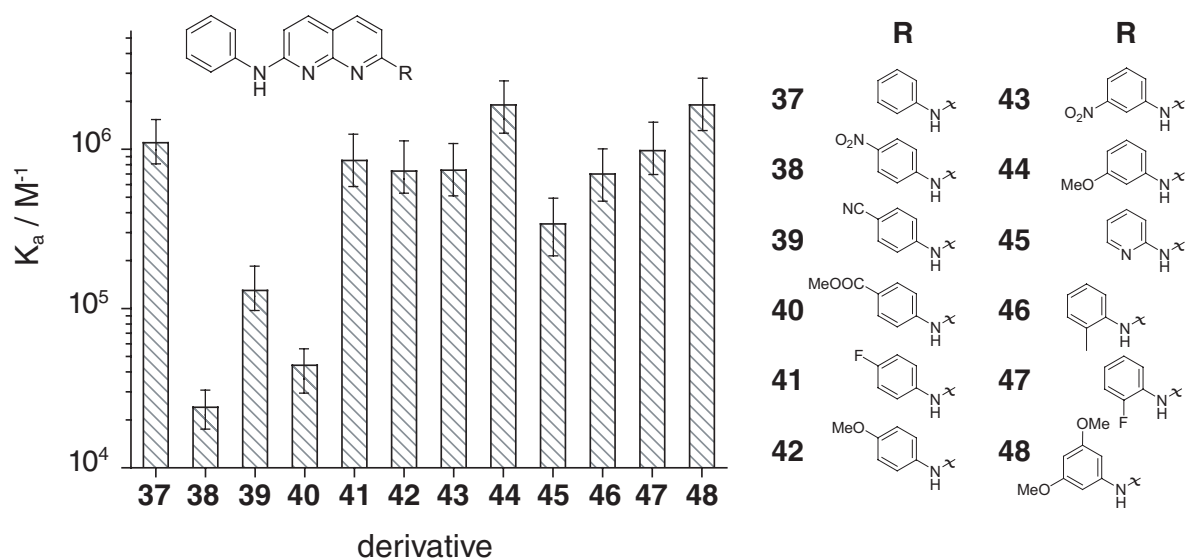
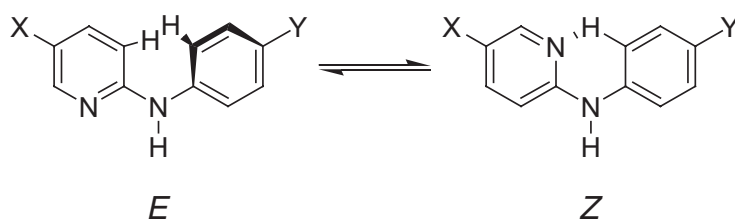


Figure 5.11 Graphic representation of association constants with systematic errors of UPy 1 with Napy derivatives 37 - 48 in $CDCl_3$ at 298 K.

A possible rationale for the unexpected weak binding of derivatives 38 to 40 can be found in the fact that conformations of 2-(arylamino)pyridines have been described in terms of *E-Z* isomerism in solution as well as in the solid.⁴⁸⁻⁵² In the *Z*-isomer the phenyl and pyridine rings are coplanar and are connected by a weak intramolecular hydrogen bond. The C(3)-H on the β -position of the phenyl ring is a hydrogen bond donor while the pyridine nitrogen behaves as an acceptor. In the *E*-form, the aromatic rings are not coplanar owing to repulsion between the β -positions of the aromatic rings (Scheme 5.4).



Scheme 5.4 *E-Z* isomerism in 2-(4-*Y*-anilino)-5-*X*-pyridines.

Takasuka *et al.* performed a systematic study on the influence of *para*-substituents on this conformational equilibrium. By infrared spectroscopy and X-ray diffraction on 2-(4-*Y*-anilino)-5-nitropyridines ($X = NO_2$) it was determined that for electron-withdrawing substituents the conformational equilibrium shifts to the *Z*-isomer. The *E*-isomer was primarily observed when electronically neutral or donating groups were applied. This phenomenon was evaluated by molecular modelling^{50,53} and explained by the presence of increased conjugation between the phenyl and amino groups for electron-withdrawing substituents on the phenyl ring therefore favouring the *Z*- over the *E*-isomer. It is reasonable to assume electronic

similarity between 5-nitropyridine and 1,8-naphthyridine. Therefore, a similar explanation can be given for the decreased binding of Napy derivatives **34** – **36**. Although the energy difference between the *E*- and *Z*-isomer for these naphthyridines is assumed to be several kJ/mol,⁵⁴ this is supposed to be sufficient to severely hamper the ability of the Napy to disrupt UPy homodimers.

5.4 The lifetime of the 2-ureido-6-[1*H*]-pyrimidinone – 2,7-diamido-1,8-naphthyridine dimer

5.4.1 Introduction

A convenient method for measuring lifetimes of associated complexes is dynamic NMR (DNMR).^{55,56} The methods involved in studying chemical exchange between different states are well-established and described in numerous books and reviews.^{57,58} In general, the parameter determined by DNMR techniques is an exchange rate between two or multiple states. For supramolecular complexes this rate is related to the dissociation and association rate constants. As a consequence, the lifetime of the observed species can be determined. Exchange NMR is the technique most commonly used to investigate supramolecular complexes in case of low to intermediate exchange rates.⁵⁹ The two-dimensional variant of this technique is the 2D-EXSY experiment,⁶⁰ which is based on the 2D-NOESY experiment.²⁸ Although in a simple two-site exchanging system coalescence analysis is usually sufficient to determine the rate constants of exchange, this is limited to fast exchanging systems. However, in case of intermediate to low exchange rates, coalescence is often not easily observed and 2D-EXSY has proven to be more successful. In principle, rate constants in the frequency domain of 1 – 10 s⁻¹ can be extracted from EXSY spectra at a single mixing time (τ_m). In a simple two-site exchange system with sites A and B of equal longitudinal relaxation times ($T_{1,A} = T_{1,B}$), the peak volumes determined in the EXSY experiment (I_{AA} and I_{BB} for diagonal peaks; I_{AB} and I_{BA} for cross-peaks) are converted into the exchange rate constant (defined as $k_{ex} = k_{AB} + k_{BA}$) via the relation in equation 5.16:

$$k_{ex} = \tau_m^{-1} \phi \quad \text{in which } \phi = \ln\left(\frac{r+1}{r-1}\right) \quad (\text{eq. 5.16})$$

as a function of mixing time, where r is the ratio between the diagonal and the cross-peaks:

$$r = 4X_A X_B \left(\frac{I_{AA} + I_{BB}}{I_{AB} + I_{BA}} \right) - (X_A - X_B)^2 \quad (\text{eq. 5.17})$$

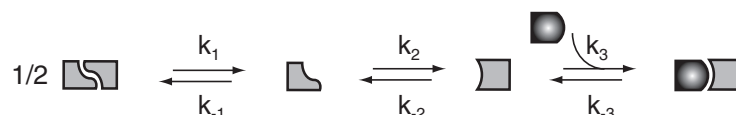
where X_A and X_B are the mole fractions of populations A and B, respectively. The logarithmic term in 5.16 is often referred to as the transfer function ϕ . The exchange rate constant can therefore easily be determined as the slope in a plot of ϕ as a function of τ_m .

5.4.2 2D-EXSY measurements

As shown in section 5.2.2, UPy - UPy and UPy - Napy are in slow exchange on the NMR time scale which meets the prerequisite for the use of dynamic NMR that the exchanging species are magnetically non-equivalent so that the reactant and product of the exchange reaction can be observed and integrated separately in the NMR spectrum. The observed interconversion of UPy homodimers and UPy - Napy heterodimer is simplified to be a two-site exchange. The observed exchange is given in equilibrium 5.4:



where U and U^* correspond to the 4[1H] and 6[1H] tautomeric forms, respectively. It has to be noted that at the measured concentrations, it is assumed that U is only present in its homodimeric form and U^* only in the UPy - Napy heterodimer. Furthermore, the exchange in the system is not necessarily a first order process and intermediates may be formed. Although several pathways for exchange may be postulated, based on previous observations a dissociative mechanism is proposed here of the homodimer to monomers followed by recombination of U^* with N. A schematic representation of this pathway is given in scheme 5.5.



Scheme 5.5 Schematic representation of the proposed pathways for exchange between U and U^* .

In order to confirm the proposed mechanism, a number of EXSY measurements were performed on 2:1 mixtures of UPy **4b** and Napy **1b** in deuterated chloroform and toluene. Assuming selective binding at 10 mM, a system is obtained in which U and U^* are of equal population.⁶¹ With equal populations, the overall exchange rate constant ($k_{ex} = k_{AB} + k_{BA}$) is equal to $2 \times k_{AB}$. Although no EXSY cross peaks were observed in chloroform and toluene solution at ambient temperature with $\tau_m < 2$ s,⁶² the exchange process can be accelerated upon increasing temperature. Indeed, exchange was observed between U and U^* in toluene solutions between 70 and 100 °C, while no exchange was observed in chloroform up to 60 °C (Figure 5.12a).

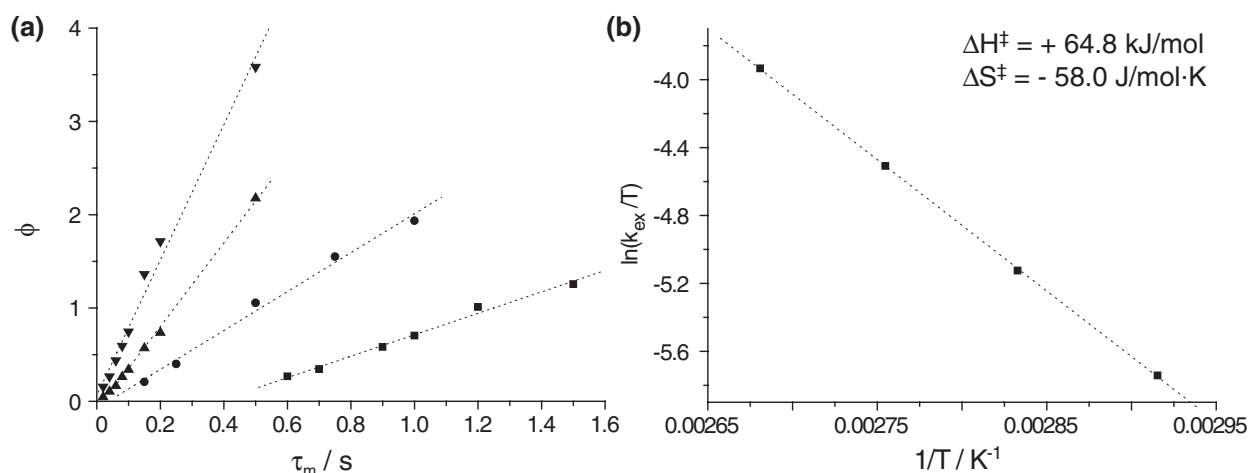


Figure 5.12 (a) Transfer function (ϕ) as a function of mixing time (τ_m) for 70 °C (■), 80 °C (●), 90 °C (▲), 100 °C (▼) at $[U_2]_0 = 10$ mM and $[N]_0 = 10$ mM in toluene- d_8 ; (b) Eyring plot with corresponding activation parameters derived from the fit. The data were fitted according to a linear relation ($r^2 = 0.999$).

The fact that ϕ is linear with mixing time τ_m for temperatures above 70 °C indicates the absence of a long-lived intermediate. Such an intermediate would cause the transfer function ϕ to approach a tangent of zero at low mixing times.⁵⁵ However, decreasing the temperature to 70 °C, causes a deviation of the linear fit. Therefore, the presence of at least one intermediate must be assumed. To study the strong temperature dependent exchange in more detail, an Eyring plot was made (Figure 5.12b). It has to be noted that even though linearity of ϕ versus τ_m is assumed in the determination of the rate constant at 70 °C, a very good fit is obtained from the Eyring plot ($r^2 = 0.999$). From the plot, the activation parameters were calculated:⁶³ $\Delta H^\ddagger = +64.8$ kJ/mol, $\Delta S^\ddagger = -58.0$ J/mol·K, ΔG^\ddagger (293 K) = +81.8 kJ/mol and E_a (293 K) = 67.2 kJ/mol. Both the activation energy (E_a) as well as the Gibbs' free energy of activation at 293 K are higher than the exchange between UPy homodimers ($E_a = 65$ kJ/mol and $\Delta G^\ddagger = 74.7$ kJ/mol in toluene- d_8). This observation may explain the slower exchange between U and U*. The positive value of ΔH^\ddagger can be rationalized when bonds are broken in the transition state. Although several explanations can be given for the observed loss in entropy, the combined data are not conclusive about the nature of the observed process.

The influence of base and acid on the exchange was subsequently studied in order to elucidate the nature of the rate determining step. It has been reported before that keto-enol tautomerization can be base and acid catalyzed.⁶⁴⁻⁶⁶ A well-known example of this rate acceleration is observed in base and acid catalyzed aldol reactions.⁶⁷ More specifically, it has been reported that the rate of prototropy⁶⁸ can be increased by the addition of catalytic amounts of base or acid.⁶⁹ The reference experiment was performed at 90 °C on a 3:2 mixture of **4b** – **1b**

in toluene- d_8 where $[N]_0 = 10$ mM and $[U_2]_0 = 7.5$ mM. In general, addition of a catalytic amount of base or acid resulted in a significant increase in exchange rate constants (Figure 5.13). Noteworthy is the difference in rate constants between the addition of 2,6-lutidine and 3,5-lutidine. Whereas both compounds have similar pK_b values, the use of 3,5-lutidine which lacks steric hindrance of the methyl substituents shows a more pronounced increase in k_{ex} . Although pyridine has a lower pK_b value, it has a larger rate accelerating effect than 2,6-lutidine but smaller than 3,5-lutidine. These data suggest that a physical proton transfer is involved in the exchange mechanism and is probably the rate determining step in the exchange reaction.

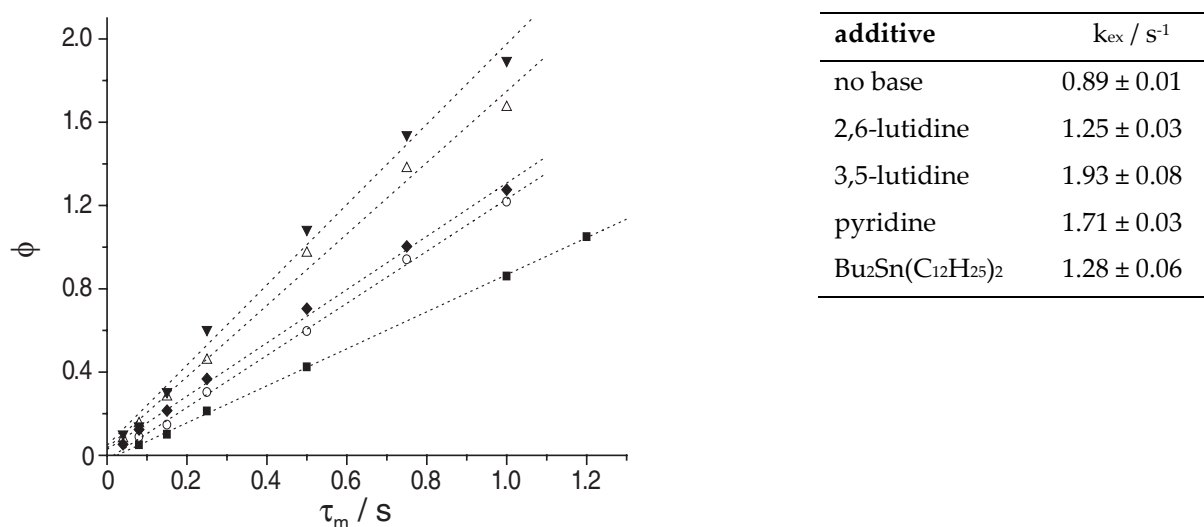


Figure 5.13 Transfer function (ϕ) as a function of mixing time (τ_m) for 3:2 mixtures of **4b** – **1b** in toluene- d_8 with $[N]_0 = 10$ mM and 0.5 v/v% base: no base (■), 2,6-lutidine (○), dibutyltin dilaurate (◆), pyridine (△) and 3,5-lutidine (▼); Determined exchange rate constants with errors estimated from the relevant fitting factors.

The dependence of the exchange rate constant on overall concentration was investigated at 90 °C in toluene- d_8 (Figure 5.14a). The exchange rate constants found for 2:1 mixtures of **4b** – **1b** with 2.5, 10, 30 and 50 mM $[N]_0$ were 4.72, 4.48, 3.02 and 1.75 s^{-1} , respectively. The determined rate constants imply an increase in reaction rate upon decreasing concentration. This would exclude the possibility of an associative mechanism in the rate determining step of the exchange. Additionally, a linear relation is observed when k_{ex} is plotted versus the concentration (Figure 5.14b). The data therefore suggest a first order process as the rate determining step which agrees with the proposed mechanism in Scheme 5.5.

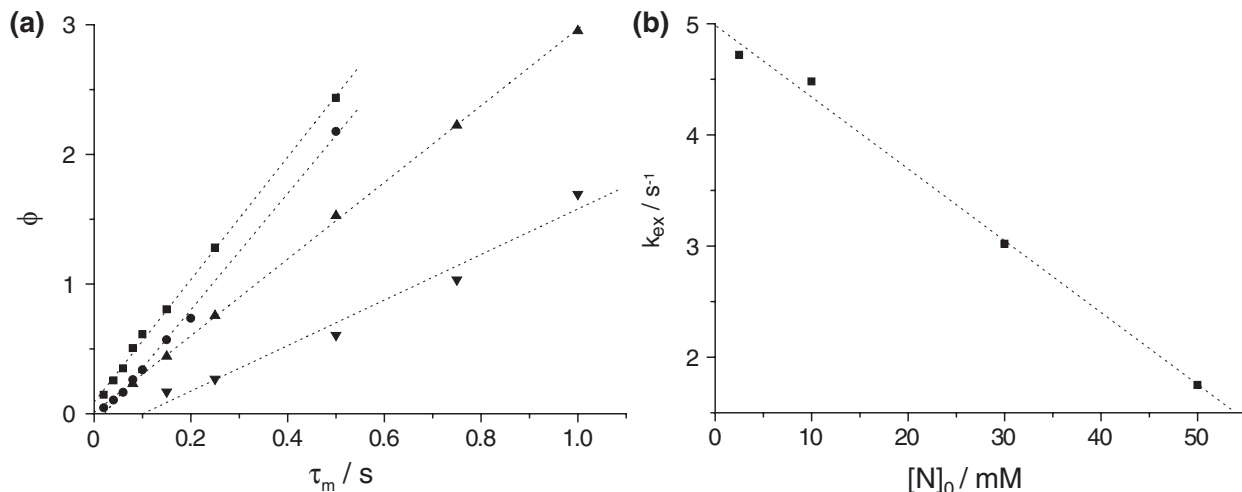


Figure 5.14 (a) Transfer function (ϕ) at 90 °C as a function of mixing time (τ_m) for 2:1 mixtures of **4b** – **1b** in toluene- d_8 with $[N]_0 = 2.5$ mM (■), 10 mM (●), 30 mM (▲) and 50 mM (▼); (b) Exchange rate constant as a function of $[N]_0$.

5.4.3 Kinetic equilibration measurements

In order to validate the results obtained by 2D EXSY NMR experiments, equilibration in UPy – Napy mixtures below room temperature was investigated. When 50 μ L of a 200 mM solution of UPy **4b** in toluene- d_8 was injected rapidly into 1.0 mL of 10 mM Napy **1b**, the equilibration of the homodimer into the heterodimer was followed with 1H NMR (Figure 5.15).

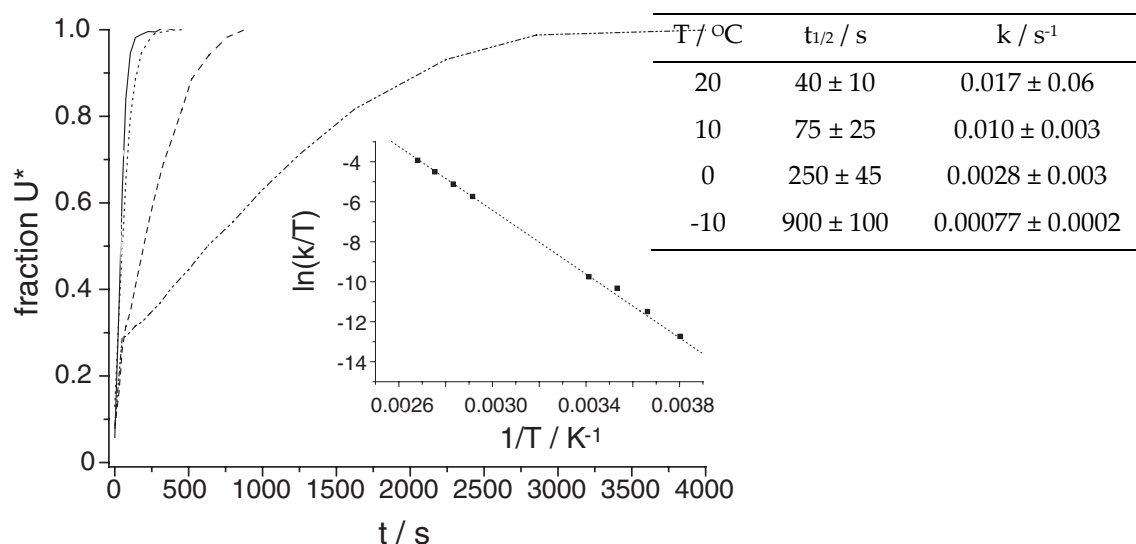


Figure 5.15 Fraction U^* as a function of time as determined with 1H NMR in toluene- d_8 at 20 °C (straight line), 10 °C (dotted line), 0 °C (dashed line) and -10 °C (dash-dot-dot line); the inset shows an Eyring plot of the rate constants obtained from 2D EXSY and kinetic equilibration measurements; half-life times and rate constants determined at different temperatures with estimated errors.

In this manner, a plot obeying a pseudo first order relationship is obtained. From the half-life time ($t_{1/2}$) the rate constant at different temperatures was determined. At 20 °C, this corresponds to a lifetime of 40 s in toluene. Analogous experiments were performed in CDCl_3 from which a lifetime of 20 s was determined. Moreover, combining the determined rate constants with the exchange rate constants obtained from 2D EXSY NMR experiments in an Eyring plot resulted in values of the activation parameters that are in excellent agreement with the values discussed in the previous section (ΔG^\ddagger (293 K) = + 81.5 kJ/mol, E_a (293 K) = 68.7 kJ/mol).

5.5 Discussion

Due to its dynamic tautomeric equilibria, the UPy is a prime example of a true supramolecular chameleon, changing from monomeric to homodimeric and heterodimeric structures depending on external stimuli such as solvent polarity, concentration and complementary compounds such as 1,8-naphthyridines (Figure 5.17). While the UPy exists in its AADD (4[1H]-pyrimidinone) or ADAD (pyrimidin-4-ol) homodimeric form in solution, these tautomeric equilibria are completely shifted towards the ADDA (6[1H]-pyrimidinone) form upon addition of a 2,7-diamido- or di(arylamino)-1,8-naphthyridine. Even though, it has been documented for related uracils and isocytosines that the monomeric 6[1H]-pyrimidinone tautomer is more stable than the monomeric 4[1H]-pyrimidinone tautomer,⁷⁰ the driving force for heterodimerization is most probably enthalpic in nature due to the formation of 8 hydrogen bonds per mole of UPy homodimer.

In contrast to several reports which reported a linear free energy relationship (LFER) between substituent effects and binding ability, an LFER is not found for the association of 2,7-disubstituted 1,8-naphthyridines with a UPy molecule. This is probably related to the intricate combination of steric and electronic effects on the conformational equilibria, acidity of the amino proton and basicity of the naphthyridine ring. However, the importance of size and shape complementarity as well as the importance of high acidity of the Napy NH protons has clearly been delineated.

Although a decrease in association constant of two orders of magnitude from $5 \times 10^6 \text{ M}^{-1}$ to $5 \times 10^4 \text{ M}^{-1}$ may not seem considerable, the selectivity of the heterodimerization reaction changes dramatically due to the mass-action law. Using the equations presented in section 5.2.5, simulated curves were generated for three different values of K_a and a constant value for

the UPy dimerization constant of $6 \times 10^7 \text{ M}^{-1}$ (Figure 5.16a). As discussed before, selectivities of UPy-Napy heterocomplexation in 1:1 mixtures of UPy and Napy are a function of concentration. It is evident that selectivity in a 1:1 UPy/Napy mixture at 10 mM decreases from 93% to 28% heterodimerization when the K_a decreases from 5×10^6 to $5 \times 10^4 \text{ M}^{-1}$. In order to achieve selective heterodimerization of a UPy for a K_a value of $5 \times 10^5 \text{ M}^{-1}$, more than two equivalents are necessary (Figure 5.16b). When constructing supramolecular architectures which require precise stoichiometry, a small decrease in association constant will therefore impose severe limitations.

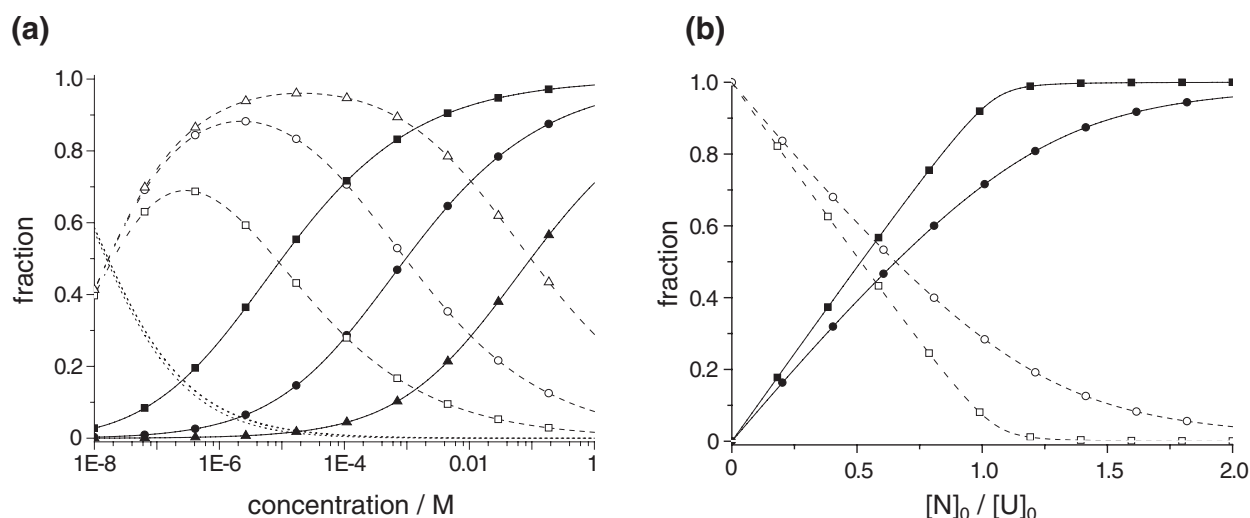


Figure 5.16 (a): Concentration dependent selectivity of different K_a values. Fractions of UPy in UPy-Napy (straight line), UPy - UPy (dashed line), and free UPy (dotted line) as a function of concentration (M) in a 1:1 mixture of UPy and Napy for $K_a = 5 \times 10^6$ (■), $K_a = 5 \times 10^5$ (●), $K_a = 5 \times 10^4$ (▲); (b) Napy to UPy ratio ($[N]_0/[U]_0$) as a function of UPy - Napy association constant.

While slow guest exchange processes have been described for a number of supramolecular hosts based on multiple hydrogen bonding,⁷¹⁻⁷⁴ most exchange processes in linear multiple hydrogen bonding arrays are fast on the NMR time scale. An increase in association constant is expected to lead to slower exchange kinetics. It was shown previously by Söntjens *et al.* that UPy homodimers are in slow exchange ($k_1 = 0.4 \text{ s}^{-1}$ in toluene at 293 K) which was attributed to a slow tautomerization step.¹⁸ As is evident from the data provided in previous sections, the exchange kinetics between UPy homodimer and UPy – Napy heterodimer are even slower ($k_{\text{ex}} = 0.02 \text{ s}^{-1}$ in toluene at 293 K). In the latter process, several tautomerization steps could be involved, thus decreasing the overall rate of equilibration. It was shown by Hammes that for strong threefold hydrogen bonds in organic solvents, the association rate constant (k_{-1} , k_{-1}^* and k_5 in Figure 5.17) is diffusion controlled.¹⁵ A realistic estimate of this rate constant can be made based on solvent viscosity using the Stokes-Einstein

relation and Debye equations which gives a rate constant of $7.3 \times 10^9 \text{ M}^{-1}\cdot\text{s}^{-1}$ in toluene (293 K).⁷⁵ Assuming that association rate constant k_{-1} is diffusion controlled and k_1 is 0.4 s^{-1} , this implies that K_2 (defined as the ratio of k_2 to k_{-2}) is in the order of 30. An important observation in the monitored equilibrium is the fact that no pyrimidin-4-ol dimer is observed while this tautomer is observed in significant amounts in toluene. This would indicate a change in equilibrium constants in the bimolecular system compared to the monomolecular UPy system. When it is assumed that conformer (a) of the two possible 6[1H]-pyrimidinone structures is the more stable monomeric form,⁷⁶ K_4 is smaller than unity and K_3 is smaller than K_2 . Subsequent association of conformer (b) with a free Napy is again assumed to be diffusion controlled. This leads to a reasonable estimate for k_{-5} of $10^2 - 10^4 \text{ s}^{-1}$. In conclusion, although these assumptions would qualitatively explain the observed slow exchange, the exact mechanism of exchange remains unclear. Furthermore, it has to be noted that the dynamics are faster in chloroform.

Whether in main-chain or side-chain supramolecular polymers, the thermodynamics of the intermolecular interaction are a primary design consideration, however, the dynamics of the interaction can be of particular importance under non-equilibrium conditions such as those imposed by mechanical stress. An example of this very important effect was reported very recently by Craig and coworkers.^{22,77}

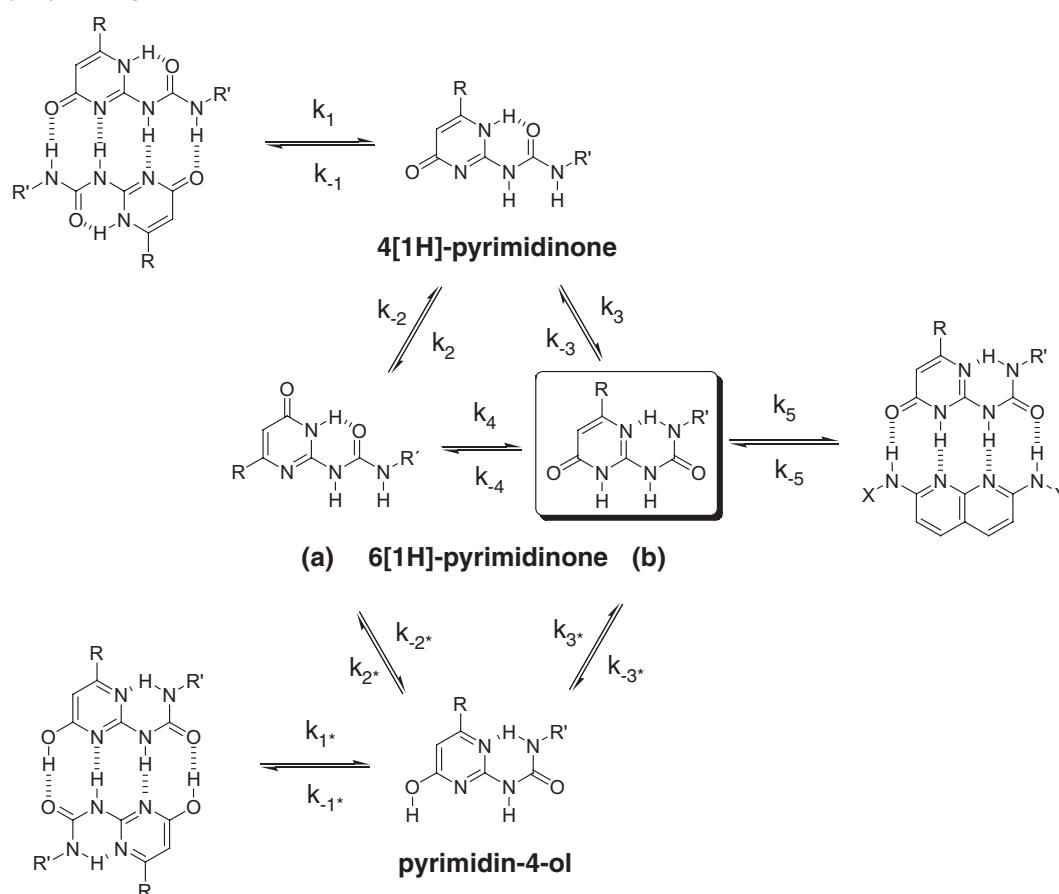


Figure 5.17 Association equilibria of tautomeric forms of UPy and Napy in organic solvents.

5.6 Conclusions

1,8-Naphthyridine derivatives bearing arylamino or amido substituents at the 2- and 7-position (Napy) are shown to disrupt the strongly dimerizing 2-ureido-4[1H]-pyrimidinone (UPy) and to induce a tautomeric shift of the UPy to the 6[1H]-pyrimidinone upon formation of a heterodimer which displays a complementary DAAD – ADDA array. Strong binding ($K_a = 5 (\pm 2) \times 10^6$ and $> 1 \times 10^7$ in CDCl_3 and toluene- d_8 , respectively) was confirmed by NMR and UV/Vis spectroscopy. A concentration dependent selectivity was shown upon dilution of 1:1 mixtures. The association behavior is complicated by several tautomeric equilibria which can not be monitored and results in slow exchange between UPy homodimer and UPy – Napy heterodimer primarily due to slow tautomerization steps. Sterically demanding substituents were shown to have a pronounced detrimental effect on the selectivity of heterocomplex formation while the introduction of electron-withdrawing or -donating substituents on an arylamino group resulted in smaller deviations of the association constant. The complementarity with respect to hydrogen bonding is advantageous for a multitude of supramolecular purposes. In combination with the ease of synthesis presented in Chapter 3 and 4, the unique change from homodimer to heterodimer with high selectivity opens the way to special supramolecular architectures.

5.7 Experimental procedures

General methods. See General methods Chapter 2.

^1H NMR experiments. ^1H NMR single point binding experiments were performed on a 300, 400 or 500 MHz NMR spectrometer and the temperature was maintained at 298 ± 0.5 K with a temperature control module that had been calibrated using the resonances of methanol. T_1 relaxation times for UPy, Napy and their heterocomplex were measured by the standard inversion recovery experiment. Spectra were obtained with a delay time of at least 3 seconds to ensure elimination of systematic errors due to differences in relaxation times. Integration was used to determine the concentration of UPy in UPy – Napy and UPy_2 in order to obtain K_a values. In general, in order to obtain equal integrals of the homo- and heterodimer UPy alkylidene, 1.2 to 2 equivalents UPy were added to a 10 mM Napy solution. K_a values $< 10^5$ were determined by addition of 0.5 to 1 equivalents UPy to a 10 mM Napy solution. Errors were determined taking into account a 5% systematic error of integration and weighing.

Kinetic experiments. Standard solutions of 200 mM UPy **4b** and 10 mM Napy **1b** in toluene- d_8 were prepared for the kinetic experiments. The exchange was monitored by ^1H NMR (500 MHz) with the probe maintained at constant temperature (± 0.5 K). The components were mixed by injection of 50 μL

200 mM UPy **4b** solution which was equilibrated at the temperature of the measurement. Data acquisition was automatically performed using an acquisition delay. The rate constants (k) presented in Figure 5.10 were determined from the half-life ($t_{1/2}$) assuming pseudo first order reaction kinetics up to 90% conversion ($k = \ln 2/t_{1/2}$).

Thermodynamics. The Gibbs free energy (ΔG^0) for any reaction can be expressed as a simple function of the thermodynamic equilibrium constant (K) as: $\Delta G^0 = -RT \ln(K)$ where R is the gas constant and T is the temperature. The Eyring equation describes the effect of the temperature on the rate of the reaction (k) by $k = (k_B T/h) \exp(-\Delta G^\ddagger/RT)$ where k_B is the Boltzmann constant and h is Planck's constant. The free energy of activation ΔG^\ddagger is defined as $\Delta G^\ddagger = \Delta H^\ddagger - T \Delta S^\ddagger$. An Eyring plot is obtained by plotting $\ln(k/T)$ versus $1/T$ and provides the kinetic activation parameters ΔH^\ddagger from the slope $-(\Delta H^\ddagger/R)$ and ΔS^\ddagger from the y-intercept ($\Delta S^\ddagger/R + \ln(k_B/h)$). The energy of activation E_a in solution is defined as $E_a = \Delta H^\ddagger + RT$.

UV/Vis titrations. UV/Vis spectra were recorded using 10 mm path length cells on a Perkin Elmer Lambda 40P equipped with a PTP-1 Peltier temperature control system. A series of spectra was obtained by the addition of μL amounts of a stock solution containing 25.7 μM Napy **1b** and 300 μM UPy **4b** to a cell containing 2.0 mL 25.7 μM Napy **1b** solution. All obtained traces were base-line corrected. The reported values of absorbance as a function of the concentration of UPy **4b** were fitted to the binding model described in section 5.2.4 using Matlab 6.1.

Fluorescence titrations. OPV4-UPy **6** was excited at 440 nm, and fluorescence from UPy-PERY **7** which is caused by efficient energy transfer from **6** was detected at 575.5 nm at 25 °C. Experimental conditions: Slit-length for emission and excitation was 2.5 nm and 10 nm, respectively. Scan rate was 100 nm/min and measured emission spectra between 450 nm to 700 nm. All obtained traces were base-line corrected. A representative preparation of solutions for fluorescence experiments is described below:

Preparation of stock solutions of 6, 7 and 8: UPy **6** (0.537 mg) was dissolved in 25 mL of chloroform to obtain 1.402×10^{-5} M stock solution (Solution A). UPy **7** (0.272 mg) was also dissolved in 25 mL of chloroform to yield 8.314×10^{-6} M stock solution (Solution B). Napy stock solution (1.589×10^{-4} M) was prepared by dissolving 1.957 mg of **8** in 25 mL of chloroform (Solution C).

Preparation of stock solutions of mixtures containing 6 and 7 or 6, 7 and 8: 4.28 mL of Solution A, 7.22 mL of Solution B, and 18.5 mL of chloroform were mixed to obtain a 30 mL of stock solution in which $[6] = [7]$ was 2 μM (Solution D). 1.43 mL of Solution A, 2.41 mL of Solution B, 2.51 mL of Solution C, and 3.65 mL of chloroform were mixed and stirred overnight for the equilibration to obtain the stock solution in which concentrations of **6**, **7** and **8** are 2 μM , 2 μM , and 40 μM , respectively (Solution E). Solution D and E were diluted four times to obtain Solution F, and G which contained 0.5 μM of **6** and **7** (Solution F), 0.5 μM of **6** and **7** and 10 μM of **8** (Solution G), respectively.

Preparation of a series of solutions to observe the decrease of the energy transfer from 6 to 7: 2 mL of Solution D and 0, 50, 100, 150, 200, 220, 300, 500, and 1000 μL of Solution E were mixed and stand for overnight for the equilibration to yield solutions for a titration experiment, in which ratios of total UPy

concentration and Napy concentration are 1:0, 1:0.243, 1:0.476, 1:0.697, 1:0.909, 1:0.991, 1:1.304, 1:2, and 1:3.33. For 1:10 solution, Solution E was used as it is. These solutions were used for the determination of the selectivity of UPy-Napy heterodimerization at 4 μ M. In the same manner, a series of solutions for titration to evaluate the selectivity of UPy-Napy heterodimerization at 1 μ M was prepared from Solution F, and G.

Synthesis. 2-*n*-Butylureido-6-methyl-4[1H]-pyrimidinone **4a** was prepared as reported by Beijer *et al.*²⁹; 2,7-diamino-1,8-naphthyridine was prepared according to Corbin *et al.*⁸ 2-(2-Ethylhexanoylamino)-7-acetylamino-1,8-naphthyridine **1b**, 2,7-bis-(dodecanoylamino)-1,8-naphthyridine **1c** and 2,7-bis-(10-undecenoylamino)-1,8-naphthyridine **8** were synthesized as reported by Ligthart *et al.*⁷⁸ (see also Chapter 3 of this thesis); (E,E,E)-4-[4-{4-(3,4,5-tridodecyloxystyryl)-2,5-bis[(S)-2-methylbutoxy]styryl}-2,5-bis[(S)-2-methylbutoxy]styryl]-ureido-6-ethylpentyl-4[1H]-pyrimidinone (UPy-OPV-4) **6** and N,N-(1-ethylpropyl)-{4-[2-ureido-6-(1-ethylpentyl)-4[1H]-pyrimidinone]-2,5-di-*t*-butylphenyl}-1,7-(3',5'-di-*t*-butylphenoxy)perylene-3,4,9,10-tetracarboxylic-bisimide (UPy-PERY) **7** were synthesized according to Dudek *et al.*⁷⁹ The synthesis of Napy derivatives **9 – 11** and **14 – 24** has been reported in Chapter 3 of this Thesis and reference 78. The synthesis of Napy derivatives **25 – 48** has been reported in Chapter 4.

2,7-Bis-(butanoylamino)-1,8-naphthyridine 1a: A mixture of 2,7-diamino-1,8-naphthyridine (320 mg, 2.0 mmol), triethylamine (1.0 mL), butyryl chloride (0.54 g, 5.0 mmol) and 4-N,N'-dimethylamino-pyridine (12.4 mg, 5 mol%) in 30 mL dry THF was heated to reflux and stirred for 16 h. The black mixture was evaporated to dryness and purified by column chromatography (SiO₂, 2 v/v% methanol/chloroform) to obtain crude product. Crystallization 1:1 from ethanol/water afforded the pure title compound as light yellow needles (51 mg, 8%). M.P. decomposes > 160 °C; ¹H NMR (CDCl₃): δ = 9.08 (br, 2H, *NH*), 8.46 (d, 2H, *J* = 8.8 Hz), 8.11 (d, 2H, *J* = 8.8 Hz), 2.44 (t, 4H, *J* = 7.4 Hz), 1.75 (q, 4H, *J* = 7.4 Hz), 0.97 (t, 3H, *J* = 7.4 Hz) ppm; ¹³C NMR (CDCl₃): δ = 172.4, 154.0, 153.4, 138.9, 118.1, 113.5, 39.5, 18.5, 13.5 ppm; MALDI-TOF-MS: (m/z) calcd: 300.16; observed: 301.07 (M+H⁺), 323.05 (M+Na⁺); FTR-IR (ATR): ν = 3297, 3139, 2958, 2870, 1684, 1606, 1544, 1495, 1385, 1311, 1280, 1191, 1167, 1136, 853, 802 cm⁻¹; Anal. Calcd. for C₁₆H₂₀N₄O₂: C 63.98, H 6.71, N 18.65; found: C 63.61, H 6.61, N 18.48.

2-Hexylureido-6-(3-heptyl)-4[1H]-pyrimidinone 4b: UPy-imidazolide⁸⁰ (3.3 g, 10.8 mmol) and 1-hexylamine (0.55 g, 5.4 mmol) were dissolved in dry chloroform (20 mL) and the solution was stirred for 3 h under nitrogen. To the reaction mixture 50 mL of chloroform was added and the organic layer was washed with 20 mL 1N HCl, 20 mL sat. NaHCO₃, and 20 mL brine. The organic layer was evaporated to dryness and the title compound was obtained as a white solid after purification by column chromatography (SiO₂, 1 v/v% methanol/chloroform) (1.08 g, 59%) M.P. 51 °C; ¹H NMR (CDCl₃): δ = 13.26 (s, 1H), 11.91 (s, 1H), 10.19 (s, 1H), 5.82 (s, 1H), 3.26 (m, 2H), 2.30 (m, 1H), 1.72-1.48 (m, 6H), 1.45-1.20 (m, 8H) 0.92-0.85 (m, 9H) ppm; ¹³C NMR (CDCl₃): δ = 173.3, 156.8, 155.5, 155.0, 106.4, 45.5, 40.3, 33.1, 29.6, 29.5, 26.9, 26.8, 22.8, 22.7, 14.2, 14.1, 11.9 ppm. MALDI-TOF-MS: (m/z) calcd: 336.25; observed: 337.20 (M+H⁺); FTR-IR (ATR): ν = 3210, 2956, 2926, 2859, 1195, 1648, 1581, 1524, 1459, 1305, 1254, 852, 801 cm⁻¹; Anal. Calcd. for C₁₈H₃₂N₄O₂: C 64.25, H 9.59, N 16.65; found: C 64.66, H 9.72, N 16.64.

2-Acetamido-7-dodecylamino-1,8-naphthyridine 12: A mixture of 7-acetamido-2-chloro-1,8-naphthyridine (221 mg, 1.0 mmol) in dodecylamine (1.8 g, 10 mmol) was heated to 100 °C and stirred for 16 h. The excess amine was removed by kugelrohr distillation. Purification by column chromatography (SiO₂, 2 v/v% methanol/chloroform) afforded the title compound as a viscous yellow oil (0.48 g, 96%). ¹H NMR (CDCl₃): δ = 7.82 (d, 2H, J = 8.1 Hz), 7.42 (d, 1H, J = 8.3 Hz), 7.21 (br, 1H, NH), 6.45 (d, 1H, J = 8.4 Hz), 5.31 (br, 1H, NH), 3.46 (m, 2H), 2.20 (s, 3H), 1.66 (m, 2H), 1.39-1.27 (m, 18H), 0.88 (t, 3H, J = 7.3 Hz) ppm; ¹³C NMR (CDCl₃): δ = 169.7, 162.7, 157.3, 154.3, 132.4, 131.8, 110.6, 110.2, 42.0, 32.0, 29.5-28.7 (6), 27.1, 24.0, 22.7, 14.1 ppm; MALDI-TOF-MS: (m/z) calcd: 370.23; observed: 371.28 (M+H⁺).

2,7-Bis-(dodecylamino)-1,8-naphthyridine 13: A mixture of 2,7-dichloro-1,8-naphthyridine (201 mg, 1.0 mmol) in dodecylamine (3.9 g, 21 mmol) was heated to 100 °C and stirred for 16 h. The excess amine was removed by kugelrohr distillation and the resulting black mixture purified by column chromatography (SiO₂, 2 v/v% methanol / chloroform) to obtain the title compound as a dark yellow oil (0.48 g, 96%). ¹H NMR (CDCl₃): δ = 7.56 (d, 2H, J = 8.5 Hz), 6.35 (d, 2H, J = 8.7 Hz), 5.20 (br, 2H, NH), 3.42 (m, 4H), 1.62 (m, 4H), 1.37-1.26 (m, 36H), 0.88 (t, 6H, J = 7.1 Hz) ppm; ¹³C NMR (CDCl₃): δ = 159.3, 155.9, 137.4, 110.1, 105.5, 42.0, 32.0, 29.7-29.0 (6), 27.0, 22.7, 14.1 ppm; MALDI-TOF-MS: (m/z) calcd: 496.45; observed: 497.56 (M+H⁺).

2,7-Bis-(S-2-hydroxypropanoylamino)-1,8-naphthyridine 18: To a 100 mL of round bottle flask, charged with 2,7-bis-{S-2-(tert-butyldimethylsilyloxy)propanoylamino}-1,8-naphthyridine **17** (1.00 g, 1.88 mmol), 25 mL of dry THF was added. The solution was deoxygenated by the argon flow, followed by the addition of triethylamine tri-hydrofluoride (908 mg, 5.63 mmol). The reaction mixture was stirred at room temperature under inert atmosphere for 2 h. Additional triethylamine tri-hydrofluoride (454 mg, 2.82 mmol) was added and stirred further 1 h at room temperature. To the reaction vessel, 50 mL of ether was added in order to precipitate the desired product together with some salts. Resulting white precipitate was collected by glass filter and washed with ether successively. White powder was again washed as it was on the filter by water to remove the salt and dried in vacuo (60 °C, overnight) to yield the title compound as a white powder (482 mg, 95%). M.P.: > 236 °C (degrades); ¹H NMR (DMSO-*d*₆): δ = 9.99 (br, 2H), 8.38 (d, 2H, J = 8.4 Hz), 8.29 (d, 2H, J = 8.8 Hz), 5.95 (br, 2H), 4.28 (q, 2H, J = 6.6 Hz), 1.33 (d, 6H, J = 6.6) ppm; ¹³C NMR (DMSO-*d*₆): δ = 175.2, 154.5, 154.2, 140.2, 118.6, 113.3, 68.2, 21.3 ppm; MALDI-TOF-MS: (m/z) calcd: 304.12; observed: 305.08 (M+H⁺), 327.06 (M+Na⁺), 343.03 (M+K⁺); FTR-IR (ATR): ν = 3456, 3348, 2988, 1692, 1610, 1533, 1504, 1382, 1314, 1287, 1186, 1125, 1085, 967, 881, 851, 800 cm⁻¹; Anal. Calcd. for C₁₄H₁₆N₄O₄: C 55.26, H 5.30, N 18.41; found: C 54.44, H 5.11, N 18.09.

5.8 References

- (1) Jorgensen, W. L.; Pranata, J. *J. Am. Chem. Soc.* **1990**, *112*, 2008-10.
- (2) Zimmerman, S. C.; Corbin, P. S. *Struct. Bonding (Berlin)* **2000**, *96*, 63-94.
- (3) Prins, L. J.; Reinhoudt, D. N.; Timmerman, P. *Angew. Chem. Int. Ed.* **2001**, *40*, 2382-2426.
- (4) Sijbesma, R. P.; Meijer, E. W. *Chem. Commun.* **2003**, 5-16.
- (5) Steed, J. W.; Atwood, J. L. *Supramolecular Chemistry*; John Wiley & Sons Ltd.: West Sussex, 2000.
- (6) Corbin, P. S.; Zimmerman, S. C. *J. Am. Chem. Soc.* **1998**, *120*, 9710-9711.

- (7) Luning, U.; Kuhl, C. *Tetrahedron Lett.* **1998**, 39, 5735-5738.
- (8) Corbin, P. S.; Zimmerman, S. C.; Thiessen, P. A.; Hawryluk, N. A.; Murray, T. J. *J. Am. Chem. Soc.* **2001**, 123, 10475-10488.
- (9) Luning, U.; Kuhl, C.; Uphoff, A. *Eur. J. Org. Chem.* **2002**, 4063-4070.
- (10) Zhao, X.; Wang, X.-Z.; Jiang, X.-K.; Chen, Y.-Q.; Li, Z.-T.; Chen, G.-J. *J. Am. Chem. Soc.* **2003**, 125, 15128-15139.
- (11) Park, T.; Zimmerman, S. C.; Nakashima, S. *J. Am. Chem. Soc.* **2005**, 127, 6520-6521.
- (12) Park, T.; Todd, E. M.; Nakashima, S.; Zimmerman, S. C. *J. Am. Chem. Soc.* **2005**, 127, 18133-18142.
- (13) Corbin, P. S.; Zimmerman, S. C. *J. Am. Chem. Soc.* **2000**, 122, 3779-3780.
- (14) Wang, X.-Z.; Li, X.-Q.; Shao, X.-B.; Zhao, X.; Deng, P.; Jiang, X.-K.; Li, Z.-T.; Chen, Y.-Q. *Chem. Eur. J.* **2003**, 9, 2904-2913.
- (15) Hammes, G. G.; Park, A. C. *J. Am. Chem. Soc.* **1968**, 90, 4151-7.
- (16) Mogck, O.; Pons, M.; Boehmer, V.; Vogt, W. *J. Am. Chem. Soc.* **1997**, 119, 5706-5712.
- (17) Szabo, T.; Hilmersson, G.; Rebek, J., Jr. *J. Am. Chem. Soc.* **1998**, 120, 6193-6194.
- (18) Söntjens, S. H. M.; Sijbesma, R. P.; van Genderen, M. H. P.; Meijer, E. W. *J. Am. Chem. Soc.* **2000**, 122, 7487-7493.
- (19) Folmer, B. J. B.; Sijbesma, R. P.; Kooijman, H.; Spek, A. L.; Meijer, E. W. *J. Am. Chem. Soc.* **1999**, 121, 9001-9007.
- (20) Castellano, R. K.; Craig, S. L.; Nuckolls, C.; Rebek, J., Jr. *J. Am. Chem. Soc.* **2000**, 122, 7876-7882.
- (21) Yount, W. C.; Loveless, D. M.; Craig, S. L. *Angew. Chem. Int. Ed.* **2005**, 44, 2746-2748.
- (22) Yount, W. C.; Loveless, D. M.; Craig, S. L. *J. Am. Chem. Soc.* **2005**, 127, 14488-14496.
- (23) Connors, K. A. *Binding Constants*; Wiley: New York, 1987.
- (24) Fielding, L. *Tetrahedron* **2000**, 56, 6151-6170.
- (25) A K_d of < 10 M⁻¹ for a dimeric binding motif of Napy was determined previously in refs. 8 & 22.
- (26) Li, X.-Q.; Jiang, X.-K.; Wang, X.-Z.; Li, Z.-T. *Tetrahedron* **2004**, 60, 2063-2069.
- (27) An example for complexation induced tautomeric shift was previously reported for a 2-ureido-[3H]-pyrido-(2,3-d)pyrimidin-4-one derivative, see ref. (6).
- (28) Macura, S.; Huang, Y.; Suter, D.; Ernst, R. R. *J. Magn. Reson.* **1981**, 43, 259-81.
- (29) Beijer, F. H.; Sijbesma, R. P.; Kooijman, H.; Spek, A. L.; Meijer, E. W. *J. Am. Chem. Soc.* **1998**, 120, 6761-6769.
- (30) Beijer, F. H., Eindhoven University of Technology, Thesis, 1998.
- (31) Stauffer, D. A.; Barrans, R. E., Jr.; Dougherty, D. A. *J. Org. Chem.* **1990**, 55, 2762-7.
- (32) Adrian, J. C., Jr.; Wilcox, C. S. *J. Am. Chem. Soc.* **1991**, 113, 678-80.
- (33) Ashton, P. R.; Fyfe, M. C. T.; Hickingbottom, S. K.; Fraser Stoddart, J.; White, A. J. P.; Williams, D. J. *J. Chem. Soc., Perkin Trans. 2* **1998**, 2117-2128.
- (34) Due to a smaller shift upon complexation and hence lower accuracy, the pyrimidinone-methyl proton integrals were not taken into account.
- (35) Neuteboom, E. E.; Beckers, E. H. A.; Meskers, S. C. J.; Meijer, E. W.; Janssen, R. A. *J. Org. Biomol. Chem.* **2003**, 1, 198-203.
- (36) Brown, D. J.; Teitei, T. *Aust. J. Chem.* **1965**, 18, 559-68.
- (37) Erkin, A. V.; Krutikov, V. I. *Russ. J. Gen. Chem.* **2005**, 75, 639-644.
- (38) Buhlmann, P.; Simon, W. *Tetrahedron* **1993**, 49, 7627-36.
- (39) See Chapter 3.3 of this Thesis.
- (40) Peng, T.; Murase, T.; Goto, Y.; Kobori, A.; Nakatani, K. *Bioorg. Med. Chem. Lett.* **2005**, 15, 259-262.
- (41) Hammett, L. P.; Pfluger, H. L. *J. Am. Chem. Soc.* **1933**, 55, 4079-89.
- (42) Hammett, L. P. *J. Chem. Ed.* **1966**, 43, 464-9.
- (43) Hansch, C.; Leo, A.; Taft, R. W. *Chem. Rev.* **1991**, 91, 165-95.
- (44) Hansch, C. *Acc. Chem. Res.* **1993**, 26, 147-53.
- (45) Islam, M. S.; Pethrick, R. A.; Pugh, D.; Wilson, M. J. *J. Chem. Soc., Faraday Trans.* **1997**, 93, 387-392.

- (46) Reek, J. N. H.; Priem, A. H.; Engelkamp, H.; Rowan, A. E.; Elemans, J. A. A. W.; Nolte, R. J. M. *J. Am. Chem. Soc.* **1997**, *119*, 9956-9964.
- (47) Hunter, C. A.; Low, C. M. R.; Rotger, C.; Vinter, J. G.; Zonta, C. *Proc. Natl. Acad. Sci. USA* **2002**, *99*, 4873-4876.
- (48) Mizuno, T.; Hirota, M.; Hamada, Y.; Ito, Y. *Tetrahedron* **1971**, *27*, 6011-21.
- (49) Hirota, M.; Kobayashi, K. *Bull. Chem. Soc. Jpn.* **1981**, *54*, 1583-4.
- (50) Takasuka, M.; Nakai, H.; Shiro, M. *J. Chem. Soc., Perkin Trans. 2* **1986**, 1969-78.
- (51) Polamo, M.; Repo, T.; Leskelae, M. *Acta Chem. Scand.* **1997**, *51*, 325-329.
- (52) Bensemman, I.; Gdaniec, M.; Polonski, T. *New J. Chem.* **2002**, *26*, 448-456.
- (53) Box, V. G. S.; Yu, H. W. *J. Chem. Ed.* **1997**, *74*, 1293-1296.
- (54) Obviously, the energy difference is solvent dependent. However, the Z-isomer will be more favorable in less polar solvents.
- (55) Perrin, C. L.; Dwyer, T. J. *Chem. Rev.* **1990**, *90*, 935-67.
- (56) Dwyer, T. J.; Norman, J. E.; Jasien, P. G. *J. Chem. Ed.* **1998**, *75*, 1635-1640.
- (57) Claridge, T. D. W. *High-Resolution NMR Techniques in Organic Chemistry*; Elsevier Science Ltd.: Oxford, 1999.
- (58) Bain, A. D. *Prog. Nucl. Mag. Reson. Spectrosc.* **2003**, *43*, 63-103.
- (59) Pons, M.; Millet, O. *Prog. Nucl. Mag. Reson. Spectrosc.* **2001**, *38*, 267-324.
- (60) Jeener, J.; Meier, B. H.; Bachmann, P.; Ernst, R. R. *J. Chem. Phys.* **1979**, *71*, 4546-53.
- (61) This assumption is actually more valid in toluene than in chloroform.
- (62) The long lifetimes of the exchanging species predominantly leads to T1 relaxation instead of exchange at higher mixing times.
- (63) See Experimental procedures.
- (64) Watarai, H.; Suzuki, N. *Bull. Chem. Soc. Jpn.* **1979**, *52*, 2778-82.
- (65) Groth-Andersen, H.; Soerensen, P. E. *Acta Chem. Scand.* **1989**, *43*, 32-8.
- (66) Iglesias, E. *New J. Chem.* **2005**, *29*, 625-632.
- (67) Smith, M. B.; March, J. *Advanced Organic Chemistry: Reactions, Mechanisms and Structure*; 5th ed.; Wiley-Interscience: New York, 2001.
- (68) Prototropy is the most common type of tautomerism and involves a proton shift.
- (69) Barra, M.; Chen, N. *J. Org. Chem.* **2000**, *65*, 5739-5744.
- (70) Elguero, J.; Marzin, C.; Katritzky, A. R.; Linda, P. *Advances in Heterocyclic Chemistry, Supplement 1: The Tautomerism of Heterocycles*, 1976.
- (71) Santamaria, J.; Martin, T.; Hilmersson, G.; Craig, S. L.; Rebek, J., Jr. *Proc. Natl. Acad. Sci. USA* **1999**, *96*, 8344-8347.
- (72) Hof, F.; Nuckolls, C.; Craig, S. L.; Martin, T.; Rebek, J., Jr. *J. Am. Chem. Soc.* **2000**, *122*, 10991-10996.
- (73) Kerckhoffs, J. M. C. A.; van Leeuwen, F. W. B.; Spek, A. L.; Kooijman, K.; Crego-Calama, M.; Reinhoudt, D. N. *Angew. Chem. Int. Ed.* **2003**, *42*, 5717-5722.
- (74) Wu, A.; Mukhopadhyay, P.; Chakraborty, A.; Fetting James, C.; Isaacs, L. *J. Am. Chem. Soc.* **2004**, *126*, 10035-43.
- (75) Connors, K. A. *Chemical Kinetics: The Study of Reaction Rates in Solution*; VCH Publishers, Inc: New York, 1990.
- (76) The assumption can be made based on calculations in the gas phase, see ref. 30.
- (77) Loveless, D. M.; Jeon, S. L.; Craig, S. L. *Macromolecules* **2005**, *38*, 10171-10177.
- (78) Ligthart, G. B. W. L.; Ohkawa, H.; Sijbesma, R. P.; Meijer, E. W. *J. Org. Chem.* **2006**, *71*, 375-378.
- (79) Dudek, S. P.; Pouderoijen, M.; Abbel, R.; Schenning, A. P. H. J.; Meijer, E. W. *J. Am. Chem. Soc.* **2005**, *127*, 11763-11768.
- (80) Keizer, H. M.; Sijbesma, R. P.; Meijer, E. W. *Eur. J. Org. Chem.* **2004**, 2553-2555.

6

Supramolecular block copolymers based on the UPy - Napy binding motif

Abstract

The strong and complementary association via quadruple hydrogen bonds between 2,7-diamido-1,8-naphthyridine (Napy) and 2-ureido-6[1H]-pyrimidinone (UPy) units allows for the formation of supramolecular main-chain polymers. The self-assembly of small, bifunctional UPy and Napy molecules results in the selective formation of cyclic heterodimers as substantiated by viscometry as well as diffusion ordered ^1H NMR spectroscopy. Furthermore, a gradual change in heterocomplex composition can be observed from purely cyclic to predominantly linear structures upon an increase in concentration. Additionally, selective incorporation of small bifunctional Napy derivatives into a linear supramolecular UPy polymer based on a high molecular weight spacer between two UPy units was demonstrated by viscometry experiments. A new methodology based on a retrosynthetic approach from supramolecular block copolymers has been developed that combines ring-opening metathesis polymerization with chain-transfer agents for the formation of UPy and Napy telechelic polymers with a degree of functionalization of exactly two. Telechelic UPy and Napy polymers were synthesized in the presence of a polar UPy derivative that serves as a supramolecular protecting group. Subsequent studies in solution by viscometry and in the bulk by atomic force microscopy confirmed the formation of supramolecular block copolymers. Due to the dual binding modes of UPy, the UPy – Napy heterocomplex is eminently suitable for the supramolecular synthesis of block copolymers with polymeric properties over a broad composition range.

6.1 Introduction

The majority of polymers currently used today in commercial applications are homopolymers. However, more and more sophisticated applications are being developed that require combinations of properties that cannot be obtained with homopolymers but require block copolymers or polymer blends. As a rule, most polymer blends are immiscible, which result in macrophase separation. The formation of such a macrophase-separated morphology generally results in poor mechanical properties. In block copolymers, however, two or more polymer blocks are linked by means of a strong chemical interaction. The competition between the strong chemical connection and repulsion between different polymer blocks leads to a wealth of interesting microphase structures (Figure 6.1; typical length scale is about 5 - 50 nm, depending on the individual length of the blocks).

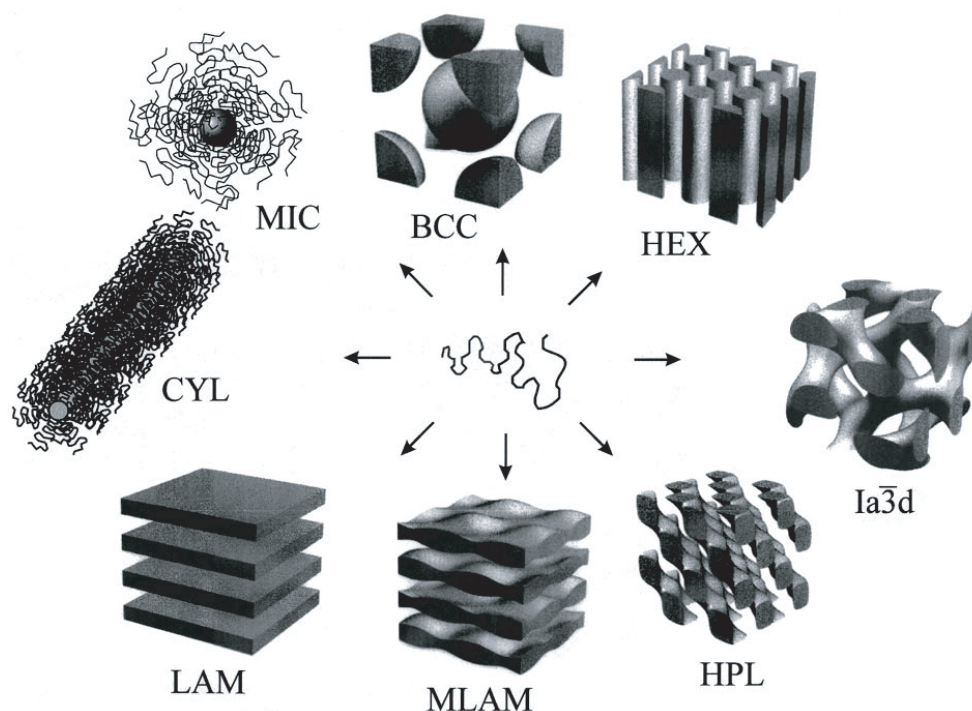


Figure 6.1 Self-organization of a diblock copolymer by phase separation into regularly ordered microstructures.¹

Phase separation may occur due to energetically favorable demixing of the two blocks combined with a low entropy of mixing.² The extent to which a covalently linked diblock copolymer phase separates and which type of morphology is obtained, is governed by the fractional composition f and parameter χN , where N is the degree of polymerization and χ is the Flory-Huggins interaction parameter between the blocks.³⁻⁵ The remarkable micro- and nanophase behavior of block copolymers and the resulting properties make them very useful as stabilizers, coatings and thermoplastic elastomers.

Recent developments in the field of supramolecular chemistry have shown that small, complementary as well as self-complementary building blocks can lead to large, well-defined structures through self-assembly. Provided that the applied non-covalent interaction is strong and the value of χ_N is sufficiently high, supramolecular copolymers will have the possibility to display microphase separation. Advantages of assembling multi-block copolymers through strong reversible non-covalent interactions include a modular approach in synthesis, ease of processing, self-healing properties, facile and selective removal of sacrificial blocks, and an extra level of hierarchical control in self-organization of functional materials.⁶⁻⁹ The strength of the non-covalent interaction affixed to the polymers will be essential in overcoming the forces driving phase-separation. Therefore, strong non-covalent interactions are required to ensure the formation of regular arrays of alternating blocks. Although examples of supramolecular block copolymers were reported recently using non-symmetrical metal-ligand complexes,^{10,11} strong metal-ligand interactions are generally kinetically inert. In this respect, hydrogen bonding arrays are more appropriate because of their synthetic accessibility, their directionality and because they easily allow the tuning of binding constants between 10 M^{-1} up to 10^9 M^{-1} in organic solvents.^{12,13} When the non-covalent interaction between two monomers is self-complementary, the block-size is not fixed, and depending on the conditions, the structure may vary from a random copolymer through a microstructure to a macrophase separated blend. Stadler *et al.* reported microphase separated poly(isoprene)-*block*-poly(1,3-butadiene) diblock copolymers with weak hydrogen bonding units based on phenylurazole.¹⁴ It was shown that hydrogen bonding induced microphase separation in an originally miscible block copolymer and resulted in the formation of a thermoreversible network. Additionally, when strong, self-complementary ureido-s-triazine units were used in a supramolecular main-chain rod-coil block-copolymer, kinetically stable microphases could be observed in the bulk.¹⁵ Therefore, the use of complementary binding motifs is a prerequisite for thermodynamically stable microphase-separated structures. Pioneering work by Lehn and co-workers in this field led to the formation of alternating supramolecular copolymers assembled from small bifunctional molecules in solution using motifs based on triple and six-fold hydrogen bonds.¹⁶⁻¹⁸ Mixtures of poly(etherketones) and poly(isobutylenes) functionalized on the termini with multiple hydrogen bonding arrays were investigated by Binder and co-workers.¹⁹⁻²¹ It was reported that the strength of the hydrogen bonding motifs was essential in preventing macrophase separation in the solid state. Higher association constants ($K_a = 10^3 - 10^5\text{ M}^{-1}$) lead to the formation of regular arrays of alternating polymers, whereas low K_a values lead to immiscibility of the individual polymers in the bulk.²² Important in this respect was the reversibility of the binding process which can be induced by temperature mediated breaking of

the bonds. While weak binding motifs can stabilize microphase separation up to the glass transition temperature, the microphase-separated structure is retained with strong binding motifs. Although polystyrene-*block*-poly(isoprene) polymers bearing multiple hydrogen bonding moieties at the termini were synthesized in the group of Long, microphase separated morphologies of these polymers were not studied to date.²³ Multiple hydrogen bond motifs with very high K_a values were incorporated by the groups of Rebek and Gong. While Rebek and co-workers showed microstructures in the solid phase and viscoelastic behavior of polycap networks,²⁴ Gong and co-workers reported the microphase separation of polystyrene and polyethylene-oxide polymers monofunctionalized with a linear complementary six-fold hydrogen bond motif based on oligo-amides ($K_a > 10^9 \text{ M}^{-1}$).²⁵ Even though an elegant study by Rowan and co-workers on the combination of hydrophobic interactions and weak hydrogen bonds based on nucleobase derivatized poly(tetrahydrofuran) (pTHF) showed polymer-like properties for otherwise low-molecular weight material,²⁶ it is generally believed that strong complementary binding motifs are necessary to ensure block copolymer formation in solution and especially in the bulk.

Recently, Li and coworkers have reported the strong and selective complexation of the 6[1H] tautomeric form of a 2-ureido-pyrimidinone (UPy) derivative **1** with 2,7-diamido-1,8-naphthyridines^{27,28} **2** (Napy) via quadruple hydrogen bonding between ADDA and DAAD arrays (Figure 6.2).²⁹⁻³³ As shown in the previous chapter, the dual complexation modes of the UPy result in concentration dependent selectivity, favoring UPy-Napy heterocomplexation over UPy homodimerization by a factor of $> 20:1$ above 0.1 M ($K_a = 5 \times 10^6 \text{ M}^{-1}$ in CHCl_3).³⁴ Because of this high selectivity and strength, the UPy-Napy heterodimer seems eminently suitable for constructing supramolecular block copolymers with high degrees of polymerization (DP) in solution as well as in the bulk.

The introduction of a Napy unit into bifunctional molecules and its influence on self-assembly in solution as well as the solid state with bifunctional UPy molecules is investigated in more detail in this chapter. The first part will focus on the synthesis and complexation behavior of small bifunctional Napy molecules with bifunctional UPy derivatives containing small or polymeric spacers in solution. In the second part, a strategy based on ring opening metathesis polymerization (ROMP) leading to the synthesis of pure bifunctional UPy and Napy containing polymers is introduced. The formation of supramolecular, alternating copolymers is examined in solution. The resulting phase-segregating behavior is subsequently studied in the bulk.

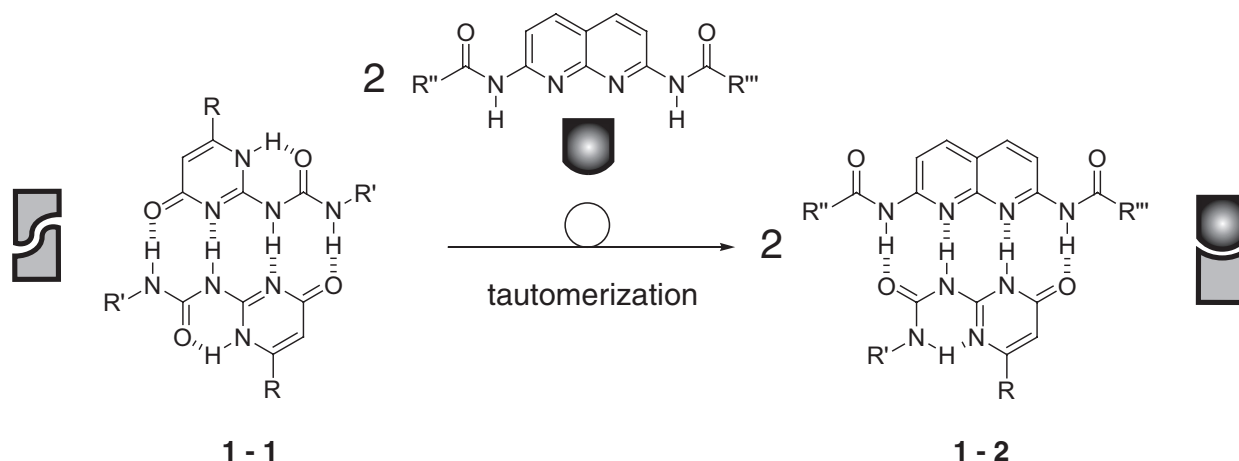
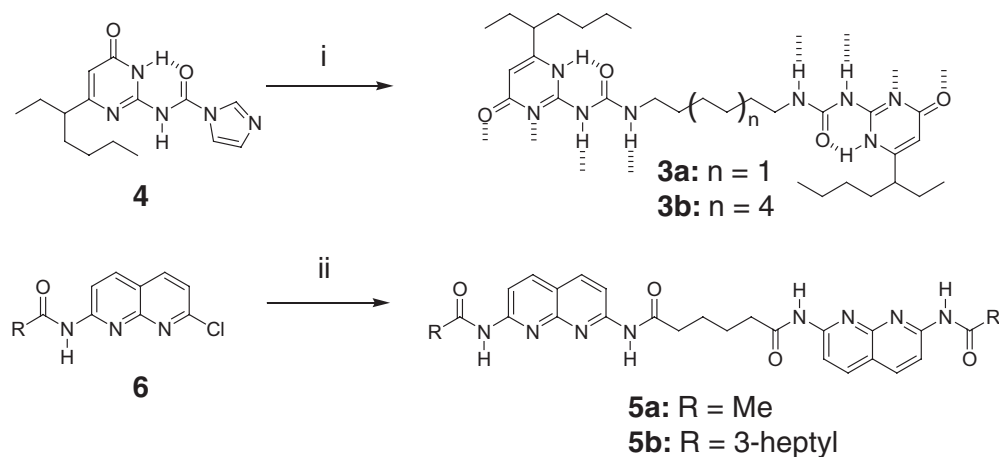


Figure 6.2 Dynamic equilibrium between UPy homodimers through an AADD self-complementary quadruple hydrogen bonding motif and UPy – Napy heterodimer through an ADDA – DAAD complementary motif.

6.2 Supramolecular systems based on small bifunctional Napy molecules

6.2.1 Synthesis and characterization

The study of UPy-Napy supramolecular copolymers requires a multi-gram synthesis of both bifunctional UPy as well as Napy derivatives. Due to both ease of purification and mild reaction conditions, UPy derivatives **3** were synthesized by reaction of alkyl diamines with imidazolidine-activated 6(3-heptyl)-isocytosine **4** (Scheme 6.1).³⁵ Products **3a** and **3b** containing either a hexyl or a dodecyl spacer were obtained after multiple precipitations in 95 and 90% yield, respectively. Both compounds were highly soluble in a range of organic solvents and gave highly viscous solutions in chloroform and toluene indicating supramolecular polymer formation.³⁶ Bifunctional Napy derivatives **5a** and **5b** were prepared using the efficient palladium-catalyzed Buchwald-Hartwig amidation³⁷ reaction between 7-amido-2-chloro-1,8-naphthyridines and hexanedioic amide as described in Chapter 3 (Scheme 6.1).²⁸ Amidation of 7-acetamido-2-chloro-1,8-naphthyridine **6a** and 7-(2-ethylhexanoyl)amino-2-chloro-1,8-naphthyridine **6b** afforded compounds **5a** and **5b** in 25 and 50% yield, respectively, after purification by column chromatography. In contrast to its 3-heptyl analogue, derivative **5a** was considerably less soluble in organic solvents such as chloroform and toluene. However, it was possible to dissolve the compound completely in chloroform upon addition of 2.5 equivalents of a monofunctional UPy derivative. Investigation by ¹H NMR spectroscopy showed the formation of UPy – Napy heterodimers as discussed in Chapter 5.



Scheme 6.1 Synthesis of bifunctional UPy and Napy molecules with small spacers; (i) alkyl-diamine, CHCl_3 , 66 °C; (ii) $\text{Pd}(\text{OAc})_2$, Xantphos, K_2CO_3 , adipamide, 1,4-dioxane, 18 h, 100 °C.

6.2.2 Towards UPy – Napy based supramolecular alternating copolymers

A characteristic property of polymeric structures, which distinguishes them from small aggregates, is their relatively high solution viscosity. For very pure bifunctional UPy derivatives with linear alkyl spacers, Sijbesma *et al.*³⁶ reported very high specific viscosities (η_{sp}). UPy-Napy complexation in UPy-based supramolecular polymers in chloroform was studied by addition of monofunctional Napy **2** ($R'' = R''' = \text{undecyl}$) to a 40 mM solution of bifunctional UPy **3a** in chloroform. The strong reduction of specific viscosity that results from addition of small amounts of **2** (Figure 6.3a), is similar to the effect of adding monofunctional

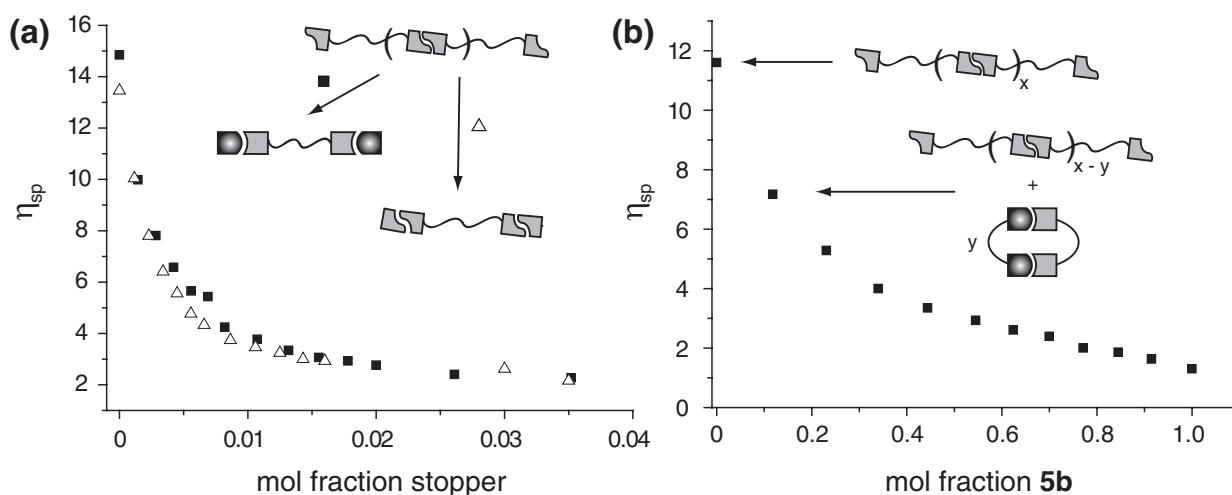


Figure 6.3 (a): Specific viscosity of 40 mM bisUPy **3a** in chloroform as a function of added monofunctional Napy **2** (■) and UPy **1** (△) and a graphical representation of the end-capping processes; (b): Specific viscosity of 40 mM bisUPy **3b** in chloroform as a function of added bisNapy **5b** (■) and a graphical representation of the cycle formation process.

UPy **1** (R = methyl, R' = butyl),³⁶ confirming the selectivity of heterocomplex formation. Thus, as the amount of **2** increases, UPy-telechelic polymers of decreasing DP are formed which are end-capped with Napy groups. These results indicate a similar unidirectionality in hydrogen bonding of **2** as a chain-stopper as compared to monofunctional UPy **1**.

It was anticipated that the addition of a concentrated solution of a bifunctional Napy derivative to a solution of bifunctional UPy compound would lead to an increase or equally high specific viscosity due to incorporation of the Napy derivative and concomitant elongation of supramolecular polymers. However, titration of a 40 mM solution of bifunctional UPy **3b** with bifunctional Napy **5b** led to a strong decrease in η_{sp} (Figure 6.3b). This result can be rationalized considering the combined effects of selective heterocomplexation and the propensity of small monomers to form cyclic dimers. It is well-documented that supramolecular polymers form randomly coiled linear chains that are in dynamic equilibrium with cyclic structures in solution. The ring-chain equilibrium is characterized by a critical polymerization concentration (CPC),^{38,39} which is determined by chain length and the presence of ring strain. Below the CPC, only cyclic aggregates are present. Above this concentration, polymeric aggregates are formed while the concentration of cyclic oligomers is constant. This phenomenon has been studied using NMR spectroscopy and viscometry for a range of hydrogen bonded supramolecular polymers.⁴⁰ While for UPy derivatives similar to **3a** a CPC < 10 mM was determined, preorganization of the spacer between two UPy functionalities was shown to result in a significant increase of CPC (10 – 300 mM)^{36,41-43} or even exclusive formation of extremely robust dimers with a tetramethyl-*m*-xylylene linker.⁴⁴ Therefore, cycle formation from short monomers **3b** and **5b** is anticipated to be significant. The extent to which this occurs in the titration may be probed by comparing the effects of *adding* fraction *y* of **5b** and *removing* fraction *y* of **3b** from a solution of **3b**. The changes in viscosity were remarkably similar. For example, when 4.7 mM of **5b** was added to a 40 mM solution of **3b** ($\eta_{sp} = 11.6$), η_{sp} decreased to 7.2, while a value of 7.4 was observed when the concentration of **3b** was reduced by 5 mM. In summary, the viscosity data strongly suggest the quantitative formation of cyclic heterodimers **3b** – **5b**. Due to the relatively short spacers, the cyclic species are suggested to be predominantly dimeric. Cycle formation in this system was investigated further by diffusion-ordered NMR experiments discussed in the next section. In addition, CPK modeling confirmed the possibility of dimeric cycle formation with these bifunctional molecules.

6.2.3 Diffusion-ordered 2D NMR (DOSY) experiments

The dynamic nature of the hydrogen bond is a feature which can be addressed by external stimuli such as polarity of a solvent, temperature and pH. Diffusion-ordered ^1H NMR spectroscopy (DOSY) measurements have been applied for the characterization of supramolecular aggregates and have provided useful information about the size of these aggregates.^{45,46} As shown in the previous section, bifunctional UPy derivative **3b** and mixtures of this compound with bifunctional Napy derivative **5b** form cyclic and linear hydrogen bonded aggregates, depending on the concentration of the solution. Linear polymers are formed from **3b**, while cyclic heterodimers **3b** – **5b** are formed upon addition of **5b**. As described in the previous chapter, the linear supramolecular UPy homopolymer and the heterodimeric UPy-Napy cycle give rise to different resonances in ^1H NMR. These two sets of signals will give rise to distinct signals in the second dimension due to the difference in diffusion rate between polymeric and cyclic species. Therefore, in order to investigate the ring-chain transition in chloroform solution of 1.5:1 mol% mixtures of **3b** – **5b**, 2D-DOSY NMR experiments were performed using heptakis(2,3,6-tri-O-methyl)- β -cyclodextrin (CD) as an internal standard (MW = 1429 g/mol). Figure 6.4 shows part of the 2D-DOSY spectra with graphic representations of the species present in the mixture. In addition, Table 6.1 summarizes the relative diffusion coefficients of the supramolecular UPy polymer and the UPy-Napy signals. At low concentration, three regions are observed which are attributed to UPy polymer, UPy homodimeric cycle and the UPy-Napy cycle, respectively. Upon increase in concentration, the UPy polymer increases in size (i.e. the degree of polymerization increases from x to $x + y$). Additionally, a higher diffusion coefficient is observed for the heterodimer. This probably indicates the presence of small heterodimeric rings that are in equilibrium with larger rings or alternating copolymers. Further increase of the concentration led to a very viscous solution. The DOSY-NMR spectrum shows two signals belonging to aggregates with low diffusion constants. These indicate a gradual change in heterocomplex composition from purely cyclic to predominantly polymeric material upon increase in concentration exchanging fast on the NMR time scale. It has to be noted that, in contrast to UPy homodimers, no separate signals are observed for UPy – Napy heterodimers in cyclic or polymeric aggregates.

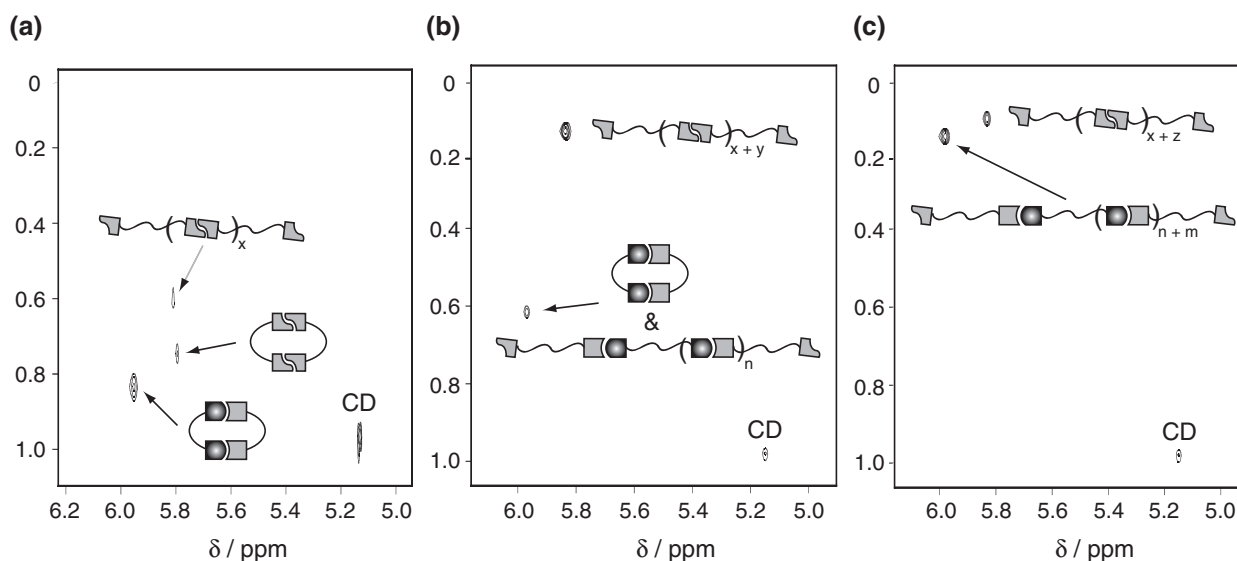


Figure 6.4 Partial 2D DOSY NMR spectrum including the internal reference (CD) and graphical representations of the species present in solution at different concentrations; (a): 15 mM **3b** and 10 mM **5b**; (b): 40 mM **3b** and 4.8 mM **5b**; (c): 150 mM **3b** and 100 mM **5b**.

Table 6.1 Diffusion coefficients of **3b** – **5b** mixtures relative to CD at different concentrations.

	concentration 3b – 5b		
	15 – 10 mM	40 – 4.8 mM	150 – 100 mM
Cyclodextrin	1.0	1.0	1.0
UPy-polymer	0.62	0.16	0.11
UPy-Napy	0.86	0.62	0.16

6.2.4 Increasing spacer length to induce alternating copolymer formation

In order to minimize the fraction of cyclic species that is formed, the supramolecular functionalities need to be separated by polymeric spacers. Therefore, readily available macromonomer **7** was chosen as the bifunctional UPy compound in which the UPy functionalities are separated by a poly(tetrahydrofuran) (pTHF) ($M_n = 10^3$ g/mol) spacer (Figure 6.5). This compound was prepared previously by Keizer *et al.* by reaction of a commercially available hydroxy telechelic pTHF with a UPy-isocyanate synthon.⁴⁷ As mentioned previously, an important aspect in supramolecular polymer systems is the degree of functionalization (F) of the hydroxyl groups of the pTHF since small amounts of monofunctional UPy-pTHF can act as chain stoppers in the polymer. A convenient method for determining hydroxy end groups in polymers is quantitative ^{19}F NMR spectroscopy,⁴⁸ which has recently been employed for the determination of the degree of functionalization of UPy telechelic poly(ethylenebutylene).⁴⁹ The hydroxy end groups in **7** were quantified by ^{19}F NMR through reaction of the hydroxy end

groups with hexafluoroacetone (HFA) to form the hemiacetal HFA adduct. Using the HFA adduct of *p*-nitrobenzylalcohol as an internal standard, the fraction of hydroxy end groups per chain was determined to be 1.8%. Assuming that all other end groups are UPy-functionalized, a degree of functionalization of > 1.98 was determined for **7**.

Titration of a 25 mM solution of this UPy telechelic pTHF **7** ($F > 1.98$) with **5b** resulted in a viscosity plot with two distinct regions (Figure 6.5a). Upon addition of less than 1 equivalent of **5b**, only a small decrease in viscosity was observed, changing from $\eta_{sp} = 10.4$ for the pure solution of **7** to $\eta_{sp} = 8.5$ in the presence of 0.99 equivalents of **5b**. This must imply that **5b** is incorporated into the supramolecular polymer main chain. Hence, at the equivalence point a true alternating supramolecular copolymer is obtained. This was also substantiated by the absence of UPy homodimer signals in the ^1H NMR spectrum at the equivalence point. When a further 0.1 equivalent of **5b** was added, however, the η_{sp} was dramatically reduced to 4.3. At this stage, additional molecules of **5b** can no longer be incorporated into the polymer chains. They therefore act as chain stoppers, and the DP of the alternating copolymer is progressively reduced. The observed effect in the last stage of the titration is analogous to the effect of adding monofunctional UPy **1** or monofunctional Napy **2** to a 25 mM solution of **7** in CHCl_3 (Figure 6.5b).

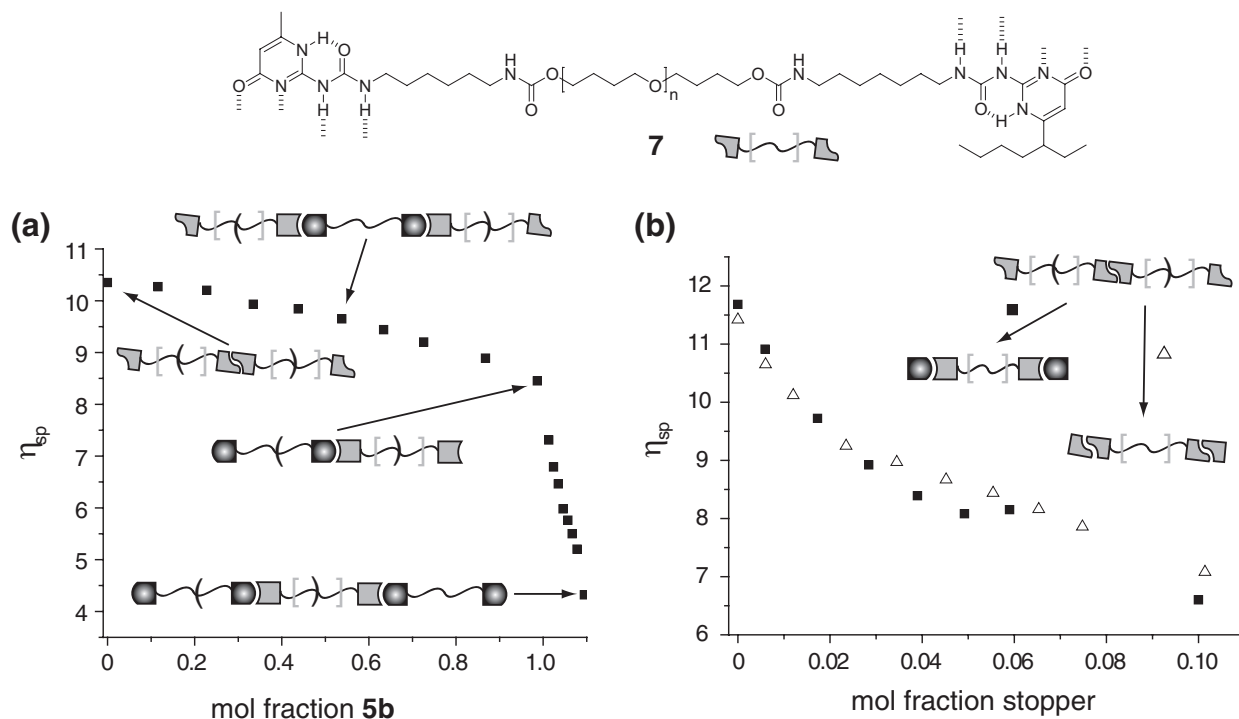


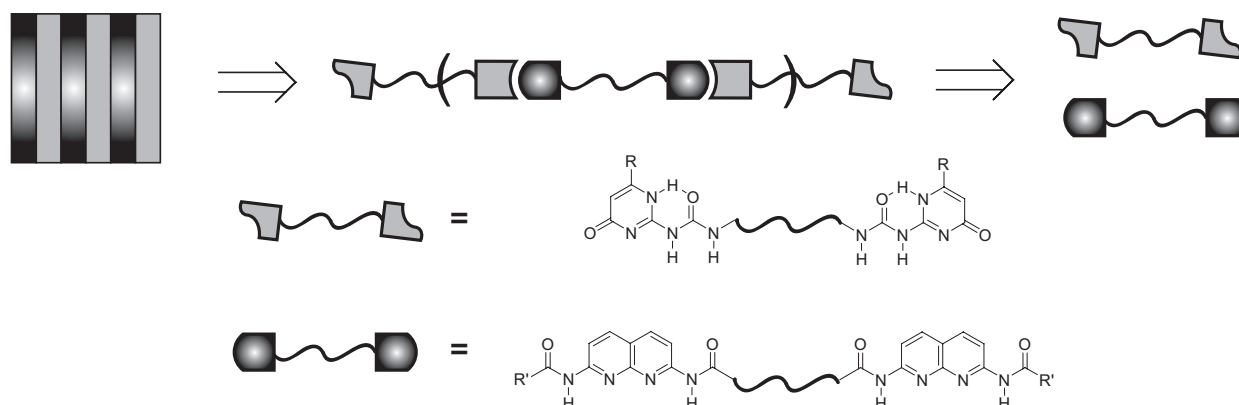
Figure 6.5 Specific viscosity of 25 mM **7** in chloroform as a function of (a): added bisNapy **5b** (■) and a graphic representation of the associated processes; (b): added monofunctional Napy **2** (■) and UPy **1** (△) and a graphic representation of the end-capping processes.

These results can be rationalized by considering the combined effects of selective heterocomplexation and the differences in ring-chain equilibrium between **3b** and **7**. While significant cycle formation has been observed for small bifunctional molecules, only a limited amount of cyclic heterodimer is expected to be formed upon titration of macromonomer **7** with **5b**. In summary, the data proves that supramolecular polymers based on bifunctional UPy and Napy molecules are able to retain a high DP over a broad composition range. This is in contrast to previously reported polymer systems which were solely based on complementary hydrogen bonding units.

6.3 Supramolecular systems based on polymeric bifunctional Napy molecules

6.3.1 Introduction

Recent developments in the field of supramolecular polymer chemistry have shown that low molecular weight building blocks equipped with complementary as well as self-complementary units can lead to well-defined structures through self-assembly. However, in order to obtain materials with desired macroscopic properties in the bulk, the multiple hydrogen bonding arrays need to be separated by polymeric spacers. To this end, a retrosynthetic approach towards $(AB)_n$ supramolecular block copolymers, as schematically depicted in Scheme 6.2, can be envisioned. For the last decades, the concept of retrosynthetic analysis has aided synthetic chemists who were interested in reconstructing complex natural molecules or other chemical targets.⁵⁰ However, this approach has yet to be introduced in supramolecular polymer chemistry. Application of this synthetic strategy to supramolecular polymeric materials could start from a simple diblock copolymer structure or morphology which possesses the intended materials properties. From thereon, its individual blocks are derived containing the appropriate hydrogen bonding motifs. Additionally, the previous section already illustrated the use of UPy – Napy heterodimerization in supramolecular copolymers. Therefore, using a retrosynthetic approach, a specific type of microphase separated morphology is expected to be obtained by simple mixing of the appropriate amount of bifunctional UPy and Napy monomer with the desired chain lengths.



Scheme 6.2 Schematic representation of a supramolecular retrosynthetic approach towards block copolymers containing a complementary quadruple hydrogen bonding array based on UPy and Napy groups.

The preparation of supramolecular block copolymers can be achieved with X – X and Y – Y bi-functional macro-monomers, which are telechelic polymers bearing UPy (X) and Napy (Y) endgroups. During last decade, several groups have reported the preparation of main-chain supramolecular polymers using post-polymerization modification routes on commercially available telechelic polymers.^{15,20,21,23,26,47,51-53} While this approach might be viable for small molecules and a polymer chain of low molecular weight (MW), complete transformation at every chain end is not realistic for higher MW polymers. With M_n values > 30-40 kg/mol, it is nearly impossible with common spectroscopic methods to discern whether or not complete transformation of an end group has occurred. Hence, post-polymerization-based strategies can easily lead to small, yet significant percentages of mono-functional polymer chains which will act as chain stoppers. Even a small percentage of mono-functional polymer (< 1%) can lead to a dramatic reduction in the degree of polymerization (DP),³⁶ and hence, polymer properties.⁵⁴ In addition, post-polymerization-based strategies often lack functional group compatibility due to competitive reactions and commercially available telechelic (main chain) polymers do not always display a degree of functionality of exactly 2 ($F = 2.0$).

The preparation of telechelic polymers with an end-group functionality of precisely two can be attained easily by starting with a pure small molecule which already contains the two UPy or Napy motifs and growing a polymer chain in between the end groups. This can be accomplished through ring-opening metathesis polymerization (ROMP) of a cyclic olefin in the presence of a bifunctional chain transfer agent (CTA).⁵⁵⁻⁵⁷ Figure 6.6 illustrates the ROMP of an unsubstituted cyclic olefin in the presence of a bis-UPy or bis-Napy CTA. The versatility of this polymerization technique was illustrated by the synthesis of a wide variety of polar,⁵⁶ non-polar⁵⁸ and even conducting polymers⁵⁹ by ROMP with the highly active, second generation

Grubbs ruthenium catalyst.⁶⁰ Although the concept for the synthesis of telechelic polymers with supramolecular binding motifs via ROMP has been reported very recently, true copolymer properties were not substantiated in solution or in the bulk.⁶¹

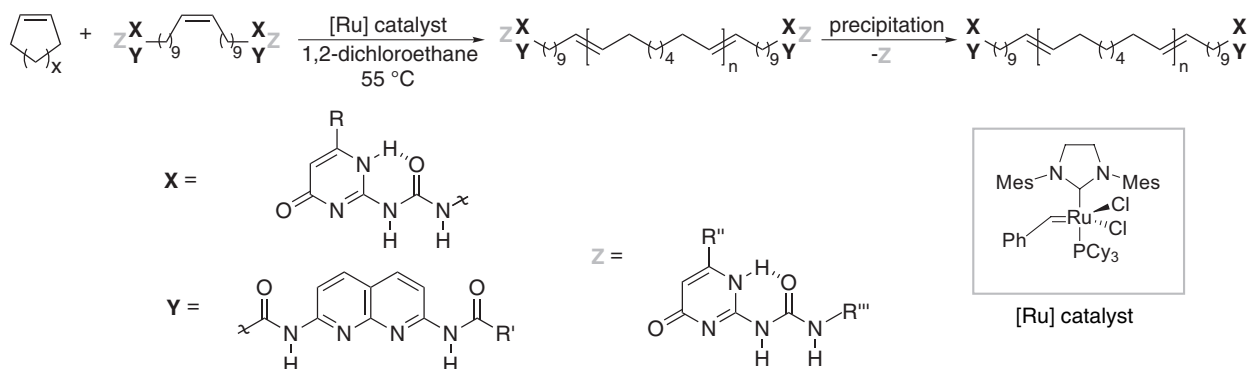


Figure 6.6 ROMP of a cyclic olefin with a CTA containing supramolecular functionalities X or Y, in the presence of a supramolecular UPy protecting group Z.

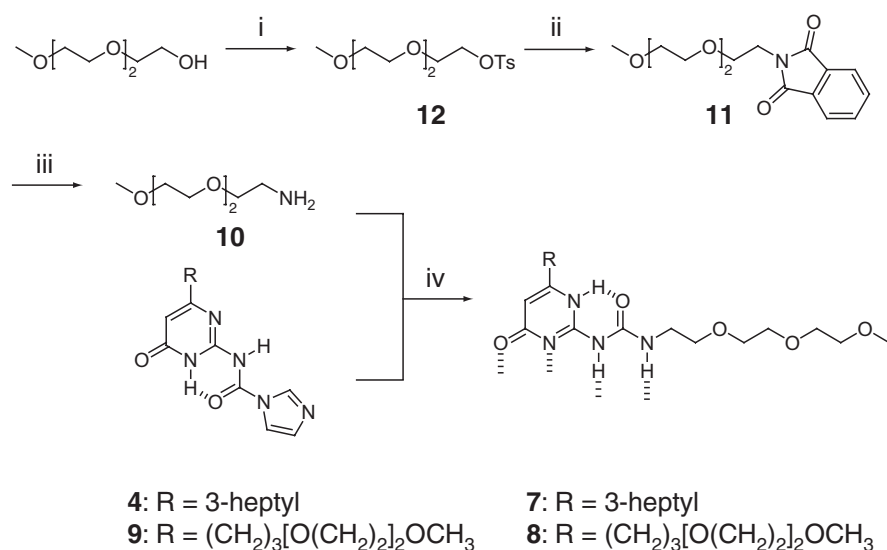
Analogous to a number of covalent reactions applying protective group strategies, the use of a supramolecular protecting group (Z) is anticipated to be very important during the polymerization process. When the CTA contains UPy functionalities, the mono-functional UPy protecting group would serve to limit build-up of viscosity during the polymerization. When the functionality of the CTA is a Napy, the protecting group will be necessary to inhibit coordination of the Napy to the active ruthenium center. Indeed, 1,8-naphthyridine derivatives have been studied before as ligands forming di- and mono-nuclear complexes with transition metals⁶² and ruthenium-Napy complexes have been isolated and studied as homogenous catalysts.⁶³⁻⁶⁵ In addition, it was found that the color of a reaction mixture containing both Grubbs' catalyst and Napy turned from yellow/orange to green suggesting that the Napy moiety deactivates the Grubbs' catalyst by coordination.⁶⁶

Finally, the ROMP of a cyclic monomer with a CTA not only allows for a large structural variation of the main chain polymer with UPy/Napy endgroups but also enables control over DP by simple adjustment of the ratio of monomer to CTA. Therefore, simple alteration of the cyclic olefin monomer followed by mixing of the X – X and Y – Y macro-monomers will result in the self assembly of many new supramolecular block copolymers with tunable properties. A straightforward example could be the combination of a telechelic bis-UPy polyethylene (hard block) with a telechelic bis-Napy polybutadiene (hard block) to create dynamic thermoplastic elastomers (TPE). The work described in the following sections was performed in collaboration with Dr. Oren A. Scherman.

6.3.2 Synthesis and characterization

6.3.2.1 UPy protecting groups

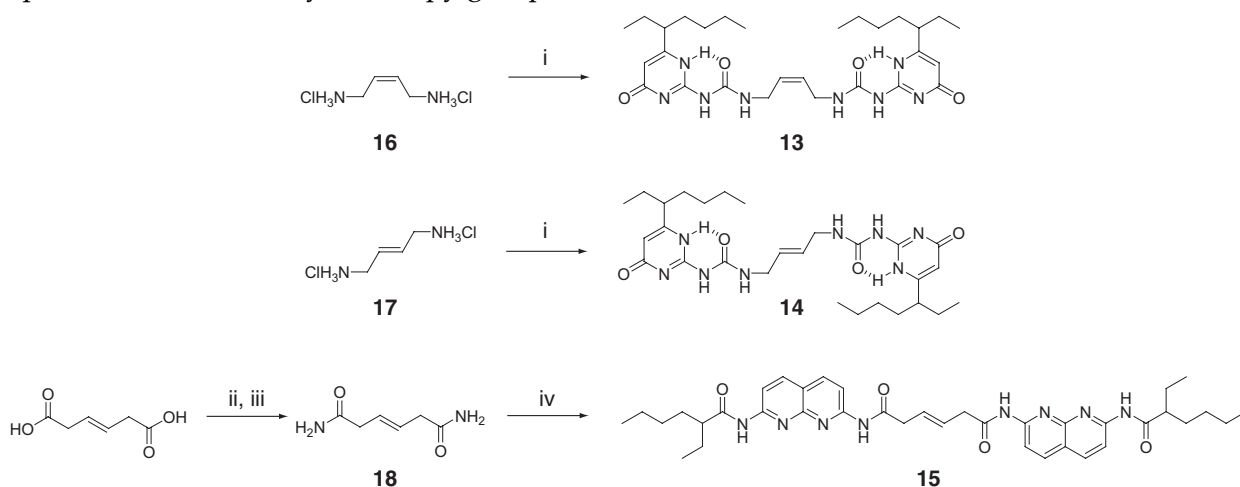
Supramolecular protecting groups using metathesis polymerization techniques have been reported before for the protection of triple hydrogen bond arrays with thymine derivatives.^{67,68} However, the applied protecting groups cannot be used when UPy and Napy functionalities are the hydrogen bonding moieties. Because of their dual binding modes, UPy derivatives are able to bind both UPy as well as Napy compounds in chloroform and toluene. Furthermore, due to its strong binding a small excess of 1.2 equivalents to the UPy or Napy functionality ensures quantitative protection. In order to facilitate their removal from an apolar metathesis polymer, UPy derivatives **7** and **8** bearing one or two triethylene glycol tails respectively were designed. Due to both ease of purification of UPy imidazolides and the mild reaction conditions,³⁵ the derivatives were synthesized from their corresponding imidazolides **4** and **9** in 90 and 92% yield for **7** and **8**, respectively. Amino-triethylene glycol **10** was synthesized in 62% yield from tosylate **12** by in situ deprotection of phthalimide **11** by hydrazine monohydrate. While phthalimide **11** was not isolated, tosylate **12** could be obtained in 95% from the reaction of commercially available triethyleneglycol monomethylether with tosyl chloride. Due to the 3-heptyl substituent on the pyrimidinone ring and the triethylene glycol tail, UPy **7** displays high solubility in a variety of solvents including THF and ethanol. More polar UPy **8** is even readily soluble in methanol.



Scheme 6.3 Synthesis of UPy protecting groups; i): NaOH, TsCl, THF/H₂O, 2 h, RT; ii): potassium phthalimide, DMF, 3 h, 110 °C; iii): NH₂NH₂·H₂O/EtOH, 16 h, 110 °C; iv): CHCl₃, 16 h, 50 °C.

6.3.2.2 Bifunctional UPy and Napy CTAs

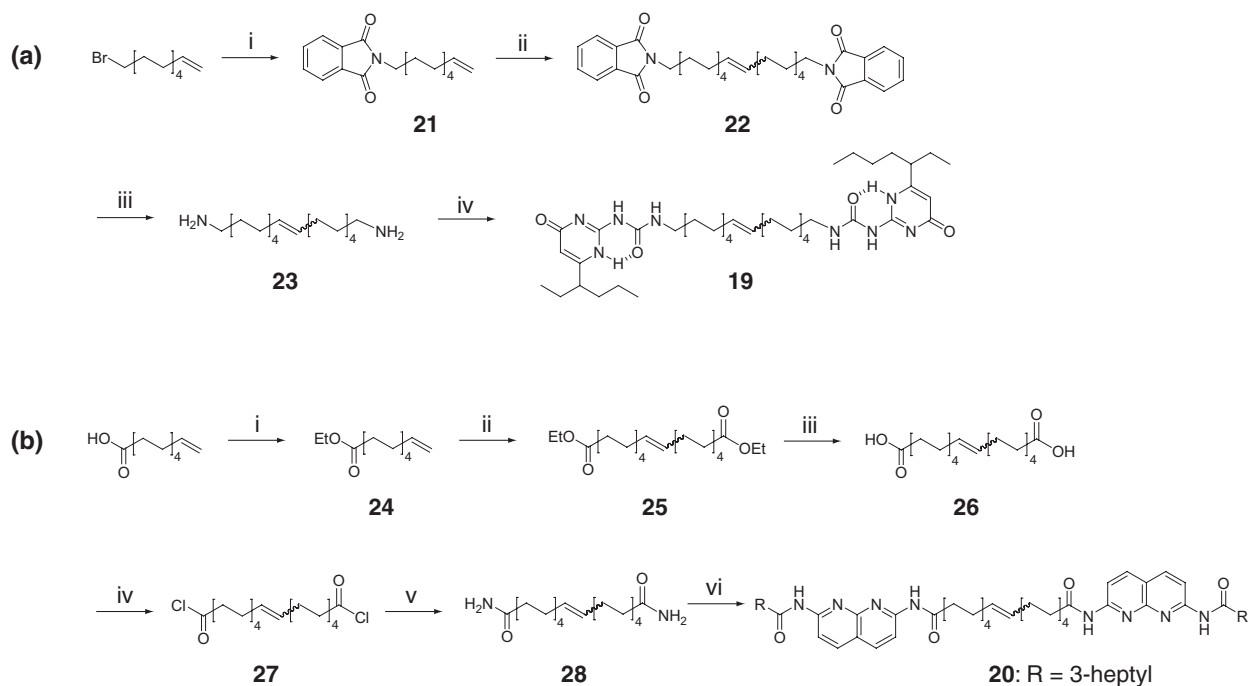
The basic design of CTAs employed in ROMP requires symmetric, acyclic olefins. Many CTAs reported in literature are based on *cis*-2-butene spacers.^{55,69-72} For synthetic ease,⁷³ both *cis*- and *trans*-bis-UPy CTAs **13** and **14** with a C4 spacer as well as the *trans*-bis-Napy CTA **15** with a C6 spacer (Scheme 6.4) were prepared. *Cis*- and *trans*-1,4-diamino-2-butene·2HCl CTAs **16** and **17** were easily synthesized according to literature procedures.^{72,74} Subsequent condensation of these salts with an excess of UPy-imidazolidine **4** followed by isolation by precipitation afforded bifunctional UPy CTAs **13** and **14** as white powders in 64% and 80%, respectively. Diamide CTA **18** was synthesized in 50% by acid chloride formation of *trans*- β -hydromuconic acid followed by precipitation in aqueous ammonia and crystallization from water. Palladium catalyzed amidation of 7-(2-ethylhexanoyl)amino-2-chloro-1,8-naphthyridine **6b** with **18** gave bifunctional Napy CTA **15** in 48% yield after purification by column chromatography. Although these CTAs are easily prepared, the relative steric crowding of the supramolecular moieties around the internal olefin could potentially interfere in the ROMP of a cyclic olefin. Therefore, in addition to CTAs **13** – **15**, two new CTAs were prepared with a larger carbon spacer between the UPy and Napy groups.



Scheme 6.4 Synthesis of UPy and Napy CTAs based on C4 and C6 spacers; i): UPy-imidazolidine **4**, Et₃N, CHCl₃, 24 h, 45 °C; ii): SOCl₂, 5 h, 80 °C; iii): NH₃/H₂O, 20 h, RT; iv): chloroNapy **6b**, Pd(OAc)₂, Xantphos, K₂CO₃, 1,4-dioxane, 18 h, 100 °C.

The synthetic routes to CTAs **19** and **20** with a C20 spacer, both based on a C11 terminal olefin which is commercially available, are depicted in Scheme 6.5. The synthesis of bis-UPy CTA **19** (Scheme 6.5a) commences with the reaction of potassium phthalimide with undecenebromide to phthalimide **21** in 78% yield. Bis-phthalimide CTA **22** was prepared in 60% yield utilizing a homo-dimerization through olefin cross metathesis reaction in the presence of 2nd

generation Grubbs' ruthenium catalyst. Deprotection of **22** with hydrazine monohydrate resulted in quantitative conversion to bis-amino CTA **23**. Subsequent reaction with UPy-imidazolidine **4** provided bis-UPy CTA **19** in 62% isolated yield. Ester **24** was obtained in 92% yield by simple acid catalyzed esterification of 10-undecenoic acid (Scheme 6.5b). By a procedure analogous to the synthesis of **22**, ethyl ester functionalized CTA **25** was obtained in 71% yield through ruthenium catalyzed olefin cross metathesis. Subsequent hydrolysis, acid activation and amidation gave intermediate CTAs **26** – **28** in 85%, 97% and >99% yield, respectively. Finally, bis-Napy CTA **20** was obtained in 65% yield by using the palladium catalyzed amidation procedure described in Chapter 3.



Scheme 6.5 (a) Synthesis of UPy CTA **19**; i): potassium phthalimide, DMF, 18 h, 75 °C; ii): 2nd gen. [Ru], 21 h, 55 °C, vacuum; iii): $\text{NH}_2\text{NH}_2 \cdot \text{H}_2\text{O}$, THF, 24 h, 70 °C; iv): UPy-imidazolidine **4**, Et_3N , CHCl_3 , 24 h, 50 °C; (b): Synthesis of Napy CTA **20**; i): H_2SO_4 , EtOH, 24 h, 80 °C; ii): 2nd gen. [Ru], 3 d, 55 °C, vacuum; iii): NaOH, EtOH, 24 h, 100 °C; iv): SOCl_2 , 4 h, 60 °C; v): conc NH_3 (aq), 1 d, RT; vi): chloroNapy **6b**, $\text{Pd}(\text{OAc})_2$, Xantphos, K_2CO_3 , 1,4-dioxane, 18 h, 100 °C.

Since any mono-functional UPy or Napy CTA would be detrimental in the preparation of α - ω -telechelic polymers, special attention was given to the removal of any non-dimerized phthalimide **22** or ethylester **25** by successive re-crystallization or column chromatography, respectively. Furthermore, bis-UPy CTA **19** was purified by multiple precipitations from MeOH and bis-Napy CTA **20** was purified by column chromatography. Both **19** and **20** were confirmed to be pure by NMR spectroscopy, elemental analysis and MALDI-ToF-MS.

6.3.2.3 UPy and Napy telechelic polymers

With the CTAs described in the previous section, ROMP experiments of 1,5-cyclooctadiene (COD) and cyclooctene (CO) were performed. These monomers were chosen for a number of reasons: i) their well-known reactivity in ROMP; ii) the produced poly(butadiene) (PBD) and poly(cyclooctene) (pCO) are commercially interesting polymers and can be hydrogenated to the even more interesting poly(ethylene); iii) the possibility to expand the scope towards ROMP of cyclooctatetraene^{59,75} to obtain conducting supramolecular polymers or functionalized cyclooctene.^{76,77} It has to be noted that PBD polymers have a higher tendency towards cross-linking than pCO polymers and hence form insoluble networks. This can be decreased substantially by the addition of 2,6-di-*t*-butyl-4-methylphenol (BHT) as a radical scavenger. All polymerizations were performed with the 2nd generation Grubbs' ruthenium catalyst in either dry toluene or 1,2-dichloroethane (DCE) at 55 °C. Typically, monomer to catalyst ratios of 7000-5000 : 1 were used at monomer concentrations between 1.5 and 3 M and reactions were stopped after 48 hours. In order to investigate the influence of a supramolecular protecting group, a number of polymerizations were performed with the CTAs under various conditions. In addition, ROMP with 3-hexene **29** as a CTA was carried out to obtain a reference polymer with no interacting chain ends. The results of the polymerization reactions are displayed in Table 6.2.

UPy and Napy CTAs **13 - 15** with short linkers were first polymerized to prepare the α - ω -telechelic polymers by ROMP (entries 1-5). Unfortunately, steric crowding of the supramolecular moieties around the internal olefin severely limited the use of these CTAs in the ROMP of COD. Generally, upon addition of ruthenium catalyst, the yellow COD/CTA solution turned light orange and gelled immediately even when UPy **7** was applied as a supramolecular protecting group. In contrast, when bisNapy CTA **15** is used, the solution turns green and polymerization is inhibited (entry 4). Addition of UPy **7** to a solution of **15** indeed prevents coordination of the Napy moiety to the ruthenium catalyst (entry 5). However, the ROMP reaction was not controlled in entries 1-5 and high molecular weight polymer is primarily formed without functional end groups. Controlled polymerization of cyclooctene was possible when bisUPy CTA **19** was used in combination with UPy **7** (entry 6). After addition of catalyst the reaction solution turned yellow and gelled within 5 minutes as mentioned earlier. However, as the reaction proceeded, the CTA was incorporated into the initially formed large chains and smaller chains were being formed leading to a less viscous solution. When UPy **8** was used as the protecting group, less control was observed in the

polymerization process (entry 7). Possible explanations of this result could involve ligation of the oxygen atoms in the two triethylene glycol tails to the active ruthenium center which can potentially disturb the metathesis. Furthermore, although the association constants of **7** and **8** are similar ($K_a = 2.4 \times 10^6$ and $1.9 \times 10^6 \text{ M}^{-1}$, respectively)⁷⁸ it has been known that larger ethylene glycol groups result in a smaller dimerization constant ($K_{\text{dim}} < 2 \cdot 10^4 \text{ M}^{-1}$).⁷⁹ Apparently, UPy **7** has the right balance between protection of the UPy or Napy functionality, ease of removal and compatibility with the metathesis catalyst.

Table 6.2 Synthesis and characterization for the ROMP of cyclic monomers with CTAs **13** – **15**, **19**, **20** and **29**.

entry	Monomer	CTA	[M]/[CTA]	SPG ^c	M _n ^{d,e} kg/mol	M _w ^d kg/mol	PDI	polymer	yield (%)
1 ^a	COD	13	34	-	22.7	118	5.2	30a	20
2 ^a	COD	13	34	7	13.9	96.9	6.9	30b	33
3 ^a	COD	14	20	7	25.6	92.1	3.6	30c	62
4 ^a	COD	15	38	-	-	-	-	31a	-
5 ^a	COD	15	38	7	45.6	121	2.7	31b	32
6 ^b	CO	19	28	7	10 (5.2)	22.0	2.2	32a	88
7 ^b	CO	19	28	8	18.7	60.0	3.2	32b	70
8 ^b	CO	20	28	7	8.0 (5.1)	13.0	1.6	33a	60
9 ^b	CO	20	10	7	3.4 (3.8)	8.1	2.4	33b	47
10 ^b	CO	20	28	8	44.5	73.4	1.7	33c	70
11 ^b	CO	29	19	-	5.7 (2.8)	10.6	1.8	34	91

^a Toluene as a solvent; ^b DCE as a solvent; ^c SPG stands for supramolecular protecting group ^d determined by GPC in THF relative to polystyrene standards with detection at 270 nm; ^e the M_n value in parentheses was determined by ¹H NMR.

Similar results were obtained when bis-Napy CTA **20** was applied in the ROMP of CO (entries 8-10). While good control of the polymerization process is observed when UPy **7** is used as the protecting group, the use of UPy **8** clearly leads to the formation of higher MW polymer (entry 10 vs entry 8). As a consequence of the loss of low MW functionalized polymer during multiple precipitation purifications when low monomer over CTA ratios are used, the isolated yield of polymer **33b** was lower than for polymers **32a** and **33a**. Noteworthy is the fact that UPy **7** can be recycled when CTAs **19** and **20** are used by collecting the filtrates of each precipitation and purifying by regular silica chromatography. Finally, reference polymer **34** could easily be obtained and purified (entry 11).

As stated before, in order to obtain supramolecular materials with $F_n = 2.0$ the UPy protection group needs to be removed quantitatively from the telechelic polymer. Therefore, all polymers were purified by multiple precipitations from THF solutions into methanol. After complete deprotection, both telechelic UPy and Napy ROMP polymers were characterized by a variety of methods as described in the following paragraphs. For both polymers, GPC was used to obtain the number of repeat units between the supramolecular moieties and thus an M_n value. For polymers with an $M_n < 20$ kg/mol, ^1H NMR was employed to determine the M_n value and confirm complete removal of the protecting group. Figure 6.7a shows the downfield ^1H NMR spectrum of bisNapy polymer **33b** after 1 (bottom) and 3 (top) precipitations. After the first precipitation, characteristic peaks of the UPy – Napy heterodimer are clearly visible,⁸⁰ while the mono-functional UPy is completely removed from the polymer and hydrogen bonding peaks are absent in the NMR spectrum.

Even though analysis by MALDI-ToF-MS was not successful in the characterization of bisUPy-telechelic polymers **32a** and **32b**, it proved useful when low MW bisNapy-telechelic ROMP polymer **33b** was used. A representative spectrum can be seen in Figure 6.7b. One set of polymer peaks can be observed with a mass difference of 110.1 amu and the number of repeat units varies from 3 to 13 in this spectrum. The inset clearly shows that the H^+ , Na^+ and K^+ adducts each fly readily and the masses can be ascribed to a polymer with a precise number of cyclooctene units inserted into the original CTA. The m/z peak at 1429.1 arises from exactly 5 cyclooctene monomers (110.1 g/mol), the original mass of CTA **20** (876.6 g/mol) plus 1 proton.

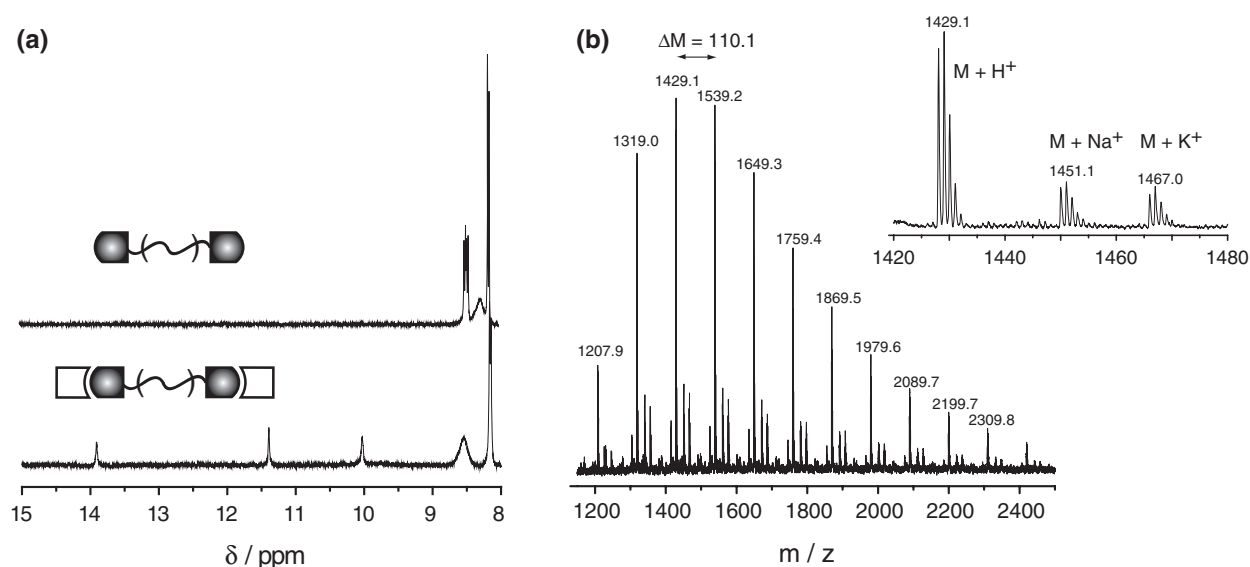


Figure 6.7 Characterization of bisNapy-pCO **33b**; (a): ^1H NMR spectra of **33b** after 1 (bottom) and 3 (top) precipitations; (b): MALDI-TOF MS of **33b** ionized from a CHCA matrix.

Moreover, the supramolecular protecting group and the parent CTA were not observed in the spectrum. In addition to MALDI-ToF MS and ^1H NMR, both FT-IR and UV/Vis spectrometry provided useful information about the deprotection of UPy **7** from the telechelic Napy polymer. When all of the UPy was removed, the FT-IR spectrum revealed a pronounced NH absorption at 3311 cm^{-1} indicating that the NH groups of the Napy moieties were not hydrogen bonded to any UPy. Prior to complete deprotection, a broader peak around 3300 cm^{-1} was observed. The UV/Vis spectrum of free Napy shows an absorption starting at 300 and ending sharply at 350 nm, with a maximum at 346 and several vibronic sub peaks at lower wavelengths. Upon UPy heterocomplexation, however, a new shoulder appears at 355 nm. After three precipitations, the UV/Vis of the telechelic bisNapy polymer **33b** did not display a shoulder at 355 nm, indicative of complete removal of the UPy **7**.

As stated previously in this chapter, the purity of UPy telechelic polymers is essential in the formation of elongated supramolecular polymers with high DP through self-assembly of the self-complementary hydrogen bond motifs. It has been theoretically predicted by Cates⁸¹⁻⁸³ and shown experimentally with solutions of small molecule bisUPys³⁶ that there is a strong dependence of specific viscosity vs. concentration (above the overlap concentration); $\eta_{\text{sp}} \sim c^{3.5-3.7}$ for pure bifunctional supramolecular materials (Figure 6.8, \blacklozenge). With respect to their purity, a number of bisUPy materials were characterized by Ubbelohde viscometry in chloroform (Figure 6.8). Previously, telechelic UPy polymers prepared by post-polymerization modification routes, such as UPy₂-PDMS (\blacksquare),⁸⁴ have yielded slopes of < 2 . This is most probably due to the presence of mono-functional polymer chains which are either due to incomplete functionalization of the commercially available starting materials or incomplete modification of the reactive chain end. These mono-functional chains can act as chain stoppers and severely limit the virtual DP and hence specific viscosity of the polymer solutions. After purification of bisUPy telechelic polymer **32a** by multiple precipitations, viscosity measurements revealed a specific viscosity vs. concentration dependence of 3.72 on a double logarithmic plot (\bullet) after surpassing the overlap concentration. To conclusively show that the slope arises from the absence of chain stoppers, and hence complete functionalization or deprotection of the chain ends, the Ubbelohde viscometry experiment was repeated with a chloroform solution of **32a** to which 2 mol% of UPy **7** was added. The corresponding data set (\odot) clearly shows that the slope (over the same concentration range) has decreased to 2.62. Furthermore, a slope of 1.32 was determined when a viscometry experiment was carried out on reference polymer **34** (\blacktriangle) verifying the absence of non-covalently interacting end groups.

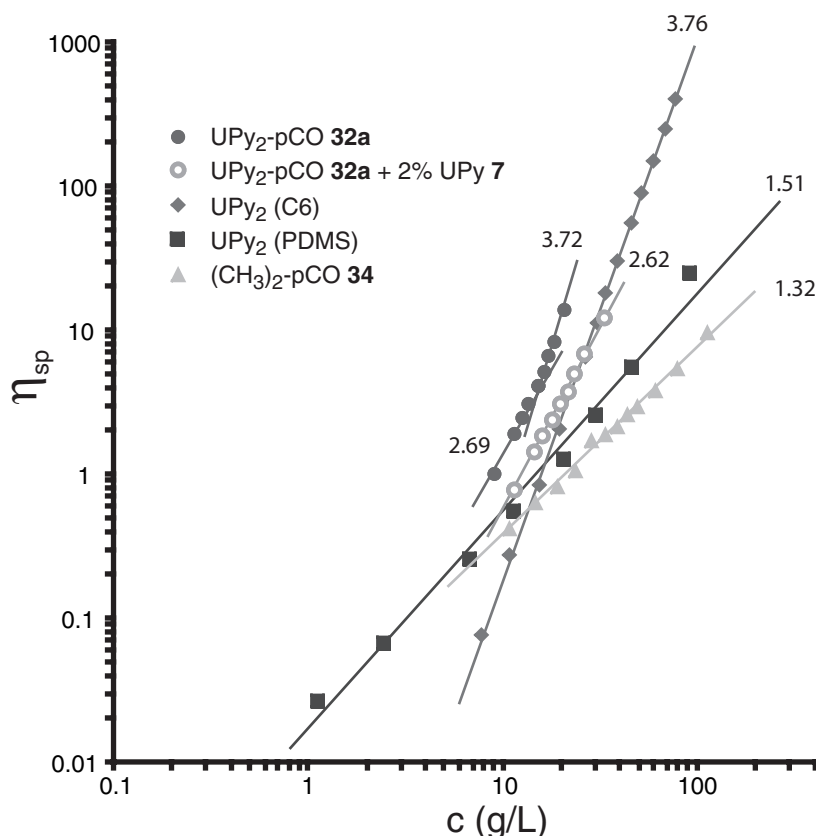


Figure 6.8 Double logarithmic plot of specific viscosity (η_{sp}) vs. concentration (g/L) for several supramolecular materials in chloroform.

6.3.3 Supramolecular block copolymer formation in solution

Once both UPy and Napy telechelic polymers were prepared and characterized as described in the previous section, preparation of $(AB)_n$ type supramolecular block copolymers was attempted. Again Ubbelohde viscometry was used, however this time to illustrate supramolecular block copolymer formation in solution. A major advantage of using the dual binding capability of UPy is that it enables the preparation of materials with a wide range of UPy:Napy ratios. To this end, a chloroform solution containing bisNapy polymer **33b** and bisUPy CTA **19** was prepared in a 1:5 w/w ratio. BisUPy **19** was chosen for two reasons: i) it allows higher solubility of the copolymer mixture and ii) it allows better characterization of the same viscometry solution by both ^1H NMR and UV/Vis compared to the use of bisUPy telechelic polymer **32a**. Figure 6.9a shows a double-logarithmic plot of specific viscosity vs. concentration for the supramolecular $(AB)_n$ system with a slope of 3.48 (●). In this solution, the shorter bisUPy **19** monomers undergo self-assembly to form a supramolecular polymer and the Napy telechelic ROMP polymers **33b** are selectively incorporated into the supramolecular polymer chains by formation of complementary quadruple hydrogen bonding arrays. The

result is a block copolymer with short C20 units and long polyoctenomer units in the same chain. In comparison, viscometry on pure bisNapy-polymer **33a** demonstrates that the Napy end groups interact to some extent giving rise to a slope of 1.7 below and 2.4 above the overlap concentration (\bullet). The incorporation of bisNapy-polymer into a supramolecular bisUPy-material is further confirmed by UV/Vis data. Figure 6.9b illustrates a titration of bisUPy **19** into Napy telechelic ROMP polymer **33b** in chloroform ranging from 0 to 15 equivalents (straight to dashed curve). When all of the Napy endgroups undergo heterodimerization with the UPy moieties, a shoulder at 355 nm is visible in the UV/Vis spectrum, *vide supra*.⁸⁵ This is clearly the case in the **33b** – **19** chloroform solution used in the viscometry experiment as shown by its normalized UV/Vis spectrum (Figure 6.9b, grey curve).

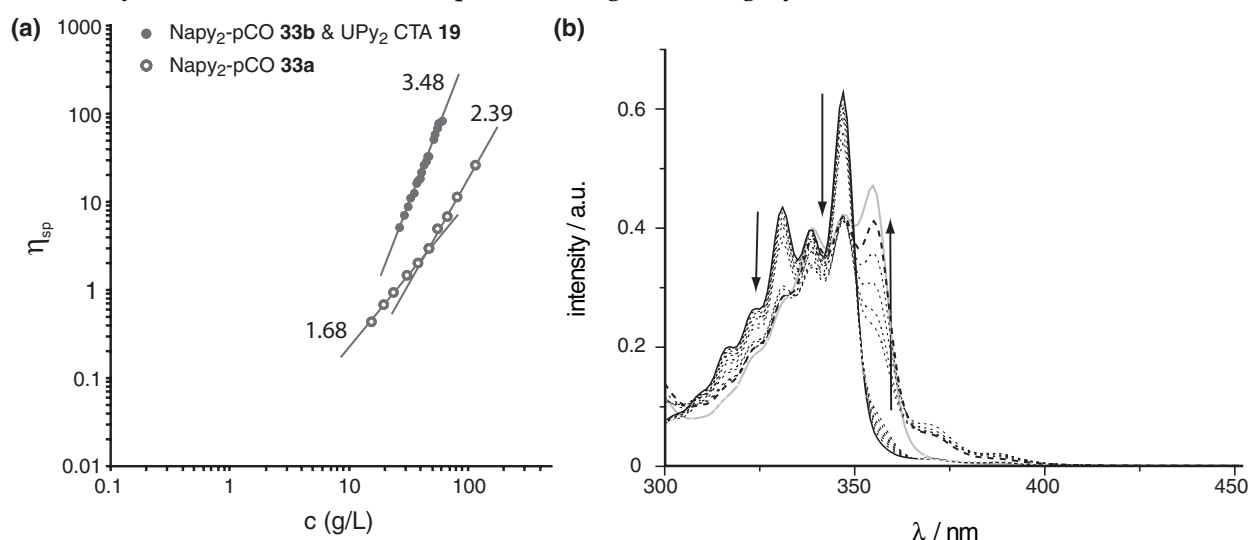
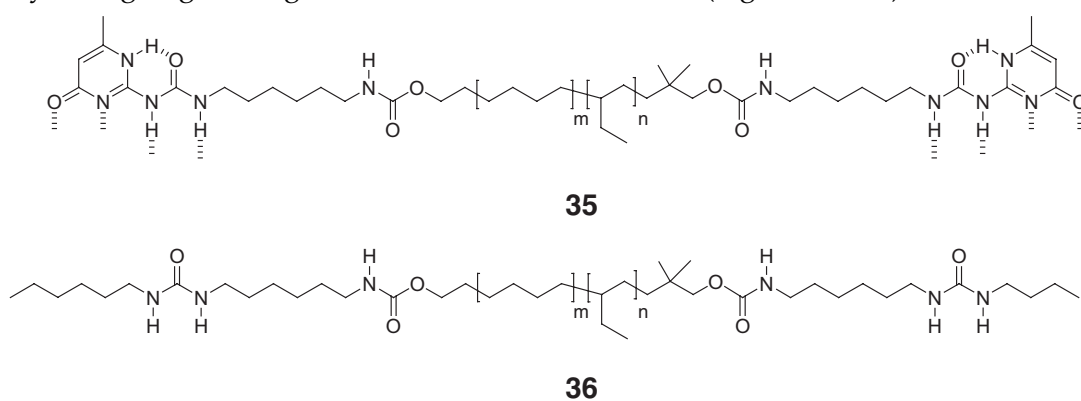


Figure 6.9 (a) Double logarithmic plot of specific viscosity (η_{sp}) vs. concentration of supramolecular block copolymer **19** – **33b** and pure **33a** in chloroform; (b): UV/Vis spectra of **33b** (black trace) upon addition of 15 equivalents of **19** (blue trace) in chloroform and the normalized UV/Vis spectrum of the chloroform solution used for the viscosity measurements in (a) (red curve).

6.3.4 Supramolecular block copolymer formation in the bulk

One of the key goals of this investigation was to determine whether the high association constant between the UPy and Napy motifs would allow the formation of block copolymers in the bulk with stable microphase separation. This would ultimately lead to controlled formation of many block copolymer morphologies by the supramolecular assembly of the individual component blocks. Atomic force microscopy (AFM) has proven to be a useful technique in order to study different morphologies in block copolymer films. Therefore, films of bisNapy-polymer **33b** and UPy telechelic poly(ethylene-butylene) **35** (bisUPy-PEB, Scheme 6.6) ($M_n = 4100$ g/mol)⁴⁹ were studied by Tapping Mode AFM (TM-AFM) by Dr. Ir. Pascal Jonkheijm.

Films were prepared by simple solution-blending of the individual components in toluene followed by drop-casting on glass slides. In contrast to pure **33b**, mixtures with bisUPy-PEB **35** yield macroscopically homogeneous films. In order to determine the existence of microphase-separated domains and determine the distribution and size of the domains, additional information was obtained by AFM measurements on 30/70 and 70/30 mol% **33b:35** films (Figure 6.10). The phase image (Figure 6.10a) of the 30/70 film shows microphase separation, which demonstrates the formation of domains consisting of two chemically different blocks. The topographic (height) image (Figure 6.10b), however, still shows a flat and homogeneous film (root mean square (rms) roughness = ± 1 nm). The pronounced contrast in the phase image indicates that chemical inhomogeneities have developed through microphase separation. A typical feature size of 15 nm can be derived from this image. Since a mol ratio of 30/70 Napy:UPy was used, these small features were attributed to the bisNapy-pCO. The assignment of the light (hard) features to the pCO hard block was confirmed by an increase in these features when a 70/30 **33b:35** film was measured. In addition to the higher density of hard domains with a similar domain size in the phase image (Figure 6.10c), a smooth and largely homogeneous film surface with a rms roughness of ± 3 nm was observed (Figure 6.10d). Moreover, the data suggests that the hard domains exist *in* the films rather than laying *on top* of the films as indicated by the smooth height images. In contrast to the mixtures with both hydrogen bonding end groups at the termini, reference experiments carried out with films of mixtures of **33b** and reference PEB polymer **36** that does not bear any UPy groups at the chain ends (Scheme 6.6), did not give rise to microphase-separated structures. Rather, these mixtures produced turbid films and macrophase-separated domains as can be clearly seen in the AFM images yielding large z-ranges and rms values for the films (Figure 6.10e-f).



Scheme 6.6 BisUPy-PEB **35** and reference PEB polymer **36**.

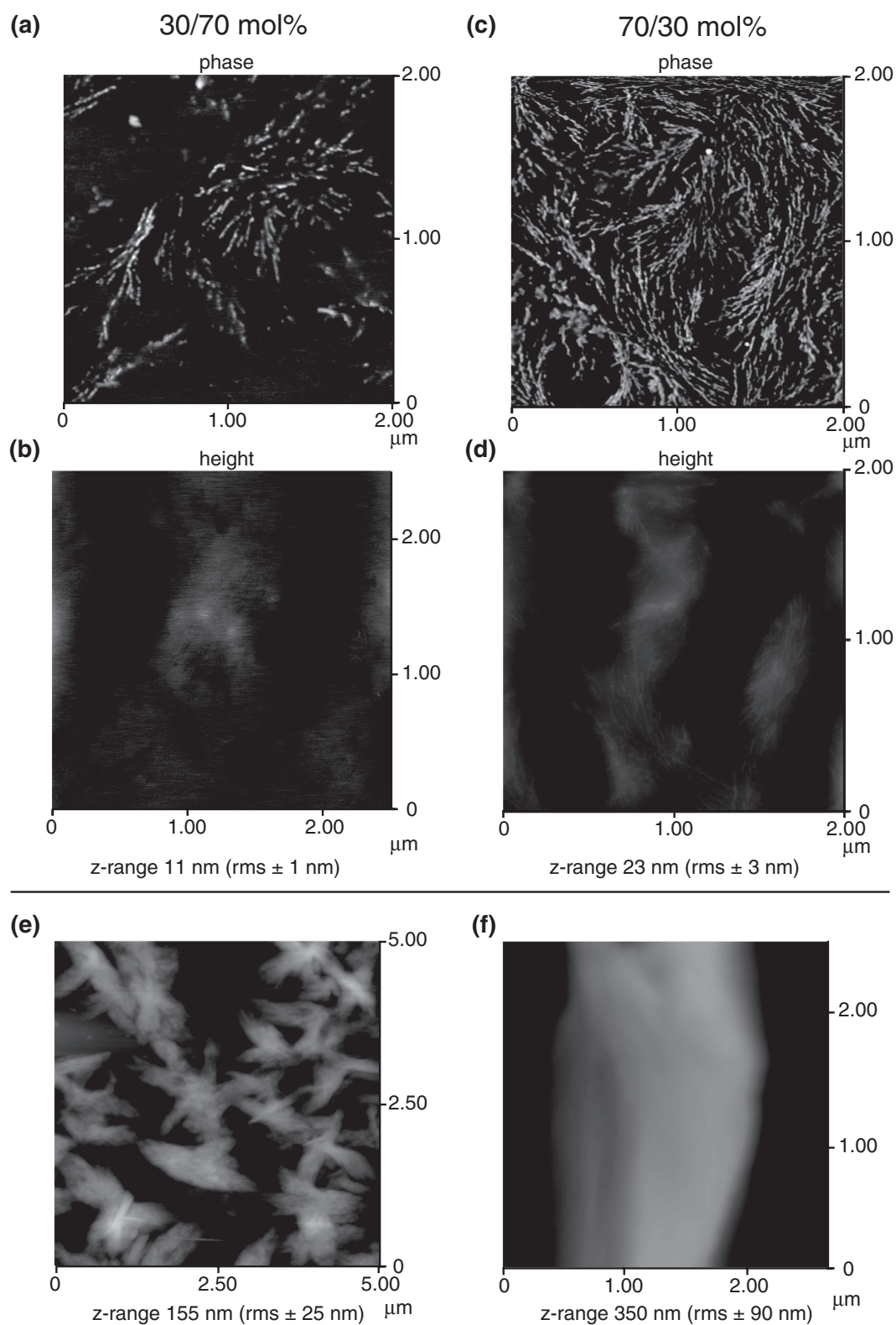


Figure 6.10 TM-AFM-images of drop-cast films of bisNapy-pCO **33b** and bisUPy-PEB **35**; (a): phase image of a 30/70 mol% **33b**:**35** film; (b): height image of a 30/70 mol% **33b**:**35** film; (c): phase image of a 70/30 mol% **33b**:**35** film; (d): height image of a 70/30 mol% **33b**:**35** film; (e): height image of a **33b** film; (f): height image of a 30/70 mol% **33b**:**36** film.

Differential scanning calorimetry (DSC) measurements were performed by Dr. Oren A. Scherman on **33b**, **35** and mixtures correlating to the supramolecular copolymer films imaged with AFM. When bisUPy-PEB **35** was added to bisNapy polyoctenamer **33b**, the melting peak arising from the semi-crystalline polyoctenamer block shifted to lower temperatures accordingly (Table 6.3, entries 1-4). Moreover, the amount of crystallinity in the block copolymers decreased with increasing weight percentage of the amorphous PEB blocks. This data is consistent with the AFM images in Figure 6.10, indicating that a supramolecular block copolymer is indeed formed. However, when DSC was carried out on a mixture of **33b** with an excess of reference PEB **36**, the crystallinity due to the polyoctenamer actually increased (entry 5). This can be rationalized by a macrophase separation of the blend as depicted in Figure 6.10f. The smaller weight fraction of **33b** in a matrix of amorphous PEB **36** undergoes macrophase separation in the melt which results in confinement and a more compact and ordered crystalline domain upon cooling.

Table 6.3 DSC-data for supramolecular block copolymers.

entry	polymer ^a	T _m (°C)	ΔH (J/g)	T _g (°C)
1	33b	48.2	37.8	-10.7
2	35	-	-	-58.5
3	33b:35 (64:36)	47.5	34.2	-59.6
4	33b:35 (25:75)	46.7	32.2	-58.2
5	33b:36 (24:76)	45.3	41.3	-61.9

^a weight fractions are indicated in parentheses.

6.4 Discussion and conclusions

The first part of the chapter focused on the self-assembly of low molecular weight bifunctional UPy and Napy molecules. Bifunctional Napy compounds were synthesized by palladium catalyzed amidation reactions of low molecular weight diamides and 7-amido-2-chloro-1,8-naphthyridines. It was shown that selective formation of cyclic heterodimers occurs in mixtures of bifunctional UPy and Napy molecules separated by low molecular weight linkers. This is due to the fact that the heterodimer, with a ring size of 18 single bonds and 2 hydrogen bonding arrays, is virtually strainless.⁸⁶ In addition, the effects of *adding* bisNapy and *removing* bisUPy from a solution of bisUPy are remarkably similar. Therefore, the data strongly suggests selective and quantitative formation of cyclic heterodimers. However, it was shown with diffusion ordered ¹H NMR that upon an increase in concentration, a gradual change in heterocomplex composition occurs from purely cyclic to predominantly polymeric material.

Moreover, when a bifunctional UPy derivative containing a high molecular weight linker is used, the formation of alternating supramolecular copolymers is induced. Upon addition of a small bifunctional Napy derivative to a bifunctional UPy macromonomer, viscometry experiments demonstrated the selective incorporation of the bisNapy molecule into the supramolecular UPy polymer. This can be rationalized considering the combined effects of selective heterocomplexation and the differences in ring-chain equilibrium between low and high molecular weight linkers. While significant cycle formation is anticipated for small bifunctional molecules, only a limited amount of cyclic aggregate is expected to be formed upon mixing large bifunctional molecules. Contrary to most supramolecular polymers bearing complementary binding motifs where a high DP can be obtained when the stoichiometry is exactly 1:1 (Figure 6.11a), a supramolecular copolymer formed from telechelic bisUPy and bisNapy polymers retains a high DP over a large range of UPy/Napy ratios (Figure 6.11b). A future goal in order to obtain supramolecular materials with polymer properties over the full composition range would therefore be the development of two hydrogen bonding moieties which are not only able to self-associate but are also complementary to each other.

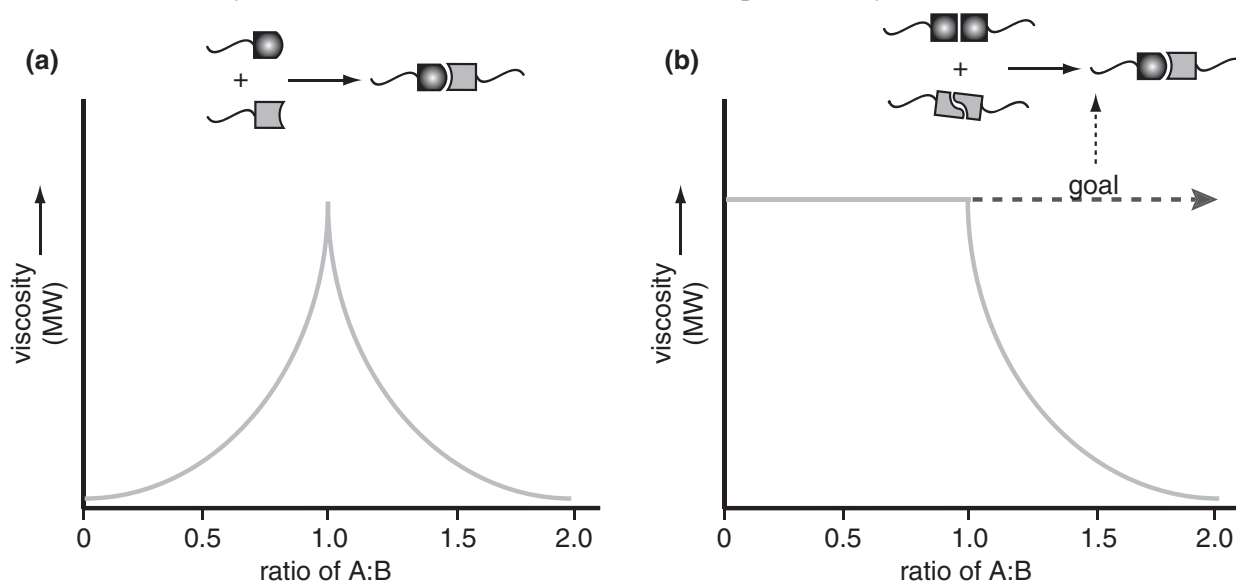


Figure 6.11 (a) Viscosity (or virtual MW) of a supramolecular copolymer vs. the ratio of component A and B when A and B are complementary; (b) Viscosity (or virtual MW) of a supramolecular copolymer vs. the ratio of component A and B when A is both self-complementary as well as complementary to B; the dashed line displays a future goal in obtaining supramolecular block copolymers with high virtual MW at every ratio of A to B.

In the second part of this chapter, a retrosynthetic approach was outlined in order to obtain supramolecular block copolymers. The successful preparation of UPy and Napy telechelic polymers with an end-group functionality of precisely two was achieved by ROMP of a cyclic monomer with a bifunctional CTA in the presence of 2nd generation Grubbs'

ruthenium catalyst in either dry toluene or DCE at 55 °C. Bifunctional CTAs equipped with either UPy or Napy moieties were synthesized from either small bifunctional molecules bearing an internal olefin or by a homodimerization through olefin cross metathesis reaction yielding C20 CTAs. In order to circumvent coordination of the Napy moiety to the ruthenium catalyst or the build-up of viscosity at the initial stage of the polymerization in case of a bisUPy CTA, a protecting group strategy based on the association of a polar UPy derivative with the UPy and Napy CTAs was developed. Whereas the polymerization reaction with small spacer CTAs was uncontrolled, ROMP of the C20 CTAs went smoothly. The UPy protecting groups could easily be removed from the crude reaction mixture by multiple precipitations in methanol. It should be mentioned that the design of the UPy protecting group is a delicate balance between the ease of removal (i.e. polarity of the derivative) and affinity for self-association in combination with association to Napy derivatives. UPy derivatives bearing ethylene glycol substituents longer than three repeat units display a lower K_{dim} value and are able to coordinate to a transition metal. Moreover, it has been demonstrated before⁶⁶ that one triethylene glycol substituent is necessary to provide sufficient solubility in polar solvents such as methanol. The purity of the polymers was substantiated using ¹H NMR, MALDI-ToF-MS, FT-IR and UV/Vis spectroscopy. Self-assembly of the UPy and Napy telechelic polymers into supramolecular block copolymers was subsequently confirmed in chloroform solution by a variety of techniques including Ubbelohde viscometry and UV/Vis spectroscopy. Initial studies on the solid state of mixtures of these polymers by TM-AFM indicate that microphase separated structures are formed. In order to elucidate the morphologies in further detail, an extensive study should be performed using TEM and X-ray scattering techniques. The outlined retrosynthetic methodology in combination with the supramolecular protection methodology will allow for the design and preparation of new block copolymer systems based on supramolecular polymers.

6.5 Experimental procedures

General methods. See General methods Chapter 2. ¹⁹F NMR spectra were recorded on Varian Mercury 400. ¹⁹F NMR was measured with $t_{\text{ac}} = 9.999$ s, $\text{np} = 90,000$, $\text{sw} = 4500.5$ Hz and $d1 = 4.0$ s. Chemical shifts in ¹⁹F NMR are in ppm with HFA·H₂O as the reference peak. Analytical gel permeation chromatography (GPC) was carried out in THF on two PL Gel single pore size (100Å) 30 cm columns, with a particle size of 3 μm (Polymer Labs) connected in series with a SPD-M10Avp photodiode array UV/Vis detector (Shimadzu) measuring between 190 and 370 nm. Reported molecular weight values were obtained against PS-standards. Thermal analysis by DSC was carried out using a Perkin Elmer Differential Scanning Calorimetry Pyris 1 with Pyris 1 DSC Autosampler and Perkin Elmer CCA7 cooling element

under a nitrogen atmosphere with heating rates of 40 °C/min and cooling rates of 10 °C/min. Unless stated otherwise, thermal parameters were determined from the second heating curve.

Viscosity measurements. Solution viscosities were measured using Schott-Geräte Ubbelohde microviscometers with suspended level bulb in automated setups with Schott-Geräte AVS/S measurement tripods and AVS 350 measurement devices. The micro-viscometers were thermostated in a water bath at 25.00 (\pm 0.01) °C. Samples were filtered over 1.0 μ m PTFE filters before measurement. Specific viscosities were corrected using the appropriate Hagenbach correction factors.

^{19}F NMR on HFA adduct of **7.** The HFA solution in CDCl_3 was prepared according to a literature procedure.⁴⁹ A ^{19}F NMR sample of the HFA adduct of the hydroxyl groups of **7** was prepared by dissolving 43.6 μ mol **7** and 9.1 μ mol *p*-nitrobenzylalcohol in 1.0 mL of the previously prepared HFA/ CDCl_3 solution.

AFM measurement. Atomic force microscopy (AFM) images were recorded under ambient conditions using a Digital Instrument Multimode Nanoscope IV operating in the tapping-mode regime using micro-fabricated silicon cantilever tips (PPP-NCH, 300-330 kHz, 42 N/m, tip radius 10 nm), scanner 5962EV was used with scan rates 0.5-1.25 Hz, scan angle 0°, feedback signals were optimized, A_{sp}/A_0 was adjusted to 0.6. Images shown are subjected to a first-order plane-fitting procedure to compensate for sample tilt. The phase images were recorded simultaneously with the topographic images. The roughness data are root-mean-square (rms) values which are derived as standard deviations of all height values in an image. Films were drop cast onto glass slides from a 5 wt% (total) toluene solution.

Synthesis. 2-*n*-Butylureido-6-methyl-4[1H]-pyrimidinone **1** was prepared as reported by Beijer *et al.*⁸⁷; 2,7-bis-(dodecanoylamino)-1,8-naphthyridine **2** and 7-(2-ethyl-hexanoylamino)-2-chloro-1,8-naphthyridine **6b** were synthesized as reported by Ligthart *et al.*³⁴; UPy-imidazolidine **4** was prepared as reported by Keizer *et al.*³⁵; 7-acetamido-2-chloro-1,8-naphthyridine **6a** was synthesized as reported by Corbin *et al.*⁸⁸; 4-(2-(2-(2-methoxy-ethoxy)-ethoxy)-ethyl)isocytosine **9** was prepared as reported by Hoogenboom *et al.*⁷⁹; *cis*- and *trans*-1,4-diamino-2-butene-2HCl **16** and **17** were prepared according to literature procedures.^{72,74} bisUPy-PEB **35** and reference polymer **36** were obtained from Henk Keizer and Holger Kautz, respectively.

General procedure of ROMP polymerizations with CTA: A dried 50 mL round-bottom flask was charged with CTA (0.29 mmol) and UPy protecting group (0.65 mmol). Dry DCE (0.7 mL) was added under argon and after stirring a clear solution was obtained to which the appropriate amount of monomer was added. Subsequently, a solution of 2nd generation Grubbs' ruthenium catalyst (1.0 mg, 1.2 μ mol) in DCE (0.5 mL) was injected. The reaction mixture immediately turned highly viscous and was stirred at 55 °C for 48 h. The solution was cooled to RT and 1.0 mL of chloroform was added. The viscous solution was added dropwise into 100 mL methanol with added BHT to prevent cross linking. The white

precipitate was isolated by centrifugation. The precipitation process was repeated twice which afforded the supramolecular polymers as white powders which were free of the UPy protecting group.

N⁰,N^{0'}-(1,6-Hexanediy1)-bis-(2-ureido-6-(3-heptyl)-4[1H]-pyrimidinone, 3a: UPy-imidazolidine **4** (6.0 g, 15.5 mmol) and 1,6-hexamethylene-diamine (0.78 g, 6.74 mmol) were dissolved in 10 mL of CHCl₃ and this solution was stirred for 3 h under nitrogen. To the reaction mixture 50 mL of CHCl₃ was added and the organic layer was washed with 20 mL 1N HCl, 20 mL sat. NaHCO₃, and 20 mL brine. The organic layer was dried with Na₂SO₄ and was reduced to about 5 mL by evaporation in vacuo. To this concentrated solution 30 mL of acetone was added under vigorous stirring, which resulted in a precipitate. The precipitate was filtered off, and washed thoroughly with MeOH. The resulting white powder was obtained in a yield of 95%. M.P. 131-133 °C; ¹H NMR (CDCl₃): δ = 13.25 (s, 2H, NH), 11.90 (s, 2H, NH), 10.19 (s, 2H, NH), 5.81 (s, 2H), 3.24 (m, 4H), 2.30 (m, 2H), 1.72-1.48 (m, 12H), 1.40 (m, 4H), 1.35-1.18 (m, 8H) 0.93 (m, 12H) ppm; ¹³C NMR (CDCl₃): δ = 173.1, 156.6, 155.3, 154.8, 106.1, 45.2, 39.9, 32.8, 29.3, 29.2, 26.7, 26.5, 22.3, 13.8, 11.6 ppm; MALDI-TOF-MS: (m/z) calcd. 586.39; observed: 587.39 (M+H⁺), 609.35 (M+Na⁺); FTR-IR (ATR): ν = 2929, 2859, 1690, 1644, 1568, 1520, 1458, 1381, 1335, 1299, 1250, 1223, 1129, 1067, 985, 949, 843, 802, 723 cm⁻¹; Anal. Calcd. for C₃₀H₅₀N₈O₄: C 61.41, H 8.59, N 19.10 found: C 60.54, H 8.59, N 18.79.

N⁰,N^{0'}-(1,12-Dodecanediyl)-bis-(2-ureido-6-(3-heptyl)-4[1H]-pyrimidinone, 3b: UPy-imidazolidine **4** (2.89 g, 9.55 mmol) and 1,12-diaminododecane (0.80 g, 4.0 mmol) were dissolved in 10 mL of CHCl₃ and this solution was stirred for 48 h under nitrogen. Subsequently, 20 mL of CHCl₃ was added and the organic layer was washed with 1N HCl (2 x 20 mL), H₂O (2 x 20 mL) and brine (20 mL). The organic layer was dried with Na₂SO₄ and was reduced to about 5 mL by evaporation in vacuo. To this concentrated solution 80 mL of MeOH was added to under vigorous stirring, which resulted in a solid precipitate after being cooled to 5 °C for 4 h. The precipitate was ground, filtered off, and washed thoroughly with MeOH. The resulting white powder was obtained in a yield of 90%. M.P. 134 - 137 °C; ¹H NMR (CDCl₃): δ = 13.26 (s, 2H, NH), 11.91 (s, 2H, NH), 10.19 (s, 2H, NH), 5.85 (s, 2H), 3.24 (m, 4H), 2.29 (m, 2H), 1.75-1.45 (m, 22H), 1.40-1.15 (m, 14H) 0.88 (m, 12H) ppm; ¹³C NMR (CDCl₃): δ = 173.0, 156.6, 155.3, 154.8, 106.1, 45.2, 40.0, 32.8, 29.4, 29.2, 26.9, 26.5, 22.4, 13.8, 11.6 ppm; MALDI-TOF-MS: (m/z) calcd. 670.47; observed: 671.44 (M+H⁺), 693.42 (M+Na⁺), 709.41 (M+K⁺); FTR-IR (ATR): ν = 2929, 2859, 1690, 1644, 1568, 1520, 1458, 1381, 1335, 1299, 1250, 1223, 1129, 1067, 985, 949, 843, 802, 723 cm⁻¹; Anal. Calcd. for C₃₆H₆₂N₈O₄: C 64.45, H 9.31, N 16.70 found: C 64.28, H 9.45, N 19.89.

N⁰,N^{0'}-[Bis-(7-acetamido-1,8-naphthyridine-2-yl) hexanediamide], 5a: A pre-dried Schlenk tube was charged with 7-acetamido-2-chloro-1,8-naphthyridine **6a** (221 mg, 1.0 mmol), adipamide (101 mg, 0.70 mmol), K₂CO₃ (193 mg, 1.4 mmol), Xantphos (35 mg, 0.060 mmol), Pd(OAc)₂ (mg, 0.0619 mmol) and 13 mL of dry 1,4-dioxane. The tube was vacuumed and refilled with N₂ three times. The reaction mixture was stirred at 100 °C for 18 h. The mixture was cooled to room temperature followed by removal of the solvent by evaporation under reduced pressure. The residue was triturated with water and filtered to afford a solid. Further purification was done by column chromatography (SiO₂, 5% methanol in CHCl₃) and yielded the title compound as a white solid (50 mg, 25%). M.P. > 315 °C (degrades); ¹H NMR (DMSO-*d*₆): δ = 10.76 (s, 4H, NH), 8.27 (m, 8H), 3.42 (m, 4H) 2.18 (m, 6H), 1.68 (m, 8H) ppm. ¹³C NMR

(DMSO-*d*₆): δ = 172.9, 170.1, 154.4, 154.0, 138.9, 117.3, 113.0, 36.2, 24.5, 24.3 ppm. MALDI-TOF-MS: (m/z) calcd. 514.21; observed: 515.12 (M+H⁺), 537.11 (M+Na⁺); FTR-IR (ATR): ν = 3323, 3008, 2945, 1670, 1611, 1542, 1504, 1394, 1287, 1170, 1146, 974, 853, 803 cm⁻¹; Anal. Calcd. for C₂₆H₂₆N₈O₄: C 60.69, H 5.09, N 21.78 found: C 59.23, H 4.98, N 20.88.

N^o,N^{o'}-[Bis-((7-(2-ethyl-hexanoyl)-amino-1,8-naphthyridine-2-yl) hexanediamide], 5b: A pre-dried Schlenk tube was charged with 7-(2-ethyl-hexanoyl)-amino-2-chloro-1,8-naphthyridine **6b** (801.2 mg, 2.62 mmol), adipamide (288.4 mg, 2.00 mmol), K₂CO₃ (506.7 mg, 3.66 mmol), Xantphos (46.3 mg, 0.0800 mmol), Pd(OAc)₂ (13.9 mg, 0.0619 mmol) and 13 ml dry 1,4-dioxane. The tube was vacuumed and refilled with N₂ three times. The reaction mixture was stirred at 100 °C for 18 h. The mixture was cooled to room temperature, filtered over diatomaceous earth and the solvent was evaporated under reduced pressure. Further purification by column chromatography (SiO₂, 2 % MeOH in CHCl₃) yielded 902 mg (50%) of yellow/orange product. M.P. 165-170 °C; ¹H NMR (CDCl₃): δ = 9.72 (s, 1H), 9.18 (s, 1H), 8.45 (d, 2H, *J* = 8.4 Hz), 8.08 (d, 2H, *J* = 8.6 Hz), 3.05 (m, 4H), 2.25 (m, 2H), 1.73-1.45 (m, 12H), 1.26-1.123 (m, 8H), 0.91 (t, 6H, *J* = 6.5 Hz), 0.82 (t, 6H, *J* = 6.4 Hz) ppm. ¹³C NMR (CDCl₃): δ = 175.9, 172.9, 154.4, 154.3, 153.3, 139.0, 138.8, 117.9, 114.0, 49.8, 36.6, 32.0, 29.5, 25.6, 24.2, 22.6, 13.8, 11.8 ppm. MALDI-TOF-MS: (m/z) calcd. 682.39; observed: 683.35 (M+H⁺), 705.33 (M+Na⁺), 721.31 (M+K⁺); FTR-IR (ATR): ν = 3297, 3204, 3136, 2978, 2929, 2860, 1683, 1607, 1583, 1537, 1498, 1379, 1311, 1280, 1168, 1133, 1118, 852, 802, 728 cm⁻¹; Anal. Calcd. for C₃₈H₅₀N₈O₄: C 66.84, H 7.38, N 16.41 found: C 66.05, H 7.39, N 16.36.

(2-(2-(2-Methoxyethoxy)-ethoxy)-ethyl)-(2-ureido-6-(3-heptyl))-4[1H]-pyrimidinone, 7: To a solution of 4-(3-heptyl)-isocytosine (5.16 g, 24.7 mmol) in 30 mL dry chloroform in a 50 mL round-bottom flask, 1, 1'-carbonyl-diimidazole (5.20 g, 32.0 mmol) was added and stirred for 4 h at room temperature under inert atmosphere. To the mixture 30 mL CHCl₃ was added, washed with water (3 x 10 mL), dried over MgSO₄ and evaporated to give the crude imidazolide which was used immediately for the next step. The UPy-imidazolide was dissolved in 20 mL of chloroform, followed by the addition of 2-(2-(2-methoxyethoxy)ethoxy)ethyl amine **10** (3.72 g, 22.8 mmol) and stirred overnight (16 h) at 50°C under inert atmosphere. The solution was cooled to RT and chloroform (120 mL) was added. The solution was washed with 1N-HCl (3 x 40 mL), water (10 mL), brine (10 mL), dried over MgSO₄, and evaporated to yield the title compound as a pale-yellowish oil (8.0 g, 90 %). ¹H NMR (CDCl₃, δ): 13.11 (s, 1H, NH), 11.92 (s, 1H, NH), 10.24 (s, 1H, NH), 5.74 (s, 1H, CHCO), 3.61 (m, 6H, CH₂O), 3.42 (m, 4H, NHCH₂CH₂), 3.30 (s, 3H, OCH₃), 2.25 (m, 1H, CCH), 1.62-1.45 (m, 4H, CH₂), 1.29-1.16 (m, 4H, CH₂) ppm; ¹³C NMR (CDCl₃, δ): 172.9, 156.9, 155.3, 154.7, 71.9, 70.5, 70.3, 69.4, 59.0, 50.1, 45.3, 39.5, 32.8, 29.3, 26.6, 22.4, 13.8, 11.6 ppm; MALDI-TOF-MS: (m/z) calcd. 398.25; observed: 399.41 (M+H⁺), 421.39 (M+Na⁺), 437.37 (M+K⁺); FTR-IR (ATR): ν = 3224, 2959, 2929, 2873, 1697, 1656, 1609, 1584, 1556, 1528, 1453, 1394, 1351, 1316, 1253, 1200, 1106, 1029, 921, 842, 803 cm⁻¹.

(2-(2-(2-Methoxyethoxy)-ethoxy)-ethyl)-(2-ureido-6-(2-(2-(2-methoxy-ethoxy)-ethoxy)-ethyl))-4[1H]-pyrimidinone, 8: To a solution of 4-(2-(2-(2-methoxy-ethoxy)-ethoxy)-ethyl)isocytosine **9** (1.63 g, 6.0 mmol) in dry chloroform (10 mL) 1, 1'-carbonyl-diimidazole (1.26 g, 7.8 mmol) was added and the resulting solution was stirred for 5 h at RT. The solution was evaporated to dryness followed by recrystallization of the imidazolide from acetone to afford an off-white powder. The UPy-imidazolide

and 2-(2-(2-methoxyethoxy)ethoxy)ethyl amine **10** (0.70 g, 4.3 mmol) were dissolved in dry chloroform (5 mL) and stirred for 4 days at 50 °C. The solution was cooled to RT and chloroform (40 mL) was added. The solution was washed with 1N HCl (2 x 20 mL) and brine (1 x 10 mL), dried over Na₂SO₄, and evaporated to yield the title compound as a waxy solid (1.83 g, 92 %). ¹H NMR (CDCl₃, δ): 13.08 (s, 1H, NH), 11.95 (s, 1H, NH), 10.18 (s, 1H, NH), 5.84 (s, 1H, CHCO), 3.65 (m, 22H, CH₂O), 3.37 (s, 6H, CH₃), 2.60 (m, 2H, CCH₂), 1.93 (m, 2H, CCHCH₂) ppm; ¹³C NMR (CDCl₃, δ): 172.9, 156.9, 155.3, 154.7, 71.9, 70.5, 70.3, 69.4, 59.0, 50.1, 45.3, 39.5, 32.8, 29.3, 26.6, 22.4, 13.8, 11.6 ppm; MALDI-TOF-MS: (m/z) calcd. 460.25; observed: 461.19 (M+H⁺), 483.18 (M+Na⁺), 499.14 (M+K⁺); FTR-IR (ATR): ν = 2870, 1698, 1659, 1614, 1586, 1562, 1453, 1328, 1255, 1199, 1103, 939, 848 cm⁻¹.

2-(2-(2-Methoxyethoxy)ethoxy)ethyl amine, 10: A 100 mL three-necked round-bottom flask was charged with a solution of triethyleneglycol monomethylether tosylate **12** (11.65 g, 36.6 mmol) in 25 mL of DMF before potassium phthalimide (9.0 g, 49 mmol) was added. The mixture was stirred at 110 °C for 3 h under inert atmosphere. After cooling to RT, 150 mL of diethylether was added to facilitate the precipitation of excess phthalimide. The resulting precipitate was removed by filtration. The solution was washed with 1N-NaOH solution (2 x 25 mL), water (25 mL) (do not shake), dried over MgSO₄, and evaporated under high vacuum. The crude phthalimide derivative **11** (7.66 g, 26.1 mmol) was used without further purification after checking with ¹H-NMR. The crude phthalimide derivative was dissolved in a 1/1 v/v% mixture of 25 mL hydrazine monohydrate and ethanol, followed by heating to reflux temperature (110 °C) overnight (16 h) under inert atmosphere. After cooling down to room temperature, the product was extracted with toluene (4 x 80 mL) from the pale-yellowish precipitate. The combined organic layers were collected and evaporated to yield the title compound as a yellow oil (3.72 g, 22.8 mmol, 62 %) which should be stored under inert atmosphere (after two weeks, the color of the product turned to orange-color probably because of the oxidation). ¹H NMR (CDCl₃, δ): 3.64 (m, 6H, CH₂O), 3.55-3.48 (m, 4H, NH₂CH₂CH₂, CH₂OCH₃), 3.36 (s, 3H, OCH₃), 2.85 (t, 2H, J = 5.3 Hz, CH₂NH₂) ppm; ¹³C NMR (CDCl₃, δ): 72.8, 71.5, 70.1, 70.1, 69.8, 58.6, 41.2 ppm.

2-(2-(2-Methoxyethoxy)ethoxy)ethyl tosylate, 12: A 300 mL three-necked round-bottom flask was charged with a solution of triethyleneglycol monomethylether (40 g, 0.244 mol) in 80 mL of THF. Sodium hydroxide (20.0 g, 0.500 mol) dissolved in 80 mL of water was added upon vigorous stirring on an ice bath. To this mixture, a solution of tosyl chloride (60 g, 0.314 mol) in 80 mL of THF was added dropwise over 15 min at 0 °C. The reaction mixture was allowed to warm to room temperature and stirred for 2 h under inert atmosphere. Subsequently, 600 mL of diethylether was added and the organic layer was separated and washed with 1N-NaOH solution (3 x 50 mL) **without shaking** (shaking can lead to the formation of an inseparable emulsion due to the amphiphilicity of the product). Again, the organic layer was washed with water (2 x 50 mL), dried over MgSO₄, followed by evaporation and drying in vacuo, to yield the title compound as a pale-yellowish liquid (73.6 g, 95%). ¹H NMR (CDCl₃, δ): 7.82 (d, 2H, J = 6.6 Hz, CH), 7.39 (d, 2H, J = 7.3 Hz, CH), 4.19 (t, 2H, J = 6.0 Hz, CH₂OSO₂), 3.70-3.52 (m, 10H, OCH₂), 3.39 (s, 3H, OCH₃), 2.42 (s, 3H, CCH₃) ppm; ¹³C NMR (CDCl₃, δ): 144.8, 133.0, 129.8, 127.9, 71.9, 70.7, 70.5, 69.2, 68.6, 59.0, 21.6 ppm.

N⁰,N^{0'}-(1,4-(*Cis*-2-butene)diyl)-bis-(2-ureido-6-(3-heptyl)-4[1H]-pyrimidinone, 13: A 250 mL round-bottom flask which contained UPy-imidazolide **4** (1.15 g, 3.8 mmol) was charged with a stirbar and *cis*-1,4-diamino-2-butene-2HCl **16** (0.251 g, 1.58 mmol) and dry chloroform (12 mL). The mixture was heated to 45 °C and a solution of triethylamine (0.8 mL) in dry chloroform (5 mL) was added. The resulting solution was stirred at 45 °C for 24 h. The solution was cooled and extra chloroform (10 mL) was added before washing with 1N HCl (3 x 30 mL), NaHCO₃ (sat) (1 x 30 mL) and brine (1 x 30 mL). The organic layer was dried over Na₂SO₄, filtered and concentrated followed by precipitation of the viscous solution into cold ethanol. The title compound was obtained after filtration and drying in vacuo as a white powder (0.56 g, 64%). ¹H NMR (CDCl₃+TFA): δ = 6.17 (s, 2H, COCH), 5.62 (m, 2H, CH₂CH), 4.02 (m, 4H, NHCH₂), 2.48 (m, 2H, CH(CH₂)₂), 1.81-1.56 (m, 8H, CH₂), 1.40-1.18 (m, 8H, CH₂), 0.94 (m, 12H, CH₃) ppm; ¹³C NMR (CDCl₃): δ = 173.1, 156.8, 155.7, 154.9, 151.4, 128.3, 106.5, 45.5, 37.4, 33.1, 29.5, 27.8, 26.8, 22.6, 14.0, 11.9 ppm; MALDI-TOF-MS: (m/z) calcd. 556.35; observed: 557.31 (M+H⁺), 579.33 (M+Na⁺); FTR-IR (CDCl₃ solution): ν = 3201, 2960, 2932, 2873, 1696, 1656, 1582, 1525, 1461, 1298, 1250, 1131, 1025, 919, 848, 805 cm⁻¹.

N⁰,N^{0'}-(1,4-(*Trans*-2-butene)diyl)-bis-(2-ureido-6-(3-heptyl)-4[1H]-pyrimidinone, 14: A 250 mL round-bottom flask which contained UPy-imidazolide **4** (1.17 g, 3.9 mmol) was charged with a stirbar and *trans*-1,4-diamino-2-butene-2HCl **17** (0.254 g, 1.60 mmol) and dry chloroform (19 mL). The mixture was heated to 45 °C and a solution of triethylamine (0.8 mL) in dry chloroform (5 mL) was added. The resulting solution was stirred at 45 °C for 24 h. The solution was cooled and extra chloroform (10 mL) was added before washing with 1N HCl (3 x 30 mL), NaHCO₃ (sat) (1 x 30 mL) and brine (1 x 30 mL). The organic layer was dried over Na₂SO₄, filtered and concentrated. To the concentrated viscous solution, cold methanol (50 mL) was added dropwise to precipitate the product. The title compound was obtained after filtration and drying in vacuo as a white powder (0.71 g, 80%). ¹H NMR (CDCl₃): δ = 13.08 (s, 2H, NH), 11.93 (s, 2H, NH), 10.37 (s, 2H, NH), 5.74 (s, 4H, COCH & CH₂CH), 3.82 (m, 4H, NHCH₂), 2.21 (m, 2H, CH(CH₂)₂), 1.64-1.45 (m, 8H, CH₂), 1.31-1.10 (m, 8H, CH₂), 0.89 (m, 12H, CH₃) ppm; ¹³C NMR (CDCl₃): δ = 173.8, 156.8, 155.9, 154.9, 128.2, 106.5, 45.6, 41.4, 33.1, 29.6, 26.8, 22.7, 14.1, 11.9 ppm; MALDI-TOF-MS: (m/z) calcd. 556.35; observed: 557.33 (M+H⁺), 579.32 (M+Na⁺); FTR-IR (CDCl₃ solution): ν = 3203, 2960, 2931, 2873, 1697, 1656, 1582, 1526, 1459, 1306, 1250, 1146, 1020, 969, 849, 805 cm⁻¹.

N⁰,N^{0'}-[Bis-((7-(2-ethyl-hexanoyl)-amino-1,8-naphthyridine-2-yl)-3-hexenediamide], 15: A pre-dried Schlenk tube was charged with 7-(2-ethyl-hexanoyl)-amino-2-chloro-1,8-naphthyridine **6b** (296.6 mg, 0.97 mmol), 3-hexenediamide **18** (75 mg, 0.53 mmol), K₂CO₃ (199.7 mg, 1.44 mmol), Xantphos (9.8 mg, 0.017 mmol), Pd(OAc)₂ (2.4 mg, 0.00107 mmol) and 4 mL dry 1,4-dioxane. The tube was pulled vacuum and back-filled with N₂ three times. The reaction mixture was stirred at 100 °C for 18 h and subsequently cooled to RT followed by filtration over diatomaceous earth. The solvent was evaporated under reduced pressure. Crude product was obtained after purification by column chromatography (SiO₂, 3 % MeOH in CHCl₃). The title compound was obtained as a white powder by precipitation of the crude product in n-pentane (160 mg, 48%). M.P. 156 °C; ¹H NMR (CDCl₃): δ = 8.92 (s, 2H, NH), 8.51 (m, 4H), 8.38 (s, 2H, NH), 8.09 (m, 2H), 5.28 (m, 2H), 3.35 (m, 4H), 2.25 (m, 2H), 1.78-1.42 (m, 12H), 1.25-1.12 (m, 8H), 0.95-0.78 (m, 12H) ppm; ¹³C NMR (DMSO-*d*₆): δ = 176.0, 175.5, 154.5, 154.4, 154.0, 153.9, 153.5, 153.0, 139.0, 138.9,

138.6, 117.4, 117.2, 113.3, 113.0, 55.0, 47.8, 47.5, 31.8, 31.6, 29.2, 25.6, 22.2 (2), 13.9, 13.8, 11.7 ppm; MALDI-TOF-MS: (m/z) calcd. 680.38; observed: 681.42 (M+H⁺), 703.4 (M+Na⁺), 719.38 (M+K⁺); FTR-IR (ATR): ν = 3287, 2959, 2931, 2872, 1697, 1607, 1549, 1498, 1378, 1349, 1312, 1283, 1228, 1171, 1136, 989, 852, 802 cm⁻¹; Anal. Calcd. for C₃₈H₄₈N₈O₄: C 67.04, H 7.11, N 16.46 found: C 66.78, H 6.85, N 16.32.

3-Hexenediamide, 18: Similar to a procedure reported by Strulov *et al.*⁸⁹; To a mixture of *trans*-3-hexenedioic acid (1.0 g, 6.9 mmol) in oxalyl chloride (2.5 mL) was added one drop of DMF and stirred for 5 h at 80 °C under argon atmosphere. Diethyl ether was added after the solution was evaporated to dryness and the resulting solution was added dropwise under vigorous stirring to concentrated NH₃ (10 mL, 25% in water). The mixture was stirred at RT for 20 h. The resulting precipitate was collected via filtration and the title compound was obtained by crystallization from water (500 mg, 50%). M.P. 210-211 °C; ¹H NMR (DMSO-*d*₆): δ = 7.24 (s, 1H, NH), 6.78 (s, 1H, NH), 5.55 (m, 2H, CH), 2.79 (d, 4H, CH₂) ppm; ¹³C NMR (DMSO-*d*₆): δ = 172.8, 127.2, 39.4 ppm; FTR-IR (ATR): ν = 3370, 3181, 2900, 1630, 1414, 1394, 1330, 1256, 1132, 974, 923, 873, 790 cm⁻¹; Anal. Calcd. for C₆H₁₀N₂O₂: C 50.69, H 7.09, N 19.71 found: C 50.51, H 6.81, N 19.85.

N^o,N^{o'}-(1,20-(10-Eicosene)diyl)-bis-[2-ureido-6-(3-heptyl)-4[1H]-pyrimidinone], 19: A solution of eicos-10-enediamine **23** (2.20 g, 7.17 mmol), triethylamine (14.3 g, 0.14 mol) and UPy-imidazolide **4** (7.9 g, 26 mmol) in chloroform (100 mL) was stirred at 50 °C for 24 h. The solution was cooled to RT and washed with 1N HCl (2 x 50 mL), NaHCO₃ (sat) (2 x 50 mL) and brine (1 x 50 mL) followed by drying over Na₂SO₄. The title compound could be obtained as a white powder after multiple precipitations in methanol (5.60 g, 62%). ¹H NMR (CDCl₃): δ = 13.21 (s, 2H, NH), 11.88 (s, 2H, NH), 10.17 (s, 2H, NH), 5.80 (s, 2H, COCH), 5.37 (m, 2H, CH₂CH), 3.22 (m, 4H, NHCH₂), 2.28 (m, 2H, CH(CH₂)₂), 1.96 (m, 4H, CHCH₂), 1.60 (m, 12H, CH₂), 1.28 (m, 32H, CH₂), 0.88 (m, 12H, CH₃) ppm; ¹³C NMR (CDCl₃): δ = 172.9, 156.5, 155.4, 154.6, 130.2, 106.1, 45.20, 39.9, 32.7, 32.5, 29.2 (m), 26.8, 26.5, 22.4, 13.8, 11.6 ppm; MALDI-TOF-MS: (m/z) calcd. 780.60; observed: 781.58 (M+H⁺), 803.57 (M+Na⁺), 819.54 (M+K⁺); FTR-IR (ATR): ν = 3215, 2958, 2923, 2853, 1696, 1644, 1581, 1563, 1523, 1455, 1318, 1249, 1006, 966, 919, 845, 802 cm⁻¹; Anal. Calcd. for C₄₄H₇₆N₈O₄: C 67.66, H 9.81, N 14.35 found: C 67.31, H 9.82, N 14.88.

2-Undec-10-enyl-isoindole-1,3-dione, 21: A 1.0 L round-bottom flask was charged with 10-undecene bromide (57.65 g, 0.235 mol) and DMF (150 mL). A stirbar was added followed by potassium phthalimide (47.61 g, 0.254 mol) and extra DMF (100 mL). The mixture was stirred at 75 °C for 6 hours and then at 50 °C for 12 h. The mixture was filtered and washed with diethylether. Subsequently, the organic layer was washed with water (3 x 175 mL), saturated KCl (aq) (2 x 150 mL) and dried over Na₂SO₄. The solvent was removed in vacuo and the title compound was obtained as white crystals after multiple crystallizations from methanol (54.54 g, 78%). ¹H NMR (CDCl₃): δ = 7.83 (m, 2H, ArH), 7.69 (m, 2H, ArH), 5.80 (m, 1H, CHCH₂), 4.96 (m, 2H, CHCH₂), 3.67 (t, 2H, J = 7.4 Hz, NCH₂), 2.02 (q, 2H, J = 7.3 Hz, CH₂CHCH₂), 1.67 (m, 2H, NCH₂CH₂), 1.57-1.22 (m, 12H, CH₂) ppm; ¹³C NMR (CDCl₃): δ = 134.0, 123.4, 114.3, 38.3, 34.0, 29.6, 29.4, 29.3, 29.1, 28.8, 27.0 ppm; FTR-IR (ATR): ν = 3081, 2926, 2855, 1773, 1711, 1640, 1616, 1467, 1437, 1395, 1368, 1057, 910 cm⁻¹.

Eicos-10-endiyl di(isoindole-1,3-dione), 22: A 0.5 L round-bottom flask was charged with 2-undec-10-enyl-isoindole-1,3-dione **21** (58.46 g, 0.195 mol) and a stirbar. Upon heating to 55 °C, the solid melted and

a solution of 2nd generation Grubbs' catalyst (25.8 mg, 29.2 μ mol, 0.015 mol%) in dry DCM was added. The purple/red solution was pulled vacuum and stirred under vacuum for 21 hours at 55 °C. The solution was cooled to RT and the title compound was recrystallized from methanol (33.36 g, 60%) ¹H NMR (CDCl₃): δ = 7.83 (m, 4H, ArH), 7.69 (m, 4H, ArH), 5.35 (m, 2H, CHCH₂), 3.67 (t, 4H, *J* = 7.3 Hz, NCH₂), 1.97 (q, 4H, *J* = 7.3 Hz, CHCH₂), 1.65 (m, 4H, NCH₂CH₂), 1.31-1.23 (m, 24H, CH₂) ppm; ¹³C NMR (CDCl₃): δ = 168.7, 134.0, 132.4, 130.5, 123.3, 38.3, 32.8, 29.8, 29.8, 29.7, 29.5, 29.4, 28.8, 27.1 ppm.

Eicos-10-endiamine, 23: Eicos-10-endiyl di(isoindole-1,3-dione) **22** (4.09 g, 7.17 mmol) and THF (160 mL) were charged into a 0.5 L round-bottom flask and hydrazide-monohydrate (14.0 mL) was added to the stirring mixture by a syringe. The mixture was stirred at 70 °C for 24 hours. A yellow/green precipitate had formed which was filtered and washed with THF and hexane. The organic layer was washed with 1M NaOH (5 x 75 mL) and brine (1 x 100 mL) followed by drying over Na₂SO₄. The product was obtained as a white solid after filtration and drying in vacuum (2.20 g, 100%). ¹H NMR (CDCl₃): δ = 5.33 (m, 2H, CHCH₂), 2.62 (t, 4H, *J* = 7.0 Hz, CH₂NH₂), 1.92 (m, 4H, CHCH₂), 1.40-1.17 (m, 28H, CH₂) ppm; ¹³C NMR (CDCl₃): δ = 130.6, 42.5, 34.1, 32.8, 29.9-29.7 (4), 29.4, 27.1 ppm.

N⁰,N^{0'}-[Bis-((7-(2-ethyl-hexanoyl)-amino-1,8-naphthyridine-2-yl) eicos-10-enediamide], 20: A pre-dried Schlenk tube was charged with 7-(2-ethyl-hexanoyl)-amino-2-chloro-1,8-naphthyridine **6b** (4.07 g, 13.3 mmol), eicos-10-enediamide **28** (2.37 g, 7.00 mmol), K₂CO₃ (2.57 g, 18.6 mmol), Xantphos (320 mg, 0.55 mmol), Pd(OAc)₂ (61 mg, 0.27 mmol) and 60 ml dry 1,4-dioxane. The tube was pulled vacuum and back-filled with N₂ three times. The reaction mixture was stirred at 100 °C for 20 h and subsequently cooled to RT. Filtration over diatomaceous earth and evaporation of the solvent under reduced pressure gave a red oil. Crude product was obtained after purification by column chromatography (SiO₂, 10% acetone in CHCl₃). The title compound was obtained as a white powder by precipitation of the crude product in n-heptane (3.79 g, 65%). M.P. 116-119 °C; ¹H NMR (CDCl₃): δ = 9.38 (s, 2H, NH), 8.92 (s, 2H, NH), 8.56 (d, 2H, *J* = 8.5 Hz), 8.51 (d, 2H, *J* = 8.4 Hz), 8.18 (d, 4H, *J* = 8.6 Hz), 5.37 (m, 2H, CH₂CH), 2.48 (t, 4H, *J* = 7.1 Hz, CH₂CO), 2.25 (m, 2H, (CH₂)CH), 1.98 (m, 4H, CHCH₂), 1.81-1.24 (m, 28H, CH₂), 0.99-0.81 (m, 12H, CH₃) ppm; ¹³C NMR (CDCl₃): δ = 175.5, 172.6, 154.1, 153.9, 153.4, 138.8 (2), 130.2, 129.7, 118.1, 113.6, 50.4, 37.6, 32.3, 32.1, 29.5, 29.4, 29.3, 29.1 (2), 29.0, 28.7, 25.7, 25.1, 22.5, 13.7, 11.8 ppm; MALDI-TOF-MS: (m/z) calcd. 876.6; observed: 877.61 (M+H⁺), 899.59 (M+Na⁺), 915.57 (M+K⁺); FTR-IR (ATR): ν = 3304, 2925, 2855, 1687, 1608, 1539, 1501, 1381, 1312, 1283, 1168, 1134, 967, 853, 802 cm⁻¹; Anal. Calcd. for C₅₂H₇₆N₈O₄: C 71.20, H 8.73, N 12.77 found: C 70.71, H 8.62, N 12.62.

Ethyl undec-10-enoate, 24: A solution of 10-undecenoic acid (freshly distilled, 49.8 g, 0.27 mol) in ethanol (250 mL) and concentrated sulphuric acid (2.5 mL) was heated to reflux and stirred for 24 h. The solvent was evaporated and the resulting oil dissolved in dichloromethane (250 mL). The organic layer was washed with saturated NaHCO₃ solution (3 x 100 mL), water (1 x 100 mL) and brine (1 x 100 mL) and subsequently dried over Na₂SO₄ to give the title compound as a light-yellow oil (52.7 g, 92%). ¹H NMR (CDCl₃): δ = 5.81 (m, 1H, CH), 4.96 (m, 2H, CH₂CH), 4.16 (q, 2H, 7.2 Hz, OCH₂), 2.31 (t, 3H, *J* = 7.3 Hz, CH₂CO), 2.02 (m, 2H, CH₂CHCH₂), 1.62 (m, 2H, CH₂CH₂CO), 1.38-1.27 (m, 10H), 1.21 (t, 3H, *J* = 6.6 Hz, OCH₂CH₃) ppm; ¹³C NMR (CDCl₃): δ = 173.9, 139.1, 114.1, 60.1, 34.4, 33.8, 29.3, 29.2, 29.1, 29.0, 28.9, 25.0, 14.2 ppm; FTR-IR (ATR): ν = 2927, 2855, 1736, 1464, 1372, 1177, 1034, 994, 909, 859, 724 cm⁻¹

Diethyl eicos-10-enedioate, 25: A solution of ethyl undec-10-enoate **24** (21.1 g, 0.10 mol) and 2nd generation Grubbs' catalyst (40.1 mg, 0.0047 mmol, 0.05 mol%) was pulled vacuum and stirred under vacuum for 3 days at 55 °C. Conversion was checked by ¹H NMR to be 91%. The title compound was obtained by column chromatography (SiO₂, 3 v/v% ethylacetate in n-hexane) as a colorless oil (14.0 g, 71%). ¹H NMR (CDCl₃): δ = 5.38 (m, 2H, CH), 4.16 (q, 4H, J = 7.3 Hz, OCH₂), 2.29 (t, 6H, J = 7.3 Hz, CH₂CO), 1.99 (m, 4H, CHCH₂), 1.62 (m, 4H, CH₂CH₂CO), 1.38-1.27 (m, 20H) 1.21 (t, 6H, J = 6.6 Hz, OCH₂CH₃) ppm; ¹³C NMR (CDCl₃): δ = 173.9, 130.3, 129.8, 60.0, 34.4, 32.5, 29.7, 29.6, 29.3 (2), 29.2, 29.1 (2), 27.2, 25.0, 14.3 ppm; FTR-IR (ATR): ν = 2925, 2854, 1735, 1464, 1372, 1177, 1034, 967, 859, 724 cm⁻¹.

Eicos-10-enedioic acid, 26: Similar to a hydrolysis procedure of dimethyl eicos-10-enedioate reported by Ruzicka *et al.*⁹⁰; To a solution of diethyl undec-10-enedioate **25** (7.0 g, 17.6 mmol) in ethanol (50 mL) was added 50 mL 2M NaOH and the resulting mixture was stirred vigorously at 100 °C for 24 h. The mixture was acidified with concentrated sulphuric acid followed by extraction into dichloromethane (3 x 150 mL) and dried over MgSO₄. Evaporation in vacuo and followed by recrystallization from ethylacetate afforded the product as white plate-like crystals (5.1 g, 85%). M.P. 82 °C; ¹H NMR (CDCl₃): δ = 5.38 (m, 2H, CH), 2.37 (t, 4H, J = 7.4 Hz, CH₂CO), 1.97 (m, 4H, CHCH₂), 1.64 (m, 4H, CH₂CH₂CO), 1.31-1.28 (m, 20H) ppm; ¹³C NMR (CDCl₃): δ = 180.6, 130.5, 130.0, 34.3, 32.7, 29.8, 29.7, 29.4, 29.3, 29.2, 27.3, 24.8 ppm; FTR-IR (ATR): ν = 3015, 2917, 2850, 2668, 1689, 1471, 1431, 1409, 1286, 1253, 1220, 1191, 963, 921 cm⁻¹; Anal. Calcd. for C₂₀H₃₆O₄: C 70.55, H 10.66, N 18.79 found: C 70.75, H 10.97, N 18.92.

Eicos-10-enedioyl dichloride, 27: Undec-10-enedioic acid **26** (5.10 g, 15.0 mmol) was dissolved in thionylchloride (50 mL) and refluxed for 4 h. Excess thionylchloride was evaporated under reduced pressure to yield the acid chloride as a brown oil (5.48 g, 97%). ¹H NMR (CDCl₃): δ = 5.38 (m, 2H, CH), 2.88 (t, 4H, J = 7.4 Hz, CH₂CO), 1.97 (m, 4H, CHCH₂), 1.74 (m, 4H, CH₂CH₂CO), 1.31-1.28 (m, 20H) ppm; ¹³C NMR (CDCl₃): δ = 173.7, 130.2, 46.9, 32.4, 29.4, 29.0, 28.9, 28.8, 28.2, 24.8 ppm.

Eicos-10-enediamide, 28: A solution of eicos-10-enedioyl dichloride **27** (5.48 g, 4.5 mmol) in dichloromethane (15 mL) was added dropwise to vigorously stirring concentrated ammonia (25%, 250 mL). Stir for 1 day at RT followed by filtration and washing with water. The solid was dried in vacuo at 50 °C for 6 h to yield the title compound as an off-white powder (4.9 g, 100%). M.P. 136-139 °C; ¹H NMR (CDCl₃): δ = 5.65 (d, 2H, NH), 5.38 (m, 2H, CH), 2.23 (t, 4H, J = 7.1 Hz, CH₂CO), 1.97 (m, 4H, CHCH₂), 1.62 (m, 4H, CH₂CH₂CO), 1.36-1.24 (m, 20H) ppm; ¹³C NMR (DMSO-*d*₆): δ = 174.8, 130.5, 130.1, 35.6, 32.4, 29.6, 29.4, 29.3, 29.2, 29.1, 25.6 ppm; MALDI-TOF-MS: (m/z) calcd. 338.18; observed: 339.32 (M+H⁺); FTR-IR (ATR): ν = 3387, 3189, 2922, 2850, 1645, 1467, 1418, 1124, 963, 804 cm⁻¹; Anal. Calcd. for C₂₀H₃₈N₂O₂: C 70.96, H 11.31, N 8.27 found: C 71.08, H 10.87, N 7.92.

Polymer characterization for UPy₂pCO, 32a: ¹H NMR (CDCl₃): δ = 13.14 (s, 2H, NH), 11.90 (s, 2H, NH), 10.18 (s, 2H, NH), 5.82 (s, 2H, COCH), 5.38 (m, pCO-CH₂CH), 3.82 (m, 4H, NHCH₂), 2.25 (m, 2H, CH(CH₂)₂), 1.97 (m, pCO-CHCH₂), 1.68-1.47 (m, 16H, CH₂), 1.40-1.19 (m, pCO-CH₂), 0.89 (m, 12H, CH₃) ppm; FTR-IR (ATR): ν = 3218, 2919, 2850, 1704, 1655, 1577, 1468, 1249, 1181, 1070, 966 cm⁻¹; GPC(THF): M_w = 22.0 kg/mol, M_n = 10.0 kg/mol, PDI = 2.20.

Polymer characterization for Napy₂pCO, 33a and 33b: ¹H NMR (CDCl₃): δ = 8.62 (d, 2H, J = 8.6 Hz), 8.57 (d, 2H, J = 8.5 Hz), 8.32 (s, 4H, NH), 8.18 (d, 4H, J = 8.7 Hz), 5.42 (m, pCO-CH₂CH), 2.51 (t, 4H, J = 7.3 Hz,

CH₂CO), 2.40 (m, 2H, (CH₂)CH), 1.98 (m, pCO-CHCH₂), 1.78-1.48 (m, 8H, CH₂), 1.42-1.22 (m, pCO-CH₂), 0.99-0.81 (m, 12H, CH₃) ppm; ¹³C NMR (CDCl₃): δ = 173.2, 171.8, 154.1, 153.7, 153.4, 138.7 (2), 130.3 (*trans*, pCO), 129.9 (*cis*, pCO), 118.3, 113.9, 113.6, 50.2, 38.0, 32.4 (pCO), 29.6 (pCO), 29.3 (pCO), 28.7 (3), 25.9, 25.3, 22.5, 14.1, 11.9 ppm; MALDI-TOF-MS (**33b**): (m/z) observed: distribution between 987 and 2420 g/mol (M+H⁺) as depicted in Figure 6.3(b); FTR-IR (ATR): ν = 3311, 2922, 2852, 1708, 1688, 1609, 1540, 1505, 1463, 1436, 1388, 1314, 1287, 1168, 1136, 965, 855, 803 cm⁻¹; GPC(THF) (**33a**): M_w = 13.0 kg/mol, M_n = 8.0 kg/mol, PDI = 1.63; GPC(THF) (**33b**): M_w = 8.1 kg/mol, M_n = 3.4 kg/mol, PDI = 2.38.

Methyl end-capped pCO, 34: A solution of *trans*-3-hexene **29** (66 mg, 0.78 mmol) and cyclooctene (1.7 g, 14.7 mmol) in a dried 5 mL vial was heated to 55 °C. A solution of 2nd generation Grubbs' catalyst (2.4 mg, 2.8 μmol, 0.36 mol% CTA) in dry DCE (0.8 mL) was added under argon. The solution immediately gelled and was stirred at 55 °C for 28 h. The solution was cooled to RT and 1.0 mL of chloroform was added. The viscous solution was added dropwise into 100 mL methanol with added BHT to prevent cross linking. The mixture was cooled overnight in the fridge followed by isolation of the white precipitate by centrifugation. ¹H NMR (CDCl₃): δ = 5.39 (m, 52H, pCO-CH₂CH), 1.98 (m, 104H, pCO-CHCH₂), 1.28 (m, 208H, pCO-CH₂), 0.97 (t, 6H, J = 6.8 Hz, CH₃) ppm; ¹³C NMR (CDCl₃): δ = 138.7 (2), 130.5 (*trans*, pCO), 130.0 (*cis*, pCO), 32.8 (pCO), 29.8 (pCO), 29.2 (pCO), 27.4, 25.7, 14.2 ppm; GPC(THF): M_w = 10.6 kg/mol, M_n = 5.7 kg/mol, PDI = 1.85.

6.6 References

- (1) Förster, S.; Antonietti, M. *Adv. Mater.* **1998**, *10*, 195-217.
- (2) Hamley, I. W. *The Physics of Block Copolymers*; Oxford Science Publications: Oxford, 1998.
- (3) Flory, P. J. *J. Chem. Phys.* **1942**, *10*, 51-61.
- (4) Huggins, M. L. *J. Am. Chem. Soc.* **1942**, *64*, 1712-19.
- (5) Matsen, M. W.; Bates, F. S. *Macromolecules* **1996**, *29*, 1091-8.
- (6) Whitesides, G. M.; Grzybowski, B. *Science* **2002**, *295*, 2418-2421.
- (7) Muthukumar, M.; Ober, C. K.; Thomas, E. L. *Science* **1997**, *277*, 1225-1232.
- (8) Stupp, S. I.; LeBonheur, V.; Walker, K.; Li, L. S.; Huggins, K. E.; Keser, M.; Amstutz, A. *Science* **1997**, *276*, 384-389.
- (9) Ikkala, O.; ten Brinke, G. *Chem. Commun.* **2004**, 2131-7.
- (10) Lohmeijer, B. G. G.; Schubert, U. S. *Angew. Chem. Int. Ed.* **2002**, *41*, 3825-3829.
- (11) Fustin, C.-A.; Lohmeijer, B. G. G.; Duwez, A.-S.; Jonas, A. M.; Schubert, U. S.; Gohy, J.-F. *Adv. Mater.* **2005**, *17*, 1162-1165.
- (12) Zimmerman, S. C.; Corbin, P. S. *Struct. Bonding (Berlin)* **2000**, *96*, 63-94.
- (13) Sijbesma, R. P.; Meijer, E. W. *Chem. Commun.* **2003**, 5-16.
- (14) Freitas, L. d. L.; Jacobi, M. M.; Goncalves, G.; Stadler, R. *Macromolecules* **1998**, *31*, 3379-3382.
- (15) Hirschberg, J. H. K. K.; Ramzi, A.; Sijbesma, R. P.; Meijer, E. W. *Macromolecules* **2003**, *36*, 1429-1432.
- (16) Fouquey, C.; Lehn, J. M.; Levelut, A. M. *Adv. Mater.* **1990**, *2*, 254-7.
- (17) Kotera, M.; Lehn, J. M.; Vigneron, J. P. *J. Chem. Soc., Chem. Commun.* **1994**, 197-9.
- (18) Berl, V.; Schmutz, M.; Krische, M. J.; Khoury, R. G.; Lehn, J.-M. *Chem. Eur. J.* **2002**, *8*, 1227-1244.
- (19) Binder, W. H.; Kunz, M. J.; Ingolic, E. *J. Polym. Sci., Part A : Polym. Chem.* **2003**, *42*, 162-172.
- (20) Kunz, M. J.; Hayn, G.; Saf, R.; Binder, W. H. *J. Polym. Sci., Part A : Polym. Chem.* **2004**, *42*, 661-674.
- (21) Binder, W. H.; Kunz, M. J.; Kluger, C.; Hayn, G.; Saf, R. *Macromolecules* **2004**, *37*, 1749-1759.

- (22) Binder, W. H.; Bernstorff, S.; Kluger, C.; Petraru, L.; Kunz, M. J. *Adv. Mater.* **2005**, *17*, 2824-2828.
- (23) Yamauchi, K.; Lizotte, J. R.; Hercules, D. M.; Vergne, M. J.; Long, T. E. *J. Am. Chem. Soc.* **2002**, *124*, 8599-8604.
- (24) Castellano, R. K.; Clark, R.; Craig, S. L.; Nuckolls, C.; Rebek, J., Jr. *Proc. Natl. Acad. Sci. USA* **2000**, *97*, 12418-12421.
- (25) Yang, X.; Hua, F.; Yamato, K.; Ruckenstein, E.; Gong, B.; Kim, W.; Ryu, C. Y. *Angew. Chem. Int. Ed.* **2004**, *43*, 6471-6474.
- (26) Rowan, S. J.; Suwanmala, P.; Sivakova, S. J. *Polym. Sci., Part A : Polym. Chem.* **2003**, *41*, 3589-3596.
- (27) Corbin, P. S.; Zimmerman, S. C. *J. Am. Chem. Soc.* **1998**, *120*, 9710-9711.
- (28) Ligthart, G. B. W. L.; Ohkawa, H.; Sijbesma, R. P.; Meijer, E. W. *J. Org. Chem.*, in press.
- (29) Wang, X.-Z.; Li, X.-Q.; Shao, X.-B.; Zhao, X.; Deng, P.; Jiang, X.-K.; Li, Z.-T.; Chen, Y.-Q. *Chem. Eur. J.* **2003**, *9*, 2904-2913.
- (30) Zhao, X.; Wang, X.-Z.; Jiang, X.-K.; Chen, Y.-Q.; Li, Z.-T.; Chen, G.-J. *J. Am. Chem. Soc.* **2003**, *125*, 15128-15139.
- (31) Li, X.-Q.; Jiang, X.-K.; Wang, X.-Z.; Li, Z.-T. *Tetrahedron* **2004**, *60*, 2063-2069.
- (32) Li, X.-Q.; Feng, D.-J.; Jiang, X.-K.; Li, Z.-T. *Tetrahedron* **2004**, *60*, 8275-8284.
- (33) Li, X.-Q.; Jia, M.-X.; Wang, X.-Z.; Jiang, X.-K.; Li, Z.-T.; Chen, G.-J.; Yu, Y.-H. *Tetrahedron* **2005**, *61*, 9600-9610.
- (34) Ligthart, G. B. W. L.; Ohkawa, H.; Sijbesma, R. P.; Meijer, E. W. *J. Am. Chem. Soc.* **2005**, *127*, 810-811.
- (35) Keizer, H. M.; Sijbesma, R. P.; Meijer, E. W. *Eur. J. Org. Chem.* **2004**, 2553-2555.
- (36) Sijbesma, R. P.; Beijer, F. H.; Brunsveld, L.; Folmer, B. J. B.; Hirschberg, J. H. K. K.; Lange, R. F. M.; Lowe, J. K. L.; Meijer, E. W. *Science* **1997**, *278*, 1601-1604.
- (37) Yin, J.; Buchwald, S. L. *J. Am. Chem. Soc.* **2002**, *124*, 6043-6048.
- (38) Jacobson, H.; Beckmann, C. O.; Stockmayer, W. H. *J. Chem. Phys.* **1950**, *18*, 1607-12.
- (39) Ercolani, G.; Mandolini, L.; Mencarelli, P.; Roelens, S. J. *Am. Chem. Soc.* **1993**, *115*, 3901-8.
- (40) ten Cate, A. T.; Sijbesma, R. P. *Macromol. Rapid Commun.* **2002**, *23*, 1094-1112.
- (41) Folmer, B. J. B.; Sijbesma, R. P.; Meijer, E. W. *J. Am. Chem. Soc.* **2001**, *123*, 2093-2094.
- (42) Söntjens, S. H. M.; Sijbesma, R. P.; van Genderen, M. H. P.; Meijer, E. W. *Macromolecules* **2001**, *34*, 3815-3818.
- (43) ten Cate, A. T.; Kooijman, H.; Spek, A. L.; Sijbesma, R. P.; Meijer, E. W. *J. Am. Chem. Soc.* **2004**, *126*, 3801-3808.
- (44) Folmer, B. J. B.; Sijbesma, R. P.; Kooijman, H.; Spek, A. L.; Meijer, E. W. *J. Am. Chem. Soc.* **1999**, *121*, 9001-9007.
- (45) Timmerman, P.; Weidmann, J.-L.; Jolliffe, K. A.; Prins, L. J.; Reinhoudt, D. N.; Shinkai, S.; Frish, L.; Cohen, Y. *J. Chem. Soc., Perkin Trans. 2* **2000**, 2077-2089.
- (46) Olenyuk, B.; Levin, M. D.; Whiteford, J. A.; Shield, J. E.; Stang, P. J. *J. Am. Chem. Soc.* **1999**, *121*, 10434-10435.
- (47) Keizer, H. M.; Sijbesma, R. P.; Jansen, J. F. G. A.; Pasternack, G.; Meijer, E. W. *Macromolecules* **2003**, *36*, 5602-5606.
- (48) Ho, F. F. L. *Anal. Chem.* **1973**, *45*, 603-5.
- (49) Keizer, H. M.; van Kessel, R.; Sijbesma, R. P.; Meijer, E. W. *Polymer* **2003**, *44*, 5505-5511.
- (50) Corey, E. J.; Cheng, X.-M. *The Logic of Chemical Synthesis*; John Wiley & Sons, Inc.: New York, 1995.
- (51) Ky Hirschberg, J. H. K.; Beijer, F. H.; van Aert, H. A.; Magusin, P. C. M. M.; Sijbesma, R. P.; Meijer, E. W. *Macromolecules* **1999**, *32*, 2696-2705.
- (52) Folmer, B. J. B.; Sijbesma, R. P.; Versteegen, R. M.; van der Rijt, J. A. J.; Meijer, E. W. *Adv. Mater.* **2000**, *12*, 874-878.
- (53) Yamauchi, K.; Lizotte, J. R.; Long, T. E. *Macromolecules* **2002**, *35*, 8745-8750.

- (54) Knoen, W.; Besseling, N. A. M.; Bouteiller, L.; Cohen Stuart, M. A. *Phys. Chem. Chem. Phys.* **2005**, *7*, 2390-2398.
- (55) Hillmyer, M. A.; Grubbs, R. H. *Macromolecules* **1995**, *28*, 8662-7.
- (56) Scherman, O. A.; Kim, H. M.; Grubbs, R. H. *Macromolecules* **2002**, *35*, 5366-5371.
- (57) The benzylidene on the ruthenium catalyst can be transferred to the polymer producing a monofunctional chain. The amount of monofunctional species is governed by the CTA to catalyst ratio. In this case, CTA/catalyst is 250 - 400 which results in << 0.4% benzylidene end-capped species.
- (58) Grubbs, R. H. *Handbook of Metathesis*; Wiley-VCH: Weinheim, 2003.
- (59) Scherman, O. A.; Rutenberg, I. M.; Grubbs, R. H. *J. Am. Chem. Soc.* **2003**, *125*, 8515-8522.
- (60) Bielawski, C. W.; Grubbs, R. H. *Angew. Chem. Int. Ed.* **2000**, *39*, 2903-2906.
- (61) Higley, M. N.; Pollino, J. M.; Hollembeak, E.; Weck, M. *Chem. Eur. J.* **2005**, *11*, 2946-2953.
- (62) Bodner, R. L.; Hendricker, D. G. *Inorg. Chem.* **1973**, *12*, 33-7.
- (63) Staniewicz, R. J.; Hendricker, D. G. *J. Am. Chem. Soc.* **1977**, *99*, 6581-8.
- (64) Boelrijk, A. E. M.; van Velzen, M. M.; Neenan, T. X.; Reedijk, J.; Kooijman, H.; Spek, A. L. *J. Chem. Soc., Chem. Commun.* **1995**, 2465-7.
- (65) Boelrijk, A. E. M.; Neenan, T. X.; Reedijk, J. *J. Chem. Soc., Dalton Trans.* **1997**, 4561-4570.
- (66) Ohkawa, H.; Ligthart, G. B. W. L.; Sijbesma, R. P.; Meijer, E. W. *manuscript in preparation*.
- (67) Bazzi, H. S.; Sleiman, H. F. *Macromolecules* **2002**, *35*, 9617-9620.
- (68) Stubbs, L. P.; Weck, M. *Chem. Eur. J.* **2003**, *9*, 992-999.
- (69) Hillmyer, M. A.; Nguyen, S. T.; Grubbs, R. H. *Macromolecules* **1997**, *30*, 718-721.
- (70) Gibson, V. C.; Okada, T. *Macromolecules* **2000**, *33*, 655-656.
- (71) Bielawski, C. W.; Morita, T.; Grubbs, R. H. *Macromolecules* **2000**, *33*, 678-680.
- (72) Morita, T.; Maughon, B. R.; Bielawski, C. W.; Grubbs, R. H. *Macromolecules* **2000**, *33*, 6621-6623.
- (73) The *cis*- and *trans*-2-butene-1,4-dihalides as well as *trans*-3-hexenedioic acid are commercially available.
- (74) He, Z.; Nadkarni, D. V.; Sayre, L. M.; Greenaway, F. T. *Biochim. Biophys. Acta* **1995**, *1253*, 117-27.
- (75) Scherman, O. A.; Grubbs, R. H. *Synth. Met.* **2001**, *124*, 431-434.
- (76) Hillmyer, M. A.; Laredo, W. R.; Grubbs, R. H. *Macromolecules* **1995**, *28*, 6311-16.
- (77) Scherman, O. A.; Walker, R.; Grubbs, R. H. *Macromolecules* **2005**, *38*, 9009-9014.
- (78) These *K_a* values were determined using the single-point method described in Chapter 5.
- (79) Hoogenboom, R.; Keizer, H. M.; Sijbesma, R. P.; Meijer, E. W. "Quadruple Hydrogen Bonding in Water," Technische Universiteit Eindhoven, 2001.
- (80) See Chapter 5 for NMR characterization of the heterodimer.
- (81) Cates, M. E. *Macromolecules* **1987**, *20*, 2289-96.
- (82) Cates, M. E.; Candau, S. J. *J. Phys.: Condens. Matter* **1990**, *2*, 6869-92.
- (83) Granek, R.; Cates, M. E. *J. Chem. Phys.* **1992**, *96*, 4758-67.
- (84) Hirschberg, J.; Beijer, F. H.; van Aert, H. A.; Magusim, P.; Sijbesma, R. P.; Meijer, E. W. *Macromolecules* **1999**, *32*, 2696-2705.
- (85) For a more detailed discussion about the changes in the UV/Vis absorption of the Napy group upon heterodimerization, see section 5.2.5 in Chapter 5.
- (86) Mandolini, L. *Adv. Phys. Org. Chem.* **1986**, *22*, 1-111.
- (87) Beijer, F. H.; Sijbesma, R. P.; Kooijman, H.; Spek, A. L.; Meijer, E. W. *J. Am. Chem. Soc.* **1998**, *120*, 6761-6769.
- (88) Corbin, P. S.; Zimmerman, S. C.; Thiessen, P. A.; Hawryluk, N. A.; Murray, T. J. *J. Am. Chem. Soc.* **2001**, *123*, 10475-10488.
- (89) Strukov, O. G.; Smirnov, S. K.; Dubov, S. S.; Danilina, L. L. *Zh. Org. Khim.* **1969**, *5*, 1257-9.
- (90) Ruzicka, L.; Plattner, P. A.; Widmer, W. *Helv. Chim. Acta* **1942**, *25*, 604-20.

7

Supramolecular graft-copolymers based on 2,7-diamido-1,8-naphthyridines

Abstract

Two supramolecular graft-copolymers containing a quadruple hydrogen bond motif in the main-chain have been prepared by acyclic diene metathesis (ADMET) of an α,ω -diene and by the polycondensation of a bis-hydroxy monomer containing a 2,7-diamido-1,8-naphthyridine (Napy) unit. Both polymerization reactions yielded materials with number average degrees of polymerization of approximately 11. During the ADMET-polymerization, a supramolecular protection strategy was applied in order to prevent naphthyridine coordination to the ruthenium catalyst. The 2-ureido-4[1H]-pyrimidinone (UPy) derivatives used as protecting groups also allowed for detection of the supramolecular graft-copolymers with size exclusion chromatography. Deprotection by simple treatment with a polar solvent afforded free Napy binding sites on the main-chain. The condensation polymer displayed a slightly weaker binding towards UPy derivatives than the reference compound containing a single Napy unit. This is presumably due to an increased polarity of the local binding environment. Reversible grafting of UPy derivatives of various sizes onto the free poly-Napy was demonstrated by diffusion ordered NMR experiments.

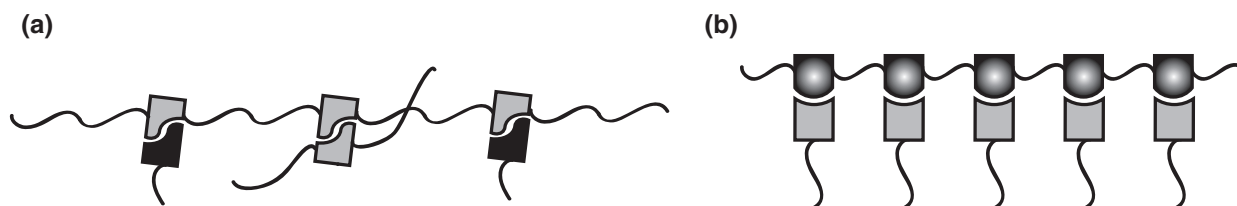
7.1 Introduction

The reversibility and versatility of non-covalent assemblies in Nature has always inspired man to design and organize new soft and/or biocompatible materials. Especially the construction of supramolecular polymers and other dynamic architectures using strategies based on non-covalent interactions has evolved tremendously over the last decade.¹⁻³ Such synthetic strategies make use of hydrogen bonding,^{4,5} metal coordination,⁶ and hydrophobic interactions.⁷ Supramolecular polymers are typically divided into two categories: i) side-chain and ii) main-chain polymers. Pioneering work in the area of side-chain polymers was first reported for the synthesis of liquid crystalline materials.⁸⁻¹³ A limitation of these early and more recent examples of side-chain functionalized polymer systems based on hydrogen bonding is the lack of binding strength of the recognition motif. Typical examples employ single hydrogen bonds,^{14,15} with fewer examples extending up to triple hydrogen bonding.¹⁶⁻²⁰ Although such weak side-chain self-assembly has been applied to materials design,^{21,22} a methodology to increase both the degree of functionalization as well as the strength of the binding motif is desirable.

In the past, it was shown that supramolecular polymers with high degrees of polymerization in excess of several hundreds can be formed by small monomers containing self-complementary 2-ureido-4[1H]-pyrimidinone (UPy) groups.²³⁻²⁵ These molecules form extremely stable homodimers in chloroform solution (dimerization constant $K_{\text{dim}} = 6 \times 10^7 \text{ M}^{-1}$ in CHCl_3).²⁶ This last feature makes the UPy group very suitable for application in various polymeric systems. However, for use in side-chain functionalized systems, the self-complementary UPy units will result in a collapsed polymeric aggregate due to intramolecular binding within the chain. Furthermore, a statistical mixture of hetero versus homodimers can be expected upon functionalization with a UPy pendant group (Scheme 7.1a). Although UPy heterodimers have been reported before,²⁷ the need for a strong complementary multiple hydrogen bond motif is evident. Fortunately, due to its ability to form an intramolecular hydrogen bond and prototropy on the pyrimidinone ring, the UPy unit is able to selectively form strong heterodimers in one of its tautomeric forms via a hydrogen bonding acceptor-donor-donor-acceptor (ADDA) array with the DAAD array of 2,7-diamido-1,8-naphthyridines (Napy).^{28,29}

In chapters 5 and 6, it was described that these dual complexation modes of UPy result in concentration dependent selectivity, favoring UPy-Napy heterocomplexation over UPy dimerization by a factor of > 20:1 above 0.1 M in 1:1 mixtures ($K_{\text{a}}(\text{UPy-Napy}) > 10^6 \text{ M}^{-1}$).^{30,31} Furthermore, UPy-Napy based supramolecular copolymers were prepared.^{30,32} The high

selectivity for heterodimerization makes the UPy-Napy system eminently suitable to explore the possibilities of obtaining supramolecular graft-copolymers with Napy units in the main-chain and UPy molecules as the side-chains (Scheme 7.1b).

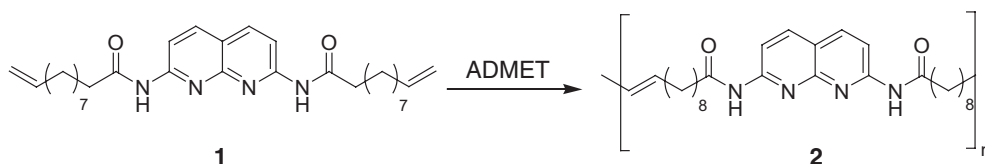


Scheme 7.1 Schematic representation of UPy (a), and Napy-based graft-copolymer (b) with UPy pendant groups.

In this chapter, two polymerization procedures involving bifunctional Napy units are explored to obtain strictly linear polymers with a DAAD quadruple hydrogen bonding motif in the main chain. Characterization of the grafted and ungrafted poly-Napy is done by ^1H NMR analysis and size exclusion chromatography. Finally, the possibility of reversible grafting with different UPy derivatives is investigated with diffusion ordered NMR spectroscopy.

7.2 Oligo-2,7-bis(9-decenoylamino)-1,8-naphthyridines via acyclic diene metathesis polymerization

Among various polymerization techniques that can be used to obtain strictly linear polymers, acyclic diene metathesis (ADMET) polymerization has proven a valuable tool for the construction of new polymer architectures due to the high catalytic activity of the applied ruthenium catalysts and the high functional group tolerance these catalysts display.^{33,34} 2,7-Bis-(10-undecenoylamino)-1,8-naphthyridine (**1**) was chosen as the Napy monomer since ADMET polymerization reactions are normally performed on α,ω -dienes (Scheme 7.2). This derivative can be prepared on multi-gram scale via Pd-catalyzed Buchwald-Hartwig amidation as reported in Chapter 3.³⁵ Because of the hydrolytic instability of the amide groups on **1**, ruthenium based metathesis catalysts were applied. The work described in this section was performed in collaboration with Dr. Haruki Ohkawa.



Scheme 7.2 ADMET of acyclic Napy diene **1**.

7.2.1 Synthesis of oligo-2,7-bis(9-decenoylamino)-1,8-naphthyridines

ADMET polymerization of Napy diene **1** was performed in dry toluene at various temperatures using various ruthenium catalysts. The reaction was monitored by ^1H NMR and conversion was determined by integration of the olefinic signals at 4.94 and 5.31 ppm for **1** and **2**, respectively. Unfortunately, initial attempts to polymerize **1** using the second generation Grubbs' ruthenium catalyst (**A**) in toluene or dichloromethane did not yield any polymer (Table 1, entry 1 and 2). In order to facilitate the metathesis reaction, prolonging the lifetime of the active form of the ruthenium catalyst in which the phosphorous ligand is dissociated from the metal is a key issue as reported by Grubbs and co-workers.³⁶ For this purpose, two approaches have been used in literature. The first approach is to increase the rate of dissociation of the phosphine ligand from the catalyst. This can be achieved by replacing the ligand with one of lower basicity³⁷⁻³⁹ (Figure 7.1, approach 1). The second is to prevent re-association of the dissociated ligand by using an acid as phosphine scavenger (Figure 7.1, approach 2).^{40,41}

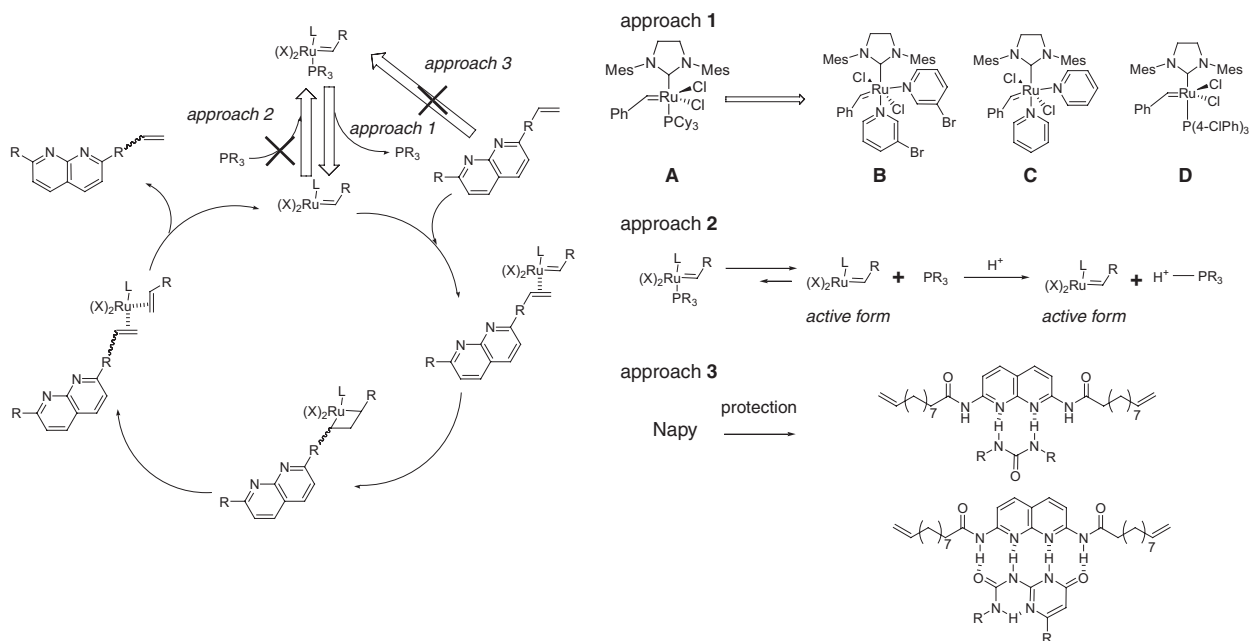
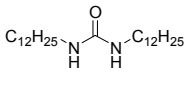
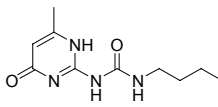
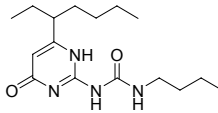
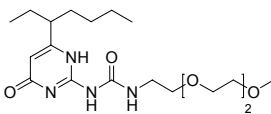


Figure 7.1 Catalytic cycle in metathesis reaction and three approaches for extending the lifetime of the active form of the Grubbs catalyst.

However, neither of these approaches was successful for efficient ADMET of Napy monomer **1**, as shown in Table 7.1 (entries 1-5). According to MALDI-ToF mass spectroscopy, only dimer, trimer, and trace amounts of tetramer of ADMET-product **2** were formed. Together with the fact that the color of the reaction mixture turned green, these results suggest that the Napy deactivates the ruthenium catalyst by coordinating to the active ruthenium center. A similar

observation was described in Chapter 6 when main-chain supramolecular polymers were prepared by ring-opening metathesis (ROMP) polymerization using a bifunctional Napy chain transfer agent. In order to circumvent coordination of the naphthyridine to the ruthenium catalyst and subsequent catalyst death, we considered a supramolecular protective group strategy analogous to the use of protecting groups in traditional organic chemistry. Such a strategy has been used before in the controlled ring-opening metathesis polymerization (ROMP) of norbornene monomers bearing triple hydrogen bonding units.^{17,42} In these polymerizations succinimide or butylthymine was added as a protecting group to prevent the self-association of adenine⁴² and diamido-pyridine¹⁷ units, respectively. Here we propose the use of a supramolecular protective group to prevent coordination of the two nitrogen atoms on the naphthyridine ring to the catalyst (Figure 7.1, approach 3).

Table 7.1 ADMET of Napy monomer **1**.^a

entry	catalyst	additive	T (°C)	conv. ^b (%)
1	A	-	40 ^c	<20
2	A	-	50	<20
3	B	-	50	<20
4	C	-	50	<20
5	D	-	50	<20
6	A	CH ₃ COOH 2.0 eq	50	<20
7	A	 0.5 eq	50	40
8	A	 3 , 1.5 eq	50	70
9	A	 4 , 2.0 eq	50	80
10	A	 5 , 1.2eq	50	80

^a Reaction conditions: 10% [Ru], 0.2-0.5 M in dry toluene ^b conversion of **1** was determined by ¹H NMR;

^c CH₂Cl₂ was used as solvent

In a first attempt to use a supramolecular protecting group for the naphthyridine moiety, N,N'-di-dodecylurea was added (entry 6). With 1.1 equivalent of urea present, conversion of the terminal double bond of **1** improved from 20% to 40% (entry 7). Hydrogen

bonding of the urea to the naphthyridine which was substantiated by a downfield shift in NH protons of the urea in the ^1H NMR spectrum, however, was apparently not sufficient to completely prevent coordination of the naphthyridine to the ruthenium. In contrast, when UPy **3** was introduced as a protecting group, conversion was improved dramatically to 70% (entry 8). This strongly suggests efficient protection of the metathesis catalyst by selective formation of the UPy-Napy heterocomplex by the complementary quadruple hydrogen bonding shown in Figure 7.1. A further increase in conversion was obtained when more soluble UPy **4** was used (entry 9). A similar conversion of 80% was found when 1.2 equivalents of the more polar triethylene glycol UPy derivative **5** was used (entry 10).

Purification of the crude reaction mixtures **2** - **3_n** or **2** - **4_n** proved to be difficult. More than 80 % of UPy **4** could be removed from the supramolecular graft-copolymer **2** by gel permeation chromatography using 10 v/v % methanol in THF as an eluent. However, due to the poor solubility of **2** in highly polar solvents like methanol, this approach was not successful to obtain pure **2**. Furthermore, the Napy polymer chain itself seemed to aggregate, which renders it even more difficult to remove the protecting group from the polymer. Reaction mixture **2** - **5_n** was substantially easier to purify. Due to the branched 3-heptyl group on the pyrimidinone ring and the polar triethylene glycol tail, UPy **5** displays a high solubility in a variety of solvents including THF and ethanol.⁴³ Removal of **5** after ADMET of monomer **1** was successfully performed by precipitation in warm ethanol. Unreacted monomer **1** was removed by trituration in hot ethanol affording **2** in 59% yield.

7.2.2 Characterization of ADMET-polymer **2**

7.2.2.1 NMR spectroscopy

The ADMET polymerization reaction of Napy diene **1** was monitored by ^1H NMR and conversion was determined by integration of the olefinic signals. Near-quantitative conversion of monomer to polymer is standard in these polymerizations, as few side reactions occur other than a small amount of cycle formation common in all polycondensation reactions.⁴⁴ However, olefin isomerization has been reported as a side-reaction with Grubbs' second generation catalyst.⁴⁵ In the present reaction, ^1H and ^{13}C NMR analysis revealed the absence of significant amounts of isomerization products. Figure 7.2 shows a part of the spectrum of ADMET-polymer **2** grafted with UPy **5** (left) and pure polymer **2** obtained after removal of **5** (right). The NH signals characteristic of UPy – Napy heterocomplex formation were observed in the

downfield region at 13.89, 11.89, 11.36, 9.90 ppm as well as the NH signals arising from UPy homodimers at 13.32, 11.96 and 10.24 ppm. In addition, a different resonance of the alkylidene proton of the UPy is found for its ADDA tautomer ($\delta = 6.01$ ppm) compared to its AADD tautomer ($\delta = 5.87$ ppm).

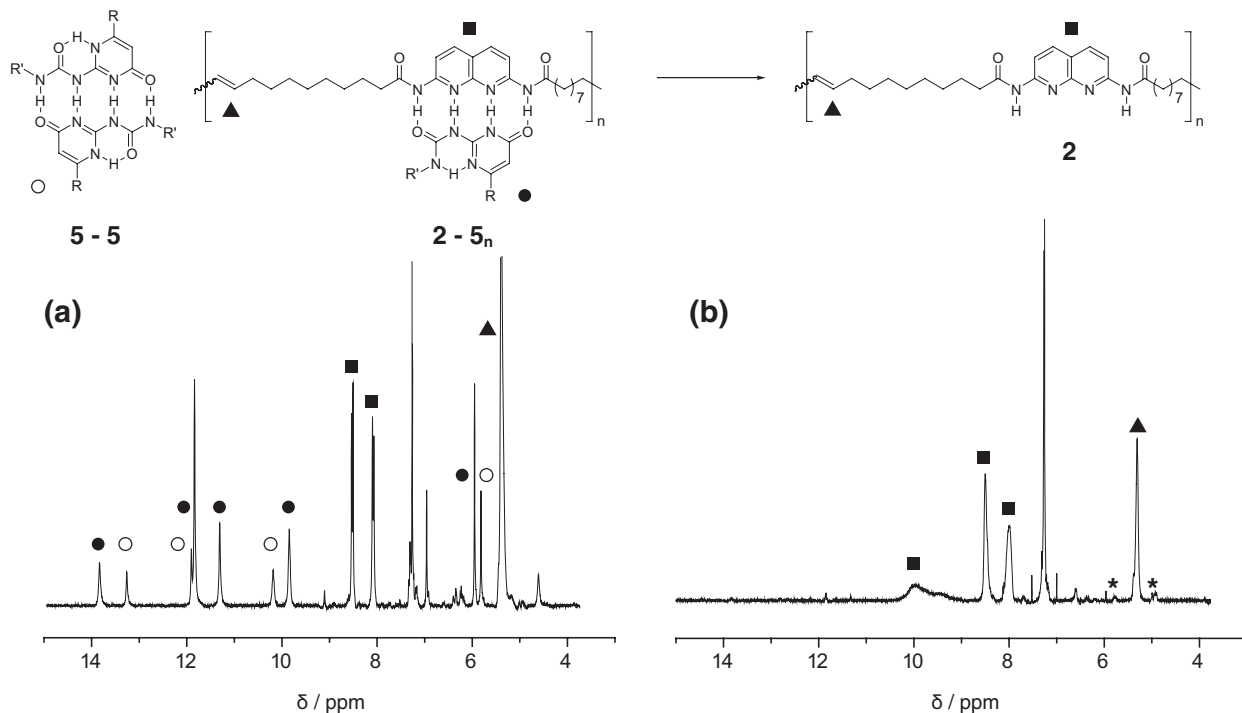


Figure 7.2 (a): ^1H NMR spectrum in CDCl_3 of **2** grafted with UPy **5**; (b): ^1H NMR spectrum in CDCl_3 of pure **2**. Symbols indicate signals from UPy in UPy dimer (○), UPy in UPy-Napy heterodimer (●), Napy (■), the internal olefin (▲). Terminal olefin end-groups are indicated with asterisks.

Unfortunately, polymer **2** is not very soluble in common organic solvents like chloroform, THF and methanol. This is also evident from its NMR spectrum in chloroform in which considerable broadening of the naphthyridine signals at 8.00 and 8.50 ppm is observed which indicates the formation of aggregates. Additionally, the broad signal around 10 ppm attributed to the NH protons is shifted downfield which probably indicates weak hydrogen bond formation to other naphthyridine units. However, using the terminal CH_2 peak at 4.94 ppm and the internal CH signal at 5.31 ppm, an average DP of 12.4 was determined by conventional end-group analysis. Although polymer **2** should be easy to protonate due to the basic nitrogen atoms in the central naphthyridine ring, analysis by MALDI-ToF-MS only showed small oligomers.

7.2.2.2 Size exclusion chromatography

Size exclusion chromatography (SEC) is a form of liquid chromatography capable of separating solute molecules according to their size and its basic principle has been explained in terms of sieving effect or size exclusion. Previously, it has been demonstrated to be an effective tool to study the size of supramolecular structures.⁴⁶⁻⁴⁸ However, important factors for the outcome of SEC experiments are the dynamics of the assemblies.⁴⁹ Although the UPy – Napy heterodimer has a high K_a value and displays slow exchange on the NMR time scale, their exchange is fast on the SEC time scale. This implies that the observed behavior of each dimer (UPy – Napy and UPy₂) on the SEC column represents a time average. Furthermore, continuous dissociation and exchange due to dilution during the elution will result in a broadened and tailed retention profile for graft polymer **2** – **5n**. As expected, reliable elution curves could not be obtained by simple injection of supramolecular graft-copolymer **2** – **5n** or ungrafted poly-Napy **2**. This can be explained by the poor solubility of **2** and the fast dynamics of the system.

An alternative methodology similar to gel filtration chromatography was therefore applied to detect the supramolecular graft-copolymer by SEC analysis in the presence of UPy in the eluent. This technique has been used to determine association constants of protein-ligand,^{50,51} protein-protein⁵² and metal-ligand complexes⁵³ on Sephadex columns. As in gel filtration chromatography, the SEC column (mixed-D Polymer Labs) was equilibrated with a 0.80 mM UPy **4** solution in chloroform. UV/Vis detection was performed at 350 and 270 nm, corresponding to the absorption maximum of Napy in the heterodimer and UPy, respectively. The baseline of the UV/Vis detector was adjusted to a 0.8 mM UPy **4** solution. As shown in Figure 7.3a, when a chloroform solution of UPy **4** was injected, the dimer was detected as a positive peak at 9.0 minutes. However, when a solution of toluene in chloroform was injected as a blank sample, a negative peak was observed at 9.0 minutes due to dilution of UPy in the eluent. The positive peak at higher retention times was attributed to toluene. A good elution curve was obtained for graft-copolymer **2** – **4n** by detection at 350 nm which is selective for 2,7-diamido-1,8-naphthyridines in the complexed form (Figure 7.3b). When completely deprotected poly-Napy **2** was injected, one positive peak of **2** and one negative peak of UPy were detected at 270 nm (Figure 7.3c). In this case, a portion of the UPy in solution in which poly-Napy **2** was dissolved, became bound to **2**. This portion of UPy, being associated with **2**, moved faster down the column than the UPy that remained unbound. This resulted in the depletion of UPy in the elution profile corresponding to the injected solution. The higher negative peak than the blank experiment, which corresponds to the decrease in UPy

concentration, is the summation of the effects of dilution and the capture of UPy **4** from the eluent by the ungrafted poly-Napy **2**. Additionally, the elution curve obtained when poly-Napy **2** was injected together with an excess of UPy **4** to yield the fully substituted supramolecular graft-copolymer, showed two positive peaks at 7.5 and 9.0 minutes, attributed to **2** – **4**_n and **4**₂, respectively (Figure 7.3d). The latter peak is due to the increase of the UPy concentration in the injected sample. The retention time of grafted poly-Napy was identical to the ungrafted poly-Napy. This is direct evidence that **2** selectively captures UPy molecules from the eluent and can therefore be detected as a supramolecular graft-copolymer. Consequently, the molecular weight of **2** – **4**_n could be determined as $M_n = 7000$, $M_w = 11690$, $M_w/M_n = 1.67$, which corresponds to a number average DP of 11.1. This value is in fair agreement with the values obtained by ^1H NMR end-group analysis and complexation analysis described in the previous section.

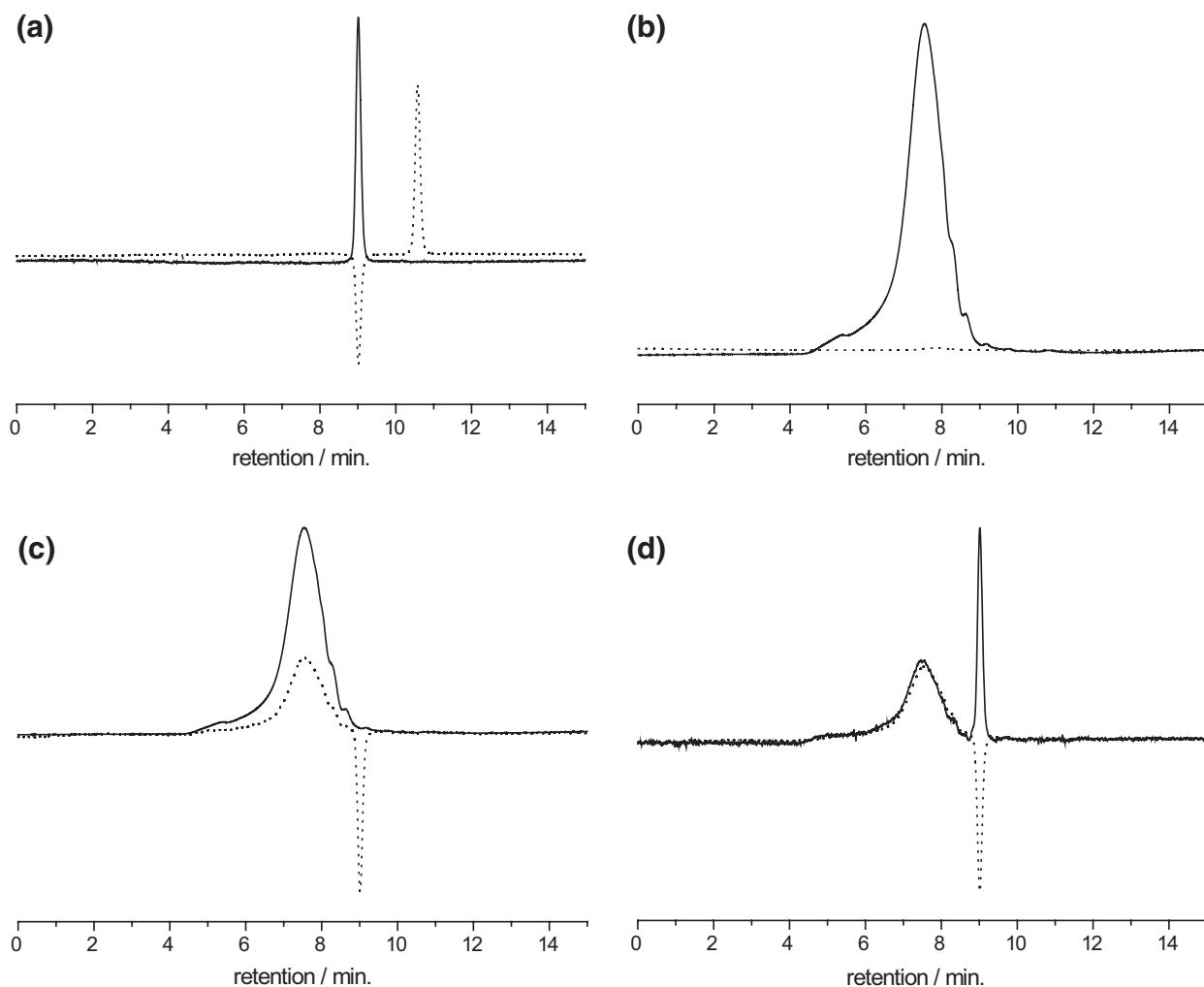
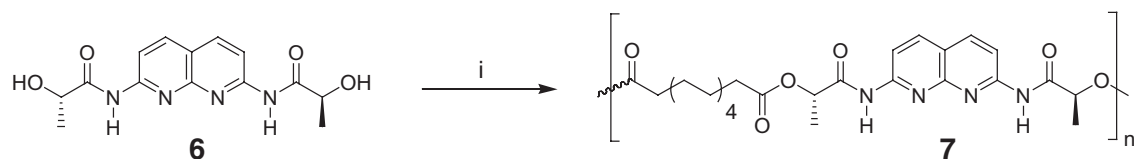


Figure 7.3 SEC elution curves; (a) full line: UPy **4**; dotted line: toluene, detection at 270 nm; (b) full line: poly-Napy·UPy **2** – **4**_n; dotted line: UPy **4**, detection at 350 nm; (c)) full line: poly-Napy·UPy **2** – **4**_n, detection at 350 nm; dotted line: poly-Napy·UPy **2** – **4**_n, detection at 270 nm; (d)) full line: poly-Napy·UPy **2** – **4**_n; dotted line: poly-Napy **2**, detection at 270 nm.

7.3 Oligo-2,7-diamido-1,8-naphthyridines via polycondensation

7.3.1 Synthesis and characterization of oligo-2,7-diamido-1,8-naphthyridine

A bifunctional Napy derivative, which has good synthetic accessibility via Pd-catalyzed Buchwald-Hartwig amidation, is 2,7-bis-(S-2-hydroxypropanoylamino)-1,8-naphthyridine **6**. Polycondensation⁵⁴ of monomer **6** with a di(acid chloride) will subsequently result in the formation of a polyester with multiple DAAD quadruple hydrogen bonding motifs in the main-chain (Scheme 7.3).



Scheme 7.3 Polycondensation of dihydroxy Napy **6**; i) dodecanedioyl dichloride (1.0 eq.), DMAP.

Table 7.2 Polycondensation of Napy monomer **6** with dodecanedioyl dichloride.^a

entry	r ^b	solvent	T (°C)	yield (%)	M _n ^c kg/mol	PDI
1	1.00	DMF	RT	36	2.76	1.45
2	1.00	CHCl ₃	RT	< 10	3.12	1.95
3	1.01	CHCl ₃	40	25	3.52	1.51
4	1.00	CHCl ₃ /DMF 4:1	40	44 ^d	5.07	1.31
5	1.05	CHCl ₃ /DMF 4:1	40	45	4.11	1.48

^a Reaction conditions: 0.1–0.2 M, 2.2 equiv. DMAP, 20 h; ^b r is the molar ratio dodecanedioyl dichloride / **6**; ^c determined by GPC in THF relative to polystyrene standards with detection at 270 nm; ^d polymer **7**.

Chloroform soluble polyester **7** was readily synthesized from **6** by condensation with dodecanedioyl dichloride using DMAP as a base (Table 7.2). The resulting polyester was obtained in moderate yields as a white solid after two precipitations of the reaction mixture in cold methanol and was characterized by GPC using THF as the eluent. Due to the low solubility of Napy monomer **6** in chloroform, DMF was initially used as solvent (entries 1 and 2). However, an increase in temperature also resulted in successful polyester formation in chloroform (entry 3). Using equimolar amounts of reactive groups in a chloroform/DMF solvent mixture, polymer **7** was obtained in 44% with a number average DP of Napy units of 10.1 (entry 4). In agreement with Carothers' theory, a lower M_n was observed when a non-equimolar mixture of reactive end-groups was polymerized (entry 5).⁵⁵

In contrast to ADMET polymer **2**, end-group analysis of polycondensation polymer **7** was not possible with ^1H NMR spectroscopy due to significant broadening and overlap of the signals, even though some acid chloride end-groups were converted to the methyl ester. However, MALDI-ToF-MS proved to be helpful in characterizing of polymer **7** (Figure 7.4). Four major sets of polymer peaks with a mass difference of 498.4 amu can be observed between 1000 and 8000 m/z in Figure 7.4a. The mass difference corresponds nicely to the monomeric unit containing one Napy moiety (**6**). The observed sets of peaks are in agreement with the formation of four oligomeric species which have different end-groups as illustrated schematically by cartoons in the figure. Figure 7.4b clearly shows that the H^+ and Na^+ adducts fly quite readily and the masses can be ascribed to a cycle or oligomeric chains with a precise number of monomeric units with either hydroxyl or carboxylic acid end-groups. For example, the m/z peak at 2493.1 arises from the protonated cycle with exactly 4 monomers. Cyclic species are formed as a consequence of cyclization instead of linear polymerization. In agreement with theoretical work on cyclization reactions in polycondensations,^{56,57} the intensity of cyclic species decreases from $m=2$ onward. The dominant species up to 4000 amu is the linear oligomer with one hydroxyl and one carboxylic acid end-group. Above 4000 amu, the oligomers with two hydroxyl end-groups are more prominent presumably due to a small excess of monomer **6** in the polymerization. Finally, oligomers with two carboxyl end-groups are also observed. As expected from the addition of a small excess of dodecanedioyl dichloride in the feed, MALDI-ToF-MS analysis of the polymer obtained from entry 5 revealed these oligomers as the dominant species.

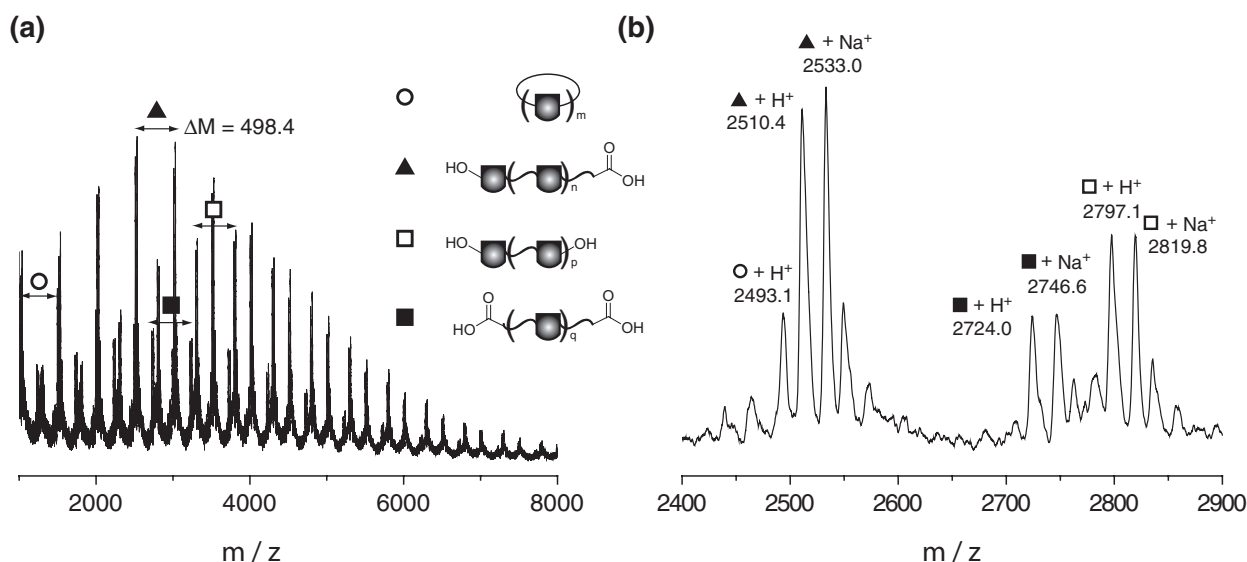


Figure 7.4 (a) MALDI-ToF-MS of **7** ionized from a CHCA matrix; the cartoons are a schematic representation of the identified species; (b) enlarged region of oligomers with $m = n = 4$ and $p = q = 5$.

A similar procedure as described in section 7.2.2.2 was applied to characterize polycondensation polymer **7** by SEC analysis using 0.80 mM UPy **4** in chloroform as the eluent. Figure 7.5 displays the SEC-traces for **7** – **4_n** with UV/Vis detection at 270 and 350 nm for (a) and (b), respectively. When a solution of ungrafted **7** in the eluent is injected onto the column, the selective binding of UPy from the eluent is illustrated by the negative peak at 9.0 minutes. A positive peak is obtained at 9.0 minutes when a solution of fully grafted **7** – **4_n** is injected. On the other hand, detection at 350 nm which is selective for Napy units in the complexed form only shows the grafted polymer. Moreover, the molecular weight of **7** – **4_n** could be determined against PS-standards as $M_n = 7640$, $M_w = 11400$, $M_w/M_n = 1.49$. These results correspond to a number average of 9.6 which is in good agreement with the value obtained by GPC analysis of ungrafted **7** in THF (DP = 10.1).

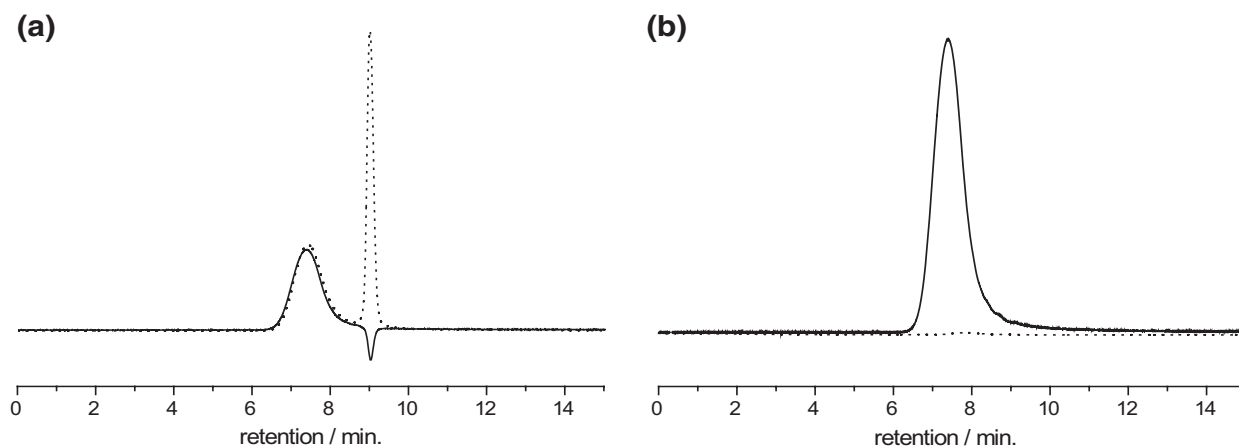
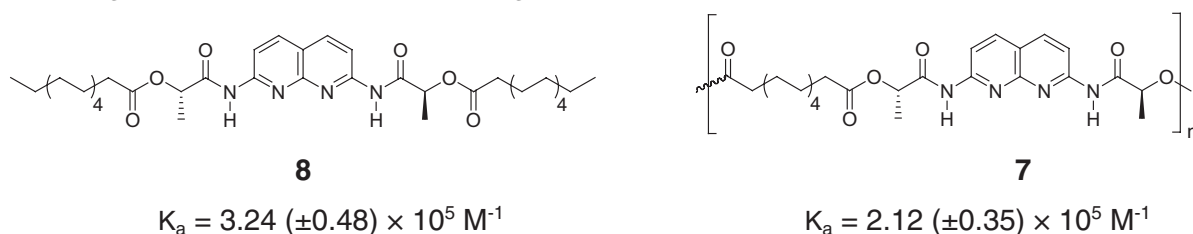


Figure 7.5 SEC elution curves; (a) full line: poly-Napy **7**; dotted line: poly-Napy-UPy **7** – **4_n**, detection at 270 nm; (b) full line: poly-Napy **7**; dotted line: UPy **4**, detection at 350 nm.

7.3.2 Recognition properties of oligo-2,7-diamido-1,8-naphthyridine

To examine the effects of a high degree of functionalization on the binding strength of polymer **7** with a UPy, reference Napy derivative **8** was synthesized. 2,7-Bis-(S-2-(dodecanoyloxy)propanoylamino)-1,8-naphthyridine **8** was synthesized in 41% yield by condensation of 2,7-bis-(S-2-hydroxypropanoylamino)-1,8-naphthyridine **6** with 2 equivalents of dodecanoyl chloride in the presence of 2.2 equivalents of DMAP. Subsequently, the single-point methodology outlined in Chapter 5 was used to determine the K_a values of UPy **4** with polymer **7** and reference compound **8**. The values given in Scheme 7.4 are average values from 5 measurements with the standard deviation in parentheses. While the K_a value of reference compound **8** with UPy **4** is $3.24 (\pm 0.48) \times 10^5 \text{ M}^{-1}$, polymer **7** displays a lower affinity for binding; $K_a = 2.12 (\pm 0.35) \times 10^5 \text{ M}^{-1}$. As stated previously in section 5.3, steric as well as

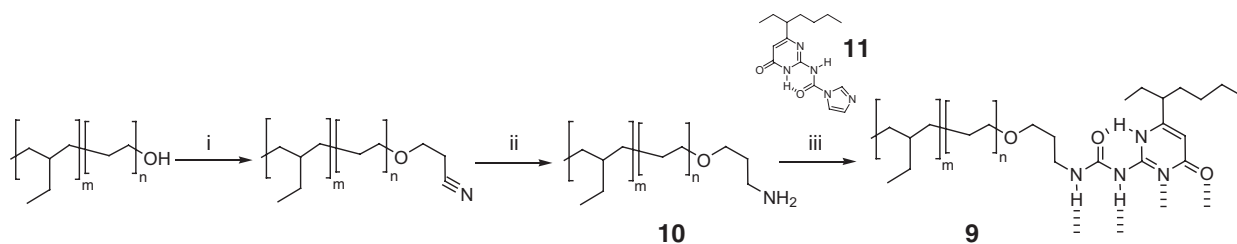
electronic effects can have a pronounced influence on the binding capability of Napy units to associate with a UPy derivative. Compared to ADMET monomer **1**, which has no branched alkyl chains on the α -position next to the carbonyl, Napy derivative **8** has a lower K_a value. This can be explained by both steric repulsion of the methyl substituent in the lactate fragment as well as by an additional repulsion between the oxygen atom of the carbonyl group and the oxygen atom of the ester group. The weaker binding displayed by polymer **7** compared to reference compound **8** is presumably the result of a more polar environment caused by the high density of polar functional groups in polymer **7**. A recent systematic study by Rotello and coworkers on the recognition properties of PMMA-embedded 2,6-diamidopyridines revealed an increase in binding efficiency as a function of molecular weight.²⁰ This was explained by an increase in local chloroform concentration with increasing molecular weight. In case of polymer **7**, an increase in alkyl linker or substitution by apolar telechelic polymers such as PS should give rise to an increased binding.



Scheme 7.4 Association constants of Napy derivatives **7** and **8** with UPy **4**

7.4 Supramolecular grafting

The dynamic nature of the non-covalent bond is a feature which can be addressed by external stimuli such as polarity of a solvent, temperature and pH. To demonstrate reversible grafting of UPy derivatives of different size on the poly-Napy main chain of **2** and **7**, diffusion-ordered ^1H NMR spectroscopy (DOSY) measurements were performed on chloroform solutions of various aggregates, using heptakis(2,3,6-tri-O-methyl)- β -cyclodextrin (CD) as an internal standard. 2D-DOSY NMR measurements have been applied for the characterization of supramolecular aggregates and have provided useful information about the relative size of these aggregates.^{58,59} In order to obtain measurable differences in diffusion behavior compared to UPy derivatives **3**, **4** and **5**, PEB-UPy (PEB = poly(ethylenebutylene)) **9** (M_w : ~ 3900) was used. PEB-UPy **9** was synthesized by UPy end-group modification of amino-functionalized PEB **10** by reaction with an activated imidazolidine **11** (Scheme 7.5). Imidazolidine **11** was obtained according to a literature procedure and was used *in situ*.⁶⁰ Amino-functionalized PEB **10** was prepared via Michael addition of α -hydroxy-PEB to acrylonitrile affording the PEB-nitrile and subsequent reduction with 1.0 M BH_3 in THF.⁶¹



Scheme 7.5 Synthesis of PEB-UPy **9**; i: acrylonitrile, NaOH/H₂O, toluene, 4 h, RT; ii: BH₃/THF, 4 h, reflux; iii: CHCl₃, 16 h, RT.

As can be seen in Table 7.3, significant differences in diffusion coefficients were measured. As expected for small molecules, monomers **1** and **6** together with UPy **4** have high normalized diffusion constants compared to the internal standard (1.16, 1.21 and 1.38, respectively; entries 1 and 2) while PEB-UPy **9** displays a low diffusion constant of 0.31 (entry 3). In contrast to ungrafted Napy polymers **2** and **7** which have low diffusion coefficients (0.36 and 0.46 for **2** and **7**, respectively; entry 4), graft-copolymers **2** – **4_n** and **7** – **4_n** had lower diffusion coefficients of 0.28 and 0.40, respectively (entry 5). This implies that the hydrodynamic radius is increased by grafting. Interestingly, when **2** or **7** were grafted with polymeric UPy **9**, even lower diffusion constants (0.17 and 0.13 for **2** – **9_n** and **7** – **9_n**, respectively; entry 6) were obtained indicating efficient grafting of the parent Napy-polymer with large grafted polyethylene-butylene side chains. In this way, reversible immobilization of different UPy derivatives is demonstrated on supramolecular graft-copolymers containing 2,7-diamido-1,8-naphthyridine moieties in the main-chain.

Table 7.3 Normalized diffusion constants of supramolecular graft-copolymers with UPy derivatives **4** or **9**.

entry		Normalized diffusion coefficients ^a	
1		1.16 (1)	1.21 (6)
2			1.38 (4)
3			0.31 (9)
4		0.36 (2)	0.46 (7)
5		0.28 (2 – 4_n)	0.40 (7 – 4_n)
6		0.17 (2 – 9_n)	0.13 (7 – 9_n)

^a Diffusion coefficients are normalized to heptakis(2,3,6-tri-O-methyl)-β-cyclodextrin; the compounds or complexes are given in parentheses.

7.5 Discussion and conclusions

In summary, the first supramolecular graft-copolymers based on the UPy-Napy heterodimer were successfully synthesized and characterized. The use of a supramolecular protecting group for the α,ω -Napy diene monomer turned out to be a prerequisite for efficient ADMET polymerization. Utilization of the UPy group capable of making a strong quadruply hydrogen bonded heterodimer with a Napy ensures conversions up to 80% of the Napy monomer in the ADMET polymerization. In contrast to UPy derivatives with alkyl substituents, the introduction of a triethylene glycol tail on the ureido position ensures increased solubility in polar solvents like ethanol and THF. Therefore, purification of the poly-Napy could be simplified to precipitation and trituration with ethanol. Confirmed by the results described in Chapter 6, the UPy protecting group approach is a powerful strategy towards constructing polymeric architectures containing 2,7-diamido-1,8-naphthyridine moieties by a wide-range of metathesis reactions. A more soluble polymer bearing Napy binding motifs in the main-chain was synthesized via polycondensation of a dihydroxy Napy derivative with a di(acid chloride). Characterization of the polymers showed number average degrees of polymerization of 10-12. Running the ADMET polymerizations under vacuum could possibly force the reaction towards higher conversion and hence higher molecular weight.

Additionally, the Napy polymers could be identified using size exclusion chromatography using a UPy solution as the mobile phase. It was shown that functionalization at low concentration of the ungrafted polymer can be achieved in the SEC run. The degrees of polymerization determined from SEC measurements were in good agreement with the DPs calculated from NMR or GPC analysis. This new method based on complementary affinity will open the way for detailed characterization studies of a variety of supramolecular architectures containing either Napy or UPy moieties. The high degree of functionality led to a decrease in binding affinity of the Napy moiety for a UPy in the Napy polycondensation polymer compared to the reference derivative. This may be the result of a high density of polar functionalities in the polymer.

Finally, reversible grafting of the Napy polymers was shown by diffusion ordered NMR experiments. Grafting of an ungrafted poly-Napy with a polymeric UPy led to a significant decrease in relative diffusion coefficient indicating a large hydrodynamic volume of the supramolecular graft-copolymers. In conclusion, we believe these results may not only open the way towards new supramolecular polymers bearing quadruple hydrogen bond arrays but also towards the synthesis of materials for reversible immobilization in solution phase

combinatorial chemistry in which Napy functionalized polymers are used to bind substrates equipped with a UPy group to a solid phase.⁶²⁻⁶⁶

7.6 Experimental procedures

General methods. See General methods Chapter 6.

Size exclusion chromatography Analytical SEC analyses were performed on a Shimadzu SEC system including a SPD-10AV UV-vis detector, using a Polymer Laboratories gel 5 μm mixed-D SEC column. A solution of 0.8 mM UPy **4** in CHCl_3 was used as eluent at a flow rate of 1.0 mL/min. 270 nm was selected to detect both Napy and UPy derivatives, while 350 nm was selected for the specific detection of the Napy chromophore. Usual sample concentration was 1 mg/mL for single injection of ungrafted polymer **2**, while for the grafted polymer **2** – **4**_n injection, a total concentration of 3 mg/mL with a 1:2 w/w% ratio of **2** and **4** was applied. Analysis was based on polystyrene standards.

Diffusion ordered 2D NMR (Table 7.3); sample preparation was as follows:

entry 1: 8 mg **1** or **6** and 1 mg CD / mL CDCl_3 ;

entry 2: 8 mg **4** and 1 mg CD / mL CDCl_3 ;

entry 3: 3 mg **2** or 8 mg **7** and 1 mg CD / mL CDCl_3 (**2** not dissolved completely);

entry 4: 5 mg **2** or 8 mg **7**, 2.36 mg **4** and 1 mg CD / mL CDCl_3 (**2** heated at 40 °C to yield a clear solution);

entry 5: 8 mg **9**, 1 mg CD / mL CDCl_3 ;

entry 6: 5 mg **2** or 7 mg **7**, 25 mg **9** and 1 mg CD / mL CDCl_3 (**2** heated at 40 °C to yield a clear solution)

Synthesis. 2-*n*-Butylureido-6-methyl-4[1H]-pyrimidinone **3** was prepared as reported by Beijer *et al.*⁶⁷; butylureido-6-(3-heptyl)-4[1H]-pyrimidinone **4** and imidazolide **11** were prepared according to Keizer *et al.*⁶⁰; {2-[2-(2-methoxy-ethoxy)-ethoxy]-ethyl}-(2-ureido-6-(3-heptyl)-4[1H]-pyrimidinone **5** was synthesized as described in Chapter 6 of this Thesis.⁴³ PEB-NH₂ **10** was synthesized as reported by Hirschberg *et al.*⁶¹

General procedure of ADMET polymerization of 2,7-bis-(10-undecenoylamino)-1,8-naphthyridine (Table 7.1, entries 1-8). To a 20 mL of Schlenk flask charged with 2,7-bis-(10-undecenoylamino)-1,8-naphthyridine **1** (100 mg, 0.202 mmol) and the additive, 1.00 mL of distilled toluene was added and deoxygenated by a freeze-pump-thaw cycle. After backfilling with argon, resulting dispersion was stirred at 50 °C until the monomer was completely dissolved. Ruthenium catalyst (**A-D**) (25 μmol) was added to this solution and stirred for 20 h as maintaining the temperature at 50 °C. The solvent was removed by the evaporation and a ¹H NMR spectrum of the crude mixture was taken.

ADMET polymerization of 2,7-bis-(10-undecenoylamino)-1,8-naphthyridine (Table 7.1, entry 9). To a 20 mL Schlenk flask charged with 2,7-bis-(10-undecenoylamino)-1,8-naphthyridine **1** (100 mg, 0.202

mmol) and UPy **4** (93.0 mg, 302 μ mol), 670 μ L of distilled toluene was added and deoxygenated by a freeze-pump-thaw cycle. After backfilling with argon, the resulting dispersion was stirred at 50 °C until the monomer was completely dissolved. Grubbs catalyst 2nd generation **A** (20.8 mg, 24.5 μ mol) was added to this solution and stirred for 24 h in argon atmosphere as maintaining the temperature at 50 °C. The solvent was removed by evaporation in vacuo. The residue was dissolved in a minimum amount of chloroform and precipitated by THF. The brownish precipitate was assembled by filtration. According to the NMR spectrum, conversion of the double bond was 80%, however still one to one heterocomplex of UPy-Napy was observed (This procedure was helpful to remove excess UPy). Neither precipitation in ethanol nor in diethyl ether enabled the cleavage of the UPy. The precipitate was again dissolved in chloroform and re-precipitated into 3 % methanol in THF (36 % removal UPy). The precipitate was dissolved in THF and purified further by gel permeation chromatography (GPC) using 8 v/v% methanol in THF (total 70 % removal UPy). At this stage the polymer was hardly soluble in any solvent. In the same way again the crude product was purified by the GPC using 10 v/v% methanol in THF as an eluent and brownish band was collected. After evaporation the naphthyridine polymer among which 74 % was free from UPy can be obtained as a brownish powder (30 mg, naphthyridine based yield 24%).

Oligo-2,7-bis(9-decenoylamino)-1,8-naphthyridines/ADMET polymer, 2 (Table 7.1, entry 10): To a 20 mL Schlenk flask charged with 2,7-bis-(10-undecenoylamino)-1,8-naphthyridine **1** (100 mg, 0.202 mmol) and UPy **5** (120.0 mg, 302 μ mol), 670 μ L of distilled toluene was added and deoxygenated by a freeze-pump-thaw cycle. After backfilling with argon, the resulting dispersion was stirred at 50 °C until the monomer was completely dissolved. Grubbs' 2nd generation ruthenium catalyst **A** (20.8 mg, 24.5 μ mol) was added to this solution and stirred for 24 h under the inert atmosphere as maintaining the temperature at 50 °C. The solvent was removed by the evaporation. The residue was dissolved in minimum amount of chloroform and precipitated by hot ethanol. The pale-brownish precipitate was assembled by filtration. According to the NMR spectrum, conversion of the double bond was 76% and 80% removal of UPy was observed. The precipitate was dispersed in ethanol and heated to reflux temperature for 1 h, followed by filtration. The precipitate was collected on a glass-filter and dried in vacuo to yield 56 mg (59%) of the Napy polymer with > 95% removal of the UPy as a pale-brownish powder. ¹H NMR (CDCl₃): δ = 10.0 (br, 2H, NH), 8.50 (2H, Napy), 8.00 (2H, Napy), 5.31 (m, 2H, C=CHCH₂), 3.70 (m, 4H, NHCH₂), 2.45 (m, 4H, C=CHCH₂), 1.93 (m, 4H), 1.66 (m, 4H), 1.55 (m, 4H), 1.26-1.19 (m, 12H) ppm; ¹³C NMR (CDCl₃): δ = 172.7, 154.5, 153.6, 139.1, 130.6, 130.1, 125.1, 118.4, 113.8, 37.9, 33.9, 29.5–29.0 (multiple peaks), 25.4 ppm; FTR-IR (ATR): ν = 3321, 3008, 2920, 2850, 1672, 1611, 1579, 1544, 1506, 1468, 1385, 1312, 1287, 1175, 1136, 1118, 968, 851, 802 cm⁻¹.

Oligo-2,7-bisamido-1,8-naphthyridines/polycondensation polymer, 7 (Table 7.2, entry 4): An oven-dried Schlenk tube was charged with 2,7-bis-(S-2-hydroxypropanoylamino)-1,8-naphthyridine **6** (200 mg, 0.657 mmol) to which CHCl₃ (4 mL) and DMF (1 mL) were added. The mixture was slowly heated until a clear solution was obtained. The vessel was pulled vacuum and back-filled with argon followed by the addition of dodecanedioyl dichloride (175.6 mg, 0.657 mmol) and DMAP (176.6 mg, 1.45 mmol). The solution was stirred at 40 °C for 20 h. The title compound was obtained as a white solid by multiple precipitations in methanol (156 mg, 44%). ¹H NMR (CDCl₃): δ = 10.6 (br, 2H, NH), 8.49 (2H, *J* = 8.8 Hz),

8.16 (2H, $J = 8.8$ Hz), 5.74 (br, 2H, CHO), 2.47 (t, 4H, $J = 4.5$ Hz, COCH₂), 1.68 (m, 4H, COCH₂CH₂), 1.57 (d, 6H, $J = 6.6$ Hz, CH₃ CHO), 1.38-1.20 (m, 8H, CH₂) ppm; ¹³C NMR (CDCl₃): $\delta = 173.8, 170.9, 155.0, 154.4, 139.4, 125.0, 118.6, 114.7, 70.4, 34.3, 29.1$ (multiple), 24.9, 18.0 ppm; MALDI-TOF-MS: (m/z) observed: distribution between 1000 and 8000 g/mol (M+H⁺) as depicted in Figure 7.4; FTR-IR (ATR): $\nu = 3310, 2928, 2855, 1712, 1609, 1542, 1501, 1454, 1389, 1312, 1285, 1175, 1135, 1095, 1047, 854, 803$ cm⁻¹; GPC(THF): $M_w = 6.64$ kg/mol, $M_n = 5.07$ kg/mol, PDI = 1.31.

2,7-Bis-(S-2-(dodecanoyloxy)propanoylamino)-1,8-naphthyridine 8: A round-bottom flask was charged with 2,7-bis-(S-2-hydroxypropanoylamino)-1,8-naphthyridine **6** (100 mg, 0.312 mmol) and CHCl₃ (2 mL) followed by the addition of DMAP (86 mg, 0.70 mmol) and dodecanoyl chloride (137 mg, 0.624 mmol). The mixture was stirred at RT for 3 h and washed with water, brine and dried over Na₂SO₄. Purification by column chromatography (SiO₂, 1/10 v/v acetone / chloroform) afforded the compound as a white powder (86 mg, 41%). ¹H NMR (CDCl₃): $\delta = 9.80$ (br, 2H, NH), 8.47 (2H, $J = 8.8$ Hz), 8.15 (2H, $J = 8.8$ Hz), 5.60 (q, 2H, $J = 7.0$ Hz, CHO), 2.45 (t, 4H, $J = 4.5$ Hz, COCH₂), 1.68 (m, 4H, COCH₂CH₂), 1.56 (d, 6H, $J = 7.0$ Hz, CH₃CHO), 1.35-1.22 (m, 36H, CH₂), 0.87 (t, 6H, $J = 5.4$ Hz, CH₃) ppm; ¹³C NMR (CDCl₃): $\delta = 173.2, 170.4, 153.9, 153.5, 139.4, 118.6, 114.4, 70.3, 34.1, 31.9, 29.6-29.0$ (5), 24.8, , 22.7, 17.8, 14.1 ppm; MALDI-TOF-MS: (m/z) calcd: 668.45; observed: 669.54 (M+H⁺), 691.51 (M+Na⁺); FTR-IR (ATR): $\nu = 3302, 2929, 2850, 1713, 1609, 1546, 1503, 1460, 1390, 1312, 1286, 1177, 1136, 1096, 1046, 854, 803$ cm⁻¹; Anal. Calcd. for C₃₈H₆₀N₄O₆: C 68.23, H 9.04, N 8.38; found: C 68.32, H 9.00, N 8.29.

UPy-functionalized poly(ethylenebutylene) (PEB-UPy) 9: To a solution of PEB-NH₂ **10** (6.50 g, 1.67 mmol) in 100 mL chloroform in a 300 mL round-bottom flask, 6-(3-heptyl)-isocytosine-N²-carbonylimidazolidine⁶⁰ **11** (1.00 g, 3.30 mmol) was added and stirred for 48 hours at 40 °C under nitrogen atmosphere. The solution was washed twice with 1N HCl aqueous solution, then brine. After drying over MgSO₄, the organic layer was filtered, concentrated by evaporation, and precipitated in methanol twice. After drying in vacuo, the title compound was obtained as a pale-yellowish, highly-viscous oil (5.75 g, 84%). ¹H NMR (CDCl₃): $\delta = 13.26$ (br, 1H, NH), 11.94 (br, 1H, NH), 10.22 (br, 1H, NH), 5.80 (s, 1H, CHCO), 3.49 (t, 2H, NHCCH₂O), 3.43 (t, 2H, CH₂O), 3.37 (m, 2H, NHCH₂CH₂), 2.29 (m, 1H, CCH), 1.91 (m, 2H, NHCH₂CH₂), 1.65-1.00 (m, 510 H, CH₂), 0.95-0.75 (m, 110 H, CH₃) ppm; ¹³C NMR (CDCl₃): $\delta = 173.1, 156.8, 155.4, 154.9, 106.2, 69.5, 68.3, 45.4, 38.9, 38.4, 37.9, 37.4, 36.7, 36.1, 34.4, 33.5, 33.4, 33.2, 32.9, 30.6, 30.2, 30.0, 29.7, 29.5, 29.3, 27.1, 26.8, 26.6, 26.4, 26.3, 26.1, 26.0$ (2), 25.9, 22.5, 19.5, 19.2, 13.9, 11.7, 11.4, 10.9, 10.7, 10.6 (2), 10.4, 10.2 ppm; FTR-IR (ATR): $\nu = 3148, 3051, 2960, 2912, 2853, 1698, 1648, 1590, 1528, 1461, 1411, 1379, 1255, 1117, 850$ cm⁻¹.

7.6 References

- (1) Lindsey, J. S. *New J. Chem.* **1991**, 15, 153-80.
- (2) Lehn, J.-M. *Supramolecular Chemistry*; Wiley-VCH, 1995.
- (3) Ciferri, A. *Supramolecular Polymers*; Marcel Dekker: New York, 2000.
- (4) Brunsveld, L.; Folmer, B. J. B.; Meijer, E. W.; Sijbesma, R. P. *Chem. Rev.* **2001**, 101, 4071-4097.
- (5) Prins, L. J.; Reinhoudt, D. N.; Timmerman, P. *Angew. Chem. Int. Ed.* **2001**, 40, 2382-2426.
- (6) Swiegers, G. F.; Malefetse, T. J. *Chem. Rev.* **2000**, 100, 3483-3537.

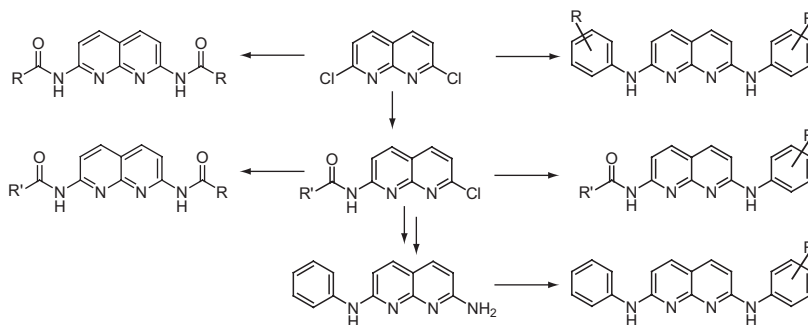
- (7) Harada, A. *Springer Series in Materials Science* **2004**, 78, 26-40.
- (8) Kato, T.; Frechet, J. M. J. *Macromolecules* **1989**, 22, 3818-19.
- (9) Kumar, U.; Kato, T.; Frechet, J. M. J. *J. Am. Chem. Soc.* **1992**, 114, 6630-9.
- (10) Kato, T.; Kihara, H.; Kumar, U.; Uryu, T.; Frechet, J. M. J. *Angew. Chem.* **1994**, 106, 1728-30.
- (11) Kato, T.; Frechet, J. M. J. *Macromol. Symp.* **1995**, 98, 311-26.
- (12) Kato, T.; Kihara, H.; Ujiie, S.; Uryu, T.; Frechet, J. M. J. *Macromolecules* **1996**, 29, 8734-8739.
- (13) Kato, T. *Science* **2002**, 295, 2414-2418.
- (14) Ruokolainen, J.; Makinen, R.; Torkkeli, M.; Makela, T.; Serimaa, R.; Ten Brinke, G.; Ikkala, O. *Science* **1998**, 280, 557-560.
- (15) Ikkala, O.; ten Brinke, G. *Chem. Commun.* **2004**, 2131-7.
- (16) Drechsler, U.; Thibault, R. J.; Rotello, V. M. *Macromolecules* **2002**, 35, 9621-9623.
- (17) Stubbs, L. P.; Weck, M. *Chem. Eur. J.* **2003**, 9, 992-999.
- (18) Boal, A. K.; Ilhan, F.; DeRouchey, J. E.; Thurn-Albrecht, T.; Russell, T. P.; Rotello, V. M. *Nature* **2000**, 404, 746-748.
- (19) Ilhan, F.; Gray, M.; Rotello, V. M. *Macromolecules* **2001**, 34, 2597-2601.
- (20) Das, K.; Nakade, H.; Penelle, J.; Rotello, V. M. *Macromolecules* **2004**, 37, 310-314.
- (21) Ten Brinke, G.; Ikkala, O. *Chemical Record* **2004**, 4, 219-230.
- (22) Pollino, J. M.; Weck, M. *Chem. Soc. Rev.* **2005**, 34, 193-207.
- (23) Sijbesma, R. P.; Beijer, F. H.; Brunsveld, L.; Folmer, B. J. B.; Hirschberg, J. H. K. K.; Lange, R. F. M.; Lowe, J. K. L.; Meijer, E. W. *Science* **1997**, 278, 1601-1604.
- (24) Ky Hirschberg, J. H. K.; Beijer, F. H.; van Aert, H. A.; Magusin, P. C. M. M.; Sijbesma, R. P.; Meijer, E. W. *Macromolecules* **1999**, 32, 2696-2705.
- (25) Folmer, B. J. B.; Sijbesma, R. P.; Versteegen, R. M.; van der Rijt, J. A. J.; Meijer, E. W. *Adv. Mater.* **2000**, 12, 874-878.
- (26) Söntjens, S. H. M.; Sijbesma, R. P.; van Genderen, M. H. P.; Meijer, E. W. *J. Am. Chem. Soc.* **2000**, 122, 7487-7493.
- (27) Söntjens, S. H. M.; Sijbesma, R. P.; van Genderen, M. H. P.; Meijer, E. W. *Macromolecules* **2001**, 34, 3815-3818.
- (28) Corbin, P. S.; Zimmerman, S. C. *J. Am. Chem. Soc.* **1998**, 120, 9710-9711.
- (29) Wang, X.-Z.; Li, X.-Q.; Shao, X.-B.; Zhao, X.; Deng, P.; Jiang, X.-K.; Li, Z.-T.; Chen, Y.-Q. *Chem. Eur. J.* **2003**, 9, 2904-2913.
- (30) Ligthart, G. B. W. L.; Ohkawa, H.; Sijbesma, R. P.; Meijer, E. W. *J. Am. Chem. Soc.* **2005**, 127, 810-811.
- (31) See Chapter 5 of this Thesis.
- (32) See also Chapter 6 of this Thesis.
- (33) Lehman, S. E.; Wagener, K. B.; Grubbs, R. H. *ADMET polymerization*; 1 ed.; Wiley-VCH: Weinheim, 2003.
- (34) Baughman, T. W.; Wagener, K. B. *Adv. Polym. Sci.* **2005**, 176, 1-42.
- (35) Ligthart, G. B. W. L.; Ohkawa, H.; Sijbesma, R. P.; Meijer, E. W. *J. Org. Chem.* **2006**, 71, 375-378.
- (36) Love, J. A.; Morgan, J. P.; Trnka, T. M.; Grubbs, R. H. *Angew. Chem. Int. Ed.* **2002**, 41, 4035-4037.
- (37) Grubbs, R. H. *Handbook of Metathesis*; Wiley-VCH: Weinheim, 2003.
- (38) Sanford, M. S.; Love, J. A.; Grubbs, R. H. *Organometallics* **2001**, 20, 5314-5318.
- (39) Love, J. A.; Sanford, M. S.; Day, M. W.; Grubbs, R. H. *J. Am. Chem. Soc.* **2003**, 125, 10103-10109.
- (40) Sanford, M. S.; Henling, L. M.; Grubbs, R. H. *Organometallics* **1998**, 17, 5384-5389.
- (41) Morgan, J. P.; Grubbs, R. H. *Org. Lett.* **2000**, 2, 3153-3155.
- (42) Bazzi, H. S.; Sleiman, H. F. *Macromolecules* **2002**, 35, 9617-9620.
- (43) Scherman, O. A.; Ligthart, G. B. W. L.; Ohkawa, H.; Sijbesma, R. P.; Meijer, E. W. *Proc. Natl. Acad. Sci. USA* **2006**, submitted.
- (44) Anhaus, J. T.; Clegg, W.; Collingwood, S. P.; Gibson, V. C. *J. Chem. Soc., Chem. Commun.* **1991**, 1720-2.

- (45) Lehman, S. E.; Schwendeman, J. E.; O'Donnell, P. M.; Wagener, K. B. *Inorg. Chim. Acta* **2003**, 345, 190-198.
- (46) Seto, C. T.; Mathias, J. P.; Whitesides, G. M. *J. Am. Chem. Soc.* **1993**, 115, 1321-9.
- (47) Ten Cate, A. T.; Dankers, P. Y. W.; Kooijman, H.; Spek, A. L.; Sijbesma, R. P.; Meijer, E. W. *J. Am. Chem. Soc.* **2003**, 125, 6860-6861.
- (48) Paulusse, J. M. J.; Huijbers, J. P. J.; Sijbesma, R. P. *Macromolecules* **2005**, 38, 6290-6298.
- (49) Lou, X.; Zhu, Q.; Lei, Z.; van Dongen, J. L. J.; Meijer, E. W. *J. Chromatogr. A* **2004**, 1029, 67-75.
- (50) Hummel, J. P.; Dreyer, W. J. *Biochim. Biophys. Acta* **1962**, 63, 530-532.
- (51) Craig, D. B. *J. Chem. Ed.* **2005**, 82, 96-98.
- (52) Wilton, R.; Myatt, E. A.; Stevens, F. J. *Methods in Molecular Biology (Totowa, NJ, United States)* **2004**, 261, 137-154.
- (53) Yoza, N. *J. Chem. Ed.* **1977**, 54, 284-287.
- (54) Carothers, W. H. *Chem. Rev.* **1931**, 8, 353-426.
- (55) Odian, G. *Principles of Polymerization*; John Wiley & Sons: New York, 1991.
- (56) Jacobson, H.; Stockmayer, W. H. *J. Chem. Phys.* **1950**, 18, 1600-6.
- (57) Flory, P. J.; Suter, U. W.; Mutter, M. *J. Am. Chem. Soc.* **1976**, 98, 5733-9.
- (58) Timmerman, P.; Weidmann, J.-L.; Jolliffe, K. A.; Prins, L. J.; Reinhoudt, D. N.; Shinkai, S.; Frish, L.; Cohen, Y. *J. Chem. Soc., Perkin Trans. 2* **2000**, 2077-2089.
- (59) Olenyuk, B.; Levin, M. D.; Whiteford, J. A.; Shield, J. E.; Stang, P. J. *J. Am. Chem. Soc.* **1999**, 121, 10434-10435.
- (60) Keizer, H. M.; Sijbesma, R. P.; Meijer, E. W. *Eur. J. Org. Chem.* **2004**, 2553-2555.
- (61) Hirschberg, J. H. K. K.; Ramzi, A.; Sijbesma, R. P.; Meijer, E. W. *Macromolecules* **2003**, 36, 1429-1432.
- (62) Yoshida, J.; Itami, K. *Chem. Rev.* **2002**, 102, 3693-3716.
- (63) Zhang, S.-Q.; Fukase, K.; Izumi, M.; Fukase, Y.; Kusumoto, S. *Synlett.* **2001**, 590-596.
- (64) Zhang, S.-Q.; Fukase, K.; Kusumoto, S. *Peptide Science* **1999**, 36th, 151-154.
- (65) Fang, S.; Bergstrom, D. E. *Tetrahedron Lett.* **2004**, 45, 7987-7990.
- (66) Fukase, K.; Takashina, M.; Hori, Y.; Tanaka, D.; Tanaka, K.; Kusumoto, S. *Synlett.* **2005**, 2342-2346.
- (67) Beijer, F. H.; Sijbesma, R. P.; Kooijman, H.; Spek, A. L.; Meijer, E. W. *J. Am. Chem. Soc.* **1998**, 120, 6761-6769.

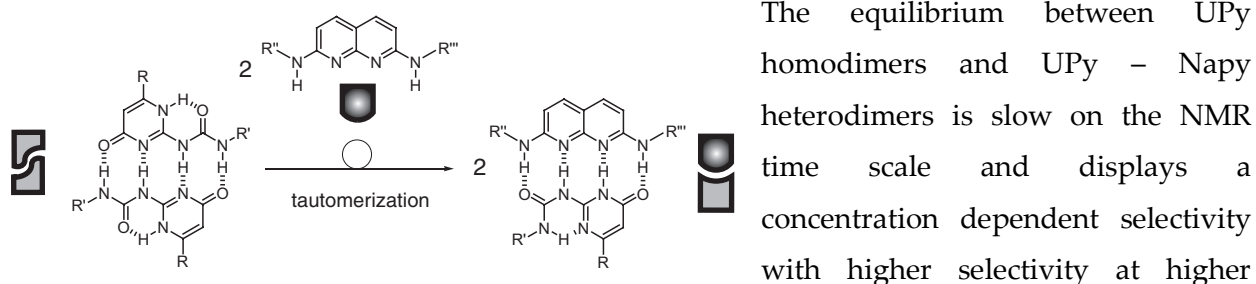
Summary

The self-assembly of small and large molecules into complex structures plays an important role in biological processes. The non-covalent interactions that determine the resulting physical properties and functions of these assemblies can be used to design new supramolecular structures with unique material properties. Whereas supramolecular chemistry has focused on the development of well-defined, discrete aggregates using either complementary or self-complementary non-covalent interactions between individual building blocks, supramolecular polymer chemistry has applied these reversible interactions for the development of polymeric architectures. This class of materials has the potential for possessing unprecedented properties not found in traditional polymers as a result of the reversibility of the non-covalent interactions. This thesis describes the design and synthesis of new complementary binding motifs based on multiple hydrogen bond interactions and their application in supramolecular polymeric architectures.

A general overview of the field of supramolecular polymers is presented in **Chapter 1** and focuses on the use of hydrogen bonding units to obtain polymeric properties in solution or in the bulk. The synthesis and characterization of two new hydrogen bonded complexes based on a 3-ureido-benzo-1,2,4-triazine-1-N-oxide or an acyclic imide motif are described in **Chapter 2**. While pre-organization of the imide motif in the *Z,Z* conformation leads to stable binding of complementary urea motifs, non-specific binding is observed for 3-butylureido-benzo-1,2,4-triazine-1-N-oxide with seemingly complementary partners. *Ab initio* calculations confirm these experimentally found binding properties of the benzotriazine-N-oxide complexes. Promising building blocks in the development of complementary quadruple hydrogen bonded complexes are 2,7-diamido-1,8-naphthyridines (Napy) which display donor-acceptor-acceptor-donor (DAAD) hydrogen bonding motifs. A generally applicable palladium-catalyzed amidation procedure of 2-chloro- and 2,7-dichloro-1,8-naphthyridines towards 2,7-diamido-1,8-naphthyridines (Napy) is described in **Chapter 3**. It is shown that various symmetric and non-symmetric derivatives bearing functional groups were obtained in moderate to good yields. The simplicity and functional group tolerance makes this an attractive method for synthesizing Napy-functionalized molecules. Additionally, 2,7-diamido-1,8-naphthyridines were found to be prone to both



acidic and alkaline hydrolysis unless an alkyl substituent is present at the α -position next to the amide carbonyl. Therefore, a palladium-catalyzed amination and arylation route was explored and optimized for the synthesis of 2-aryl-amino- and 2,7-di(aryl-amino)-1,8-naphthyridines in **Chapter 4**. These derivatives present a previously unexplored class of DAAD hydrogen bonding molecules which are not susceptible to alkaline degradation. In **Chapter 5**, the heterodimer based on the association of 2-ureido-6[1H]-pyrimidinones (UPy) and 2,7-diamino-1,8-naphthyridines was studied in solution by NMR, UV/Vis and fluorescence spectroscopy.

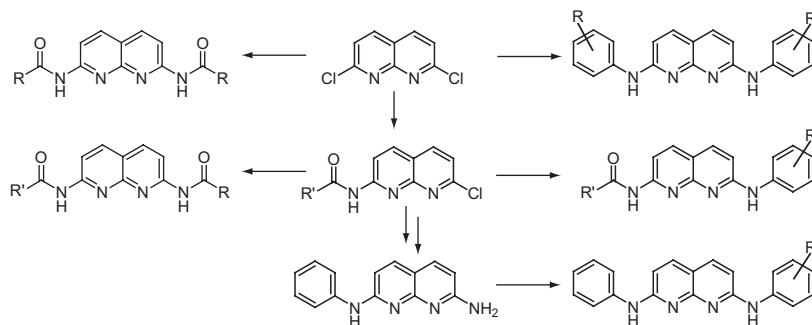


The equilibrium between UPy homodimers and UPy – Napy heterodimers is slow on the NMR time scale and displays a concentration dependent selectivity with higher selectivity at higher concentrations with an association constant of $5 (\pm 2) \times 10^6 \text{ M}^{-1}$ in chloroform. In addition, the strength of binding can be tuned by steric and electronic effects of the amino-substituents of the 1,8-naphthyridine and binding constants can be determined using a single-point ^1H NMR method. With this complementary quadruple hydrogen bonding array available, the results described in **Chapter 6** focus on an application of this array in supramolecular block copolymers. When small bifunctional UPy and Napy building blocks are used, viscometry measurements and DOSY NMR spectroscopy reveal the selective formation of small cyclic structures. Increasing the spacer length between the UPy end-groups was shown to lead to the formation of alternating copolymers. In order to synthesize large bifunctional UPy- and Napy-telechelics via ring-opening metathesis polymerization, a supramolecular protecting group strategy based on quadruple hydrogen bonding with a UPy protecting group was introduced. Supramolecular block copolymer formation was substantiated in solution with viscometry, UV/Vis and infrared spectroscopy as well as in the bulk with AFM and DSC. Finally, acyclic diene metathesis polymerization employing the UPy-protection strategy and a polycondensation procedure using bifunctional Napy units are described in **Chapter 7** in an effort to obtain strictly linear polymers with a high degree of DAAD quadruple hydrogen bond motifs in the main-chain. These polymers were characterized by size exclusion chromatography and diffusion-ordered NMR as grafted and ungrafted copolymers in solution. In conclusion, the results described in this thesis illustrate the versatility of the UPy – Napy heterodimer in the construction of a broad range of supramolecular architectures.

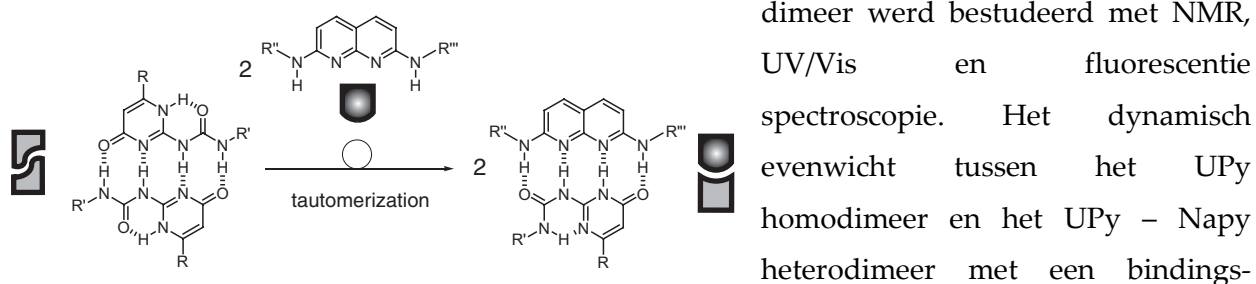
Samenvatting

De zelf-assemblage van kleine en grote moleculen tot complexe structuren speelt een grote rol in biologische processen. De niet-covalente interacties die de resulterende fysische eigenschappen en functies van deze structuren bepalen, kunnen worden gebruikt om nieuwe supramoleculaire structuren te ontwerpen met unieke materiaaleigenschappen. Terwijl supramoleculaire chemie zich richt op goed gedefinieerde aggregaten gebruik makend van zelf-complementaire en complementaire bindingsmotieven, gebruikt de supramoleculaire polymeerchemie deze reversibele interacties om polymere architecturen te ontwikkelen. Door gebruik te maken van reversibele interacties hebben deze nieuwe materialen eigenschappen die kunnen reageren op veranderingen in de omgeving (zogenaamde 'slimme materialen'). Dit proefschrift beschrijft studies om nieuwe complementaire bindingsmotieven te verkrijgen op basis van meervoudige waterstofbruggen en het gebruik ervan in supramoleculaire polymeerstructuren.

Een introductie tot het onderzoeksveld van supramoleculaire polymeren wordt gegeven in **Hoofdstuk 1** waarbij de nadruk wordt gelegd op het verkrijgen van polymeereigenschappen door gebruik van waterstofgebrugde bindingsmotieven. **Hoofdstuk 2** beschrijft de synthese en karakterisering van twee nieuwe waterstofgebrugde complexen gebaseerd op enerzijds een 3-ureido-benzo-1,2,4-triazine-1-N-oxide en anderzijds een acyclisch imide. Hoewel preorganisatie van het imide motief in de *Z,Z* conformatie leidt tot een stabiel complex met een complementair urea molecuul, wordt niet-specifieke binding waargenomen voor het benzotriazine-N-oxide derivaat met schijnbaar complementaire moleculen. Ab initio berekeningen bevestigden deze resultaten. Veelbelovende bouwstenen in de ontwikkeling van complementaire complexen via viervoudige waterstofbrugvorming zijn de 2,7-diamido-1,8-naphthyridines (Napy) die een rij van donor-acceptor-acceptor-donor (DAAD) waterstofbrugfunctionaliteiten vormt. Een algemeen toepasbare syntheseroute voor deze moleculen via palladium-gekatalyseerde amidering van 2-chloro- en 2,7-dichloro-1,8-naphthyridines staat beschreven in **Hoofdstuk 3**. Op deze manier werden verschillende symmetrische en niet-symmetrische derivaten met functionele groepen verkregen met goede opbrengsten. De eenvoud en tolerantie voor functionele groepen van de amidering zorgt ervoor dat dit een aantrekkelijke methode is



om Napy-gefunctionaliseerde moleculen te maken. De gemaakte derivaten zijn echter gevoelig voor zure en basische hydrolyse tenzij er zich een vertakte alkyl staart bevindt naast de amide carbonyl groep. De palladium-gekatalyseerde aminering en arylering tot 2-arylamino- and 2,7-di(arylamino)-1,8-naphthyridines wordt beschreven in **Hoofdstuk 4**. Deze nieuwe klasse verbindingen met DAAD waterstofbrugfunctionaliteiten worden niet afgebroken onder basische omstandigheden. **Hoofdstuk 5** rapporteert de associatie van 2,7-diamido-1,8-naphthyridines met 2-ureido-6[1H]-pyrimidinones (UPy) tot een stabiel heterodimeer. Het



constante van $5 (\pm 2) \times 10^6 \text{ M}^{-1}$ in chloroform, is langzaam op de NMR tijdschaal en vertoont een concentratie-afhankelijke selectiviteit waarbij hogere selectiviteit voor het heterodimeer wordt waargenomen bij hogere concentraties. De sterkte van de binding kan worden gevarieerd door middel van sterische en elektronische effecten van de aminosubstituenten van het 1,8-naphthyridine. Het toepassen van het UPy – Napy complex in supramoleculaire blok-copolymeren wordt in **Hoofdstuk 6** beschreven. Viscosimetrie en DOSY NMR metingen lieten zien dat het combineren van kleine bifunctionele UPy en Napy bouwstenen resulteert in de vorming van kleine cyclische structuren. Door het vergroten van de verbinding tussen de twee UPy eindgroepen werd de vorming van alternerende copolymeren aangetoond. Een supramoleculaire beschermings-strategie op basis van viervoudige waterstofbrugvorming met een UPy beschermgroep werd ontwikkeld om UPy- en Napy-getermineerde polymeren te maken via ring-opening metathese polymerisatie. De vorming van supramoleculaire blok-copolymeren werd met viscosimetrie, UV/Vis en infrarood spectroscopie bevestigd in oplossing en met AFM en DSC in de vaste fase. Tenslotte beschrijft **Hoofdstuk 7** de acyclische dieen metathese polymerisatie waarbij de UPy-beschermgroep strategie werd gebruikt en een polycondensatie van bifunctionele Napy moleculen om lineaire polymeren te verkrijgen met een hoge functionalisatiegraad van DAAD waterstofbrugfunctionaliteiten in de hoofdketen. Met behulp van SEC en DOSY NMR spectroscopie kon worden aangetoond dat deze polymeren in oplossing kunnen worden gefunctionaliseerd met UPy moleculen. De resultaten beschreven in dit proefschrift illustreren derhalve de veelzijdigheid van het UPy – Napy heterodimeer voor de constructie van een breed scala aan supramoleculaire structuren.

Curriculum Vitae



Ronald (G.B.W.L.) Ligthart is geboren op 23 augustus 1977 te Breda. Na het voltooien van het VWO aan het Riethil College in Raamsdonksveer in 1995 begon hij aan de studie Scheikundige Technologie aan de Technische Universiteit Eindhoven. Tijdens deze studie deed hij een stage bij AkzoNobel Surface Chemistry LLC in McCook, Illinois, USA. De studie werd in 2001 afgerond met een onderzoek naar katalytische oxidaties van alcoholen. Vanaf februari 2002 werkte hij als promovendus van de Technische Universiteit Eindhoven binnen de capaciteitsgroep Macromoleculaire en Organische Chemie van de faculteit Scheikundige Technologie. Onder leiding van prof.dr. E.W. Meijer en dr. R.P. Sijbesma werkte hij tot maart 2006 aan zijn promotieonderzoek naar het ontwikkelen van nieuwe, complementaire bindingsmotieven gebaseerd op meervoudige waterstofbrug interacties en de toepassing van deze complexen in supramoleculaire polymeerstructuren. De belangrijkste resultaten van dit onderzoek staan beschreven in dit proefschrift.

Ronald (G.B.W.L.) Ligthart was born on Augustus 23, 1977 in Breda, The Netherlands. He completed high school in 1995 at the Riethil College in Raamsdonksveer. In the same year, he started studying Chemical Engineering and Chemistry at the Eindhoven University of Technology. During his master study, he did an international internship at AkzoNobel Surface Chemistry LLC in McCook, Illinois, USA. He obtained his master degree in 2001 with an investigation on the catalytic oxidation of alcohols. The author started his Ph.D. research in February 2002 at the Eindhoven University of Technology in the laboratories of Macromolecular and Organic Chemistry at the department of Chemical Engineering and Chemistry. Under supervision of prof.dr. E.W. Meijer and dr. R.P. Sijbesma, the author has worked on the design and synthesis of new complementary binding motifs based on multiple hydrogen bond interactions and their application in supramolecular polymeric architectures until March 2006. The most important results of this Ph.D. research are described in this thesis.

Publications

- Ligthart, G.B.W.L.; Cörvers, C.F.; Sijbesma, R.P.; Meijer, E.W. "Pd-Catalyzed Amination to 2-Amino- and 2,7-Diamino-1,8-naphthyridines", *Eur. J. Org. Chem.*, **2006**, in preparation.
- Ligthart, G.B.W.L.; Guo, D.; Zuilhof, H.; Sijbesma, R.P. "On the Quadruple Hydrogen Bonding of a 3-Ureido-benzo-1,2,4-triazine-1N-oxide Motif", *J. Chem. Phys.*, **2006**, submitted.
- Ohkawa, H.; Ligthart, G.B.W.L.; Sijbesma, R.P.; Meijer, E.W. "Supramolecular Graft-Copolymers Based on 2,7-Diamido-1,8-naphthyridines", *Macromolecules*, **2006**, submitted.
- Scherman, O.A.; Ligthart, G.B.W.L.; Ohkawa, H.; Sijbesma, R.P.; Meijer, E.W. "Olefin Metathesis and Quadruple Hydrogen Bonding: A Powerful Combination in Multi-step Supramolecular Synthesis", *Proc. Natl. Acad. Sci. USA*, **2006**, submitted.
- Ligthart, G.B.W.L.; Scherman, O.A.; Sijbesma, R.P.; Meijer, E.W. "Supramolecular Polymer Engineering", contribution in: "Macromolecular Engineering: From Precise Macromolecular Synthesis to Macroscopic Materials Properties and Applications, Ed. Matyjaszewski, K.; Gnanou, Y.; Leibler, L., **2006**, in press.
- Scherman, O.A.; Ligthart, G.B.W.L.; Sijbesma, R.P.; Meijer, E.W. "A Selectivity Driven Supramolecular Polymerization of an AB Monomer", *Angew. Chem. Int. Ed.*, **2006**, 45, 2072-2076.
- Ligthart, G.B.W.L.; Ohkawa, H.; Sijbesma, R.P.; Meijer, E.W. "Pd-Catalyzed Amidation of 2-Chloro- and 2,7-Dichloro-1,8-naphthyridines", *J. Org. Chem.*, **2006**, 71, 375-378.
- Ligthart, G.B.W.L.; Ohkawa, H.; Sijbesma, R.P.; Meijer, E.W. "Complementary quadruple hydrogen bonding for supramolecular architectures", *Polym. Prepr.*, **2005**, 46, 1098-1099.
- Ligthart, G.B.W.L.; Ohkawa, H.; Sijbesma, R.P.; Meijer, E.W. "Complementary Quadruple Hydrogen Bonding in Supramolecular Copolymers", *J. Am. Chem. Soc.*, **2005**, 127, 801-811.
- Meijer, R.H.; Ligthart, G.B.W.L. Meuldijk, J.; Vekemans, J.A.J.M.; Hulshof, L.A.; Mills, A.M.; Kooijman, H.; Spek, A.L. "Triruthenium dodecacarbonyl/triphenyl-phosphine catalyzed dehydrogenation of primary and secondary alcohols", *Tetrahedron*, **2004**, 60, 1065-1072.
- Meijer, R.H.; Ligthart, G.B.W.L. Meuldijk, J.; Vekemans, J.A.J.M.; Hulshof, L.A.; "RuCl₂[S-BINAP]-catalyzed synthesis of aldehydes and ketones by dehydrogenation of alcohols", *J. Mol. Cat. A*, **2004**, 218, 29-40.
- Ligthart, G.B.W.L.; Meijer, R.H.; Donners, M.P.J.; Meuldijk, J.; Vekemans, J.A.J.M. ; Hulshof, L.A. "Highly sustainable catalytic dehydrogenation of alcohols with evolution of hydrogen gas", *Tetrahedron Lett.*, **2003**, 44, 1507-1509.
- Sijbesma, R.P.; Ligthart, G.B.W.L.; Versteegen, R.M.; Koevoets, R.; Meijer, E.W. "Molecular recognition in polymers using multiple hydrogen bonds: Expanding the toolbox", *Polym. Prepr.*, **2003**, 44, 457-458.

Dankwoord

Met heel veel plezier en voldoening kijk ik terug op de afgelopen vier jaar. Bij deze wil ik dan ook graag iedereen bedanken die een bijdrage heeft geleverd aan dit onderzoek. Een aantal mensen wil ik echter in het bijzonder bedanken.

Allereerst ben ik mijn promotor **Bert Meijer** en copromotor **Rint Sijbesma** zeer dankbaar voor hun enthousiaste begeleiding, leerzame discussies en vertrouwen. Jullie hebben me altijd zeer gemotiveerd. Rint, je ideeën en suggesties zijn onmisbaar geweest voor mijn onderzoek.

I would also like to thank prof. **Bob Grubbs** and prof. **Jim Feast** for participating in my examination committee and for the suggestions on my thesis; I am truly honored. Prof. **Bert Hulshof** wil ik ook graag bedanken voor het deelnemen aan de leescommissie en het consistent maken van mijn proefschrift. Tevens ben ik dank verschuldigd aan dr. **Marc Hillmyer** en dr. **Erik Abbenhuis** voor hun deelname aan de promotiecommissie.

A special word of thanks to both my “Napy brothers” dr. **Haruki** (Japy) Ohkawa and dr. **Oren** (one sec...) Scherman without whom the results described in chapters 6 and 7 wouldn't have been achieved. Haruki, ‘dank je wel’ for a great time and I hope you can find a way to live according to Dutch standards in Japan! Oren, ‘ontzettend bedankt’ for all your advice and a great time. I am convinced you will be an outstanding professor anywhere in the world!

Gedurende mijn promotie heb ik het voorrecht gehad met een aantal andere groepen samen te werken. Graag wil ik dan ook ir. **Bas Gruijters** en prof. **Floris Rutjes** van de Radboud Universiteit Nijmegen bedanken voor de samenwerking om niet-covalente oppervlakte-modificatie te realiseren. Dr. **Dawei Guo** en dr. **Han Zuilhof** van de Universiteit van Wageningen wil ik bedanken voor de berekeningen die hebben geleid tot een beter begrip waarom de benzotriazine-N-oxide geen goed waterstofbrugvormend molecuul is en **Wout Knoben** van dezelfde universiteit voor de samenwerking om silica te functionaliseren; we zitten er dicht tegen aan! Verder wil ik dr. **Pedro Hermkens** van Organon N.V. bedanken voor de synthetische adviezen en de faciliteiten om een aantal Napy-derivaten te verkrijgen.

Een erg leuk en leerzaam onderdeel van mijn promotie was ook het begeleiden van practicumstudenten en afstudeerders. In het bijzonder dank aan **Bart Hamers** en **Debbie Cörvers** voor de nuttige bijdragen van hun afstudeerwerk en de gezellige tijd! Bart: succes met je promotie bij SKA en Debbie: succes op de TU/e met je Master-opleiding!

Ik wil dr. **Jef Vekemans** graag bedanken voor de vele adviezen en inzichten op synthetisch gebied maar ook daarbuiten en het corrigeren van menig manuscript. Het is ongelooflijk dat je voor iedereen tijd hebt en tegelijkertijd nog de onbetwiste encyclopedie van SMO bent. Het analytische team bestaande uit **Joost van Dongen**, **Xianwen Lou** en **Ralf Bovee** ben ik zeer

erkentelijk voor de vele analyses en **Henk Eding** voor de element analyses en de gezelligheid bij de koffietafel! Het secretariaat met **Hanneke Veldhoen, Joke Rediker, Ingrid Dirkx, Carine van der Vaart** en **Sagitta Peters** ben ik dankbaar voor al hun hulp. In het bijzonder wil ik ook **Hannie van der Lee** en **Hans Damen** bedanken voor de gezelligheid en leuke gesprekken tijdens de koffiepauzes (ze werden steeds langer...), het schoonhouden van SMO en het regelen van chemicaliën. Hans: ik hoop toch dat je op het feest komt!

Gedurende de afgelopen 4 jaar heb ik ook heel wat kamergenoten gehad: **Paul, Renzo, Pascal, Rolf, Haruki, Zeljko, Maarten S.** en **Michel** bedankt voor de altijd goede sfeer op de kamer! Daarnaast wil ik mijn labgenoten, **Maarten P., Zeljko, Patricia, Henk, Holger, Subi, Freek, Pim, Jeroen, Pascal, Patrick** en **Bas** van het 'koningenlab' 3 bedanken voor de enorm leuke tijd tijdens de doodsaie kolommen en lange dagen en voor de uitstekende sfeermuziek waardoor ik altijd met een grote glimlach het lab in kwam en verliet maar ook soms met grote haast naar mijn kamer ging. De darts- en kara'OKÉ'-avonden zal ik me nog lang herinneren! Speciaal wil ik **Jos** en **Maarten B.** bedanken voor hun vriendschap en mooie momenten waardoor er altijd hard gelachen kon worden want een schaterlach is toch per definitie luid! Verder wil ik alle vroegere en huidige leden van de capaciteitsgroep Macromoleculaire en Organische Chemie bedanken voor het creëren van een sfeer waarin wederzijdse interesse en behulpzaamheid voorop staat en ook voor het delen van vele niet-wetenschappelijke momenten. In het bijzonder wil ik noemen: **Oren, Haruki, Jos, Maarten B., Sander, Linda, Patricia, Henk, Tessa, Eva, Hinke, Tom, Judith, René** en **Jolanda**.

Alle collega's van de PhilipsHarmonie, Philips Symfonie Orkest en andere orkesten waar ik regelmatig heb gespeeld wil ik bedanken voor de gezellige repetities, goede concerten en onvergetelijke tournees.

De mensen bij wie ik dag en nacht kan aankloppen om mijn hart te luchten ben ik nog het meest dankbaar voor hun luisterend oor en de speciale momenten. **Marco** en **Michel**, jullie zijn fantastische broers (echte chemical brothers!) en ik ben enorm blij dat jullie mijn paranimfen willen zijn. Verder wil ik al mijn vrienden en vriendinnen bedanken voor de nodige ontspanning tot in de late uurtjes. **Pa** en **ma**, jullie zijn geweldige ouders, bedankt voor jullie onvoorwaardelijke steun. Als laatste de belangrijkste: **Ingrid**, je betekent alles voor me. Het viel niet altijd mee als ik weer eens wat af wilde maken in de avonduren of het weekend maar ik hoop je ooit nog eens witte chocolade zonder calorieën voor te schotelen...

Ronald